TÉCNICO LISBOA

UNIVERSIDADE DE LISBOA

INSTITUTO SUPERIOR TÉCNICO

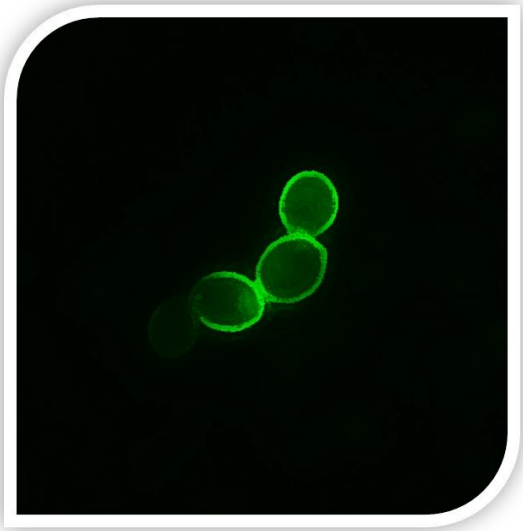

Unveiling the complex regulatory network governing antifungal drug resistance in *Candida glabrata*: from new regulators to new effectors

Pedro Henrique Magalhães Fernandes Pais

Supervisor: Doctor Miguel Nobre Parreira Cacho Teixeira

Thesis approved in public session to obtain the PhD Degree in Biotechnology and Biosciences

Jury final classification: Pass with Distinction and Honour

2019

UNIVERSIDADE DE LISBOA

INSTITUTO SUPERIOR TÉCNICO

Unveiling the complex regulatory network governing antifungal drug resistance in *Candida glabrata*: from new regulators to new effectors

Pedro Henrique Magalhães Fernandes Pais

Supervisor: Doctor Miguel Nobre Parreira Cacho Teixeira

Thesis approved in public session to obtain the PhD Degree in Biotechnology and Biosciences

Jury final classification: Pass with Distinction and Honour

Jury

Chairperson: Doctor Isabel Maria de Sá Correia Leite de Almeida, Instituto Superior Técnico, Universidade de Lisboa

Members of the Committee:

Doctor Geraldine Butler, School of Biomolecular and Biomedical Science, University College Dublin, Ireland

Doctor Isabel Maria de Sá Correia Leite de Almeida, Instituto Superior Técnico, Universidade de Lisboa

Doctor Miguel Nobre Parreira Cacho Teixeira, Instituto Superior Técnico, Universidade de Lisboa

Doctor Sandra Cristina Almeida Paiva, Escola de Ciências, Universidade do Minho

Doctor Nuno Gonçalo Pereira Mira, Instituto Superior Técnico, Universidade de Lisboa

Funding Institutions: FCT – Fundação para a Ciência e a Tecnologia

2019

Abstract

The acquisition of drug resistance has been implicated in the failure of antifungal therapy, especially against infections caused by *Candida glabrata*. It is thus crucial to understand the molecular basis of this phenomenon, in order to guide the design of more suitable therapeutic strategies. With this overall goal in mind, the work described in this thesis aims to contribute to extend knowledge on the role of transcription regulatory networks in antifungal resistance in *C. glabrata*.

The PathoYeastract database (www.pathoyeastract.org) was built, comprising a series of tools to predict and analyze transcription regulatory associations in the four major *Candida* pathogenic species. All published data on Transcription Factor (TF) regulatory associations, and DNA binding motifs was curated and stored in the database. Moreover, tools for the comprehensive analysis on gene or genome-wide transcriptional responses were developed, which further enable the prediction of regulatory networks and cross-species comparison based on orthologous associations described for other yeast species.

Additionally, the role of three transcription factors in antifungal resistance was evaluated. Although the role of the TF CgPdr1 in fluconazole resistance had been well established, that is not the case for other antifungals, especially the effect of CgPdr1 at the protein expression levels. Based on the identification of CgPdr1 as a determinant of resistance to imidazoles and 5-flucytosine, the effect of CgPdr1 expression on membrane protein levels in response to clotrimazole and 5-flucytosine was studied, using iTRAQ-MS-based proteomics. The concentration of 37 or 32 membrane proteins was found to change upon clotrimazole or 5-flucytosine stress, respectively, CgPdr1 controlling about 50% of those changes. Based on the obtained results, the Drug:H+ Antiporters CgTpo1_1 and CgTpo1_2 were found to mediate clotrimazole resistance, while CgFlr1 and CgFlr2 were found to contribute to 5-flucytosine resistance, in both cases by decreasing intracellular drug accumulation. Cell wall remodeling was also found to occur in response to both drugs, in the case of clotrimazole through the specific participation of the CgGas1 cell wall protein.

It is frequently the occurrence of Gain-of-Function (GOF) mutations in CgPdr1, leading to its activation, that results in constitutive expression of drug efflux pumps and, consequently, azole drug resistance. However, several studies reported the identification

of *C. glabrata* clinical isolates that display azole resistance, but no CgPdr1 GOF mutations, suggesting the existence of additional unknown mechanisms of antifungal resistance in this yeast. As a result of a screening for new TFs that might be involved in antifungal drug resistance, the TFs CgRpn4 and CgMar1 were found as additional determinants of fluconazole resistance in *C. glabrata*. Their role in this phenomenon, assessed through RNA-sequencing, was found to include, at least, the control of plasma membrane lipid metabolism. CgRpn4 was found to be required for the activation of ergosterol biosynthesis genes, including direct activation of the azole target *CgERG11*. CgMar1 was found to regulate sphingolipid metabolism, particularly the activation of the sphingolipid flippase CgRsb1 and the incorporation of sphingosine in the plasma membrane. Obtained results support the notion that CgRpn4 and CgMar1 participate in the control of ergosterol and sphingolipid levels during fluconazole stress, respectively, contributing to decrease plasma membrane permeability and the consequent fluconazole accumulation in *C. glabrata* cells.

Altogether, this thesis extends our understanding of how transcription regulation is orchestrated in *Candida* species by providing a new computational tool for its analysis, while presenting two novel regulatory networks that contribute to azole resistance in *C. glabrata*.

Keywords: *Candida glabrata*, azoles, 5-flucytosine, transcription factors, antifungal regulatory networks

Resumo

A aquisição de resistência a drogas tem sido associada ao insucesso da terapia antifúngica, especialmente em infeções causadas por *Candida glabrata*. Por esta razão, é crucial perceber as bases moleculares deste fenómeno, de forma a guiar o desenvolvimento de estratégias terapêuticas mais adequadas. Com este objetivo, o trabalho descrito nesta tese tem o intuito de contribuir para o conhecimento do papel de redes de regulação transcricional na resistência a antifúngicos em *Candida glabrata*.

A base de dados PathoYeastract (www.pathoyeastract.org) foi desenvolvida, incluindo um conjunto de ferramentas para analisar e prever associações regulatórias nas quatro espécies de *Candida* mais prevalentes. Toda a informação publicada relativa a associações regulatórias de Fatores de Transcrição (FT) e motivos de ligação ao DNA foi recolhida e incorporada na base de dados. Foram desenvolvidas ferramentas para a análise integrada de respostas transcricionais ao nível de genes ou genomas completos, permitindo a previsão de redes regulatórias e comparações inter-espécies baseadas em associações ortólogas descritas noutras espécies de leveduras.

O papel de três fatores de transcrição na mediação da resistência a antifúngicos foi estudado. Embora a função do FT CgPdr1 na resistência a fluconazol esteja bem estudada, o mesmo não é o caso para outros antifúngicos, especialmente o efeito do FT CgPdr1 ao nível da expressão proteica. Com base na identificação do FT CgPdr1 como sendo um determinante de resistência a imidazóis e 5-flucitosina, o efeito da sua expressão na resposta ao nível de proteínas de membrana em resposta a clotrimazol e 5-flucitosina foi estudado, usando para tal proteómica baseada em iTRAQ-MS. Verificou-se que a concentração de 37 ou 32 proteínas de membrana encontra-se alterada durante tratamento com clotrimazol ou 5-flucitosina, respetivamente, e que o FT CgPdr1 controla cerca de 50% dessas alterações. Com base nestes resultados, verificou-se que os antiportadores droga:H^+ CgTpo1_1 e CgTpo1_2 conferem resistência a clotrimazol, enquanto que os antiportadores droga:H^+ CgFlr1 e CgFlr2 conferem resistência a 5-flucitosina; em ambos os casos actuam por diminuição da acumulação intracelular de antifúngico. A remodelação da parede celular também ocorre em resposta a ambos os antifúngicos, sendo que no caso do clotrimazol o mesmo se deve, pelo menos, à presença da proteína de parede CgGas1.

A ocorrência de mutações de ganho de função no FT CgPdr1, levando à sua ativação, é frequentemente a causa da expressão constitutiva de bombas de efluxo, resultando na resistência a antifúngicos da família dos azóis. No entanto, vários estudos referem a descoberta de isolados de *C. glabrata* resistentes a azóis que não possuem mutações de ganho de função no FT CgPdr1, o que sugere a existência de mecanismos adicionais de resistência a azóis que são desconhecidos nesta levedura. Como resultado de uma triagem para encontrar novos FTs que possam estar envolvidos em resistência a antifúngicos, os FTs CgRpn4 e CgMar1 foram identificados como determinantes de resistência a fluconazol em *C. glabrata*. A sua função neste fenómeno foi avaliada através da técnica de sequenciação de RNA, tendo sido associada ao controlo do metabolismo de lípidos da membrana plasmática. O FT CgRpn4 regula a ativação de genes de síntese de ergosterol, incluindo ativação direta do gene *CgERG11*, que constitui o alvo dos azóis. O FT CgMar1 regula metabolismo de esfingolípidos, nomeadamente a ativação do translocador de esfingolípidos CgRsb1 e a incorporação de esfingosina na membrana plasmática. Os resultados obtidos mostram que os FTs CgRpn4 e CgMar1, respetivamente, participam no controlo dos níveis de ergosterol e esfingolípidos durante tratamento com fluconazol, contribuindo assim para diminuir a permeabilidade de membrana e consequentemente a acumulação do antifúngico em células de *C. glabrata*.

De modo geral, esta tese contribui para o aumento do conhecimento quanto à regulação transcricional em *C. glabrata* e como a mesma está organizada, através do desenvolvimento de ferramentas computacionais de análise e apresentando duas novas redes de regulação que contribuem para resistência a azóis em *C. glabrata*.

Palavras-chave: *Candida glabrata*, azóis, 5-flucitosina, fatores de transcrição, redes de regulação antifúngicas

Acknowledgements

I would like to acknowledge my supervisor Professor Miguel Teixeira for giving me the opportunity to carry out my PhD work under his guidance. I especially appreciate his availability, advice and unwearying dedication not only to this project, but also to my growth as a scientist. His guidance was key to perform a solid scientific work, from experimental design to the writing of papers and this PhD thesis. His expertise as a competent researcher and his commitment allowed this work to come together and motivated me to be the best student I could. I must also thank him for pushing me to learn distinct techniques and skills, which undoubtedly contributed to my professional development and allowed this thesis to be as comprehensive as it is.

I would also like to acknowledge Professor Isabel Sá-Correia, head of the Biological Sciences Research Group (BSRG) and director of the BIOTECnico PhD program. I acknowledge her for allowing me to join the BSRG and conduct this work in the context of this PhD program. The BIOTECnico program facilitated multiple training opportunities which proved quite advantageous for the development of my scientific background and this thesis.

I acknowledge the collaboration of all co-authors of the papers and manuscripts presented in this thesis. A special recognition goes to Catarina Costa, not only as a co-author, but also for guiding my early steps in the research group. I acknowledge Dr. Pedro Monteiro and the BioData.pt e-infrastructure for making the PathoYeastract project possible. I further acknowledge Professor Geraldine Butler, from the Conway Institute at University College Dublin, for accepting me at her research group to learn from their expertise during 6 months of my PhD, with the support of Mihaela Ola, who I also acknowledge.

Finally, I acknowledge “Fundação para a Ciência e a Tecnologia” (FCT) PhD grant PD/BD/113631/2015 attributed to the candidate under the framework of the Instituto Superior Técnico BIOTECnico PhD program in Biotechnology and Biosciences. The work carried out during this PhD was financed by FEDER and FCT (Contracts PTDC/EBB-BIO/119356/2010, IF/01333/2013, PTDC/BBB-BIO/4004/2014, PTDC/BII-BIO/28216/2017). Funding received by iBB from FCT (UID/BIO/04565/2013), INESC-ID from FCT (UID/CEC/50021/2013) and from

Programa Operacional Regional de Lisboa 2020 (Project N. 007312) is also acknowledged.

The following personal acknowledgements will be addressed in Portuguese:

Em primeiro lugar, gostaria de deixar um agradecimento ao meu orientador, Prof. Miguel Teixeira, pela dedicação, paciência e os conhecimentos que foi capaz de passar durante este doutoramento. Este trabalho deve muito à sua capacidade de trabalho e à atenção que presta aos seus alunos. Um obrigado especial pela confiança que depositou em mim e à porção de independência que me ofereceu durante o desenvolvimento deste trabalho, permitindo-me assim aprender a partir dos meus erros. A sua orientação e confiança nas minhas capacidades permitiu que esta tese tenha sido possível.

Como não podia deixar de ser, todas as pessoas do BSRG merecem um grande agradecimento. São os companheiros de todos os dias que pela sua boa disposição e amizade, contribuem para um bom ambiente de trabalho. Deixo um agradecimento especial à Catarina, que contribuiu para a minha aprendizagem científica. Um obrigado aos companheiros diários do 6.6.15, especialmente à Mónica, e à Mafalda; que estiveram presentes diariamente e por vezes muita paciência tiveram. Um obrigado também aos que sempre me ouviram sem restrições, que aturaram os meus devaneios e estiveram dispostos a despender do seu tempo para apenas me ajudar a desabafar um pouco, especialmente a Andreia. Um obrigado muito grande aos que acompanharam mais de perto os sabores e dissabores do doutoramento e que me ajudaram em todos os momentos dentro e fora do laboratório, especialmente à Cláudia, Amir e Soraia. Obrigado a todos estes e aos demais que contribuíram para que os dias de trabalho tenham sido passados com um sorriso na cara.

Por fim, um obrigado a todos os que me apoiaram fora do BSRG e que sempre acreditaram no sucesso desta etapa. Um obrigado à Isabel, que foi incansável. Obrigado aos meus pais, à minha avó e sua irmã, obrigado à minha prima e à minha madrinha que sempre me provocaram com “as cândidas”, e a toda a minha família.

Table of Contents

List of Figures

Figure 3.1 – Categorization, based on the biological process taxonomy of Gene Ontology, of the proteins identified in membrane-enriched fractions of *C. glabrata* cells. These genes were clustered using the GoToolBox software (http://genome.crg.es/GOToolBox/), and the most highly ranked statistically significant (p-value<10^{-10}) GO terms are displayed. The protein frequency within each class is indicated by the black bars, compared to the frequency registered for the *C. glabrata* whole genome, indicated by the grey bars, gene frequency being the percentage of the genes in a list associated to a specific GO term.

Figure 3.2 – Major functional groups found to have significant expression changes in the membrane-enriched proteome upon exposure to clotrimazole in *C. glabrata*. Proteins with significant expression changes include Ribosome components and translation machinery (22 proteins), Lipid and cell wall metabolism (2 proteins), Multidrug resistance transporters (4 proteins), Mitochondrial import (2 proteins), Oxidative phosphorylation (5 proteins) and Glucose metabolism (2 proteins).

Figure 3.3 – CgTpo1_1 and CgTpo1_2 confer resistance to azole antifungal drugs in *C. glabrata* cells. (A) Comparison of the susceptibility to inhibitory concentrations of several chemical stress inducers, at the indicated concentrations, of the *C. glabrata* KUE100, KUE100_*Δcgtpo1_1* and KUE100_*Δcgtpo1_2* strains, in YPD agar plates (SPM - spermine and SPMD - spermidine) and BM plates (remaining drugs) by spot assays. (B) Comparison of the susceptibility to several drug stress inducers, at the indicated concentrations, of the *C. glabrata* L5U1 strain, harboring the pGREG576 cloning vector (v) or the pGREG576_MTI_*CgTPO1_1* or pGREG576_MTI_*CgTPO1_2* plasmids in YPD agar plates (SPM and SPMD) and BM agar plates (remaining drugs), without uracil, by spot assays. (c) Comparison of the vector pGREG576 (v) or the derived *CgTPO1_1* or *CgTPO1_2* expression plasmids pGREG576_*CgTPO1_1* or pGREG576_*CgTPO1_2*, on BM agar plates by spot assays. The inocula were prepared as described in Experimental Procedures. Cell suspensions used to prepare the spots were 1:5 (b) and 1:25 dilutions of the cell suspension used in (a). The displayed images are representative of at least three independent experiments.

Figure 3.4 – Fluorescence of exponential phase BY4741 *S. cerevisiae* and L5U1 *C. glabrata* cells, harboring the expression plasmids pGREG576_*CgTPO1_1* and pGREG576_*CgTPO1_2*; or pGREG576_MTI_*CgTPO1_1* and pGREG576_MTI_*CgTPO1_2*, after galactose or copper-induced recombinant protein production, respectively.

Figure 3.5 – Comparison of growth curves of *C. glabrata* KUE100 (■,□), KUE100_*Δcgtpo1_1* (▲,△) and KUE100_*Δcgtpo1_2* (◆,◇) cell populations, in liquid BM medium, in the absence (open symbols) or presence of 90 mg/L clotrimazole (filled symbols), measured in terms of variation in OD_{600nm}. The displayed growth curves are representative of at least three independent experiments.

Figure 3.6 – Time-course accumulation of radiolabeled ^{3}H-clotrimazole in strains KUE100 (▪) wild-type and KUE100_*Δcgtpo1_1* (♦) (A) and KUE100 (▪) and KUE100_*Δcgtpo1_2* (♦) (B), during cultivation in BM liquid medium in the presence of 30 mg/L unlabeled clotrimazole. Accumulation values are the average of at least three independent experiments. Error bars represent the corresponding standard deviations. *p<0.05. **p<0.01.

Figure 3.7 – Comparison of the variation of the *CgTPO1_1* (A) and *CgTPO1_2* (B) transcript levels in the 66032u *C. glabrata* wild-type strain and in the derived 66032u_*Δcgpdr1* deletion mutant, before (control) and after 1h of exposure 60 mg/L clotrimazole. The presented transcript levels were obtained by quantitative RT-PCR and are relative *CgTPO1_1*/*CgACT1* or *CgTPO1_2*/*CgACT1* mRNA, relative to the values registered in the 66032u parental strain in control conditions. The indicated values are averages of at least three independent experiments. Error bars represent the corresponding standard deviations. *p<0.05.

Figure 3.8 – CgGas1 confers resistance to azole antifungal drugs in *C. glabrata* cells. (A) Comparison of the susceptibility to azole antifungal drugs, at the indicated concentrations, of the *C. glabrata* KUE100 wild-type and KUE100_*Δcggas1* strains, in BM agar plates by spot assays. The inocula were prepared as described in Experimental Procedures. Cell suspensions used to prepare the spots were 1:5 (b) and 1:25 (c) dilutions of the cell suspension used in (a). The displayed images are representative of at least three independent experiments. (B) Lyticase susceptibility in *C. glabrata* KUE100 (♦,■,▲) and KUE100_*Δcggas1* (◊,□,Δ) cells harvested in the exponential

phase of growth in the absence of stress (♦,◊) or upon 30 min of exposure to 30 mg/L clotrimazole (■,□), or in the exponential phase of growth reached upon adaptation to 30 mg/L clotrimazole (▲,Δ). After addition of 10 mg/L lyticase, the decrease in the OD_{600nm} of the cell suspension was measured periodically and indicated as a percentage of the initial OD_{600nm}. The indicated values are averages of at least three independent experiments. Error bars represent the corresponding standard deviations. **p<0.01.

Figure 3.9 – The combined action of CgTpo1_2 and CgGas1 confers resistance to azole antifungal drugs in *C. glabrata* cells. (A) Comparison of the susceptibility to azole antifungal drugs, at the indicated concentrations, of the *C. glabrata* KUE100 wild-type and KUE100_*Δcggas1* strains, in BM agar plates by spot assays. The inocula were prepared as described in Experimental Procedures. Cell suspensions used to prepare the spots were 1:5 (b) and 1:25 (c) dilutions of the cell suspension used in (a). The displayed images are representative of at least three independent experiments. (B) Comparison of growth curves of *C. glabrata* KUE100 (■,□), KUE100_*Δcggas1* (▲,Δ) and KUE100_*Δcggas1_Δcgtpo1_2* (♦,◊), in liquid BM, in the absence (open symbols) or presence of 90 mg/L clotrimazole (filled symbols), measured in terms of variation in OD_{600nm}. The displayed growth curves are representative of at least three independent experiments. (C) Time-course accumulation of clotrimazole in KUE100 (□), KUE100_*Δcggas1* (◊) and KUE100_*Δcggas1_Δcgtpo1_2* (Δ) strains, during cultivation in BM liquid medium in the presence of radiolabeled ^{3}H-clotrimazole. Accumulation values are the average of at least three independent experiments. Error bars represent the corresponding standard deviations. *p<0.05.

Figure 4.1 – Major functional groups found to have significant expression changes in the *C. glabrata* membrane-enriched proteome upon exposure to 5-flucytosine. Proteins with significant expression changes include Glucose metabolism (5 proteins), Mitochondrial function (5 proteins), Aminoacid/Nucleotide metabolism (3 proteins), Ribosome components and translation machinery (10 proteins), Lipid metabolism (3 proteins), Cell wall assembly (1 protein) and Multidrug resistance transporters (5 proteins).

Figure 4.2 – CgPdr1 confers resistance to flucytosine in *C. glabrata* cells. Comparison of the susceptibility to inhibitory concentrations of 5-flucytosine, clotrimazole and fluconazole, at the indicated concentrations, of the *C. glabrata* 66032u and 66032u_*Δcgpdr1* strains, in BM plates by spot assays. The inocula were prepared as described under "Materials and Methods". Cell suspensions used to prepare the spots were 1:5 (b) and 1:25 (c) dilutions of the cells suspension used in (a). The displayed images are representative of at least three independent experiments.

Figure 4.3 – CgFlr1 and CgFlr2 confer resistance to 5-flucytosine in *C. glabrata* cells. Comparison of the susceptibility to inhibitory concentrations of several chemical stress inducers, at the indicated concentrations, of the *C. glabrata* KUE100, KUE100_*Δcgflr1* and KUE100_*Δcgflr2* strains, in BM plates by spot assays. The inocula were prepared as described under "Materials and Methods". Cell suspensions used to prepare the spots were 1:5 (b) and 1:25 (c) dilutions of the cells suspension used in (a). The displayed images are representative of at least three independent experiments.

Figure 4.4 – CgFlr1 and CgFlr2 expression increases 5-flucytosine resistance in *C. glabrata* cells. Comparison of the susceptibility to inhibitory concentrations of several chemical stress inducers, at the indicated concentrations, of the *C. glabrata* L5U1 strain, harboring the pGREG576 cloning vector (v) or the pGREG576_MTI_*CgFLR1* or pGREG576_MTI_*CgFLR2* plasmids, in BM-U plates (50 μM $CuSO_4$ supplemented) by spot assays. The inocula were prepared as described under "Materials and Methods". Cell suspensions used to prepare the spots were 1:5 (b) and 1:25 (c) dilutions of the cells suspension used in (a). The displayed images are representative of at least three independent experiments.

Figure 4.5 – CgFlr1 and CgFlr2 confer resistance to antifungal drugs when heterologously expressed in *S. cerevisiae* cells. Comparison of the susceptibility to inhibitory concentrations of several chemical stress inducers, at the indicated concentrations, of the *S. cerevisiae* BY4741 and BY4741_*Δflr1* strains, harboring the pGREG576 cloning vector (v) or the pGREG576_*CgFLR1* of pGREG576_*CgFLR2* plasmids, in BM-U plates by spot assays. The inocula were prepared as described under "Materials and Methods". Cell suspensions used to prepare the spots were 1:5 (b) and 1:25 (c) dilutions of the cells suspension used in (a). The displayed images are representative of at least three independent experiments.

Figure 4.6 – CgFlr1 and CgFlr2 are plasma membrane proteins. Fluorescence of exponential phase BY4741 *S. cerevisiae* and L5U1 *C. glabrata* cells, harboring the expression plasmids pGREG576_*CgFLR1* and pGREG576_*CgFLR2* or pGREG576_MTI_*CgFLR1* and pGREG576_MTI_*CgFLR2*, after galactose or copper-induced recombinant protein production, respectively.

Figure 4.7 – CgFlr1 and GgFlr2 expression decreases the intracellular accumulation of ^{3}H-flucytosine. Time-course accumulation of radiolabeled ^{3}H-flucytosine in KUE100 wild-type (♦) and KUE100_*Δcgflr1* (■) (A) and KUE100 (♦) and KUE100_*Δcgflr2* (■) (B) strains, during cultivation in BM liquid medium in the presence of sub-lethal concentrations of unlabeled flucytosine. Accumulation values are the average of at least three independent experiments. Errors bars represent the corresponding standard deviations. *$p<0.05$.

Figure 4.8 – CgFlr2 expression decreases the intracellular accumulation of ^{3}H-clotrimazole. Time-course accumulation of radiolabeled ^{3}H-clotrimazole in KUE100 wild-type (♦) and KUE100_*Δcgflr2* (■) strains, during cultivation in BM liquid medium in the presence of sub-lethal concentrations of unlabeled clotrimazole. Accumulation values are the average of at least three independent experiments. Errors bars represent the corresponding standard deviations. ***$p<0.0001$.

Figure 4.9 – *CgFLR1* and *CgFLR2* transcriptional control. Comparison of the variation of the *CgFLR1* (A) and *CgFLR2* (B) transcript levels in the 66032u *C. glabrata* wild-type strain and in the derived 66032u_*Δcgpdr1* deletion mutant; and in the 84u *C. glabrata* wild-type strain and in the derived 84u_*Δcgyap1* deletion mutant, before and after 1h of exposure to 60 mg/L clotrimazole, 80 mg/L fluconazole, 8 mg/L flucytosine and 20 mg/L mancozeb. The presented transcript levels were obtained by quantitative RT-PCR and are relative *CgFLR1/CgACT1* or *CgFLR2/CgACT1* mRNA, relative to the values registered in the 66032u or 84u parental strains in control conditions. The indicated values are averages of at least three independent experiments. Error bars represent the corresponding standard deviations. *$p<0.05$; **$p<0.01$.

Figure 5.1 – *CgRPN4* confers resistance to fluconazole in *C. glabrata*. (A) Comparison of the susceptibility to azole antifungals, at the indicated concentrations, of the KUE100 and KUE100_Δ*cgrpn4 C. glabrata* strains, in BM agar plates, by spot assays. (B) Comparison of the susceptibility to azole antifungals, at the indicated concentrations, of the L5U1 *C. glabrata* strain harboring the pGREG576 cloning vector (v) or the pGREG576_MTI_*CgRPN4* in BM-U agar plates supplemented with 50 μM $CuSO_4$, by spot assays. The inocula were prepared as described in the materials and methods section. Cell suspensions used to prepare the spots were 1:5 (b) and 1:25(c) dilutions of the cell suspensions used in (a). The displayed images are representative of at least three independent experiments.

Figure 5.2 – *CgRPN4* regulated functional groups. Differentially expressed genes in exponential-phase KUE100_Δ*cgrpn4 C. glabrata* cells, comparing to KUE100 cells, after 1h fluconazole exposure. (A) CgRpn4-activated genes (downregulated in the mutant strain). (B) CgRpn4-repressed genes (upregulated in the mutant strain).

Figure 5.3 – Comparison of ergosterol and heme related genes expression patterns in wild-type and Δ*cgrpn4* cells upon fluconazole stress. Expression profiles of differentially expressed *ERG* and *HEM* genes in at least one dataset. *C. glabrata* genes names are shown. In cases were no gene name has been assigned, the designation of their *S. cerevisiae* homolog is shown.

Figure 5.4 – CgRpn4 increases its relative distribution to the nucleus upon fluconazole stress. Assessment of the subcellular localization of fluorescence in exponential-phase L5U1 *C. glabrata* cells harboring the pGREG576_MTI_*CgRPN4* plasmid after 5h of recombinant protein production in control conditions or after 1h fluconazole exposure. (A) Representative images of CgRpn4_GFP localization in L5U1 *C. glabrata* cells. (B) Results are shown in the percentage of cells showing nuclear localization of the CgRpn4_GFP fusion protein. Error bars represent the corresponding standard deviation. **$p<0.01$.

Figure 5.5 – CgRpn4 regulates ergosterol levels in *C. glabrata* cells during fluconazole stress, affecting permeability and drug accumulation. (A) KUE100 and KUE100_Δ*cgrpn4 C. glabrata* cells were harvested after 15h of growth in YPD medium (control) or after 3h or 6h fluconazole stress. Ergosterol was extracted and quantified through HPLC. Cholesterol was used as an internal standard to evaluate yield of the ergosterol extraction. The displayed ergosterol content is representative of at least six independent experiments. Error bars represent the correspondent standard deviations. (B) Comparison of plasma membrane permeability of exponential-phase KUE100 (squares), KUE100_Δ*cgrpn4* (diamonds) in control conditions or upon 1h fluconazole stress. The estimation of plasma membrane permeability is based on the fluorescence intensity values exhibited by yeast cells upon passive accumulation of propidium iodide. Error bars represent the corresponding standard deviation. (C) Time-course accumulation of radiolabeled ^{3}H-fluconazole in strains KUE100 (squares) and KUE100_Δ*cgrpn4* (diamonds), during cultivation in liquid BM in the presence of 150 mg/L unlabeled fluconazole. Accumulation values are the average of at least three independent experiments. Error bars represent the corresponding standard deviations. *p<0.05, **p<0.01, ***p<0.001, ****p<0.0001.

Figure 5.6 – Overrepresented sequences in the promoters of CgRpn4-activated genes and possible CgRpn4 recognition sequence. (A) Motifs found to be overrepresented in the promoters of CgRpn4-activated genes, as found by the DREME tool. Sequences located upstream (-1000 to -1 bp) of the genes found to be activated by CgRpn4 were retrieved from PathoYeastract and submitted to DREME. The prediction was made with default parameters. The sequences shown correspond to the motifs outputted by DREME, excluding TATA-box motifs. (B) The putative CgRpn4 recognition sequence in the promoter of *CgERG11* is in the complementary strand. The numbers refer to the position of the consensus site relative to the first ATG of the coding region. The wild-type sequence is shown underlined below the box, with asterisks denoting the base substitutions generated by site-directed mutagenesis. Below the resulting mutated sequence is shown. (C) Comparison of the variation of lacZ transcript levels determined by RT-PCR in L5U1 cells harboring the pYEP354_*CgERG11*prom_lacZ or pYEP354_mut_*CgERG11*prom_lacZ plasmids in control conditions or after 1h fluconazole exposure. Transcript levels of *CgRDN25* were used for normalization. Expression values are the average of at least three independent experiments. Error bars represent the corresponding standard deviations. **p<0.01, ***p<0.001.

Figure 6.1 – *CgMAR1* confers resistance to fluconazole in *C. glabrata*. (A) Comparison of the susceptibility to azole antifungals, at the indicated concentrations, of the KUE100 and KUE100_Δ*cgmar1 C. glabrata* strains, in BM agar plates, by spot assays. (B) Comparison of the susceptibility to azole antifungals, at the indicated concentrations, of the L5U1 *C. glabrata* strain harboring the pGREG576 cloning vector (v) or the pGREG576_PDC1_*CgMAR1* in BM-U agar plates, by spot assays.

Figure 6.2 – CgMar1 is activated upon fluconazole stress. Fluorescence of exponential-phase L5U1 *C. glabrata* cells harboring the pGREG576_PDC1_*CgMAR1* plasmid after 5h of recombinant protein production in control conditions (A) or after 1h fluconazole exposure (B), respectively.

Figure 6.3 – *CgMAR1* regulated genes in response to fluconazole stress. Differentially expressed genes in exponential-phase KUE100_Δ*cgmar1 C. glabrata* cells, comparing to KUE100 cells, after 1h fluconazole exposure. (A) CgMar1-activated genes (downregulated in the mutant strain). (B) CgMar1-repressed genes (upregulated in the mutant strain).

Figure 6.4 – CgMar1 and CgRbs1-dependent localization of NBD-DHS in *C. glabrata* cells. Comparison of 5 µM NBD-dihydrosphingosine (NBD-DHS) subcellular localization in *C. glabrata*, after 30 minutes incubation, in (A) KUE100 *C. glabrata* cells or (B) in KUE100_Δ*cgrsb1* cells or (C) KUE100_Δ*cgmar1* cells.

Figure 6.5 – CgMar1 and CgRsb1 regulate plasma membrane permeability and fluconazole accumulation in *C. glabrata* cells. (A) Comparison of plasma membrane permeability of exponential-phase KUE100 (squares), KUE100_Δ*cgmar1* (diamonds) or KU100_Δ*cgrsb1* (triangles) in control conditions or upon 1h fluconazole stress. The estimation of plasma membrane permeability is based on the fluorescence intensity values exhibited by yeast cells upon passive accumulation of propidium iodide. Error bars represent the corresponding standard deviation. (B) Time-course accumulation of radiolabeled ^{3}H-fluconazole in strains KUE100 (diamonds) and KUE100_Δ*cgmar1* (squares) or (C) KUE100 (diamonds) and KUE100_Δ*cgrsb1* (squares), during cultivation in BM liquid medium in the presence of 150 mg/L unlabeled fluconazole. Accumulation values are the average of at least three independent experiments. Error bars represent the corresponding standard deviations. *p<0.05, **p<0.01, ***p<0.001, ****p<0.0001.

Figure 6.6 – Overrepresented sequences in the promoters of CgMar1-activated genes. Motifs found to be overrepresented in the promoters of CgMar1-activated genes, as found by the DREME tool. Sequences located upstream (-1000 to -1 bp) of the genes found to be activated by CgMar1 were retrieved from PathoYeastract and submitted to DREME. The prediction was made with default parameters. The sequences shown correspond to the motifs outputted by DREME, excluding TATA-box motifs.

Figure 7.1 – Proposed model for the knowledge gathered in this thesis work on new regulators and effectors involved in azole and flucytosine resistance, integrated with known resistance mechanisms in *C. glabrata*. Red inverted triangles represent novel genes or mechanisms identified in this thesis. [1] Sanglard *et al.* AAC 43:2753-2765, 1999.; [2] Miyazaki *et al.* AAC 42(7):1695-701, 1998.; [3] Torelli *et al.* Mol Microbiol 68:186-201, 2008.; [4] Costa *et al.* AAC 57(7):3159-67, 2013.; [5] Costa *et al.* Front Microbiol 4:170, 2013.; [6] Costa *et al.* JAC 69:1767-76, 2014.; [7] Pais *et al.* MCP 15(1):57-72, 2016.; [8] Pais *et al.* Front Microbiol 7:2045, 2016.; [9] Costa *et al.* PLoS One 10(8):e0135110, 2015.

Figure 7.2 – Comprehensive regulatory network of the MDR transporters identified in this thesis as antifungal resistance determinants. The presented associations were drawn using the tools available at the PathoYeastract database.

Figure S4.1 – CgFlr1 and CgFlr2 are expressed in *C. glabrata* cells harboring the pGREG576_MT1_*CgFLR1* and the pGREG576_MT1_*CgFLR2* plasmids. Comparison of the level of expression of CgFlr1-GFP or CgFlr2-GFP fusion proteins in L5U1 *C. glabrata* cells upon exposure to the indicated CuSO4 concentrations, based on anti-GFP immuno-detection. Cells harboring the pGREG576 cloning vector (control), exposed to the same CuSO4 concentrations were used as a negative control.

List of Tables

The following supplementary tables are available at:
https://docs.google.com/spreadsheets/d/1V_n1mfdNbAQRiwKL70LvbRn8R2M8EIX-dzwetBfiqA0/edit?usp=sharing

List of Acronyms

2,4-D	2,4-Dichlorophenoxyacetic Acid
4-NQO	4-nitroquinoline-N-oxide
5-FC	5-flucytosine
5-FOA	5-fluoroorotic Acid
5-FU	5-fluorouracil
5-FUMP	5-fluorouridine Monophosphate
5-FdUMP	5-fluorodeoxyuridine Monophosphate
ABC	ATP-Binding Cassette
ATP	Adenosine Triphosphate
bHLH	Basic Helix-Loop-Helix
BLASTp	Basic Local Alignment Search Tool protein
BM	Basal Medium
BSI	Blood Stream Infection
cDNA	Complementary DNA
CDR	Candida Drug Resistance
CGD	Candida Genome Database
ChIP	Chromatin Immuno Precipitation
ChIP-seq	Chromatin Immuno Precipitation-sequencing
CWI	Cell Wall Integrity
DHA	Drug:H^+ Antiporter
DMCDD	Dimethylcholesta-8,24(28)-dien-3β,6α-diol
DMSO	Dimethyl Sulfoxide
DNA	Deoxyribonucleic Acid
DRE	Drug Response Element
DREME	Discriminative Regular Expression Motif Elicitation
dTTP	Deoxythymidine Triphosphate
dUTP	Deoxyuridine Triphosphate
EMSA	Electrophoretic Mobility Shift Assay
ER	Endoplasmic Reticulum
GFP	Green Fluorescent Protein
GO	Gene Ontology
GOF	Gain-of-Function
GPI	GlicosylPhosphatidylInositol
HACS	High Affinity Ca^{2+} uptake System
HPLC	High-Performance Liquid Chromatography
iTRAQ-MS	Isobaric Tag for Relative and Absolute Quantitation – Mass Spectroscopy
MCPA	2-Methyl-4-ChloroPhenoxyacetic Acid
MDR	MultiDrug Resistance
MFS	Major Facilitator Superfamily
MIC	Minimum Inhibitory Concentration

MIPC	Mannosyl-inositol Phosphorylceramide
MMTS	Methyl Methane Thiosulfonate
mRNA	Messenger RNA
MRP	Multidrug Resistance Protein
NBD	Nucleotide-Binding Domain
NBD-DHS	7-nitrobenz-2-oxa-1,3-diazol-4-yl-dihydrosphingosine
NGS	Next Generation Sequencing
OD_{600nm}	Optical Density at 600nm
ORF	Open Reading Frame
OSR	Oxidative Stress Resistance
PathoYeastract	Pathogenic Yeast Search for Transcriptional Regulators And Consensus Tracking
PBS	Phosphate Buffered Saline
PCR	Polymerase Chain Reaction
PDR	Pleiotropic Drug Resistance
PDRE	Pleiotropic Drug Response Element
PI	Propidium Iodide
PKC	Protein Kinase C
PMSF	PhenylMethylSulfonyl Fluoride
RNA	Ribonucleic Acid
RNA-seq	RNA sequencing
ROS	Reactive Oxygen Species
rpm	Rotations per Minute
RSAT	Regulatory Sequence Analysis Tool
RT-PCR	Real Time–PCR
SPM	Spermine
SPMD	Spermidine
SREBP	Sterol Regulatory-element Binding Protein
TCEP	Tris(2-CarboxyEthyl)Phosphine
TEAB	TetraEthylAmmonium Bromide
TF	Transcription Factor
TM	Trizma base-MES hydrate
TMD	Transmembrane Domain
TOM	Translocase of Outer Membrane
TRANSFAC	Transcription Factor database
UDP	Uridine Diphosphate
UMP	Uridine Monophosphate
UPR	Unfolded Protein Response
UTP	Uridine Triphosphate
WT	Wild-type
YEASTRACT	Yeast Search for Transcriptional Regulators And Consensus Tracking
YPD	Yeast extract-Peptone-Dextrose
YPED	Yale Protein Expression Database

αHPC	α-hydroxyphytoceramide

1 General Introduction

Excerpts of this chapter are based on review articles/book chapter published by the candidate on the context of this thesis.

Most of Section 1.3 corresponds to published work on the book chapter:

Pais, P., Galocha, M., Teixeira, M.C. 2019. Genome-wide response to drugs and stress in the pathogenic yeast *Candida glabrata*. Chapter In: Yeasts in Biotechnology and Human Health (Isabel Sá-Correia, Ed.), Springer, *Prog Mol Subcell Biol*, **58:**155-193.

Most of Section 1.5 corresponds to published work on the review paper:

Pais, P., Costa, C., Cavalheiro, M., Romão, D., Teixeira, M.C. 2016. Transcriptional control of drug resistance, virulence and immune system evasion in pathogenic fungi: a cross-species comparison. *Front Cell Infect Microbiol*, **6:** 131.

Both beforementioned sections, as well as other portions of this chapter, are also based on the published review paper:

Pais, P., Galocha, M., Viana, R., Cavalheiro, M., Pereira, D., Teixeira, M.C. 2019. Microevolution of the pathogenic yeasts *Candida albicans* and *Candida glabrata* during antifungal therapy and host infection. *Microb Cell*, **6:**142-159.

1.1 Thesis Outline

The acquisition of Multiple Drug Resistance (MDR), a phenomenon with serious consequences on the control of infections by fungal pathogens, depends often on the activity of transcription factors (TFs) that regulate the expression of drug efflux pumps from the ATP-Binding Cassette (ABC) and Major Facilitator Superfamily (MFS) families. The understanding of the global regulatory mechanisms that control the response to antifungal drugs is crucial to design suitable strategies to diagnose and eradicate persistent infections. The conjugation of computational and experimental tools seems to be the only suitable way to tackle this problem at a genomic scale. The work described in this thesis aims at increasing current understanding of gene expression regulation on response and resistance to antifungal drugs in the opportunistic pathogenic yeast *Candida glabrata*, the second most common cause of candidaemia, frequently displaying azole drug resistance and considered a good model for the study of pathogenesis and drug resistance in fungi.

The first chapter provides a literature review on current knowledge on the existing antifungal drug families and their modes of action. The efficiency of each antifungal class is evaluated, together with their known side-effects. A brief overview of the evolution and development of new generation drugs from these antifungal families is also analyzed. Special emphasis is given to the typical resistance mechanisms applied by *Candida* to overcome antifungal toxic effects. Current knowledge on regulatory networks that play a role in the development of antifungal resistance phenotypes is also reviewed. Due to the significance of azole antifungals in clinical practice, emphasis is given to the regulation of azole resistance mechanisms in pathogenic fungi in this chapter. This introductory chapter comprises several segments that have been published by the candidate, namely two review papers published in *Frontiers in Cellular and Infection Microbiology* [1] and *Microbial Cell* [2], as well as a book chapter published in *Yeasts in Biotechnology and Human Health*, Springer (Sá-Correia I, Ed.) [3].

In Chapter 2 the development of the PathoYeastract database, a bioinformatics resource to explore regulatory associations between transcription factors and target genes in *Candida* species, is described. Making use of the expertise and structure of the previously built YEASTRACT (www.yeastract.com) [4–8], Chapter 2 describes the development of the PathoYeastract database, which contains, upon expert curation by

the iBB-IST team, all published information on transcriptional regulation in the four most prevalent *Candida* species: *C. albicans*, *C. glabrata*, *C. parapsilosis* and *C. tropicalis*. This approach allows the prediction of genomic regulation based on orthologous associations described in other yeast species, enabling a comparative genomics setup. Chapter 2 also details the features of PathoYeastract and how its bioinformatics tools can be used to execute comprehensive evaluations based on regulation of genome-wide transcriptional responses, experimental conditions and promoter analysis. The work described in this chapter has been published in *Nucleic Acids Research* [9]. The role of the PhD candidate, as second author of this paper, was the collection and curation of all available data, as well as the design of some of the newly developed comparative genomics tools.

In Chapter 3 the role of the TF CgPdr1, the master regulator of azole resistance, in the membrane proteome response of *C. glabrata* to clotrimazole stress is studied. This chapter arises from the relative lack of studies addressing proteomics response to antifungal drugs. The membrane proteome is a promising target to study antifungal response, given the dependence of *C. glabrata* on membrane MDR transporters as major effectors of antifungal resistance. Given that most studies addressing azole resistance use fluconazole as a model drug, the work presented in chapter 3 also aimed at getting more knowledge into the conservation of azole resistance mechanisms among imidazoles, such as clotrimazole. This chapter details the use of iTRAQ-MS to probe changes in membrane protein abundance during clotrimazole-challenged *C. glabrata* and the role of CgPdr1 in this response. This approach enabled the characterization of the role of the MFS transporters CgTpo1_1 and CgTpo1_2 in mediating clotrimazole resistance. The role of each transporter is examined by susceptibility profiling of the corresponding deletion mutants to a wide range of antifungal agents and their role in clotrimazole resistance associated with a decreased drug accumulation in *C. glabrata* cells. Chapter 3 also elucidates a role for cell wall remodeling, via CgGas1, in clotrimazole stress resistance. The results described in this chapter have been published in *Molecular and Cellular Proteomics* [10].

In Chapter 4 the membrane proteome response of *C. glabrata* to 5-flucytosine stress is described. This chapter arises from the finding that CgPdr1 is involved in 5-flucytosine resistance and that 5-flucytosine is used in combination therapy with azoles. The work detailed in this chapter was performed concurrently with the one described in Chapter 3,

following the same structure as the previous chapter to detail changes in the membrane proteome of 5-flucytosine-challenged cells, together with the role of CgPdr1 in such changes. This approach enabled the characterization of the role of the MFS transporters CgFlr1 and CgFlr2 in mediating 5-flucytosine resistance. The role of each transporter is examined by susceptibility profiling of the corresponding deletion mutants to a wide range of antifungal agents and their role in 5-flucytosine resistance associated with a decreased drug accumulation in *C. glabrata* cells. Chapter 4 also demonstrates differential transcriptional regulation of *CgFLR1* and *CgFLR2* genes by the TFs CgPdr1 and CgYap1 in distinct environmental conditions. The results described in this chapter have been published in *Frontiers in Microbiology* [11].

Chapter 5 focuses on a new transcriptional regulatory pathway activated during fluconazole stress in *C. glabrata*, controlled by the TF CgRpn4. CgRpn4 is characterized as a new determinant of azole resistance. Its role in this context was evaluated through RNA-seq-based transcriptomics. Global data analysis described in this chapter, and the following, was supported by a 6-month stay of the PhD candidate in Geraldine Butler's Lab, UCD, Ireland, to whom acknowledgments are specifically addressed. The identification of CgRpn4 targets, activated under fluconazole stress, enabled the identification of CgRpn4 as a regulator of ergosterol biosynthesis. A link between this pathway, membrane permeability and fluconazole accumulation mediated by CgRpn4 is described in this chapter. The results presented in this chapter have been submitted for publication.

Chapter 6 details work performed concurrently with that present in Chapter 5 in the elucidation of new transcriptional networks governing azole resistance. This chapter describes the role of the TF CgMar1 during fluconazole stress in *C. glabrata*, based on the characterization of the CgMar1 regulon through RNA-seq transcriptomics. Based on these results, a role for CgMar1 in the incorporation of sphingolipids in the plasma membrane, shown to affect membrane permeability via its target gene *CgRSB1* is established. This work adds new light into the complex regulation of plasma membrane homeostasis and its potential to influence azole susceptibility in *C. glabrata*. The results presented in this chapter are included in a manuscript in preparation.

Chapter 1

Chapter 7 provides a final discussion where all the obtained results are integrated. The major contributions of this thesis to the advance of knowledge in its field are highlighted. Future perspectives and open avenues are also discussed in terms of potential impact and applications, while setting the steps of what is believed to be the crucial aspects that should be addressed in the next few years in the field of drug resistance in *C. glabrata*.

1.2 Infections by Fungal Pathogens: Emergence of *Candida glabrata*

The prevalence of fungal infections in the clinical setting has been increasing in the last decades and is now recognized as a major public health problem worldwide [12]. The rise in difficult to treat infections by pathogenic fungi is mainly associated with less effective treatment options, supported by the development of antifungal resistance phenotypes. *Aspergillus*, *Cryptococcus*, and *Candida* species constitute the most relevant human fungal pathogens. Infections caused by these pathogens are especially severe in immunocompromised patients, particularly cancer patients, transplant recipients and HIV-infected patients [13–15]. Aspergillus fumigatus is responsible for pulmonary diseases [16], while *Cryptococcus neoformans* causes central nervous system conditions such as meningitis or meningoencephalitis [17]. *Candida albicans* and *Candida glabrata* are the most prevalent *Candida* species, followed by *Candida parapsilosis* and *Candida tropicalis*, being responsible for more than 400,000 life-threatening infections worldwide every year and persistent mucosal infections [18].

Candida species are commensal yeasts that asymptomatically colonize the gastrointestinal and vaginal tracts in healthy individuals but act as opportunistic pathogens in immunocompromised patients [13]. Often, they cause localized superficial infections (candidiasis), most commonly in the vaginal, oral tracts or skin. In worst case scenarios, *Candida* infections can reach the bloodstream and cause disseminated infections (candidemia) with quite high mortality rates [19,20]. Besides immunocompromised patients, additional risk factors for disseminated infections include long-term hospitalization or the use of invasive medical technologies, such as intravascular catheters [21].

Infections caused by *Candida* species are recognized as the 4th most common cause of hospital acquired bloodstream infections in the USA [18,22,23], *C. glabrata* being the second most common cause of candidemia after *C. albicans* [22,24]. Although *C. albicans* remains the predominant causative agent of all forms of candidiasis, candidemia epidemiology has changed in the past few decades. This change is characterized by a shift in species distribution, from a preponderance of *C. albicans* to more frequent isolation of less drug-susceptible *Candida* species such as *C. glabrata*, which now represents 15–30% of these infections in humans [25]. The increase in *C.*

glabrata prevalence has been associated with its ability to resist antifungal therapy [26,27]. Indeed, *C. glabrata* clinical isolates display either intrinsic resistance to azole antifungals or an unusual ability to rapidly acquire resistance during antifungal treatment, which limits their clinical effectiveness [28].

C. glabrata is a haploid ascomycete yeast, closely related to the model *Saccharomyces cerevisiae*, both belonging to the whole genome duplication clade (Figure 1.1) [29,30]. It is phylogenetically, genetically and phenotypically distinct from *C. albicans* and other *Candida* species from the CTG clade [29,30], which reassigned the leucine CUG codons to serine [31,32]. The fact that *C. glabrata* displays high azole resistance makes it a good model to study antifungal resistance mechanisms in fungal pathogens. Moreover, the close phylogenetic relationship with the model *S. cerevisiae* suggests that the huge amount of information gathered during decades of study might be easily transferred to *C. glabrata*.

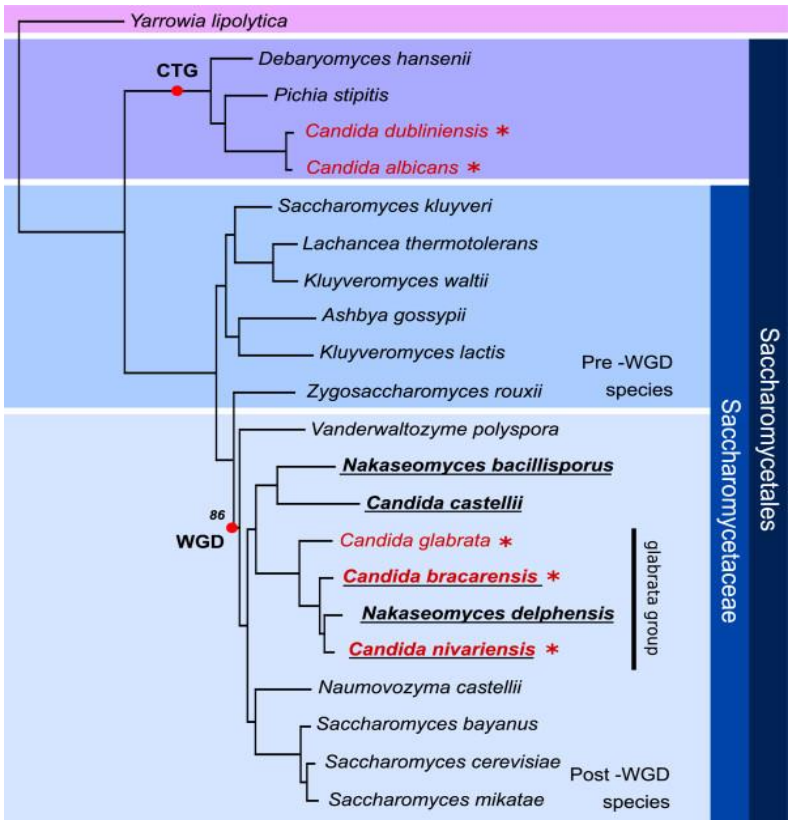

Figure 1.1 – Relationships of the *C. glabrata* species group. Underlined species were sequenced in the referred study. Pathogenic species are shown in red and are indicated with an asterisk. CTG, CTG clade; WGD, whole-genome duplication. From Gabaldón *et al.* [30].

1.3 Antifungal Drugs and Resistance Mechanisms in *Candida* species

1.3.1 Azole mode of action

Azoles have been the most widely employed antifungal family, commonly used as prophylaxis and first-line drugs against most *Candida* species because of their safety profile and availability in both oral and intravenous formulations [33–36]. They exert their function through the impairment of ergosterol biosynthesis, leading to fungal growth inhibition. Azoles bind to and inhibit the activity of the cytochrome P450 lanosterol 14-α-sterol-demethylase, which is a key enzyme in the ergosterol biosynthesis pathway encoded by the *ERG11* gene in yeasts (*Candida* species and *C. neoformans*) and *cyp51A* and *cyp51B* in fungi (e.g., *A. fumigatus*) [37] (Figure 1.2). Ergosterol is the main sterol component in fungal cell membranes and its depletion affects cell membrane resulting in defective structural properties, loss of fluidity and altered functions such as signaling, transport, exocytosis and endocytosis [37–39]. Inhibition of Erg11 activity leads to the accumulation of alternate and toxic sterol intermediates produced by Erg3, for instance lanosterol, 4,14α-dimethyl zymosterol and 14,24-dimethylcholesta-8,24(28)-dien-3β,6α-diol (DMCDD), leading to growth inhibition [37–39].

Azoles are five-membered heterocyclic synthetic compounds containing a nitrogen atom and at least one other non-carbon atom (e.g. nitrogen, sulphur, or oxygen) as part of the ring [40]. They can be divided into imidazole (clotrimazole, miconazole, thioconazole, econazole and ketoconazole) and triazole (fluconazole, itraconazole, voriconazole and posaconazole) subfamilies, as they have two or three nitrogen atoms in their azole ring, respectively. The imidazole class (particularly ketoconazole) was a tremendous breakthrough and quickly became the drug of choice for many fungal infections for nearly a decade. However, because of their limited spectrum of activity, high toxicity, severe side effects and numerous interactions with other drugs, they were replaced by the triazoles and are currently limited to the treatment of superficial mycosis [41]. The first-generation triazoles (fluconazole and itraconazole) were groundbreaking, exhibiting a broader antifungal activity spectrum as compared to imidazoles and having a significantly improved safety profile. However, both have clinical limitations such as their fungistatic nature instead of fungicidal, leading to

increased probability of resistance outbreaks. To solve this problem, second-generation triazoles (voriconazole and posaconazole) were developed. They are considered fungicidal and have a broad spectrum of activity [33]. Nevertheless, although being inactive against infections caused by filamentous fungi and having a narrower spectrum activity, the first-generation triazole fluconazole is still the most widely used drug in the treatment of *Candida* infections due to its favorable bioavailability and safety profile [42].

The fungistatic nature of azoles imposes strong directional selection for the evolution of resistance. Additionally, some *Candida* species, such as *C. glabrata*, are intrinsically less susceptible to this class of antifungal drugs. In fact, *C. glabrata* presents higher levels of intrinsic resistance to azoles than *C. albicans* and develops further resistance during prolonged azole therapy. Previous studies reported that the average fluconazole minimum inhibitory concentration (MIC) for *C. glabrata* is 32- fold higher than for *C. albicans* [43]. Accordingly, *C. glabrata* has risen dramatically in frequency as a significant cause of blood stream infection (BSI) since the introduction of azole drugs in the 1980s [43]. The increase in the prophylactic use of azoles for high-risk individuals contributed to the increasing development of *C. glabrata* resistance to these antifungal drugs, which are significantly effective in eradicating infections caused by other *Candida* species [44–46]. Moreover, these antifungals are inactive against biofilm-associated infections, which is a significant public health problem due to the increasing usage of medical devices [47].

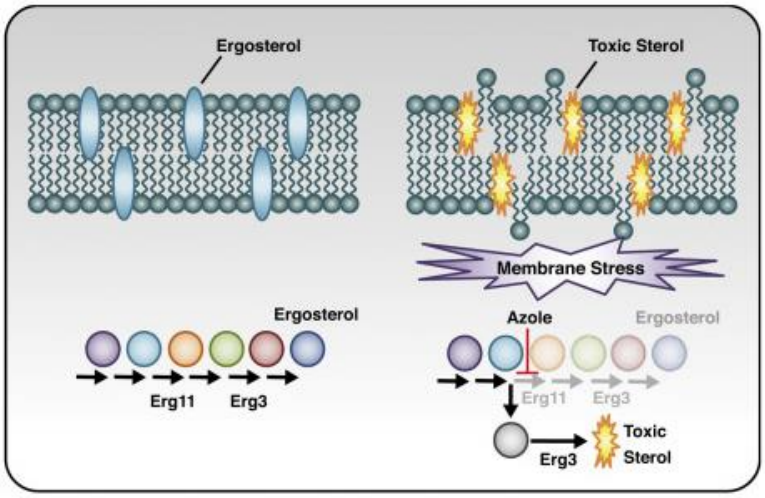

Figure 1.2 – Azole mode of action on ergosterol biosynthesis inhibition in fungal cells. Adapted from Revie *et al.* [37].

1.3.2 Azole resistance mechanisms

Azole resistance in *C. albicans* is mainly associated with the expression of multidrug resistance transporters, alterations in the azole target CaErg11 and inactivation of CaErg3 that synthetizes the toxic sterol DMCDD [48,49]. MDR transporters act as efflux pumps in the plasma membrane that catalyze the extrusion of azole drugs. In *C. albicans*, the ABC transporters CaCdr1 and CaCdr2, together with the MFS transporter CaMdr1, represent the major transporters involved in the development of azole resistance [50–54]. Generally, the upregulation of drug efflux pumps is the result from Gain-of-Function (GOF) mutations in genes encoding the regulators of their expression, namely *CaTAC1* and *CaMRR1* [55–60], or from increased copy number of the genes through genome rearrangements such as whole chromosome and segmental aneuploidies [61–63]. In turn, CaErg11 alterations involve mutations or upregulation of the *CaERG11* gene. Mutations result in loss of affinity between azole molecules and CaErg11 [64–66], while upregulation acts as a compensatory mechanism [67,68]. Moreover, it was recently demonstrated that *C. albicans* can also gain azole resistance by altering plasma membrane sphingolipid composition via upregulation of sphingolipid biosynthesis genes [69]. Additionally, *C. albicans* strains devoid of sphingolipid synthesis genes were found to accumulate more toxic sterol and displayed reduced ergosterol levels than the wild-type, indicating a direct correlation between both lipid classes [69].

In contrast to what is observed in *C. albicans* and despite the potential for *CgERG11* point mutations to have a greater impact in the haploid *C. glabrata*, several studies suggest that mutations in *CgERG11* are not relevant in clinical azole resistance in this pathogen [70–72]. The major described mechanism of acquired azole resistance in *C. glabrata* clinical isolates is the increased drug efflux due to the upregulation of drug efflux pumps [73–76]. This is generally caused by GOF mutations in the gene encoding the master regulator of azole resistance, *CgPDR1*. CgPdr1 is responsible for the upregulation of the efflux pumps CgCdr1, CgCdr2, CgSnq2 (ABC transporters) and CgQdr2 (MFS transporter), which directly confer most of the acquired azole resistance in this pathogen and, surprisingly, was also found to enhance virulence [70,76–78].

A high frequency of acquired azole resistance *in vitro* in *C. glabrata* populations has been linked to a loss of mitochondrial function, which leads to the upregulation of ABC

transporter genes [77,79]. In fact, this human pathogen can experience loss of mitochondrial DNA (mtDNA), and the drug-resistant mutants most commonly show mitochondrial dysfunction, which is also possible in *S. cerevisiae* [80–82]. This mitochondrial deficiency is called petite phenotype and corresponds to the absence of growth on non-fermentable carbon sources, deficient growth in media supplemented with glucose, reduced oxygen consumption and partial or total mtDNA deletion [83]. It was first proposed that the respiratory deficiency observed in the petite mutants could promote the exhibited azole resistance, since the biosynthesis of P-450-dependent 14α-sterol demethylase is stimulated by anaerobic conditions [79]. This phenotype is associated with CgPdr1 expression, as mitochondrial dysfunction was shown to increase the expression of *CgPDR1*, further exacerbated by a positive auto-regulatory loop that leads to *CgPDR1* and target gene overexpression [84,85]. In dysfunctional mitochondria, changes in the membrane association characteristics of the mitochondrial inner membrane protein CgPsd1 create a signal for activation of CgPdr1, leading to upregulation of genes encoding efflux pumps which mediate drug resistance and have additional roles in phospholipid homeostasis, as well as genes required for sphingolipid metabolism [86].

It was proposed that *C. glabrata* can switch between states of mitochondrial competence (azole-susceptible) and incompetence (azole-resistant) in response to azole exposure, probably through chromatin epigenetic modifications [81]. Until recently, clinical relevance of mitochondrial mutants was questionable in light of their decreased fitness. Nevertheless, Ferrari *et al.* found that an azole-resistant *C. glabrata* clinical isolate not only exhibited mitochondrial dysfunction and upregulation of *CgCDR1* and *CgCDR2*, but also was more virulent than its susceptible counterpart in both systemic and vaginal murine infection models [80]. This report demonstrated that mitochondrial dysfunction can confer selective advantage under host conditions. Although loss of mtDNA and associated drug resistance is relatively common in *C. glabrata in vitro* cultures, very few reports of clinical azole resistance are linked to mitochondrial dysfunction, and thus, the relevance of this mechanism in the clinic remains to be studied.

1.3.3 Polyene mode of action

Polyenes are macrocyclic organic molecules usually composed by a 20–40 carbon macrolactone ring conjugated with a d-mycosimine group and they were the first antifungal drugs applied to clinical use [87]. These compounds are fungicidal and have the broadest spectrum of activity compared to any other antifungal molecules. Nystatin, natamycin and amphotericin B, natural products isolated from the cultivation broths of *Streptomyces noursei*, *Streptomyces natalensis* and *Streptomyces nodosum*, respectively, are the only three polyenes in clinical use [88]. Nystatin and natamycin are only used as topical agents due to their low absorption in the gut and their high toxicity, while amphotericin B is the most used polyene for the treatment of systemic infections.

Due to their amphipathic structure, these antifungals attach to the external lipid layer and form complexes with ergosterol, generating pores on the cell membrane, which increases cell permeability, leakage of cytoplasmic contents and oxidative damage resulting in fungal cell death [89,90]. Additionally, merely the binding of amphotericin B to ergosterol was shown to kill yeast cells, with pore formation being a complementary mechanism [91]. A distinct mode of action for amphotericin B has also been proposed, based on the formation of extramembranous aggregates that extract ergosterol from lipid bilayers [92] (Figure 1.3). Polyenes have a lower but non-negligible affinity for cholesterol. This slight affinity for cholesterol explains the high toxicity associated with these antifungals and is responsible for numerous side effects [93]. Due to its hydrophobicity and poor absorption through the gastrointestinal tract, amphotericin B is administered intravenously which might cause adverse effects in kidneys and liver [93,94]. Despite the noteworthy disadvantages, for over 50 years amphotericin B is used for the treatment of life-threatening fungal infections in humans with minimal development of microbial resistance [92]. However, resistance toward this antifungal has been found in some clinical isolates, including *C. glabrata* [95–97].

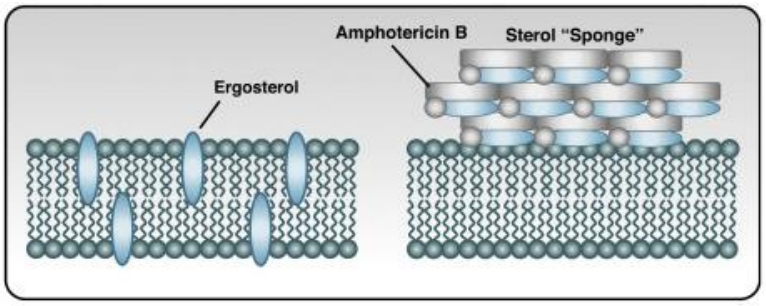

Figure 1.3 – Amphotericin B mode of action on ergosterol-polyene complex formation in fungal cells. Adapted from Revie *et al.* [37].

1.3.4 Polyene resistance mechanisms

The molecular mechanisms underlying polyene resistance are poorly documented, especially in pathogenic yeasts. It is thought that a decrease in the levels of ergosterol in the cell membrane is connected to the resistant phenotype [97,98]. Mutations in the *ERG6* gene, encoding an enzyme involved in late steps of ergosterol biosynthesis, have been found in polyene resistant clinical isolates, apparently leading to decreased ergosterol concentration in the plasma membrane and accumulation of late sterol intermediates [98,99]. Lower ergosterol concentration leads to decreased binding of amphotericin B, thus decreasing its toxic effect. It seems that *CgERG6* mutants of *C. glabrata* may be selected by the prophylactic or therapeutic use of amphotericin B [98]. Schwarzmüller and colleagues [25] generated a large-scale collection encompassing 619 *C. glabrata* mutants and found 13 amphotericin B sensitive mutants. The five mutants displaying the most pronounced susceptibilities lack genes that play diverse roles in phospho- and sphingolipid signaling, including *CgYPK1*, *CgCKA2*, *CgDEP1*, *CgSNF6* and *CgVPS15*. Additional determinants of amphotericin B resistance include *CgKRE1* and *CgSAC7*, which encode proteins implicated in glucan homeostasis, as well as *CgKTR6*, *CgKTR2*, *CgCWH41*, whose products affect surface protein glycosylation. Further studies are needed to understand the roles of cell wall, phospho- and sphingolipid metabolism as resistance mechanisms against amphotericin B in *C. glabrata*.

1.3.5 Echinocandin mode of action

Echinocandins are the only new class of antifungals to reach the clinic in decades, with three echinocandins currently available for clinical use: caspofungin, micafungin, and anidulafungin [45,49]. These antifungals target the fungal cell wall by disrupting glucan synthesis, the major component in *Candida* cell walls, through noncompetitive inhibition of the β-(1,3)-D-glucan synthase enzyme encoded by *FKS* genes [45,100] (Figure 1.4). The disruption of (1,3)-β-D-glucans impairs the structure of growing cell walls, resulting in loss of structural integrity, osmotic instability and cell death. Therefore, echinocandins have the advantage of exerting fungicidal effect, together with good safety profiles and low toxicity due to their unique target, that is absent in mammalian cells. Crucially, echinocandins have been shown to possess activity against *Candida* biofilms as the inhibition of polysaccharide production could lead to lysis and dissolution of the extracellular matrix [101,102]. This is an extremely important feature since biofilm-associated infections are hard to treat and are recurrent in patients with medical devices such as pacemakers or catheters. Considering all the advantages, the Infectious Diseases Society of America guidelines currently favor echinocandins as first-line treatment for systemic candidiasis in patients with moderate-to-severe infection and in those with prior exposure to azoles, with fluconazole held in reserve for the treatment of patients with less severe infection [103]. Moreover, the European Society of Clinical Microbiology and Infectious Diseases recommends echinocandins as first-line treatment for all patients with systemic candidiasis [104]. However, despite these advantages, the pharmacokinetic and stability properties of the currently approved echinocandins impose limitations on their use. Because of short half-lives and poor oral absorption, they were each developed for once-daily administration by intravenous infusion [105]. A novel echinocandin, rezafungin (CD101), is presently being developed as a once-weekly intravenous formulation for the treatment of candidemia and invasive candidiasis. Rezafungin has potent *in vitro* activity against *C. albicans* and *C. glabrata*, including azole- and echinocandin-resistant isolates [106]. The stability and solubility features of CD101 not only provide advantages for manufacturing and storage, but also enable expansion of echinocandin use to include weekly intravenous infusions and topical and subcutaneous forms [105].

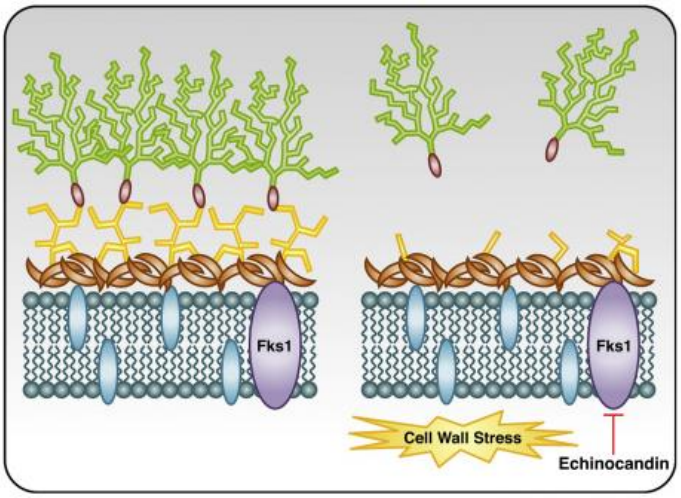

Figure 1.4 – Echinocandin mode of action on β-glucan synthesis inhibition in fungal cells. Adapted from Revie *et al.* [37].

1.3.6 Echinocandin resistance mechanisms

Generally, MICs of echinocandins are much lower than for amphotericin B and fluconazole against all *Candida* species [107] since most *Candida* have a low rate of echinocandin resistance [108]. Even so, *Candida* clinical isolates exhibiting reduced echinocandin susceptibility have been found over the past years [109–111], which is supported by mutations in the genes encoding the echinocandin target and reducing drug affinity. In *C. albicans*, this reduced susceptibility is strictly attributed to changes in the CaFks1 subunit of glucan synthase, the specific target of echinocandins. Indeed, genetically related isolates from the same patient with different mutations in *CaFKS1* were identified, suggesting that reduced susceptibility can evolve in the patient [110,112].

Some studies reported that echinocandin resistance is more common in *C. glabrata* compared to other species and that this rate can be attributed to the high potential of *C. glabrata* for developing resistance mutations [107,113]. In 2011, Costa-de-Oliveira *et al.* reported for the first time the *in vivo* acquisition of echinocandin resistance following anidulafungin therapy in a patient with *C. glabrata* invasive candidiasis, highlighting the need for antifungal susceptibility surveillance in patients under extended echinocandin therapy [111]. It has been reported that the reduced susceptibility to echinocandins is due to mutations in "hot-spot" regions of the *CgFKS1* and *CgFKS2* genes (but not *CgFKS3*), which encode subunits of the glucan synthase

enzyme [27,96,109,111,114,115]. Such mutations alter the kinetics of the target glucan synthase resulting in significantly higher MIC levels and inhibition constant [116]. Although echinocandin resistance is systematically associated with point mutations in either *CgFKS1* or *CgFKS2* genes [27,117–119], cell wall integrity signaling mediated via protein kinase C (PKC), the protein phosphatase calcineurin, and the molecular chaperone CgHsp90 are vital in enabling echinocandin drug tolerance and compensatory mechanisms such as upregulation of chitin synthesis [27,120,121]. Interestingly, it was seen that CgHsp90 and calcineurin regulate echinocandin resistance by controlling expression of *CgFKS2*, providing another mechanism via which CgHsp90 and calcineurin contribute to echinocandin resistance in *C. glabrata* [27].

A systematic phenotypic study [25] identified 48 *C. glabrata* mutants with altered caspofungin susceptibilities, 38 of which were strongly hypersensitive while another 10 were mildly sensitive. Remarkably, the group of genes found to affect caspofungin sensitivity included several genes playing a role in the PKC cell integrity signaling pathway, calcium/calcineurin signaling, general cell wall homeostasis, including mannosylation and glycosylation, as well as transcriptional regulators. Deletion of several genes encoding components of the chromatin and histone modification machinery also modulated caspofungin susceptibility, suggesting an important regulatory role for chromatin in controlling surface homeostasis and caspofungin susceptibility. Hyperresistance to echinocandins can result from mutations in glucan synthase genes as well as through the PKC pathway that mediates caspofungin tolerance in the phylogenetically close yeast *S. cerevisiae* and in *C. albicans* [122,123]. Accordingly, *C. glabrata Δwsc1, Δslt2, Δmkk1, Δbck1, Δrlm1* and *Δfks1* mutants, all lacking key genes of this central pathway, were found to be hypersensitive to caspofungin. Another study [124] also applied a global screening approach to identify caspofungin resistance genes in *C. glabrata*. These include some controlling the cell-wall integrity (CWI) pathway (*CgMKK1*, *CgCNA1* and *CgSLT2*) [125,126], reinforcing the idea that chemical modulators of the CWI pathway may increase the efficacy of caspofungin. Interestingly, it has been reported that *S. cerevisiae* strains with deletions of CWI pathway genes *ScBCK1* and *ScSLT2* are sensitive to the anti-malarial drug chloroquine, and that chloroquine and caspofungin show a synergistic effect in *S. cerevisiae, C. albicans* and in *C. glabrata* [127]. Moreover, inhibition of Ca^{2+} influx via high affinity Ca^{2+} uptake system (HACS) complex may also increase the efficacy of

echinocandins. In both screens, the disruption of the HACS members *CCH1* and *MID1* was found to confer increased caspofungin susceptibility. Nevertheless, none of the commonly found genes in both screens are currently associated with clinical resistance.

1.3.7 Pyrimidine analogs mode of action

Pyrimidine analogs such as 5-flucytosine (5-FC) were first used to treat *Cryptococcus* and *Candida* infections in the 1960s [128]. 5-flucytosine is one of the oldest synthetic antimycotic compounds, first synthesized in 1957 as an anticancer drug [129]. These antifungals have fungistatic activity exerted through the interference with pyrimidine metabolism, 5-flucytosine being the most common. 5-flucytosine itself has no antifungal activity; its antimycotic activity results from the rapid conversion of 5-flucytosine into 5-fluorouracil (5-FU) within fungal cells [130,131]. 5-flucytosine is taken up by a cytosine permease, which is also the transport system for adenine, hypoxanthine and cytosine. These compounds competitively antagonize the uptake of 5-fucytosine [132]. Once inside the cells it is converted by cytosine deaminase to 5-FU which is transformed by UMP pyrophosphorylase into 5- fluorouridine monophosphate (5-FUMP). This compound is then phosphorylated and incorporated into RNA, resulting in inhibition of protein synthesis. 5-FU also undergoes conversion into 5-FdUMP (5-fluorodeoxyuridine monophosphate), a potent inhibitor of thymidylate synthase, that inhibits fungal DNA synthesis and nuclear division [133] (Figure 1.5). 5-flucytosine has the advantage of being selectively toxic to fungi as there is little or no cytosine deaminase activity in mammalian cells [134]. However, its use is limited as it displays significant adverse effects such as myelotoxicity and hepatotoxicity and should be used in combination with other antifungals as resistance rapidly develops with monotherapy [135,136]. 5-flucytosine is administered in combination with amphotericin B as the standard of care for cryptococcal meningitis, and the drug continues to have a role in the treatment of *Candida* infections which are life threatening [137].

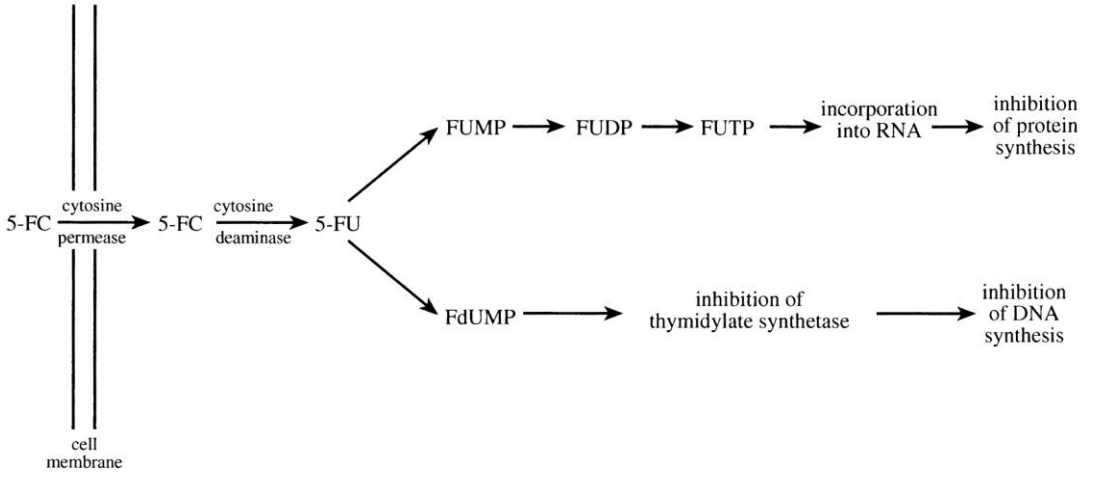

Figure 1.5 – Pathway of 5-FC conversion to 5-FU and its mode of action in inhibition of protein and DNA synthesis in fungal cells. Adapted from Vermes *et al.* [128].

1.3.8 Pyrimidine analogs resistance mechanisms

Whether it is innate in some fungal species or acquired in others, resistance to 5-flucytosine is a frequent phenomenon in pathogenic fungi. However, due to its complex mode of action, the molecular mechanisms leading to 5-flucytosine resistance have been poorly investigated. The most common mechanism of resistance to pyrimidine analogs is a point mutation in the *FUR1* gene, coding an uracil phosphoribosyltransferase [138]. In *C. albicans* and *C. glabrata*, decreased susceptibility to this drug has been related with point mutations in *FUR1* and also *FCY1/FCA1* (encoding a cytosine deaminase) that decrease the conversion of 5-flucytosine to 5-FU or 5-FUMP [137,139]. Moreover, mutations in *CgFCY2* (encoding a cytosine permease) that decrease drug uptake in *C. glabrata* [139] and overexpression of the thymidylate synthase encoded by *CgCDC21*, a key enzyme of DNA synthesis, may result in a 5-flucytosine-resistance phenotype [139]. *C. glabrata* also resorts to drug extrusion as a 5-flucytosine resistance mechanism, as *CgAQR1*, encoding a MFS transporter, and *CgFPS1* and *CgFPS2*, encoding aquaglyceroporins, contribute to decrease accumulation of flucytosine within *C. glabrata* cells [140,141].

1.4 Multidrug Resistance Phenomenon

The extensive use of azole antifungal drugs both as treatment and prophylaxis has led to a huge increase in the number of intrinsically resistant *Candida* infections. The frequency and relative high mortality levels (up to 45% for *C. glabrata*) of these infections are generally attributed to the capacity of these pathogenic yeasts to efficiently develop MDR [35,142].

MDR is a ubiquitous phenomenon causing several difficulties in the treatment of fungal infections. One of the most prominent MDR mechanisms is the expression of multidrug resistance transporters, responsible for the efflux of structurally and functionally unrelated compounds from the cytoplasm to the external medium [143,144]. These transporters allow the development of antifungal drug resistance and are generally associated with therapeutic failure [50,145]. MDR transporters belong mainly to two families: the ABC and the MFS. Both families are found across prokaryotes, eukaryotes and plants; involved in transport of substances across the plasma membrane, with physiological roles beyond drug transport [143].

The promiscuous nature of MDR transporters and their potential significance in most aspects of pathogenic fungi interaction with the human host has been recently reviewed [144]. These proteins can transport a variety of xenobiotics; including antifungals, anti-cancer molecules, antibiotics and herbicides are among known substrates. Although widely referred to as MDR transporters due to their ability to confer resistance to xenobiotics, these proteins possess physiological substrates; such as cations, carbohydrates or peptides; among others [146,147]. It is clear that MDR is a widespread phenomenon with clinical, agricultural and biotechnological implications, where MDR transporters that are presumably able to catalyze the efflux of multiple cytotoxic compounds play a key role in the acquisition of resistance [148]. Although the ability to transport multiple substrates has been well described, it is also possible that the accumulation of diverse compounds is an indirect consequence of the transport of their physiological substrates [144].

1.4.1 ABC transporters

The ABC transporters have four main domains, including two transmembrane domain (TMD) with six trans-membrane segments and two nucleotide-binding domain (NBD). In depth structural data of ABC transporters has been reviewed elsewhere [143]. Upon ATP binding to the NBD, energy resultant from ATP hydrolysis mediates a conformational change that allows primary transport of different molecules against an electrochemical gradient [149–151] (Figure 1.6). The best-studied families of fungal drug efflux pumps are those from the model *S. cerevisiae* [152]. In this model eukaryote, the ABC transporters have been classified into three main subfamilies, namely, the pleiotropic drug resistance (PDR), MDR, and multidrug resistance-associated protein (MRP), making up a total of 21 ABC drug resistance-related transporters [152,153]. ScPdr5 is a typical example of the potential for ABC transporters to confer resistance to a broad xenobiotic diversity [154–157], including fungicides, steroids and cations [153,158,159]. Genome sequencing has revealed that there is a wide repertoire of predicted ABC drug efflux pumps among pathogenic fungal species. Sequence similarity analysis predicted 28 ABC proteins in *C. albicans* [160]. The genome of *C. glabrata* is predicted to have approximately 18 ABC transporters [161]. Otherwise, much larger numbers of ABC proteins are predicted in the genomes of *A. fumigatus* and *C. neoformans.* The *A. fumigatus* genome is predicted to encode 49 ABC transporters, 35 of which are predicted to be multidrug efflux pumps [16,162]. *C. neoformans* genome is predicted to encode 54 ABC transporters [163].

Few ABC transporters have been functionally characterized in pathogenic fungi, including those that can be involved in multidrug resistance. However, those of which who have been characterized often own it to their relevance in clinical acquisition of antifungal resistance. Candida Drug Resistance (CDR) transporters are among the best studied ABC proteins in fungal pathogens due to their key role in mediating clinical azole antifungal resistance in *Candida* species. The transporters Cdr1 and Cdr2 are recognized as major effectors of azole resistance in both *C. albicans* and *C. glabrata*, as acquisition of azole resistance in clinical isolates is often associated with *CDR1/2* overexpression [50,59,74,164]. Moreover, *C. glabrata* Snq2 is yet another transporter with implications in clinical azole resistance [165]. The participation of ABC transporters in azole resistance has also been observed in other pathogenic fungi, as is the case of *A. fumigatus* AtrF and *C. neoformans* Afr1 [166,167]. Illustrating the broad

substrate specificity, other ABC transporters have been characterized in *C. albicans*, albeit participating in other stress responses and/or translocation of other molecules. This is the case of CaCdr4, which is induced as part of the core stress response to osmotic, oxidative and heavy metal stress and hypoxia [168,169] and CaYor1 involved in aureobasidin A resistance [170]. In *C. glabrata*, CgYor1 is putatively involved in azole resistance in *C. glabrata* [171], once more denoting the multidrug resistance potential of these proteins.

Some ABC proteins across yeast species play a role in controlling lipid composition of the plasma membrane. For example, CaCdr1, CaCdr2 and CaCdr3 are involved in phospholipid transport across the lipid bilayer that may help maintain plasma membrane asymmetry [172–174], as is the MFS transporter CgMdr1 [173]. The sterol transporter CgAus1 is involved in sterol scavenging in *C. glabrata*, another mechanism of azole resistance [175,176]. ScPdr5 is also involved in lipid translocation [152,177] and ScPdr18 has a role in plasma membrane sterol incorporation [178].

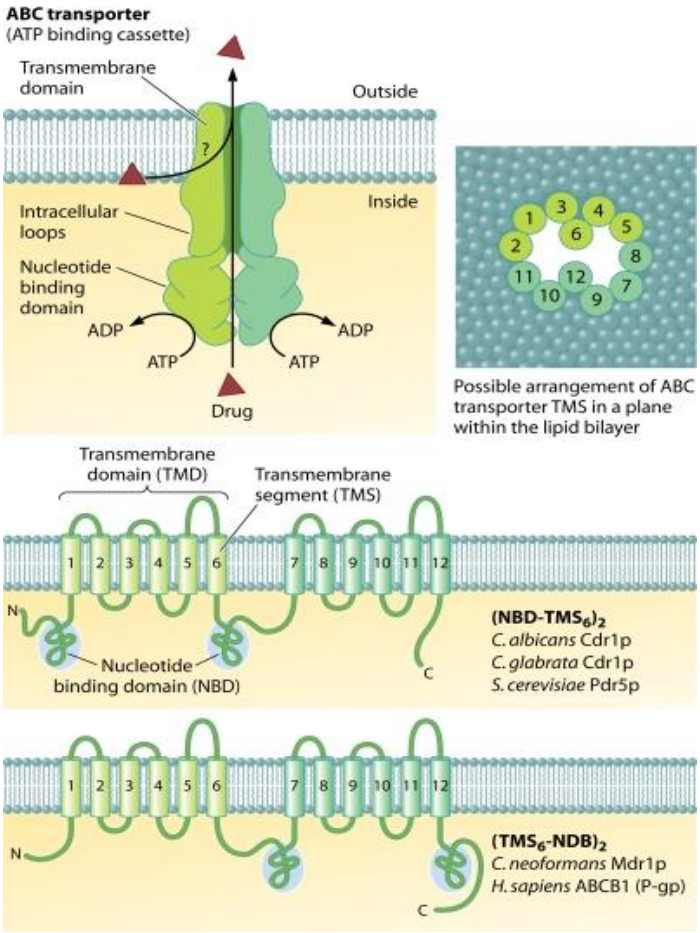

Figure 1.6 – Typical structure of ABC transporters in fungal species. From Cannon *et al.* [143].

1.4.2 MFS transporters

MFS pumps are secondary transporters that utilize the proton-motive force across the plasma membrane. Just has the ABC transporters, MFS proteins display high sequence similarity across plants, animals, bacteria and fungi. This superfamily constitutes the largest group of secondary active transporters, functioning as uniporters, symporters, or antiporters [147]. A subset of these transporters is involved in drug efflux [179]. In fungi, the MFS transporters involved in drug efflux are clustered into two subfamilies: the drug:H+ antiporter 1 (DHA1), including 12 transmembrane segment proteins, and the drug:H+ antiporter 2 (DHA2), including 14 transmembrane segment proteins [180,181] (Figure 1.7).

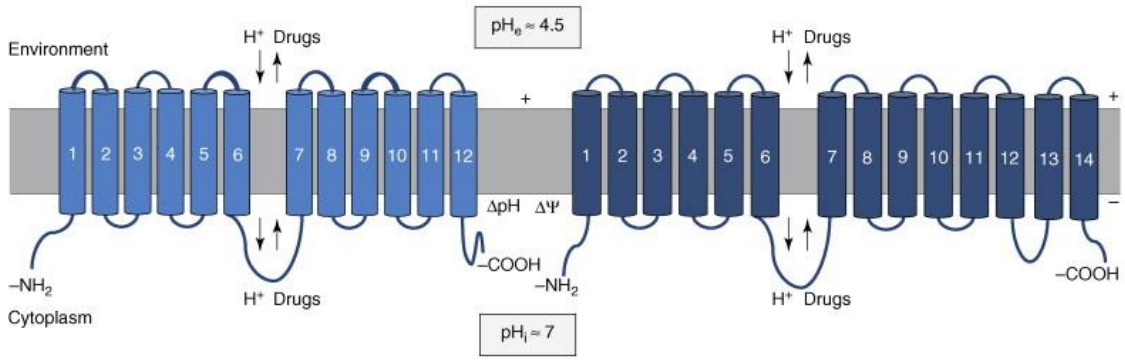

Figure 1.7 – Typical structure of MFS transporters from the DHA1 and DHA2 subfamilies in fungal species. From Sá-Correia *et al.* [182].

A total of 22 MFS drug transporters were reported in the genome of *S. cerevisiae* [183]. Based on phylogenetic analysis with *S. cerevisiae*, Costa *et al.* [183] listed the DHA-MFS transporters found to occur in *Candida* species, *A. fumigatus* and *C. neoformans*. Generally, the filamentous fungus *A. fumigatus* has much higher number of transporters, featuring 54 from the DHA1-MFS family and 32 from the DHA2-MFS family. From the yeasts, *C. neoformans* has much fewer transporters, featuring 9 from the DHA1-MFS family and 7 from the DHA2-MFS family. Within the DHA1-MFS family 18 and 10 transporters were predicted in the genomes of *C. albicans* and *C. glabrata*; while regarding the DHA2-MFS family, 8 and 5 were found as predicted transporters in their genomes.

While the role of ABC efflux pump proteins in the development of MDR is well documented, the role of MFS transporters which can also be implicated in clinical drug resistance has not received due attention. Once again, *C. albicans* MFS transporters were among the first to be characterized, such as the transporters encoded by *CaMDR1* and *CaFLU1*. CaMdr1 is a key transporter involved in clinical acquisition of azole resistance, as *CaMDR1* expression was associated with azole-resistant isolates [54,184–186]. CaMdr1 constitutes, together with CaCdr1 and CaCdr2, the trio of clinically relevant transporters in azole antifungal resistance in *C. albicans*. CaMdr1 overexpression confers resistance to cerulenin and brefeldin A in *C. albicans* [187] and benomyl and methotrexate resistance when heterologously expressed in *S. cerevisiae* [188], confirming its role in MDR. As for CaFlu1, it appears to only have a slight effect in azole resistance, but possibly a more prominent role in mycophenolic acid resistance [189,190]. Several MFS multidrug transporters have also been linked to MDR in *C. glabrata*. For example, azole resistance has been associated with the expression of the transporters CgQdr2 and CgTpo3 [75,76], while CgAqr1 and CgDtr1 have been linked primarily to acetic acid resistance and less significantly to antifungal agents (in the case of CgAqr1) [141,191]. While often overlooked compared with ABC transporters (namely CgCdr1 and CgCdr2), MFS pump genes *CgTPO1_1*, *CgTPO3*, *CgAQR1* and *CgQDR2* were shown to be upregulated in azole-resistant *C. glabrata* isolates. Moreover, the correlation between their expression and azole resistance was found to be similar to that of *CgCDR2*, suggesting that MFS drug transporters indeed have clinical relevance in antifungal resistance [145].

1.5 Transcriptional Regulation of Drug Resistance in *Candida*

MDR acquisition in clinical isolates is often related to the high expression levels of multidrug transporters, occurring as a consequence of point mutations in MDR-related transcription factors (TFs) [71]. Since the MDR phenotype can be seen as a long term genetic stabilization of the normally transient drug response [192], it is essential to understand the structure and functioning of the transcriptional networks regulating the early drug response in *Candida*, to be able to understand and circumvent the long term acquisition of drug resistance.

Considering the intrinsic variation regarding drug susceptibility among different *Candida* species and the increasing acquired resistance in several clinical isolates, it becomes evident that the genetic evolution underlying drug resistance phenomenon must continue to be investigated. Unveiling new potential targets is imperative to develop new suitable strategies to fight increasing *Candida*-associated infections and, although the nature of intrinsic resistance is unknown, the development of resistance can be studied.

Transcription factors are key players in the activation or repression of gene expression programs in response to environmental stimuli. TFs recognize specific sequences in the promoters of their target genes. For instance, CgPdr1 recognizes and binds Pleiotropic Drug Response Elements (PDREs) (TCCACCGA) to activate the expression of *CgCDR1* [85]. Regulation of gene expression is based on TF binding to target promoter regions, but there is a multitude of mechanisms that underscores TF action. A common mechanism is the interaction with co-activators or co-repressors that act as adjuvants for TF activity, from which the general repressor ScTup1 is one of the best characterized cases [193,194]. In some cases, TFs can regulate their own expression in autoregulation loops [195]. TF activity is frequently modulated by protein modifications. Typical cases involve phosphorylation in specific amino acid residues or structural changes among protein domains [196]. Such modifications will regulate TF activity to facilitate gene expression programs or can result in translocation to the nucleus as an activation mechanism. An archetype of structural changes and TF translocation is the well characterized activation of *S. cerevisiae* Yap1 by hydrogen peroxide [197,198]. Mutations in TF encoding genes, most of the times conferring TF hyperactivity, are also

commonly found to modulate target gene expression, as is well described in regulators of azole resistance in *Candida* species, such as CgPdr1 [78].

Transcriptional regulatory networks are made of intricated pathways that often control more than one cellular response. In yeast there are several well-defined cases of transcriptional regulators that participate in response to more than one environmental condition. The duo of general stress regulators ScMsn2/4 is a typical example, as these TFs are responsible for governing a series of biological processes to a wide variety of stress conditions [199,200]. Another hallmark is the overlap between pleiotropic drug resistance and other stresses, such as oxidative stress or metal stress, both centered on the regulon of ScYap1 [201,202]. The inherent complexity of transcriptional networks needs to be addressed in order to better understand adaptive mechanisms of stress response. The study of regulatory networks taking place in fungal pathogens opens new opportunities for therapeutic options, as the identification of these pathways will contribute to target specific fungal pathways in a more effective way than targeting individual effectors of drug resistance [1].

1.5.1 Regulation of MDR transporters

One of the major regulators of drug resistance in *C. glabrata* is the transcription factor CgPdr1. *C. glabrata* Pdr1 is a Zn(2)-Cys(6) DNA binding protein responsible for the activation of drug resistance genes, such as the multidrug resistance transporters CgCdr1 and CgCdr2 (also known as CgPdh1), via pleiotropic drug response elements (PDRE) [71,85,171]. Gain-of-Function (GOF) mutations in the *CgPDR1* gene have been found in clinical isolates to be responsible for increased CgPdr1 activity and consequent constitutive high expression of the ABC drug efflux pumps, as well as its positive autoregulation [78,84,85]. Although *C. glabrata* azole resistant isolates often exhibit *CgPDR1* GOF mutations, different mutations have been found to lead to various degrees of impact on CgPdr1 target genes, even if the mutations occur in the same domain of the protein [203]. For instance, strains with higher expression of *CgPDR1* seemed to always lead to higher expression levels of *CgCDR1*. On the other hand, the impact of *CgPDR1* GOF mutations on *CgCDR2* appeared to be much weaker when compared to *CgCDR1*. Moreover, not all *CgPDR1* GOF mutations lead to increased expression of *CgSQN2* [3]. Interestingly, Ferrari and co-workers [78] have

demonstrated that GOF mutations in *CgPDR1* also result in increased fitness and virulence. Additionally, the only two genes coordinately upregulated by all *CgPDR1* GOF mutations present in a set of resistant isolates were *CgCDR1* and *CgPUP1* (encoding a mitochondrial protein of unknown function). Since the increased virulence phenotype was observed for all *CgPDR1* GOF mutations, these genes are suspected to be involved. In fact, deletion of *CgCDR1* and *CgPUP1* in an azole resistant clinical isolate revealed that both genes were required for increased virulence [78]. Although typical regulatory targets of CgPdr1 include the ABC efflux pumps CgCdr1 and CgCdr2, it was also found to activate the expression of efflux pumps from the MFS family, including CgQdr2 and CgTpo3 [76,141]. Moreover, the main regulator of oxidative stress resistance, CgYap1, also regulates the expression of the MDR transporter CgFlr1, particularly in response to 4-nitroquinoline-N-oxide (4-NQO), benomyl and cadmium chloride [204]. However, there is no evidence to suggest regulation of CgFlr1 by CgYap1 in azole drug resistance [204].

Drug resistance regulation is a complex process that must be controlled according to the specific stress exerted over fungal pathogens, activating or repressing key pathways to better express the desired response. As such, a negative Zn(2)-Cys(6) regulator of azole resistance, the transcription factor CgStb5, was also addressed as a relevant regulator of drug resistance in *C. glabrata*. As a result of its negative regulation, CgStb5 overexpression leads to a higher susceptibility towards azole drugs, while its deletion causes a small increase in azole resistance [205]. Also, expression analysis showed that CgStb5 shares many transcriptional targets with CgPdr1, such as CgCdr1, CgCdr2 and CgYor1, but working as a pleiotropic drug resistance repressor [205]. Homologous proteins were identified in *C. parapsilosis* (uncharacterized, encoded by ORF CPAR2_109760) and in *C. albicans* (Stb5) in the phylome analysis. Additionally, the *C. tropicalis* protein encoded by ORF *CTRG_04421* was identified as a *C. glabrata* Stb5 homolog by BLASTp search. *C. albicans* Stb5 shares the Zn(2)-Cys(6) DNA binding domain found in *C. glabrata* Stb5, and despite the fact that its role and regulation mechanisms are still poorly characterized, it has been shown to be repressed by CaHap43 [206].

C. albicans has as its own master regulator of drug resistance CaTac1, a Zn(2)-Cys(6) DNA binding activator of drug-responsive genes such as the ABC multidrug resistance transporters CaCdr1 and CaCdr2 [207] by binding the Drug Response Element (DRE)

[208]. Onward with the transcriptional control of CaTac1 over CaCdr1 and CaCdr2 expression, changes in this transcription factor gene were described to modulate its function and consequently add an extra layer of regulation in its network. Several substitutions and small deletions were found to increase CaTac1 function [209], while chromosomal rearrangements in chromosome 5 lead to loss of heterozygosity resulting in CaTac1 dosage adjustments by overexpression of its encoding gene [62,209]. There is evidence supporting positive autoregulation of CaTac1 [210,211]. Altogether, evidence shows that *CaTAC1* controls its target genes by increasing its own expression or by GOF mutations [59,208,209]. Despite having similar functions and regulating similar gene targets, CaTac1 was not found to share sequence homology with *C. glabrata* Pdr1. Instead, CaTac1 presents high similarity with several uncharacterized proteins encoded by other CTG clade *Candida* spp. These include *C. parapsilosis* proteins encoded by ORFs CPAR2_303510, CPAR2_303520 and CPAR2_303500 and *C. tropicalis* proteins encoded by ORFs *CTRG_05307*, *CTRG_05306* and *CTRG_05308*. *C. albicans* carries yet another major regulator of multidrug resistance transporters in the form of the transcription factor CaMrr1, an activator of the MFS multidrug transporter CaMdr1, leading to acquisition of multidrug resistance in azole resistant clinical isolates [212]. As observed for *C. glabrata* Pdr1 and *C. albicans* Tac1 transcriptional regulators, CaMrr1 is a Zn(2)-Cys(6) transcription factor and its gene sequence of is subjected to GOF mutations responsible for increased protein activity [58]. As described above for CaTac1, CaMrr1 also appears to be autoregulated [213]. Additionally, it was found to be induced by Hap43 [206]. Additionally, the oxidative stress resistance regulator CaCap1 was found to be involved in drug resistance, as it regulates the expression of the multidrug transporter CaMdr1 [214]. Showing some level of functional conservation with the previous regulators is also the transcription factor CaMrr2, seen to control the expression of CaCdr1 in *C. albicans* [215]. CaMrr1 and CaMrr2 do not present significant homology to each other, but interestingly, in the search for CaMrr1 and CaMrr2 homologs, several common hits were identified in *Candida* species. Among them is a closely related *C. parapsilosis* Zn(2)-Cys(6) homolog (named CpMrr1) described to be upregulated in azole resistant strains, probably leading to the upregulation of *C. parapsilosis* Mdr1 [216]. Similarly to what is described in *C. albicans*, the upregulation of *C. parapsilosis* Mrr1 and Mdr1 is correlated with point mutations in the *CpMRR1* gene [216]. However, beyond these homologs, BLASTp analysis revealed an array of additional proteins that show some

similarity with CaMrr1 and CaMrr2. Interestingly, *C. parapsilosis* Mrr1 was also found to share sequence similarity with *C. albicans* Mrr2. Additionally, other regulators not primarily related to drug resistance display sequence similarity with CaMrr1 and CaMrr2, namely *C. albicans* Cta4 [217], a transcription factor involved in nitrosative stress resistance [218]. Nevertheless, it is relevant to point out that CaCta4 expression in *S. cerevisiae* was seen to contribute for azole drug resistance [217]. It is interesting to see that CaMrr1 and CaMrr2 display some level of similarity not only with other regulators (e.g. CaCta4), but also with several uncharacterized proteins, both in *C. albicans* and other *Candida* species.

1.5.2 Regulation of ergosterol biosynthesis

Resistance to azole drugs has often been attributed to the upregulation of ergosterol biosynthetic genes, given that these drugs act by inhibiting the activity of Erg11, thus leading to ergosterol depletion in the fungal plasma membrane [219–221]. In this context, the transcription factor CaUpc2 is an important player in azole drug resistance, being a transcriptional activator of ergosterol biosynthetic genes in *C. albicans*, but also of the MFS multidrug transporter encoding gene *CaMDR1* [48,56,58,169,222]. *C. albicans* Upc2 phylome analysis revealed a *C. parapsilosis* Upc2 homolog. In fact, *C. parapsilosis* Upc2 displays a conserved function, as it was described to confer resistance against azole drugs and to regulate the ergosterol pathway in hypoxia [223]. *C. glabrata* harbors two Upc2 regulators known to participate in the same process. *C. glabrata* Upc2A, but not Upc2B, displays the prominent role in the resistance against azoles and sterol biosynthesis inhibitors [224]. However, CgUpc2B was shown to regulate the expression of CgErg2 and CgErg3 from the ergosterol biosynthetic pathway, whereas both CgUpc2A and CgUpc2B are required for expression of the sterol transporter CgAus1 [224]. A predicted *C. tropicalis* Upc2 was also found to share significant sequence similarity with the rest of the Upc2 proteins. Interestingly, despite the further phylogenetic distance, both *C. albicans* and *S. cerevisiae* contain a Upc2 paralog, Ecm22; while *C. glabrata* harbors CgUpc2A and CgUpc2B. Several uncharacterized proteins in other CTG clade species were further predicted to share homology with *C. albicans* Ecm22. Additionally, there is also an identified Ecm22 protein in *C. neoformans*, however, it does not share significant homology with *C.*

albicans Ecm22. In most fungi, regulation of sterol biosynthesis is based on well conserved Sterol Regulatory-element Binding Proteins (SREBP), usually harboring a basic helix-loop-helix (bHLH) leucine zipper domain. However, it is interesting to note that this system has been disrupted in yeasts such as *S. cerevisiae* and *Candida* species [225]. In these species, the role of SREBPs in sterol biosynthesis has been replaced by the Zn(2)-Cys(6) Upc2 proteins, which are structurally unrelated to SREBPs. Maguire and colleagues proposed that Upc2 arose in the common ancestor of the Saccharomycotina and was created by duplication of another zinc finger protein gene, although it diverged too much from its orthologs in other species, such as *A. fumigatus* [225].

Upregulation of ergosterol synthesis upon azole drug exposure is controlled in *A. fumigatus* by the transcription factor AfSrbA, encoding a bHLH protein belonging to the SREBP family. As stated previously, this family comprises the main regulators of sterol biosynthesis in fungi outside of the Saccharomycotina lineage. AfSrbA is responsible for mediating azole drug resistance by activating the expression of *Afcyp51*, the *ERG11* ortholog in this pathogen [226–228]. Additionally, it has a secondary role in the maintenance of cell polarity, therefore directing hyphal growth [227]. AfSrbA controls the expression of a target gene with which it shares sequence similarity: *AfsrbB*. AfSrbB is another transcriptional regulator that together with AfSrbA co-regulates heme biosynthesis and sterol demethylation genes. However, it acquired new functions as it also regulates hypoxia response and virulence genes [229]. Consistent the proposal of Maguire *et al.*, there are no known AfSrbA/B homologs in *S. cerevisiae* or *Candida* species. Nonetheless, *C. neoformans* harbors the transcription factor CnSre1, another bHLH protein that despite not being found to share a phylogenetic relationship with AfSrbA or AfSrbB was found to be required for azole drug resistance [230–232]. Like *A. fumigatus* SrbA, this is due to CnSre1 involvement in the expression of genes required for ergosterol biosynthesis [227,233]. Additionally, CnSre1 is also involved in virulence, as it was found to be important for the establishment and growth of yeast cells in the brain; as well as being involved in the regulation of genes involved in iron uptake [233].

1.6 References

1. Pais, P.; Costa, C.; Cavalheiro, M.; Romão, D.; Teixeira, M.C. Transcriptional Control of Drug Resistance, Virulence and Immune System Evasion in Pathogenic Fungi: A Cross-Species Comparison. *Front. Cell. Infect. Microbiol.* **2016**, *6*, 31.

2. Pais, P.; Galocha, M.; Viana, R.; Cavalheiro, M.; Pereira, D.; Teixeira, M.C. Microevolution of the pathogenic yeasts *Candida albicans* and *Candida glabrata* during antifungal therapy and host infection. *Microb. Cell* **2019**, *6*, 142–159.

3. Pais, P.; Galocha, M.; Teixeira, M.C. Genome-Wide Response to Drugs and Stress in the Pathogenic Yeast *Candida glabrata*. In *Progress in molecular and subcellular biology* **2019**, *58*, pp. 155–193.

4. Teixeira, M.C.; Monteiro, P.T.; Palma, M.; Costa, C.; Godinho, C.P.; Pais, P.; Cavalheiro, M.; Antunes, M.; Lemos, A.; Pedreira, T.; *et al.* YEASTRACT: An upgraded database for the analysis of transcription regulatory networks in *Saccharomyces cerevisiae*. *Nucleic Acids Res.* **2018**, *46*, D348-D353.

5. Teixeira, M.C.; Monteiro, P.T.; Guerreiro, J.F.; Gonçalves, J.P.; Mira, N.P.; Dos Santos, S.C.; Cabrito, T.R.; Palma, M.; Costa, C.; Francisco, A.P.; *et al.* The YEASTRACT database: An upgraded information system for the analysis of gene and genomic transcription regulation in *Saccharomyces cerevisiae*. *Nucleic Acids Res.* **2014**, *42*, D161-D166.

6. Teixeira, M.C.; Monteiro, P.; Jain, P.; Tenreiro, S.; Fernandes, A.R.; Mira, N.P.; Alenquer, M.; Freitas, A.T.; Oliveira, A.L.; Sá-Correia, I. The YEASTRACT database: a tool for the analysis of transcription regulatory associations in Saccharomyces cerevisiae. *Nucleic Acids Res.* **2006**, *34*, D446–D451.

7. Abdulrehman, D.; Monteiro, P.T.; Teixeira, M.C.; Mira, N.P.; Lourenco, A.B.; dos Santos, S.C.; Cabrito, T.R.; Francisco, A.P.; Madeira, S.C.; Aires, R.S.; *et al.* YEASTRACT: providing a programmatic access to curated transcriptional regulatory associations in *Saccharomyces cerevisiae* through a web services interface. *Nucleic Acids Res.* **2011**, *39*, D136–D140.

8. Monteiro, P.T.; Mendes, N.D.; Teixeira, M.C.; d'Orey, S.; Tenreiro, S.; Mira, N.P.; Pais, H.; Francisco, A.P.; Carvalho, A.M.; Lourenço, A.B.; *et al.* YEASTRACT-DISCOVERER: new tools to improve the analysis of transcriptional regulatory associations in *Saccharomyces cerevisiae*. *Nucleic Acids Res.* **2008**, *36*, D132-D136.

9. Monteiro, P.T.; Pais, P.; Costa, C.; Manna, S.; Sá-Correia, I.; Teixeira, M.C. The PathoYeastract database: An information system for the analysis of gene and genomic transcription regulation in pathogenic yeasts. *Nucleic Acids Res.* **2017**, *45*, D597-D603.

10. Pais, P.; Costa, C.; Pires, C.; Shimizu, K.; Chibana, H.; Teixeira, M.C. Membrane Proteome-Wide Response to the Antifungal Drug Clotrimazole in *Candida glabrata* : Role of the Transcription Factor CgPdr1 and the Drug:H+ Antiporters CgTpo1_1 and CgTpo1_2. *Mol. Cell. Proteomics* **2016**, *15*, 57-72.

11. Pais, P.; Pires, C.; Costa, C.; Okamoto, M.; Chibana, H.; Teixeira, M.C. Membrane proteomics analysis of the *Candida glabrata* response to 5-flucytosine: Unveiling the role and regulation of the drug efflux transporters CgFlr1 and CgFlr2. *Front. Microbiol.* **2016**, *7*, 2045.

12. Pfaller, M.A.; Diekema, D.J. Epidemiology of invasive mycoses in North America. *Crit. Rev. Microbiol.* **2010**, *36*, 1–53.

13. Sims, C.R.; Ostrosky-Zeichner, L.; Rex, J.H. Invasive Candidiasis in Immunocompromised Hospitalized Patients. *Arch. Med. Res.* **2005**, *36*, 660–671.

14. Chauhan, N.; Latge, J. P.; Calderone, R. Signalling and oxidant adaptation in *Candida albicans* and *Aspergillus fumigatus*. *Nat. Rev. Microbiol.* **2006**, *4*, 435–444.

15. Schmalzle, S.A.; Buchwald, U.K.; Gilliam, B.L.; Riedel, D.J. *Cryptococcus neoformans* infection in malignancy. *Mycoses* **2016**, *59*, 542–552.

16. Ferreira, M.E. da S.; Colombo, A.L.; Paulsen, I.; Ren, Q.; Wortman, J.; Huang, J.; Goldman, M.H.S.; Goldman, G.H. The ergosterol biosynthesis pathway, transporter genes, and azole resistance in *Aspergillus fumigatus*. *Med. Mycol.* **2005**, *43 Suppl 1*, S313-319.

17. Dou, H. T.; Xu, Y.-C.; Wang, H. Z.; Li, T. S. Molecular epidemiology of *Cryptococcus neoformans* and *Cryptococcus gattii* in China between 2007 and 2013 using multilocus sequence typing and the DiversiLab system. *Eur. J. Clin. Microbiol. Infect. Dis.* **2015**, *34*, 753–762.

18. Wisplinghoff, H.; Bischoff, T.; Tallent, S.M.; Seifert, H.; Wenzel, R.P.; Edmond, M.B. Nosocomial bloodstream infections in US hospitals: analysis of 24,179 cases from a prospective nationwide surveillance study. *Clin. Infect. Dis.* **2004**, *39*, 309–317.

19. González de Molina, F.J.; León, C.; Ruiz-Santana, S.; Saavedra, P.; CAVA I Study Group Assessment of candidemia-attributable mortality in critically ill patients using propensity score matching analysis. *Crit. Care* **2012**, *16*, R105.

20. Hirano, R.; Sakamoto, Y.; Kudo, K.; Ohnishi, M. Retrospective analysis of mortality and *Candida* isolates of 75 patients with candidemia: a single hospital experience. *Infect. Drug Resist.* **2015**, *8*, 199–205.

21. Yapar, N. Epidemiology and risk factors for invasive candidiasis. *Ther. Clin. Risk Manag.* **2014**, *10*, 95.

22. Azie, N.; Neofytos, D.; Pfaller, M.; Meier-Kriesche, H.U.; Quan, S.P.; Horn, D. The PATH (Prospective Antifungal Therapy) Alliance® registry and invasive fungal infections: update 2012. *Diagn. Microbiol. Infect. Dis.* **2012**, *73*, 293–300.

23. Edmond, M.B.; Wallace, S.E.; McClish, D.K.; Pfaller, M.A.; Jones, R.N.; Wenzel, R.P. Nosocomial bloodstream infections in United States hospitals: a three-year analysis. *Clin. Infect. Dis.* **1999**, *29*, 239–244.

24. Khatib, R.; Johnson, L.B.; Fakih, M.G.; Riederer, K.; Briski, L. Current trends in candidemia and species distribution among adults: *Candida glabrata* surpasses *C. albicans* in diabetic patients and abdominal sources. *Mycoses* **2016**, *59*, 781–786.

25. Schwarzmüller, T.; Ma, B.; Hiller, E.; Istel, F.; Tscherner, M.; Brunke, S.; Ames, L.; Firon, A.; Green, B.; Cabral, V.; *et al.* Systematic Phenotyping of a Large-Scale *Candida glabrata* Deletion Collection Reveals Novel Antifungal Tolerance Genes. *PLoS Pathog.* **2014**, *10*, e1004211.

26. Le, A.; Farmakiotis, D.; Tarrand, J.J.; Kontoyiannis, D.P. Initial Treatment of Cancer Patients with Fluconazole-Susceptible Dose-Dependent *Candida glabrata* Fungemia: Better Outcome with an Echinocandin or Polyene Compared to an Azole? *Antimicrob. Agents Chemother.* **2017**, *61*, e00631-17.

27. Singh-Babak, S.D.; Babak, T.; Diezmann, S.; Hill, J.A.; Xie, J.L.; Chen, Y. L.; Poutanen, S.M.; Rennie, R.P.; Heitman, J.; Cowen, L.E. Global Analysis of the Evolution and Mechanism of Echinocandin Resistance in *Candida glabrata*. *PLoS Pathog.* **2012**, *8*, e1002718.

28. Whaley, S.G.; Rogers, P.D. Azole Resistance in *Candida glabrata*. *Curr. Infect. Dis. Rep.* **2016**, *18*, 41.

29. Turner, S.A.; Butler, G. The *Candida* Pathogenic Species Complex. *Cold Spring Harb. Perspect. Med.* **2014**, *4*, a019778–a019778.

30. Gabaldón, T.; Martin, T.; Marcet-Houben, M.; Durrens, P.; Bolotin-Fukuhara, M.; Lespinet, O.; Arnaise, S.; Boisnard, S.; Aguileta, G.; Atanasova, R.; *et al.* Comparative genomics of emerging pathogens in the *Candida glabrata* clade. *BMC Genomics* **2013**, *14*, 623.

31. Santos, M.A.S.; Gomes, A.C.; Santos, M.C.; Carreto, L.C.; Moura, G.R. The genetic code of the fungal CTG clade. *C. R. Biol.* **2011**, *334*, 607–611.

32. Krassowski, T.; Coughlan, A.Y.; Shen, X.X.; Zhou, X.; Kominek, J.; Opulente, D.A.; Riley, R.; Grigoriev, I. V; Maheshwari, N.; Shields, D.C.; *et al.* Evolutionary instability of CUG-Leu in the genetic code of budding yeasts. *Nat. Commun.* **2018**, *9*, 1887.

33. Petrikkos, G.; Skiada, A. Recent advances in antifungal chemotherapy. *Int. J. Antimicrob. Agents* **2007**, *30*, 108–117.

34. Papon, N.; Courdavault, V.; Clastre, M.; Bennett, R.J. Emerging and emerged pathogenic *Candida* species: beyond the *Candida albicans* paradigm. *PLoS Pathog.* **2013**, *9*, e1003550.

35. Fidel, P.L.; Vazquez, J.A.; Sobel, J.D. *Candida glabrata*: review of epidemiology, pathogenesis, and clinical disease with comparison to *C. albicans*. *Clin. Microbiol. Rev.* **1999**, *12*, 80-96.

36. Sheehan, D.J.; Hitchcock, C.A.; Sibley, C.M. Current and emerging azole antifungal agents. *Clin. Microbiol. Rev.* **1999**, *12*, 40–79.

37. Revie, N.M.; Iyer, K.R.; Robbins, N.; Cowen, L.E. Antifungal drug resistance: evolution, mechanisms and impact. *Curr. Opin. Microbiol.* **2018**, *45*, 70–76.

38. Ostrosky-Zeichner, L.; Casadevall, A.; Galgiani, J.N.; Odds, F.C.; Rex, J.H. An insight into the antifungal pipeline: selected new molecules and beyond. *Nat. Rev. Drug Discov.* **2010**, *9*, 719–727.

39. Whaley, S.G.; Caudle, K.E.; Vermitsky, J. P.; Chadwick, S.G.; Toner, G.; Barker, K.S.; Gygax, S.E.; Rogers, P.D. *UPC2A* is required for high-level azole antifungal resistance in *Candida glabrata*. *Antimicrob. Agents Chemother*. **2014**, *58*, 4543–4554.

40. Eicher, T.; Hauptmann, S.; Speicher, A. The chemistry of heterocycles : structure, reactions, synthesis and applications. *Wiley-VCH* **2012**, ISBN 3527669868.

41. Yan, J. Y.; Nie, X. L.; Tao, Q. M.; Zhan, S. Y.; Zhang, Y. Ketoconazole Associated Hepatotoxicity: A Systematic Review and Meta-analysis. *Biomed. Environ. Sci.* **2013**, *26*, 605–610.

42. Sun, L.; Liao, K.; Hang, C. Caffeic acid phenethyl ester synergistically enhances the antifungal activity of fluconazole against resistant *Candida albicans*. *Phytomedicine* **2018**, *40*, 55–58.

43. Borst, A.; Raimer, M.T.; Warnock, D.W.; Morrison, C.J.; Arthington-Skaggs, B.A. Rapid acquisition of stable azole resistance by *Candida glabrata* isolates obtained before the clinical introduction of fluconazole. *Antimicrob. Agents Chemother.* **2005**, *49*, 783–787.

44. Wiederhold, N. Antifungal resistance: current trends and future strategies to combat. *Infect. Drug Resist.* **2017**, *10*, 249–259.

45. Shapiro, R.S.; Robbins, N.; Cowen, L.E. Regulatory circuitry governing fungal development, drug resistance, and disease. *Microbiol. Mol. Biol. Rev.* **2011**, *75*, 213–267.

46. Anderson, J.B. Evolution of antifungal-drug resistance: mechanisms and pathogen fitness. *Nat. Rev. Microbiol.* **2005**, *3*, 547–556.

47. Mukherjee, P.K.; Chandra, J.; Kuhn, D.M.; Ghannoum, M.A. Mechanism of fluconazole resistance in *Candida albicans* biofilms: phase-specific role of efflux pumps and membrane sterols. *Infect. Immun.* **2003**, *71*, 4333–4340.

48. MacPherson, S.; Akache, B.; Weber, S.; De Deken, X.; Raymond, M.; Turcotte, B. *Candida albicans* Zinc Cluster Protein Upc2p Confers Resistance to Antifungal Drugs and Is an Activator of Ergosterol Biosynthetic Genes. *Antimicrob. Agents Chemother.* **2005**, *49*, 1745–1752.

49. Cowen, L.E.; Steinbach, W.J. Stress, drugs, and evolution: the role of cellular signaling in fungal drug resistance. *Eukaryot. Cell* **2008**, *7*, 747–764.

50. Sanglard, D.; Kuchler, K.; Ischer, F.; Pagani, J.L.; Monod, M.; Bille, J. Mechanisms of resistance to azole antifungal agents in *Candida albicans* isolates from AIDS patients involve specific multidrug transporters. *Antimicrob. Agents Chemother.* **1995**, *39*, 2378–2386.

51. Sanglard, D.; Ischer, F.; Monod, M.; Bille, J. Susceptibilities of *Candida albicans* multidrug transporter mutants to various antifungal agents and other metabolic inhibitors. *Antimicrob. Agents Chemother.* **1996**, *40*, 2300–2305.

52. Sanglard, D.; Ischer, F.; Monod, M.; Bille, J. Cloning of *Candida albicans* genes conferring resistance to azole antifungal agents: characterization of *CDR2*, a new multidrug ABC transporter gene. *Microbiology* **1997**, *143*, 405–416.

53. Siikala, E.; Rautemaa, R.; Richardson, M.; Saxen, H.; Bowyer, P.; Sanglard, D. Persistent *Candida albicans* colonization and molecular mechanisms of azole resistance in autoimmune polyendocrinopathy-candidiasis-ectodermal dystrophy (APECED) patients. *J. Antimicrob. Chemother.* **2010**, *65*, 2505–2513.

54. White, T.C. Increased mRNA levels of *ERG16*, *CDR*, and *MDR1* correlate with increases in azole resistance in *Candida albicans* isolates from a patient infected with human immunodeficiency virus. *Antimicrob. Agents Chemother.* **1997**, *41*, 1482–1487.

55. Hoot, S.J.; Smith, A.R.; Brown, R.P.; White, T.C. An A643V amino acid substitution in Upc2p contributes to azole resistance in well-characterized clinical isolates of *Candida albicans*. *Antimicrob. Agents Chemother.* **2011**, *55*, 940–942.

56. Heilmann, C.J.; Schneider, S.; Barker, K.S.; Rogers, P.D.; Morschhäuser, J. An A643T mutation in the transcription factor Upc2p causes constitutive *ERG11* upregulation and increased fluconazole resistance in *Candida albicans*. *Antimicrob. Agents Chemother.* **2010**, *54*, 353–359.

57. Flowers, S.A.; Barker, K.S.; Berkow, E.L.; Toner, G.; Chadwick, S.G.; Gygax, S.E.; Morschhäuser, J.; Rogers, P.D. Gain-of-function mutations in *UPC2* are a frequent cause of *ERG11* upregulation in azole-resistant clinical isolates of Candida albicans. *Eukaryot. Cell* **2012**, *11*, 1289–1299.

58. Dunkel, N.; Blaß, J.; Rogers, P.D.; Morschhäuser, J. Mutations in the multi-drug resistance regulator *MRR1*, followed by loss of heterozygosity, are the main cause of *MDR1* overexpression in fluconazole-resistant *Candida albicans* strains. *Mol. Microbiol.* **2008**, *69*, 827–840.

59. Coste, A.; Turner, V.; Ischer, F.; Morschhäuser, J.; Forche, A.; Selmecki, A.; Berman, J.; Bille, J.; Sanglard, D. A mutation in Tac1p, a transcription factor regulating *CDR1* and *CDR2*, is coupled with loss of heterozygosity at chromosome 5 to mediate antifungal resistance in *Candida albicans*. *Genetics* **2006**, *172*, 2139–2156.

60. Dunkel, N.; Liu, T.T.; Barker, K.S.; Homayouni, R.; Morschhäuser, J.; Rogers, P.D. A gain-of-function mutation in the transcription factor Upc2p causes upregulation of ergosterol biosynthesis genes and increased fluconazole resistance in a clinical *Candida albicans* isolate. *Eukaryot. Cell* **2008**, *7*, 1180–1190.

61. Selmecki, A.; Forche, A.; Berman, J. Aneuploidy and Isochromosome Formation in Drug-Resistant *Candida albicans*. *Science* **2006**, *313*, 367–370.

62. Selmecki, A.; Gerami-Nejad, M.; Paulson, C.; Forche, A.; Berman, J. An isochromosome confers drug resistance in vivo by amplification of two genes, *ERG11* and *TAC1*. *Mol. Microbiol.* **2008**, *68*, 624–641.

63. Selmecki, A.M.; Dulmage, K.; Cowen, L.E.; Anderson, J.B.; Berman, J. Acquisition of Aneuploidy Provides Increased Fitness during the Evolution of Antifungal Drug Resistance. *PLoS Genet.* **2009**, *5*, e1000705.

64. White, T.C. The presence of an R467K amino acid substitution and loss of allelic variation correlate with an azole-resistant lanosterol 14α demethylase in *Candida albicans*. *Antimicrob. Agents Chemother.* **1997**, *12*, 80-96.

65. Sanglard, D.; Ischer, F.; Koymans, L.; Bille, J. Amino acid substitutions in the cytochrome P-450 lanosterol 14α- demethylase (CYP51A1) from azole-resistant *Candida albicans* clinical isolates contribute to resistance to azole antifungal agents. *Antimicrob. Agents Chemother.* **1998**, *42*, 241-253-

66. Lamb, D.C.; Kelly, D.E.; White, T.C.; Kelly, S.L. The R467K amino acid substitution in *Candida albicans* sterol 14α- demethylase causes drug resistance through reduced affinity. *Antimicrob. Agents Chemother.* **2000**, *44*, 63-67.

67. Henry, K.W.; Nickels, J.T.; Edlind, T.D. Upregulation of *ERG* genes in *Candida* species by azoles and other sterol biosynthesis inhibitors. *Antimicrob. Agents Chemother.* **2000**, *44*, 2693–2700.

68. Song, J.L.; Harry, J.B.; Eastman, R.T.; Oliver, B.G.; White, T.C. The *Candida albicans* Lanosterol 14-α-Demethylase (*ERG11*) Gene Promoter Is Maximally Induced after Prolonged Growth with Antifungal Drugs. *Antimicrob. Agents Chemother.* **2004**, *48*, 1136-1144.

69. Gao, J.; Wang, H.; Li, Z.; Wong, A.H.H.; Wang, Y.Z.; Guo, Y.; Lin, X.; Zeng, G.; Wang, Y.; Wang, J. *Candida albicans* gains azole resistance by altering sphingolipid composition. *Nat. Commun.* **2018**, *9*, 4495.

70. Vermitsky, J.P.; Edlind, T.D. Azole resistance in *Candida glabrata*: coordinate upregulation of multidrug transporters and evidence for a Pdr1-like transcription factor. *Antimicrob. Agents Chemother.* **2004**, *48*, 3773–3781.

71. Caudle, K.E.; Barker, K.S.; Wiederhold, N.P.; Xu, L.; Homayouni, R.; Rogers, P.D. Genomewide expression profile analysis of the *Candida glabrata* Pdr1 regulon. *Eukaryot. Cell* **2011**, *10*, 373–383.

72. Sanguinetti, M.; Posteraro, B.; Fiori, B.; Ranno, S.; Torelli, R.; Fadda, G. Mechanisms of azole resistance in clinical isolates of *Candida glabrata* collected during a hospital survey of antifungal resistance. *Antimicrob. Agents Chemother.* **2005**, *49*, 668–769.

73. vanden Bossche, H.; Marichal, P.; Odds, F.C.; Le Jeune, L.; Coene, M.C. Characterization of an azole-resistant *Candida glabrata* isolate. *Antimicrob. Agents Chemother.* **1992**, *36*, 2602–2610.

74. Sanglard, D.; Ischer, F.; Calabrese, D.; Majcherczyk, P.A.; Bille, J. The ATP binding cassette transporter gene *CgCDR1* from *Candida glabrata* is involved in the resistance of clinical isolates to azole antifungal agents. *Antimicrob. Agents Chemother.* **1999**, *43*, 2753–2765.

75. Costa, C.; Nunes, J.; Henriques, A.; Mira, N.P.; Nakayama, H.; Chibana, H.; Teixeira, M.C. Candida glabrata drug:H+ antiporter CgTpo3 (ORF *CAGL0I10384g*): role in azole drug resistance and polyamine homeostasis. *J. Antimicrob. Chemother.* **2014**, *69*, 1767–1776.

76. Costa, C.; Pires, C.; Cabrito, T.R.; Renaudin, A.; Ohno, M.; Chibana, H.; Sá-Correia, I.; Teixeira, M.C. *Candida glabrata* drug: H+antiporter CgQdr2 confers imidazole drug resistance, being activated by transcription factor CgPdr1. *Antimicrob. Agents Chemother.* **2013**, *57*, 3159-3167.

77. Sanglard, D.; Ischer, F.; Bille, J. Role of ATP-binding-cassette transporter genes in high-frequency acquisition of resistance to azole antifungals in *Candida glabrata*. *Antimicrob. Agents Chemother.* **2001**, *45*, 1174–1183.

78. Ferrari, S.; Ischer, F.; Calabrese, D.; Posteraro, B.; Sanguinetti, M.; Fadda, G.; Rohde, B.; Bauser, C.; Bader, O.; Sanglard, D. Gain of Function Mutations in *CgPDR1* of *Candida glabrata* Not Only Mediate Antifungal Resistance but Also Enhance Virulence. *PLoS Pathog.* **2009**, *5*, e1000268.

79. Defontaine, A.; Bouchara, J.P.; Declerck, P.; Planchenault, C.; Chabasse, D.; Hallet, J.N. In-vitro resistance to azoles associated with mitochondrial DNA deficiency in *Candida glabrata*. *J. Med. Microbiol.* **1999**, *48*, 663–670.

80. Ferrari, S.; Sanguinetti, M.; De Bernardis, F.; Torelli, R.; Posteraro, B.; Vandeputte, P.; Sanglard, D. Loss of mitochondrial functions associated with azole resistance in *Candida glabrata* results in enhanced virulence in mice. *Antimicrob. Agents Chemother.* **2011**, *55*, 1852–1860.

81. Kaur, R.; Castaño, I.; Cormack, B.P. Functional genomic analysis of fluconazole susceptibility in the pathogenic yeast *Candida glabrata*: roles of calcium signaling and mitochondria. *Antimicrob. Agents Chemother.* **2004**, *48*, 1600–1163.

82. Hallstrom, T.C.; Moye-Rowley, W.S. Multiple signals from dysfunctional mitochondria activate the pleiotropic drug resistance pathway in *Saccharomyces cerevisiae. J. Biol. Chem.* **2000**, *275*, 37347–37356.

83. Brun, S.; Bergès, T.; Poupard, P.; Vauzelle-Moreau, C.; Renier, G.; Chabasse, D.; Bouchara, J.-P. Mechanisms of azole resistance in petite mutants of *Candida glabrata*. *Antimicrob. Agents Chemother.* **2004**, *48*, 1788–1796.

84. Tsai, H.F.; Krol, A.A.; Sarti, K.E.; Bennett, J.E. *Candida glabrata PDR1*, a transcriptional regulator of a pleiotropic drug resistance network, mediates azole resistance in clinical isolates and petite mutants. *Antimicrob. Agents Chemother.* **2006**, *50*, 1384–1392.

85. Paul, S.; Schmidt, J.A.; Moye-Rowley, W.S. Regulation of the CgPdr1 Transcription Factor from the Pathogen *Candida glabrata*. *Eukaryot. Cell* **2011**, *10*, 187–197.

86. Shingu-Vazquez, M.; Traven, A. Mitochondria and Fungal Pathogenesis: Drug Tolerance, Virulence, and Potential for Antifungal Therapy. *Eukaryot. Cell* **2011**, *10*, 1376–1383.

87. Mayers, D.L., Sobel, J.D., Ouellette, M., Kaye, K.S., Marchaim, D. Antimicrobial Drug Resistance. Eds.; Springer International Publishing: Cham. **2017**; ISBN 978-3-319-46716-0.

88. De Pauw, B.E. New antifungal agents and preparations. *Int. J. Antimicrob. Agents* **2000**, *16*, 147–150.

89. Rodrigues, C.F.; Silva, S.; Henriques, M. *Candida glabrata*: a review of its features and resistance. *Eur. J. Clin. Microbiol. Infect. Dis.* **2014**, *33*, 673–688.

90. Andes, D. In vivo pharmacodynamics of antifungal drugs in treatment of candidiasis. *Antimicrob. Agents Chemother.* **2003**, *47*, 1179–1186.

91. Gray, K.C.; Palacios, D.S.; Dailey, I.; Endo, M.M.; Uno, B.E.; Wilcock, B.C.; Burke, M.D. Amphotericin primarily kills yeast by simply binding ergosterol. *Proc. Natl. Acad. Sci. U. S. A.* **2012**, *109*, 2234–2239.

92. Anderson, T.M.; Clay, M.C.; Cioffi, A.G.; Diaz, K.A.; Hisao, G.S.; Tuttle, M.D.; Nieuwkoop, A.J.; Comellas, G.; Maryum, N.; Wang, S.; *et al.* Amphotericin forms an extramembranous and fungicidal sterol sponge. *Nat. Chem. Biol.* **2014**, *10*, 400–406.

93. Lemke, A.; Kiderlen, A.F.; Kayser, O. Amphotericin B. *Appl. Microbiol. Biotechnol.* **2005**, *68*, 151–162.

94. Odds, F.C.; Brown, A.J.P.; Gow, N.A.R. Antifungal agents: Mechanisms of action. *Trends Microbiol.* **2003**, *11*, 272–279.

95. Cho, E.J.; Shin, J.H.; Kim, S.H.; Kim, H.K.; Park, J.S.; Sung, H.; Kim, M.N.; Im, H.J. Emergence of multiple resistance profiles involving azoles, echinocandins and amphotericin B in *Candida glabrata* isolates from a neutropenia patient with prolonged fungaemia. *J. Antimicrob. Chemother.* **2014**, *70*, 1268–1270.

96. Krogh-Madsen, M.; Arendrup, M.C.; Heslet, L.; Knudsen, J.D. Amphotericin B and Caspofungin Resistance in *Candida glabrata* Isolates Recovered from a Critically Ill Patient. *Clin. Infect. Dis.* **2006**, *42*, 938–944.

97. Martel, C.M.; Parker, J.E.; Bader, O.; Weig, M.; Gross, U.; Warrilow, A.G.S.; Kelly, D.E.; Kelly, S.L. A Clinical Isolate of Candida albicans with Mutations in *ERG11* (Encoding Sterol 14 -Demethylase) and *ERG5* (Encoding C22 Desaturase) Is Cross Resistant to Azoles and Amphotericin B. *Antimicrob. Agents Chemother.* **2010**, *54*, 3578–3583.

98. Vandeputte, P.; Tronchin, G.; Larcher, G.; Ernoult, E.; Bergès, T.; Chabasse, D.; Bouchara, J.P. A nonsense mutation in the *ERG6* gene leads to reduced susceptibility to polyenes in a clinical isolate of *Candida glabrata*. *Antimicrob. Agents Chemother.* **2008**, *52*, 3701–9.

99. Vandeputte, P.; Tronchin, G.; Bergès, T.; Hennequin, C.; Chabasse, D.; Bouchara, J.P. Reduced susceptibility to polyenes associated with a missense mutation in the *ERG6* gene in a clinical isolate of *Candida glabrata* with pseudohyphal growth. *Antimicrob. Agents Chemother.* **2007**, *51*, 982–90.

100. Denning, D.W. Echinocandin antifungal drugs. *Lancet* **2003**, *362*, 1142–1151.

101. Bachmann, S.P.; VandeWalle, K.; Ramage, G.; Patterson, T.F.; Wickes, B.L.; Graybill, J.R.; López-Ribot, J.L. In vitro activity of caspofungin against *Candida albicans* biofilms. *Antimicrob. Agents Chemother.* **2002**, *46*, 3591–3596.

102. Kuhn, D.M.; George, T.; Chandra, J.; Mukherjee, P.K.; Ghannoum, M.A. Antifungal susceptibility of *Candida* biofilms: unique efficacy of amphotericin B lipid formulations and echinocandins. *Antimicrob. Agents Chemother.* **2002**, *46*, 1773–80.

103. Sanguinetti, M.; Posteraro, B.; Lass-Flörl, C. Antifungal drug resistance among *Candida* species: mechanisms and clinical impact. *Mycoses* **2015**, *58*, 2–13.

104. Cornely, O.A.; Bassetti, M.; Calandra, T.; Garbino, J.; Kullberg, B.J.; Lortholary, O.; Meersseman, W.; Akova, M.; Arendrup, M.C.; Arikan-Akdagli, S.; *et al.* ESCMID* *This guideline was presented in part at ECCMID 2011. European Society for Clinical Microbiology and Infectious Diseases. guideline for the diagnosis and management of Candida diseases 2012: non-neutropenic adult patients. *Clin. Microbiol. Infect.* **2012**, *18*, 19–37.

105. Krishnan, B.R.; James, K.D.; Polowy, K.; Bryant, B.J.; Vaidya, A.; Smith, S.; Laudeman, C.P. CD101, a novel echinocandin with exceptional stability properties and enhanced aqueous solubility. *J. Antibiot. (Tokyo).* **2017**, *70*, 130–135.

106. Lakota, E.A.; Ong, V.; Flanagan, S.; Rubino, C.M. Population Pharmacokinetic Analyses for Rezafungin (CD101) Efficacy Using Phase 1 Data. *Antimicrob. Agents Chemother.* **2018**, *62*, e02603-17.

107. Matsumoto, E.; Boyken, L.; Tendolkar, S.; McDanel, J.; Castanheira, M.; Pfaller, M.; Diekema, D. Candidemia surveillance in Iowa: emergence of echinocandin resistance. *Diagn. Microbiol. Infect. Dis.* **2014**, *79*, 205–208.

108. Pfaller, M.A.; Diekema, D.J. Epidemiology of invasive candidiasis: A persistent public health problem. *Clin. Microbiol. Rev.* **2007**, *20*, 133-163.

109. Katiyar, S.; Pfaller, M.; Edlind, T. *Candida albicans* and *Candida glabrata* clinical isolates exhibiting reduced echinocandin susceptibility. *Antimicrob. Agents Chemother.* **2006**, *50*, 2892–2894.

110. Park, S.; Kelly, R.; Kahn, J.N.; Robles, J.; Hsu, M.J.; Register, E.; Li, W.; Vyas, V.; Fan, H.; Abruzzo, G.; *et al.* Specific substitutions in the echinocandin target Fks1p account for reduced susceptibility of rare laboratory and clinical *Candida* sp. isolates. *Antimicrob. Agents Chemother.* **2005**, *49*, 3264–3273.

111. Costa-de-Oliveira, S.; Marcos Miranda, I.; Silva, R.M.; Pinto E Silva, A.; Rocha, R.; Amorim, A.; Gonçalves Rodrigues, A.; Pina-Vaz, C. *FKS2* mutations associated with decreased echinocandin susceptibility of *Candida glabrata* following anidulafungin therapy. *Antimicrob. Agents Chemother.* **2011**, *55*, 1312–1314.

112. Douglas, C.M.; D'Ippolito, J.A.; Shei, G.J.; Meinz, M.; Onishi, J.; Marrinan, J.A.; Li, W.; Abruzzo, G.K.; Flattery, A.; Bartizal, K.; *et al.* Identification of the *FKS1* gene of *Candida albicans* as the essential target of 1,3-beta-D-glucan synthase inhibitors. *Antimicrob. Agents Chemother.* **1997**, *41*, 2471–2479.

113. Dannaoui, E.; Desnos-Ollivier, M.; Garcia-Hermoso, D.; Grenouillet, F.; Cassaing, S.; Baixench, M.-T.; Bretagne, S.; Dromer, F.; Lortholary, O.; French Mycoses Study Group, the F.M.S. *Candida* spp. with acquired echinocandin resistance, France, 2004-2010. *Emerg. Infect. Dis.* **2012**, *18*, 86–90.

114. Katiyar, S.K.; Alastruey-Izquierdo, A.; Healey, K.R.; Johnson, M.E.; Perlin, D.S.; Edlind, T.D. Fks1 and Fks2 are functionally redundant but differentially regulated in *Candida glabrata*: implications for echinocandin resistance. *Antimicrob. Agents Chemother.* **2012**, *56*, 6304–6309.

115. Vallabhaneni, S.; Cleveland, A.A.; Farley, M.M.; Harrison, L.H.; Schaffner, W.; Beldavs, Z.G.; Derado, G.; Pham, C.D.; Lockhart, S.R.; Smith, R.M. Epidemiology and Risk Factors for Echinocandin Nonsusceptible *Candida glabrata* Bloodstream Infections: Data From a Large Multisite Population-Based Candidemia Surveillance Program, 2008–2014. *Open Forum Infect. Dis.* **2015**, *2*, ofv163.

116. Garcia-Effron, G.; Park, S.; Perlin, D.S. Correlating echinocandin MIC and kinetic inhibition of fks1 mutant glucan synthases for *Candida albicans*: implications for interpretive breakpoints. *Antimicrob. Agents Chemother.* **2009**, *53*, 112–122.

117. Sanglard, D. Emerging Threats in Antifungal-Resistant Fungal Pathogens. *Front. Med.* **2016**, *3*, 11.

118. Garcia-Effron, G.; Lee, S.; Park, S.; Cleary, J.D.; Perlin, D.S. Effect of *Candida glabrata FKS1* and *FKS2* mutations on echinocandin sensitivity and kinetics of 1,3-beta-D-glucan synthase: implication for the existing susceptibility breakpoint. *Antimicrob. Agents Chemother.* **2009**, *53*, 3690–3699.

119. Cowen, L.E.; Nantel, A.; Whiteway, M.S.; Thomas, D.Y.; Tessier, D.C.; Kohn, L.M.; Anderson, J.B. Population genomics of drug resistance in *Candida albicans*. *Proc. Natl. Acad. Sci. U. S. A.* **2002**, *99*, 9284–9289.

120. Singh, S.D.; Robbins, N.; Zaas, A.K.; Schell, W.A.; Perfect, J.R.; Cowen, L.E. Hsp90 Governs Echinocandin Resistance in the Pathogenic Yeast *Candida albicans* via Calcineurin. *PLoS Pathog.* **2009**, *5*, e1000532.

121. Stevens, D.A.; Ichinomiya, M.; Koshi, Y.; Horiuchi, H. Escape of *Candida* from Caspofungin Inhibition at Concentrations above the MIC (Paradoxical Effect) Accomplished by Increased Cell Wall Chitin; Evidence for -1,6-Glucan Synthesis Inhibition by Caspofungin. *Antimicrob. Agents Chemother.* **2006**, *50*, 3160–3161.

122. Markovich, S.; Yekutiel, A.; Shalit, I.; Shadkchan, Y.; Osherov, N. Genomic Approach to Identification of Mutations Affecting Caspofungin Susceptibility in *Saccharomyces cerevisiae*. *Antimicrob. Agents Chemother.* **2004**, *48*, 3871–3876.

123. Walker, L.A.; Munro, C.A.; de Bruijn, I.; Lenardon, M.D.; McKinnon, A.; Gow, N.A.R. Stimulation of chitin synthesis rescues *Candida albicans* from echinocandins. *PLoS Pathog.* **2008**, *4*, e1000040.

124. Rosenwald, A.G.; Arora, G.; Ferrandino, R.; Gerace, E.L.; Mohammednetej, M.; Nosair, W.; Rattila, S.; Subic, A.Z.; Rolfes, R. Identification of Genes in *Candida glabrata* Conferring Altered Responses to Caspofungin, a Cell Wall Synthesis Inhibitor. *G3 (Bethesda).* **2016**, *6*, 2893–2907.

125. Chen, Y.L.; Konieczka, J.H.; Springer, D.J.; Bowen, S.E.; Zhang, J.; Silao, F.G.S.; Bungay, A.A.C.; Bigol, U.G.; Nicolas, M.G.; Abraham, S.N.; *et al.* Convergent Evolution of Calcineurin Pathway Roles in Thermotolerance and Virulence in *Candida glabrata*. *G3(Bethesda)* **2012**, *2*, 675–691.

126. Cota, J.M.; Grabinski, J.L.; Talbert, R.L.; Burgess, D.S.; Rogers, P.D.; Edlind, T.D.; Wiederhold, N.P. Increases in *SLT2* Expression and Chitin Content Are Associated with Incomplete Killing of *Candida glabrata* by Caspofungin. *Antimicrob. Agents Chemother.* **2008**, *52*, 1144–1146.

127. Islahudin, F.; Khozoie, C.; Bates, S.; Ting, K.N.; Pleass, R.J.; Avery, S. V. Cell Wall Perturbation Sensitizes Fungi to the Antimalarial Drug Chloroquine. *Antimicrob. Agents Chemother.* **2013**, *57*, 3889–3896.

128. Vermes, A.; Guchelaar, H.J.; Dankert, J. Flucytosine: a review of its pharmacology, clinical indications, pharmacokinetics, toxicity and drug interactions. *J. Antimicrob. Chemother.* **2000**, *46*, 171–179.

129. Duschinsky, R.; Pleven, E.; Heidelberger, C. The synthesis of 5-fluoropyrimidines. *J. Am. Chem. Soc.* **1957**, *79*, 4559–4560.

130. Waldorf, A.R.; Polak, A. Mechanisms of action of 5-fluorocytosine. *Antimicrob. Agents Chemother.* **1983**, *23*, 79–85.

131. Benson, J.M.; Nahata, M.C. Clinical use of systemic antifungal agents. *Clin. Pharm.* **1988**, *7*, 424–438.

132. Polak, A.; Grenson, M. Evidence for a Common Transport System for Cytosine, Adenine and Hypoxanthine in *Saccharomyces cerevisiae* and *Candida albicans*. *Eur. J. Biochem.* **1973**, *32*, 276–282.

133. Dowell, J.A.; Knebel, W.; Ludden, T.; Stogniew, M.; Krause, D.; Henkel, T. Population Pharmacokinetic Analysis of Anidulafungin, an Echinocandin Antifungal. *J. Clin. Pharmacol.* **2004**, *44*, 590–598.

134. Zhao, C.; Huang, T.; Chen, W.; Deng, Z. Enhancement of the diversity of polyoxins by a thymine-7-hydroxylase homolog outside the polyoxin biosynthesis gene cluster. *Appl. Environ. Microbiol.* **2010**, *76*, 7343–7347.

135. Robbins, N.; Wright, G.D.; Cowen, L.E. Antifungal Drugs: The Current Armamentarium and Development of New Agents. In *The Fungal Kingdom*; American Society of Microbiology **2016**, *4*, pp. 903–922.

136. Roger, C.; Sasso, M.; Lefrant, J.Y.; Muller, L. Antifungal Dosing Considerations in Patients Undergoing Continuous Renal Replacement Therapy. *Curr. Fungal Infect. Rep.* **2018**, *12*, 1–11.

137. Hope, W.W.; Tabernero, L.; Denning, D.W.; Anderson, M.J. Molecular Mechanisms of Primary Resistance to Flucytosine in *Candida albicans*. *Antimicrob. Agents Chemother.* **2004**, *48*, 4377–4386.

138. Chapeland-Leclerc, F.; Hennequin, C.; Papon, N.; Noel, T.; Girard, A.; Socie, G.; Ribaud, P.; Lacroix, C. Acquisition of Flucytosine, Azole, and Caspofungin Resistance in *Candida glabrata* Bloodstream Isolates Serially Obtained from a Hematopoietic Stem Cell Transplant Recipient. *Antimicrob. Agents Chemother*. **2010**, *54*, 1360–1362.

139. Vandeputte, P.; Pineau, L.; Larcher, G.; Noel, T.; Brèthes, D.; Chabasse, D.; Bouchara, J.-P. Molecular Mechanisms of Resistance to 5-Fluorocytosine in Laboratory Mutants of *Candida glabrata*. *Mycopathologia* **2011**, *171*, 11–21.

140. Costa, C.; Ponte, A.; Pais, P.; Santos, R.; Cavalheiro, M.; Yaguchi, T.; Chibana, H.; Teixeira, M.C. New mechanisms of flucytosine resistance in *C. glabrata* unveiled by a chemogenomics analysis in S. cerevisiae. *PLoS One* **2015**, *10*, e0135110.

141. Costa, C.; Henriques, A.; Pires, C.; Nunes, J.; Ohno, M.; Chibana, H.; Sá-Correia, I.; Teixeira, M.C. The dual role of *Candida glabrata* drug:H+ antiporter CgAqr1 (ORF *CAGL0J09944g*) in antifungal drug and acetic acid resistance. *Front. Microbiol.* **2013**, *4*, 170.

142. Mishra, N.N.; Prasad, T.; Sharma, N.; Payasi, A.; Prasad, R.; Gupta, D.K.; Singh, R. Pathogenicity and drug resistance in *Candida albicans* and other yeast species. A review. *Acta Microbiol. Immunol. Hung.* **2007**, *54*, 201-235.

143. Cannon, R.D.; Lamping, E.; Holmes, A.R.; Niimi, K.; Baret, P. V.; Keniya, M. V.; Tanabe, K.; Niimi, M.; Goffeau, A.; Monk, B.C. Efflux-mediated antifungal drug resistance. *Clin. Microbiol. Rev.* **2009**, *22*, 291-321.

144. Cavalheiro, M.; Pais, P.; Galocha, M.; Teixeira, M. Host-Pathogen Interactions Mediated by MDR Transporters in Fungi: As Pleiotropic as it Gets! *Genes (Basel).* **2018**, *9*, 332.

145. Costa, C.; Ribeiro, J.; Miranda, I.M.; Silva-Dias, A.; Cavalheiro, M.; Costa-de-Oliveira, S.; Rodrigues, A.G.; Teixeira, M.C. Clotrimazole Drug Resistance in *Candida glabrata* Clinical Isolates Correlates with Increased Expression of the Drug:H(+) Antiporters CgAqr1, CgTpo1_1, CgTpo3, and CgQdr2. *Front. Microbiol.* **2016**, *7*, 526.

146. Prasad, R.; Banerjee, A.; Khandelwal, N.K.; Dhamgaye, S. The ABCs of *Candida albicans* Multidrug Transporter Cdr1. *Eukaryot. Cell* **2015**, *14*, 1154–1164.

147. Pao, S.S.; Paulsen, I.T.; Saier, M.H. Major facilitator superfamily. *Microbiol. Mol. Biol. Rev.* **1998**, *62*, 1–34.

148. dos Santos, S.C.; Teixeira, M.C.; Dias, P.J.; Sá-Correia, I. MFS transporters required for multidrug/multixenobiotic (MD/MX) resistance in the model yeast: understanding their physiological function through post-genomic approaches. *Front. Physiol.* **2014**, *5*, 180.

149. Prasad, R.; Khandelwal, N.K.; Banerjee, A. Yeast ABC transporters in lipid trafficking. *Fungal Genet. Biol.* **2016**, *93*, 25–34.

150. Cannon, R.D.; Holmes, A.R. Learning the ABC of oral fungal drug resistance. *Mol. Oral Microbiol.* **2015**, *30*, 425–437.

151. Del Sorbo, G.; Schoonbeek, H.; De Waard, M.A. Fungal transporters involved in efflux of natural toxic compounds and fungicides. *Fungal Genet. Biol.* **2000**, *30*, 1–15.

152. Decottignies, A.; Grant, A.M.; Nichols, J.W.; de Wet, H.; McIntosh, D.B.; Goffeau, A. ATPase and multidrug transport activities of the overexpressed yeast ABC protein Yor1p. *J. Biol. Chem.* **1998**, *273*, 12612–22.

153. Bauer, B.E.; Wolfger, H.; Kuchler, K. Inventory and function of yeast ABC proteins: about sex, stress, pleiotropic drug and heavy metal resistance. *Biochim. Biophys. Acta* **1999**, *1461*, 217–36.

154. Balzi, E.; Wang, M.; Leterme, S.; Van Dyck, L.; Goffeau, A. *PDR5*, a novel yeast multidrug resistance conferring transporter controlled by the transcription regulator *PDR1*. *J. Biol. Chem.* **1994**, *269*, 2206–2214.

155. Bissinger, P.H.; Kuchler, K. Molecular cloning and expression of the *Saccharomyces cerevisiae STS1* gene product. A yeast ABC transporter conferring mycotoxin resistance. *J. Biol. Chem.* **1994**, *269*, 4180–4186.

156. Golin, J.; Ambudkar, S. V.; May, L. The yeast Pdr5p multidrug transporter: How does it recognize so many substrates? *Biochem. Biophys. Res. Commun.* **2007**, *356*, 1–5.

157. Hirata, D.; Yano, K.; Miyahara, K.; Miyakawa, T. *Saccharomyces cerevisiae YDR1*, which encodes a member of the ATP-binding cassette (ABC) superfamily, is required for multidrug resistance. *Curr. Genet.* **1994**, *26*, 285–94.

158. Ernst, R.; Klemm, R.; Schmitt, L.; Kuchler, K. Yeast ATP-Binding Cassette Transporters: Cellular Cleaning Pumps. In *Methods in enzymology* **2005**, *400*, pp. 460–484.

159. Miyahara, K.; Mizunuma, M.; Hirata, D.; Tsuchiya, E.; Miyakawa, T. The involvement of the *Saccharomyces cerevisiae* multidrug resistance transporters Pdr5p and Snq2p in cation resistance. *FEBS Lett.* **1996**, *399*, 317–20.

160. Gaur, M.; Choudhury, D.; Prasad, R. Complete Inventory of ABC Proteins in Human Pathogenic Yeast, *Candida albicans*. *J. Mol. Microbiol. Biotechnol.* **2005**, *9*, 3–15.

161. Dujon, B.; Sherman, D.; Fischer, G.; Durrens, P.; Casaregola, S.; Lafontaine, I.; de Montigny, J.; Marck, C.; Neuvéglise, C.; Talla, E.; *et al.* Genome evolution in yeasts. *Nature* **2004**, *430*, 35–44.

162. Nierman, W.C.; Pain, A.; Anderson, M.J.; Wortman, J.R.; Kim, H.S.; Arroyo, J.; Berriman, M.; Abe, K.; Archer, D.B.; Bermejo, C.; *et al.* Genomic sequence of the pathogenic and allergenic filamentous fungus *Aspergillus fumigatus*. *Nature* **2005**, *438*, 1151–1156.

163. Loftus, B.J.; Fung, E.; Roncaglia, P.; Rowley, D.; Amedeo, P.; Bruno, D.; Vamathevan, J.; Miranda, M.; Anderson, I.J.; Fraser, J.A.; *et al.* The Genome of the Basidiomycetous Yeast and Human Pathogen *Cryptococcus neoformans*. *Science* **2005**, *307*, 1321–1324.

164. Bennett, J.E.; Izumikawa, K.; Marr, K.A. Mechanism of increased fluconazole resistance in *Candida glabrata* during prophylaxis. *Antimicrob. Agents Chemother.* **2004**, *48*, 1773–1777.

165. Torelli, R.; Posteraro, B.; Ferrari, S.; La Sorda, M.; Fadda, G.; Sanglard, D.; Sanguinetti, M. The ATP-binding cassette transporter–encoding gene *CgSNQ2* is contributing to the *CgPDR1*-dependent azole resistance of *Candida glabrata*. *Mol. Microbiol.* **2008**, *68*, 186–201.

166. Slaven, J.W.; Anderson, M.J.; Sanglard, D.; Dixon, G.K.; Bille, J.; Roberts, I.S.; Denning, D.W. Increased expression of a novel *Aspergillus fumigatus* ABC transporter gene, atrF, in the presence of itraconazole in an itraconazole resistant clinical isolate. *Fungal Genet. Biol.* **2002**, *36*, 199–206.

167. Sionov, E.; Lee, H.; Chang, Y.C.; Kwon-Chung, K.J. *Cryptococcus neoformans* Overcomes Stress of Azole Drugs by Formation of Disomy in Specific Multiple Chromosomes. *PLoS Pathog.* **2010**, *6*, e1000848.

168. Enjalbert, B.; Smith, D.A.; Cornell, M.J.; Alam, I.; Nicholls, S.; Brown, A.J.P.; Quinn, J. Role of the Hog1 Stress-activated Protein Kinase in the Global Transcriptional Response to Stress in the Fungal Pathogen *Candida albicans*. *Mol. Biol. Cell* **2006**, *17*, 1018–1032.

169. Synnott, J.M.; Guida, A.; Mulhern-Haughey, S.; Higgins, D.G.; Butler, G. Regulation of the Hypoxic Response in *Candida albicans*. *Eukaryot. Cell* **2010**, *9*, 1734–1746.

170. Ogawa, A.; Hashida-Okado, T.; Endo, M.; Yoshioka, H.; Tsuruo, T.; Takesako, K.; Kato, I. Role of ABC transporters in aureobasidin A resistance. *Antimicrob. Agents Chemother.* **1998**, *42*, 755–61.

171. Vermitsky, J.P.; Earhart, K.D.; Smith, W.L.; Homayouni, R.; Edlind, T.D.; Rogers, P.D. Pdr1 regulates multidrug resistance in *Candida glabrata*: gene disruption and genome-wide expression studies. *Mol. Microbiol.* **2006**, *61*, 704–722.

172. Balan, I.; Alarco, A.M.; Raymond, M. The *Candida albicans CDR3* gene codes for an opaque-phase ABC transporter. *J. Bacteriol.* **1997**, *179*, 7210–7218.

173. Smriti; Krishnamurthy, S.; Dixit, B.L.; Gupta, C.M.; Milewski, S.; Prasad, R. ABC transporters Cdr1p, Cdr2p and Cdr3p of a human pathogen *Candida albicans* are general phospholipid translocators. *Yeast* **2002**, *19*, 303–318.

174. Higgins, C.F. Flip-flop: the transmembrane translocation of lipids. *Cell* **1994**, *79*, 393–395.

175. Nakayama, H.; Tanabe, K.; Bard, M.; Hodgson, W.; Wu, S.; Takemori, D.; Aoyama, T.; Kumaraswami, N.S.; Metzler, L.; Takano, Y.; *et al.* The *Candida glabrata* putative sterol transporter gene *CgAUS1* protects cells against azoles in the presence of serum. *J. Antimicrob. Chemother.* **2007**, *60*, 1264–1272.

176. Nagi, M.; Tanabe, K.; Ueno, K.; Nakayama, H.; Aoyama, T.; Chibana, H.; Yamagoe, S.; Umeyama, T.; Oura, T.; Ohno, H.; *et al.* The *Candida glabrata* sterol scavenging mechanism, mediated by the ATP-binding cassette transporter Aus1p, is regulated by iron limitation. *Mol. Microbiol.* **2013**, *88*, 371–381.

177. Kihara, A.; Igarashi, Y. Cross Talk between Sphingolipids and Glycerophospholipids in the Establishment of Plasma Membrane Asymmetry. *Mol. Biol. Cell* **2004**, *15*, 4949–4959.

178. Egner, R.; Mahé, Y.; Pandjaitan, R.; Kuchler, K. Endocytosis and vacuolar degradation of the plasma membrane-localized Pdr5 ATP-binding cassette multidrug transporter in Saccharomyces cerevisiae. *Mol. Cell. Biol.* **1995**, *15*, 5879–5887.

179. Holmes, A.R.; Cardno, T.S.; Strouse, J.J.; Ivnitski-Steele, I.; Keniya, M. V; Lackovic, K.; Monk, B.C.; Sklar, L.A.; Cannon, R.D. Targeting efflux pumps to overcome antifungal drug resistance. *Future Med. Chem.* **2016**, *8*, 1485–1501.

180. Gbelska, Y.; Krijger, J.J.; Breunig, K.D. Evolution of gene families: the multidrug resistance transporter genes in five related yeast species. *FEMS Yeast Res.* **2006**, *6*, 345–355.

181. Paulsen, I.T.; Brown, M.H.; Skurray, R.A. Proton-dependent multidrug efflux systems. *Microbiol. Rev.* **1996**, *60*, 575–608.

182. Sá-Correia, I.; dos Santos, S.C.; Teixeira, M.C.; Cabrito, T.R.; Mira, N.P. Drug:H+ antiporters in chemical stress response in yeast. *Trends Microbiol.* 2009, *17*, 22–31.

183. Costa, C.; Dias, P.J.; Sá-Correia, I.; Teixeira, M.C. MFS multidrug transporters in pathogenic fungi: Do they have real clinical impact? *Front. Physiol.* **2014**, *5*, 197.

184. Perea, S.; Lopez-Ribot, J.L.; Kirkpatrick, W.R.; McAtee, R.K.; Santillan, R.A.; Martinez, M.; Calabrese, D.; Sanglard, D.; Patterson, T.F. Prevalence of Molecular Mechanisms of Resistance to Azole Antifungal Agents in *Candida albicans* Strains Displaying High-Level Fluconazole Resistance Isolated from Human Immunodeficiency Virus-Infected Patients. *Antimicrob. Agents Chemother.* **2001**, *45*, 2676–2684.

185. Dunkel, N.; Blaß, J.; Rogers, P.D.; Morschhäuser, J. Mutations in the multi-drug resistance regulator *MRR1*, followed by loss of heterozygosity, are the main cause of *MDR1* overexpression in fluconazole-resistant *Candida albicans* strains. *Mol. Microbiol.* **2008**, *69*, 827–840.

186. Popp, C.; Hampe, I.A.I.; Hertlein, T.; Ohlsen, K.; Rogers, P.D.; Morschhäuser, J. Competitive Fitness of Fluconazole-Resistant Clinical *Candida albicans* Strains. *Antimicrob. Agents Chemother.* **2017**, *61*, e00584-17.

187. Hiller, D.; Sanglard, D.; Morschhauser, J. Overexpression of the *MDR1* Gene Is Sufficient To Confer Increased Resistance to Toxic Compounds in *Candida albicans*. *Antimicrob. Agents Chemother.* **2006**, *50*, 1365–1371.

188. Fling, M.E.; Kopf, J.; Tamarkin, A.; Gorman, J.A.; Smith, H.A.; Koltin, Y. Analysis of a *Candida albicans* gene that encodes a novel mechanism for resistance to benomyl and methotrexate. *Mol. Gen. Genet.* **1991**, *227*, 318–29.

189. Calabrese, D.; Sanglard, D.; Bille, J. A novel multidrug efflux transporter gene of the major facilitator superfamily from *Candida albicans* (*FLU1*) conferring resistance to fluconazole. *Microbiology* **2000**, *146*, 2743–2754.

190. Park, S.; Perlin, D.S. Establishing Surrogate Markers for Fluconazole Resistance in *Candida albicans*. *Microb. Drug Resist.* **2005**, *11*, 232–238.

191. Romão, D.; Cavalheiro, M.; Mil-Homens, D.; Santos, R.; Pais, P.; Costa, C.; Takahashi-Nakaguchi, A.; Fialho, A.M.; Chibana, H.; Teixeira, M.C. A New Determinant of *Candida glabrata* Virulence: The Acetate Exporter CgDtr1. *Front. Cell. Infect. Microbiol.* **2017**, *7*, 473.

192. Karababa, M.; Coste, A.T.; Rognon, B.; Bille, J.; Sanglard, D. Comparison of gene expression profiles of *Candida albicans* azole-resistant clinical isolates and laboratory strains exposed to drugs inducing multidrug transporters. *Antimicrob. Agents Chemother.* **2004**, *48*, 3064–3079.

193. Courey, A.J.; Jia, S. Transcriptional repression: the long and the short of it. *Genes Dev.* **2001**, *15*, 2786–2796.

194. Smith, R.L.; Johnson, A.D. Turning genes off by Ssn6-Tup1: a conserved system of transcriptional repression in eukaryotes. *Trends Biochem. Sci.* **2000**, *25*, 325–330.

195. Khakhina, S.; Simonicova, L.; Moye-Rowley, W.S. Positive autoregulation and repression of transactivation are key regulatory features of the *Candida glabrata* Pdr1 transcription factor. *Mol. Microbiol.* **2018**, *107*, 747–764.

196. Whitmarsh, A.J.; Davis, R.J. Regulation of transcription factor function by phosphorylation. *Cell. Mol. Life Sci.* **2000**, *57*, 1172–1183.

197. Okazaki, S.; Tachibana, T.; Naganuma, A.; Mano, N.; Kuge, S. Multistep Disulfide Bond Formation in Yap1 Is Required for Sensing and Transduction of H_2O_2 Stress Signal. *Mol. Cell* **2007**, *27*, 675–688.

198. Kuge, S.; Jones, N.; Nomoto, A. Regulation of yAP-1 nuclear localization in response to oxidative stress. *EMBO J.* **1997**, *16*, 1710–1720.

199. Martínez-Pastor, M.T.; Marchler, G.; Schüller, C.; Marchler-Bauer, A.; Ruis, H.; Estruch, F. The *Saccharomyces cerevisiae* zinc finger proteins Msn2p and Msn4p are required for transcriptional induction through the stress response element (STRE). *EMBO J.* **1996**, *15*, 2227–2235.

200. Schmitt, A.P.; McEntee, K. Msn2p, a zinc finger DNA-binding protein, is the transcriptional activator of the multistress response in *Saccharomyces cerevisiae*. *Proc. Natl. Acad. Sci.* **1996**, *93*, 5777–5782.

201. Teixeira, M.C. Complex Regulatory Interplay Between Multidrug Resistance and Oxidative Stress Response in Yeast: The *FLR1* Regulatory Network as a Systems Biology Case-Study. In *Oxidative Stress - Molecular Mechanisms and Biological Effects*; InTech, **2012**, pp. 323-340.

202. Wu, A.; Wemmie, J.A.; Edgington, N.P.; Goebl, M.; Guevara, J.L.; Moye-Rowley, W.S. Yeast bZip proteins mediate pleiotropic drug and metal resistance. *J. Biol. Chem.* **1993**, *268*, 18850–18858.

203. Tsai, H.F.; Sammons, L.R.; Zhang, X.; Suffis, S.D.; Su, Q.; Myers, T.G.; Marr, K.A.; Bennett, J.E. Microarray and molecular analyses of the azole resistance mechanism in *Candida glabrata* oropharyngeal isolates. *Antimicrob. Agents Chemother.* **2010**, *54*, 3308–3317.

204. Chen, K.H.; Miyazaki, T.; Tsai, H.F.; Bennett, J.E. The bZip transcription factor Cgap1p is involved in multidrug resistance and required for activation of multidrug transporter gene *CgFLR1* in *Candida glabrata*. *Gene* **2007**, *386*, 63–72.

205. Noble, J.A.; Tsai, H.F.; Suffis, S.D.; Su, Q.; Myers, T.G.; Bennett, J.E. *STB5* is a negative regulator of azole resistance in *Candida glabrata*. *Antimicrob. Agents Chemother.* **2013**, *57*, 959–967.

206. Singh, R.P.; Prasad, H.K.; Sinha, I.; Agarwal, N.; Natarajan, K. Cap2-HAP complex is a critical transcriptional regulator that has dual but contrasting roles in regulation of iron homeostasis in *Candida albicans*. *J. Biol. Chem.* **2011**, *286*, 25154-25170.

207. Coste, A.T.; Karababa, M.; Ischer, F.; Bille, J.; Sanglard, D. *TAC1*, Transcriptional Activator of *CDR* Genes, Is a New Transcription Factor Involved in the Regulation of *Candida albicans* ABC Transporters *CDR1* and *CDR2*. *Eukaryot. Cell* **2004**, *3*, 1639–1652.

208. Coste, A.T.; Crittin, J.; Bauser, C.; Rohde, B.; Sanglard, D. Functional Analysis of *cis* - and *trans* -Acting Elements of the *Candida albicans CDR2* Promoter with a Novel Promoter Reporter System. *Eukaryot. Cell* **2009**, *8*, 1250–1267.

209. Coste, A.; Selmecki, A.; Forche, A.; Diogo, D.; Bougnoux, M.E.; D'Enfert, C.; Berman, J.; Sanglard, D. Genotypic evolution of azole resistance mechanisms in sequential Candida albicans isolates. *Eukaryot. Cell* **2007**, *6*, 1889–1904.

210. Liu, T.T.; Znaidi, S.; Barker, K.S.; Xu, L.; Homayouni, R.; Saidane, S.; Morschhäuser, J.; Nantel, A.; Raymond, M.; Rogers, P.D. Genome-wide expression and location analyses of the *Candida albicans* Tac1p regulon. *Eukaryot. Cell* **2007**, *6*, 2122–2138.

211. Znaidi, S.; De Deken, X.; Weber, S.; Rigby, T.; Nantel, A.; Raymond, M. The zinc cluster transcription factor Tac1p regulates *PDR16* expression in *Candida albicans*. *Mol. Microbiol.* **2007**, *66*, 440–452.

212. Morschhäuser, J.; Barker, K.S.; Liu, T.T.; Blaß-Warmuth, J.; Homayouni, R.; Rogers, P.D. The Transcription Factor Mrr1p Controls Expression of the *MDR1* Efflux Pump and Mediates Multidrug Resistance in *Candida albicans*. *PLoS Pathog.* **2007**, *3*, e164.

213. Schubert, S.; Barker, K.S.; Znaidi, S.; Schneider, S.; Dierolf, F.; Dunkel, N.; Aïd, M.; Boucher, G.; Rogers, P.D.; Raymond, M.; *et al.* Regulation of efflux pump expression and drug resistance by the transcription factors Mrr1, Upc2, and Cap1 in *Candida albicans*. *Antimicrob. Agents Chemother.* **2011**, *55*, 2212–2223.

214. Mogavero, S.; Tavanti, A.; Senesi, S.; Rogers, P.D.; Morschhäuser, J. Differential Requirement of the Transcription Factor Mcm1 for Activation of the *Candida albicans* Multidrug Efflux Pump *MDR1* by Its Regulators Mrr1 and Cap1. *Antimicrob. Agents Chemother.* **2011**, *55*, 2061–2066.

215. Schillig, R.; Morschhäuser, J. Analysis of a fungus-specific transcription factor family, the *Candida albicans* zinc cluster proteins, by artificial activation. *Mol. Microbiol.* **2013**, *89*, 1003–1017.

216. Silva, A.P.; Miranda, I.M.; Guida, A.; Synnott, J.; Rocha, R.; Silva, R.; Amorim, A.; Pina-Vaz, C.; Butler, G.; Rodrigues, A.G. Transcriptional profiling of azole-resistant *Candida parapsilosis* strains. *Antimicrob. Agents Chemother.* **2011**, *55*, 3546–3556.

217. Coste, A.T.; Ramsdale, M.; Ischer, F.; Sanglard, D. Divergent functions of three *Candida albicans* zinc-cluster transcription factors (*CTA4, ASG1* and *CTF1*) complementing pleiotropic drug resistance in Saccharomyces cerevisiae. *Microbiology* **2008**, *154*, 1491–1501.

218. Chiranand, W.; McLeod, I.; Zhou, H.; Lynn, J.J.; Vega, L.A.; Myers, H.; Yates, J.R.; Lorenz, M.C.; Gustin, M.C. *CTA4* Transcription Factor Mediates Induction of Nitrosative Stress Response in *Candida albicans*. *Eukaryot. Cell* **2008**, *7*, 268–278.

219. Kelly, S.L.; Lamb, D.C.; Corran, A.J.; Baldwin, B.C.; Kelly, D.E. Mode of Action and Resistance to Azole Antifungals Associated with the Formation of 14α-Methylergosta-8,24(28)-dien-3β,6α-diol. *Biochem. Biophys. Res. Commun.* **1995**, *207*, 910–915.

220. Ghannoum, M.A.; Rice, L.B. Antifungal agents: mode of action, mechanisms of resistance, and correlation of these mechanisms with bacterial resistance. *Clin. Microbiol. Rev.* **1999**, *12*, 501–517.

221. Kanafani, Z.A.; Perfect, J.R. Resistance to Antifungal Agents: Mechanisms and Clinical Impact. *Clin. Infect. Dis.* **2008**, *46*, 120–128.

222. Silver, P.M.; Oliver, B.G.; White, T.C. Role of *Candida albicans* Transcription Factor Upc2p in Drug Resistance and Sterol Metabolism. *Eukaryot. Cell* **2004**, *3*, 1391–1397.

223. Guida, A.; Lindstädt, C.; Maguire, S.L.; Ding, C.; Higgins, D.G.; Corton, N.J.; Berriman, M.; Butler, G. Using RNA-seq to determine the transcriptional landscape and the hypoxic response of the pathogenic yeast *Candida parapsilosis*. *BMC Genomics* **2011**, *12*, 628.

224. Nagi, M.; Nakayama, H.; Tanabe, K.; Bard, M.; Aoyama, T.; Okano, M.; Higashi, S.; Ueno, K.; Chibana, H.; Niimi, M.; *et al.* Transcription factors *CgUPC2A* and *CgUPC2B* regulate ergosterol biosynthetic genes in *Candida glabrata*. *Genes to Cells* **2011**, *16*, 80–89.

225. Maguire, S.L.; Wang, C.; Holland, L.M.; Brunel, F.; Neuvéglise, C.; Nicaud, J.M.; Zavrel, M.; White, T.C.; Wolfe, K.H.; Butler, G. Zinc Finger Transcription Factors Displaced SREBP Proteins as the Major Sterol Regulators during Saccharomycotina Evolution. *PLoS Genet.* **2014**, *10*, e1004076.

226. Mellado, E.; Garcia-Effron, G.; Buitrago, M.J.; Alcazar-Fuoli, L.; Cuenca-Estrella, M.; Rodriguez-Tudela, J.L. Targeted Gene Disruption of the 14- Sterol Demethylase (*cyp51A*) in *Aspergillus fumigatus* and Its Role in Azole Drug Susceptibility. *Antimicrob. Agents Chemother.* **2005**, *49*, 2536–2538.

227. Willger, S.D.; Puttikamonkul, S.; Kim, K.H.; Burritt, J.B.; Grahl, N.; Metzler, L.J.; Barbuch, R.; Bard, M.; Lawrence, C.B.; Cramer, R.A. A Sterol-Regulatory Element Binding Protein Is Required for Cell Polarity, Hypoxia Adaptation, Azole Drug Resistance, and Virulence in *Aspergillus fumigatus*. *PLoS Pathog.* **2008**, *4*, e1000200.

228. Moye-Rowley, W.S. Multiple mechanisms contribute to the development of clinically significant azole resistance in *Aspergillus fumigatus*. *Front. Microbiol.* **2015**, *6*, 70.

229. Chung, D.; Barker, B.M.; Carey, C.C.; Merriman, B.; Werner, E.R.; Lechner, B.E.; Dhingra, S.; Cheng, C.; Xu, W.; Blosser, S.J.; *et al.* ChIP-seq and In Vivo Transcriptome Analyses of the *Aspergillus fumigatus* SREBP SrbA Reveals a New Regulator of the Fungal Hypoxia Response and Virulence. *PLoS Pathog.* **2014**, *10*, e1004487.

230. Chun, C.D.; Liu, O.W.; Madhani, H.D. A Link between Virulence and Homeostatic Responses to Hypoxia during Infection by the Human Fungal Pathogen *Cryptococcus neoformans*. *PLoS Pathog.* **2007**, *3*, e22.

231. Bien, C.M.; Chang, Y.C.; Nes, W.D.; Kwon-Chung, K.J.; Espenshade, P.J. *Cryptococcus neoformans* Site-2 protease is required for virulence and survival in the presence of azole drugs. *Mol. Microbiol.* **2009**, *74*, 672–690.

232. Jung, K.W.; Yang, D.H.; Maeng, S.; Lee, K.T.; So, Y.S.; Hong, J.; Choi, J.; Byun, H.J.; Kim, H.; Bang, S.; *et al.* Systematic functional profiling of transcription factor networks in *Cryptococcus neoformans*. *Nat. Commun.* **2015**, *6*, 6757.

233. Chang, Y.C.; Bien, C.M.; Lee, H.; Espenshade, P.J.; Kwon-Chung, K.J. Sre1p, a regulator of oxygen sensing and sterol homeostasis, is required for virulence in *Cryptococcus neoformans*. *Mol. Microbiol.* **2007**, *64*, 614–629.

2 The PathoYeastract database: an information system for the analysis of gene and genomic transcription regulation in pathogenic yeasts.

This chapter contains results published in:

Monteiro, P. T., Pais, P., Costa, C., Manna, S., Sá-Correia, I., Teixeira, M.C. 2017. The PathoYeastract database: an information system for the analysis of gene and genomic transcription regulation in pathogenic yeasts. *Nucleic Acids Res*, **45:**D597-D603.

The PhD candidate contributed to the work detailed in this chapter by collecting the published data on transcriptional regulatory networks in *Candida* species that constitutes the documented data present in the database. This chapter details the original publication of the 2017 PathoYeastract database release, comprising 28,000 regulatory associations between transcription factors and target genes in *Candida albicans* and *Candida glabrata*. Since then, the database has been regularly updated with the most recent data and upgraded to include the species *Candida parapsilosis* and *Candida tropicalis* as well. The candidate also contributed for the up-to-date maintenance and expansion of the database. At this time, PathoYeastract counts with more than 49 000 regulatory associations across the four species.

2.1 Abstract

We present the PATHOgenic YEAst Search for Transcriptional Regulators And Consensus Tracking (PathoYeastract - http://pathoyeastract.org) database, a tool for the analysis and prediction of transcription regulatory associations at the gene and genomic levels in the pathogenic yeasts *Candida albicans* and *C. glabrata*.

Upon data retrieval from hundreds of publications, followed by curation, the database currently includes 28,000 unique documented regulatory associations between transcription factors (TF) and target genes and 107 DNA binding sites, considering 134 TFs in both species. Following the structure used for the YEASTRACT database, PathoYeastract makes available bioinformatics tools that enable the user to exploit the existing information to predict the TFs involved in the regulation of a gene or genome-wide transcriptional response, while ranking those TFs in order of their relative importance. Each search can be filtered based on the selection of specific environmental conditions, experimental evidence or positive/negative regulatory effect. Promoter analysis tools and interactive visualization tools for the representation of TF regulatory networks are also provided.

The PathoYeastract database further provides simple tools for the prediction of gene and genomic regulation based on orthologous regulatory associations described for other yeast species, a comparative genomics setup for the study of cross-species evolution of regulatory networks.

2.2 Introduction

Candida species are recognized as the 4th most common cause of nosocomial infections [1]. Candidiasis is considered to be responsible for more than 400,000 life-threatening infections worldwide every year. The frequency and relative high mortality levels (up to 45% for *Candida glabrata*) of these infections [2] are generally attributed to the capacity of these pathogenic yeasts to efficiently develop multidrug resistance (MDR), to tolerate host defence mechanisms, to maintain high proliferative and repopulation capacity through biofilm formation, and to activate invasive growth related genes [3,4].

Since clinically evolved phenotypes can be seen as a long term genetic stabilization of the normal transient response to new environments [5], it is essential to understand the structure and functioning of the transcription networks regulating the early response to clinically relevant environmental changes, in *Candida* species, to be able to understand and circumvent the long term acquisition of virulence and drug resistance-related phenotypes. For example, MDR acquisition in clinical isolates is often related to the high expression levels of multidrug transporters [6,7], occurring as a consequence of point mutations in MDR-related transcription factors (TFs), including *C. glabrata* Pdr1 or *C. albicans* Tac1 and Mrr1 [8]. Similarly, other infection-relevant phenomena, such as biofilm formation or tissue invasion, also occur under the control of transcription factors such as *C. albicans* Efg1 and Cph1 [9] or Cph2, Tec1 and Czf1, respectively [10]. However, the transcriptional control of infection-related phenomena appears to be much more complex than predicted. For example, it has been recently demonstrated that the carbon source in which *Candida* cells proliferate has deep impact in drug resistance and phagocytosis [11]. Additionally, a significant number of clinical isolates, especially from non-*albicans Candida* species, that evolved to become drug resistant or virulent, have often been found not to display the "typical" molecular markers associated to these phenotypes [3,12,13], showing that there is still a lot to learn in terms of the vast array of evolutionary paths that a fungal cell can undergo to reach a given infection-related phenotype.

The PathoYeastract database has been developed to provide researchers and clinicians working in the field of fungal infections with a tool to obtain a more complete understanding of the complex regulatory control that underlies the biology, pathogenicity and drug resistance capabilities of *Candida* species. Other important

pathogenic yeasts, including those from the *Cryptococcus* and *Rhodotorula* genus, were not considered in PathoYeastract. This new information system follows the footsteps of the YEASTRACT (http://yeastract.com) database that has provided to the public up-to-date information on documented regulatory associations between TFs and target genes, as well as between TFs and DNA binding sites, in *S. cerevisiae* [14–17]. However, it goes beyond YEASTRACT as it extends to pathogenic yeasts and provides the chance to run inter-species comparison of regulatory networks. Other databases focused on transcriptional regulation in yeasts and other organisms do exist, including TRANSFAC [18] or RSAT [19], but focus most of their analysis and predictive power on the understanding of promoter regions. Besides providing tools for promoter analysis in yeast, PathoYeastract is, to the best of our knowledge, the single information system that offers a complete integration of all the experimentally validated transcriptional regulatory data ever published for *C. albicans* and *C. glabrata*.

Side by side with the collected data, PathoYeastract offers an array of queries that enable users to extract the most out of the existing data. Specifically, tools are offered to predict the transcription factors that control a given transcriptional response, at the gene or at the genomic scales, suitable for the analysis of transcriptomics data. Moreover, bioinformatics tools to predict transcriptional associations based on the knowledge gathered for better known yeast species, including *S. cerevisiae* and *C. albicans* have also been devised, to compensate for the current lack of knowledge of similar processes in less well characterized yeast species, such as *C. glabrata*. These new tools provide the required backbone to be able to run cross-species comparison of transcription regulatory networks, which is expected to bring more light into the evolution of *Candida* species as competent human pathogens.

2.3 Data Collection

In its first release, PathoYeastract gathers all available (and reliable) information on transcriptional associations for the two most prevalent of pathogenic *Candida* species: *C. albicans* and *C. glabrata*.

Basic information on gene and promoter sequence, amino acid sequence and a functional description for every *C. albicans* and *C. glabrata* genes/proteins were downloaded from the Candida Genome Database (http://candidagenome.org) [20].

Promoter sequences were considered to be the first 1000bp upstream of the START codon. Additionally, Gene Ontology terms associated to all the *C. albicans* and *C. glabrata* genes/proteins, and their hierarchy, were retrieved from the GO consortium database [21,22].

The genomes of *C. albicans* and *C. glabrata* are predicted to encode 163 and 117 transcription factors, respectively. An extensive literature survey was conducted to retrieve all the available information on associations between these transcription factors and their target genes. For each paper describing TF DNA binding results or transcription data, in the dependence of a TF, the data was collected based on the criteria used by the paper authors, validated by the review process. In each case, the experimental basis of the associations between TFs and target genes was included in the database. The underlying experimental evidence was also collected and classified as either *DNA Binding* or *Expression Evidence*. *DNA Binding Evidence* was considered to be provided through: experiments directly measuring the binding of the TF to the promoter region of the target gene (e.g. Chromatin ImmunoPrecipitation (ChIP), ChIP-on-chip, ChIP-seq and Electrophoretic Mobility Shift Assay (EMSA)); or the analysis of the effect on target-gene expression of the site-directed mutation of the TF binding site in its promoter region, as strongly suggesting an interaction of the TF with that specific target promoter. *Expression Evidence* classification was attributed to experiments such as the comparative analysis of gene expression changes occurring in response to the deletion, mutation or over-expression of a given TF, based on experimental techniques that include quantitative RT-PCR, microarray analysis, RNA sequencing or expression proteomics. In the case of *Expression Evidence*-based data the effect of the transcription factor in the target gene expression was registered as positive or negative, as it may help to discard indirect effects of TF expression. Specific gene expression levels are not included in PathoYeastract at this time. Based on this classification, PathoYeastract contains a total of 12,224 regulatory associations based on DNA-binding evidence and 24,752 on expression evidence, with some overlap. Altogether, PathoYeastract includes in its July 2016 release 2,170 associations between TF and target genes in *C. glabrata*, including 1,818 unique TF-target gene pairs, based in 76 different publications, and 34,806 associations between TF and target genes in *C. albicans*, including 26,473 unique TF-target gene pairs, based in 671 different publications.

Information on associations between transcription factors and TF binding sites in both *C. albicans* and *C. glabrata* was also gathered. In the *C. glabrata* case, 11 TF have been associated with a recognized consensus nucleotide sequence, predicted based on the use of motif finding algorithms and in some cases experimentally validated (e.g. CgAmt1 [23] and CgPdr1 [24], using DNAse I footprinting assays). For *C. albicans*, a DNA binding motif has been appointed for 40 TFs, again most of which based only using bioinformatic predictions.

In all cases, the environmental condition in which the regulatory association was found to occur was included in the database, as the occurrence of these associations is extremely dependent on environmental stimuli. Published regulation data was found to be associated to a total of 995 different environmental conditions, which were then clustered into 12 groups, including: biofilm formation, carbon source quality/availability, cell cycle/morphology, human niche conditions, in vitro, ion/metal/phosphate/sulphur/vitamin availability, lipid supplementation, nitrogen source quality/availability, oxygen availability, pathogenicity, stress and unstressed log-phase growth (control). Each of these clusters is composed by sub-clusters to enable a finer filtering of the existing regulatory associations.

All TF-target gene or TF-TF binding site pairs included in the database are associated to at least one publication, whose reference and pubmed link is automatically provided.

2.4 Predicting gene and genomic regulation

The PathoYeastract database is equipped with several simple queries that aim at enabling its users to easily extract relevant information from the total underlying data. Those queries were built in a way as to respond to typical questions that a yeast biologist/research clinician may pose.

The simplest queries enable the user to obtain all the transcription factors that regulate a given gene or all the genes which are regulated by a given TF. This query can be set to rely on documented regulation data, herein coined “documented regulation”, or in prediction based on the occurrence of putative TF binding sites in the promoter region of the gene of interest, herein coined “potential regulation”. This may be extremely useful when trying to predict the function of an uncharacterized target gene/TF. For

example, the recently characterized *C. albicans* Qdr1-3 proteins, predicted to act as Drug:H+ Antiporters (DHA) of the Major Facilitator Superfamily, were shown to play instead overlapping roles in *C. albicans* virulence [25]. Using the Search by TF query in PathoYeastract it is possible to predict all the TFs that may play a role in the control of the transcription of QDR genes (Figure 2.1). Interestingly, none of the Qdr encoding genes has been shown to be controlled by the *C. albicans* multidrug resistance transcription factors Tac1 or Mrr1. Surprisingly, these three genes are associated to a rather disparate set of transcription factors. Based on the PathoYeastract analysis, CaQdr1 has been shown to be controlled by 17 different TFs, while CaQdr2 is only known to be regulated by the CaMcm1 TF, that regulates hyphal growth, and only three TF are known to control the expression of CaQdr3: CaMcm1, CaHap43, related to the control of iron homeostasis, and CaTbf1, an essential transcriptional activator that regulates ribosomal protein genes (Figure 2.1A). The transcriptional control of these homologous genes suggests, not only that indeed they play no direct role in drug resistance, but also strongly point to the hypothesis that they may serve more than paralogous roles. Indeed, the fact that *C. albicans* has 3 QDR genes in its genome sequence further suggests as much, especially, when compared to *C. glabrata* which exhibits only one QDR gene, *CgQDR2*, recently shown to play a role in azole drug resistance [26]. Interestingly, using the search for TF query in PathoYeastract the *C. glabrata QDR2* gene can be seen to be solely regulated by CgPdr1, as far as current knowledge goes, CgPdr1 being the main regulator of azole drug resistance in this yeast species (Figure 2.1B).

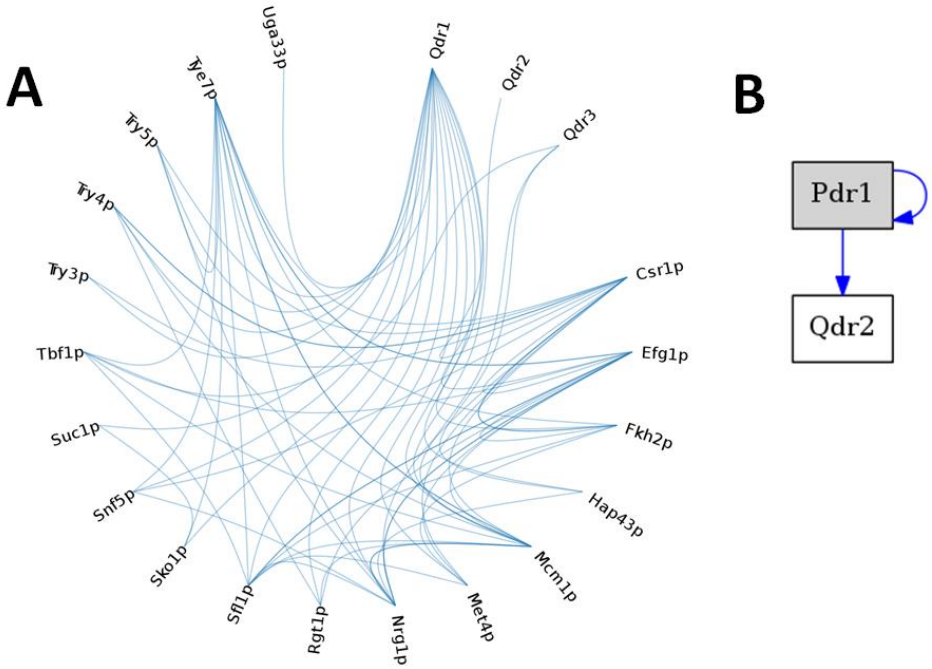

Figure 2.1 - Regulation of the QDR genes in *C. albicans* (A) and in *C. glabrata* (B).

Alternatively, using the "Search for Genes" query it is possible to pinpoint all the genes that have been shown to be regulated by a given transcription factor. Keeping to the drug resistance case study, using this tool it is possible to observe that there are 399 genes known to be regulated by the *C. glabrata* Pdr1 TF, whereas there are only 45 genes known to be regulated by the *C. albicans* Tac1 TF (Figure 2.2). Interestingly, the list of genes whose expression is controlled by CgPdr1 or CaTac1 is also quite diverse in terms of associated functions, far beyond the classical targets, the multidrug efflux pumps of the ATP-Binding Cassette superfamily Cdr1 and Cdr2. Both lists include shared genes and functions, such as Hsp12, a stress resistance related protein chaperone, the Erg11 gene, the target of azole antifungal drugs, but also genes associated to central metabolic pathways. For example, *CaADH1* and *CaSNZ1* were identified as targets of the CaTac1 TF, being related to central carbon metabolism and vitamin B synthesis, respectively. This observation raises the possibility of either CaTac1 playing additional roles in *C. albicans* biology or that CaAdh1 and CaSnz1 contribute somehow to drug resistance.

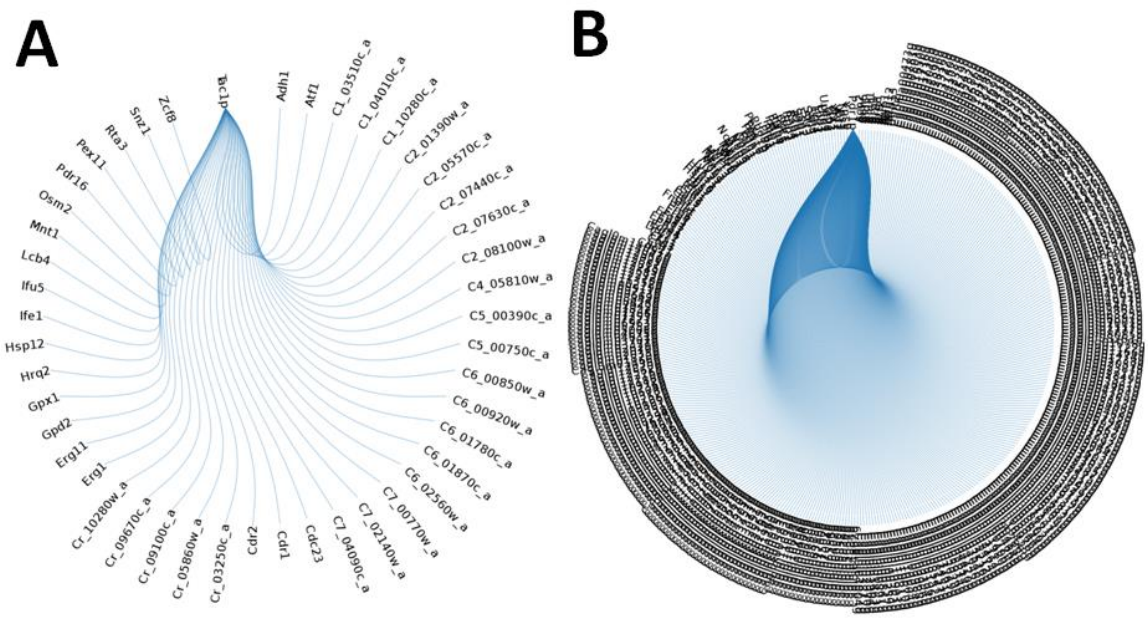

Figure 2.2 – The Tac1 / Pdr1 putative regulon in *C. albicans* (A) / *C. glabrata* (B) as obtained using the "Search for target genes" in the PathoYeastract database.

2.5 Analysing genome-wide expression data

One of the key uses of the regulatory data present in the PathoYeastract database is to predict the TF regulatory network that controls a given genome-wide expression remodelling. Specifically, the query "Rank by TF" was designed to accept as input a list of genes, for example the set of genes upregulated in a given condition, as obtained by RNA sequencing or microarray analysis, providing as output the TFs that regulate the user's gene list, ranked by relative importance. For example, a recent study on the role of the *C. glabrata* Yap1 TF, a master regulator of the oxidative stress response in yeasts, provided a list of 70 genes which are upregulated in *C. glabrata* cells exposed to stress induced by selenium, under the control of CgYap1 [27]. Using the "Rank by TF" query to analyse the same list, it is possible to observe that besides CgYap1, 14 other TFs play a role in the regulation of this gene list, suggesting that the network of TF responsible for the transcriptional remodelling occurring in these cells is much more complex than initially foreseen (Figure 2.3).

The authors of the paper describing the role of CgYap1 in the *C. glabrata* selenium response focused on the participation of some of the Yap1 homologs [27], however, TFs

such as CgPdr1, CgSkn7 or even the uncharacterized TFs encoded by ORF *CAGL0I07755g* (an homologue of the salt stress related *S. cerevisiae* Hal9 TF) or ORF *CAGL0G08844g* (an homologue of the cell wall stress related *S. cerevisiae* Asg1 TF) also appear highly ranked in this query, as they are required for the transcriptional control of more than 10% of the dataset in analysis. This result appears to suggest that selenium stress induces toxicity at several levels, beyond oxidative stress, thus activating an array of TF that control various biological functions required for *C. glabrata* cells to cope with selenium stress.

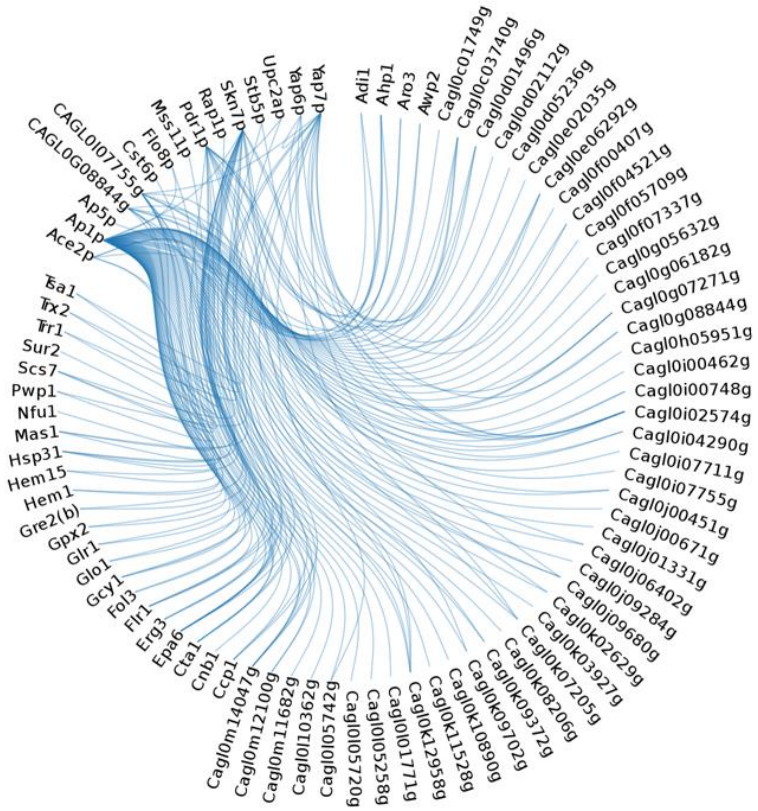

Figure 2.3 – The TF regulatory network predicted to control the Yap1-dependent response to selenium stress in *C. glabrata*, based on the PathoYeastract "Rank by TF" tool.

2.6 Predicting transcriptional regulation based on orthologous transcription regulatory networks in different yeast species

The fact that PathoYeastract comprises regulatory information on two *Candida* species enables the possibility to run cross-species comparison in terms of regulatory associations. The potential of this approach is further increased when considering the ability to further access regulatory data on the model yeast *Saccharomyces cerevisiae* in the YEASTRACT database. Such a comparison can be made at the gene, but also genomic level.

Picking up the example above, focused on the regulation of the *C. glabrata QDR2* gene [26], the Search by TF query offers the possibility to predict the transcriptional control of this gene based on the transcription of their orthologous genes in either *C. albicans* or *S. cerevisiae* (Figure 2.4). Using this query it is possible to highlight the fact that, although *C. glabrata QDR2* gene is only known to be regulated by a single TF, CgPdr1, its homologs in *C. albicans* and *S. cerevisiae* are known to be regulated by 10 and 18 TFs for which there are orthologs in *C. glabrata*, respectively. This comparison may provide interesting clues, pointing out to which additional TFs may be involved in the regulation of the *C. glabrata QDR2* gene. Additionally, the comparison between the TF network that controls *CgQDR2* regulation in these three related yeast species may provide an interesting setup for the prediction of gene regulation evolution. In this case, the regulation of *CgQDR2* appears to have diverged significantly within the three species, as there is not a single TF known to be shared by the QDR genes in the three yeast species. It is important to point out, however, that the amount of data collected for the regulation of *CgQDR2* in *C. glabrata* is resumed to a single bibliographic reference, suggesting that many more regulators of the *C. glabrata QDR2* may still be uncovered. Nonetheless, the observed variability in terms of *CgQDR2* regulation within the three species appears consistent with the fact that the function of the *CgQDR2* gene appears also to have diverged within these yeasts [25,26,28–30].

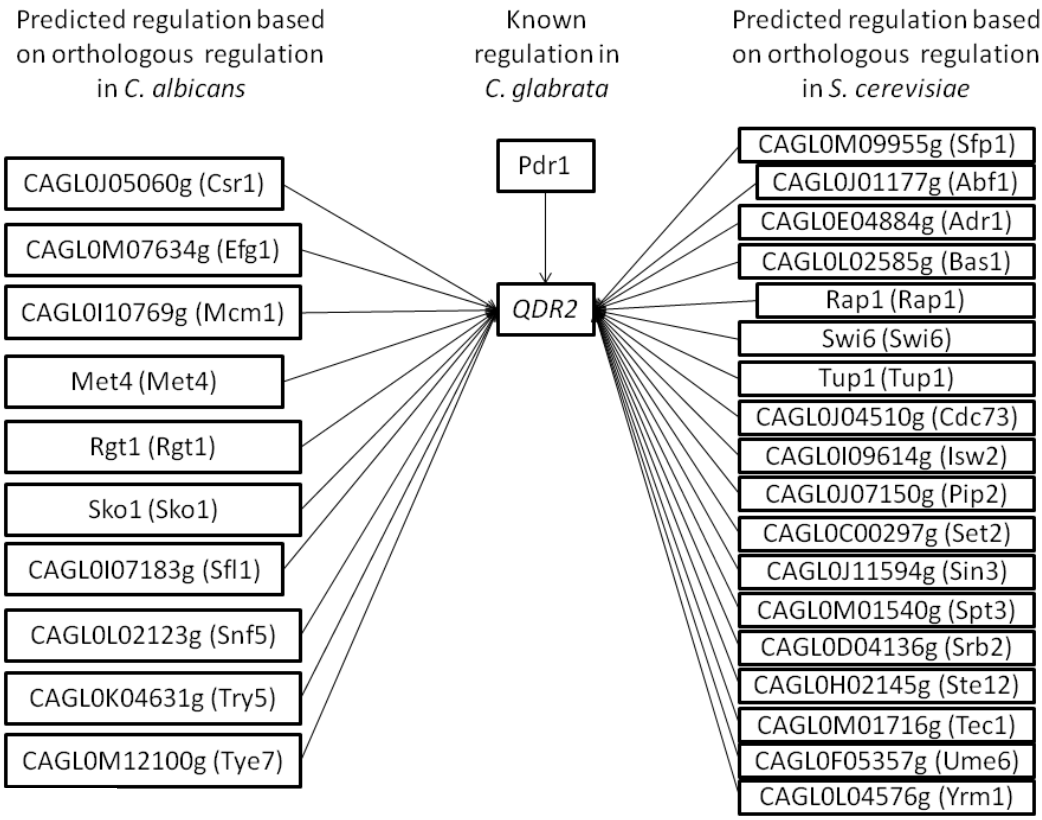

Figure 2.4 – Prediction the TFs that regulate the *C. glabrata QDR2* gene, based on knowledge gathered in *C. glabrata* or on knowledge gathered for the regulation of orthologous genes in *S. cerevisiae* and *C. albicans*, as deposited in the PathoYeastract and YEASTRACT.

2.7 Future Directions

The PathoYeastract team is committed to continue to offer updated, reliable and complete information on the field of transcriptional regulation in pathogenic yeasts to the international community working in the molecular basis of candidemia and its prophylaxis and treatment. Furthermore, the possibility to run a systematic inter-species comparison of transcription regulatory networks in different yeast will continue to be developed, especially through the development of more complex dedicated tools and the extension of the PathoYeastract database to other relevant pathogenic yeasts, including *Candida parapsilosis* and *C. dubliniensis*, but also *C. orthopsilosis*, *C. krusei* and *C. lusitaniae*.

2.8 Acknowledgements

The PathoYeastract database was constructed based on the YEASTRACT database structure (http://yeastract.com). All past and present colleagues and collaborators of the YEASTRACT project are deeply acknowledged. The information about Candida genes other than documented regulations, potential regulations and the TF binding sites contained in PathoYeastract are gathered from; Candida Genome Database (CGD), Gene Ontology (GO) Consortium and YEASTRACT. We acknowledge these three platforms for making that information available to the public in easily downloadable files.

This work was supported by national funds through FCT – Fundação para a Ciência e a Tecnologia, under the contract PTDC/BBB-BIO/4004/2014 and post-doc and PhD grants to CC (SFRH/BPD/100863/2014) and PP (SFRH/BD/110956/2015), respectively. PTM was supported by FCT grant IF/01333/2013. SM was supported by the EuSysBio ERASMUS MUNDUS MSc program in Systems Biology. Funding received by iBB-Institute for Bioengineering and Biosciences from Programa Operacional Regional de Lisboa 2020 (Project N. 007317) and received by iBB and INESC-ID from FCT (UID/BIO/04565/2013 and UID/CEC/50021/2013, respectively) is acknowledged.

2.9 References

1. Wisplinghoff, H.; Bischoff, T.; Tallent, S.M.; Seifert, H.; Wenzel, R.P.; Edmond, M.B. Nosocomial Bloodstream Infections in US Hospitals: Analysis of 24,179 Cases from a Prospective Nationwide Surveillance Study. *Clin. Infect. Dis.* **2004**, *39*, 309–317.

2. Denning, D.W.; Bromley, M.J. Infectious Disease. How to bolster the antifungal pipeline. *Science* **2015**, *347*, 1414–1416.

3. Fidel, P.L.; Vazquez, J.A.; Sobel, J.D. *Candida glabrata*: review of epidemiology, pathogenesis, and clinical disease with comparison to *C. albicans*. *Clin. Microbiol. Rev.* **1999**, *12*, 80-96.

4. Mishra, N.N.; Prasad, T.; Sharma, N.; Payasi, A.; Prasad, R.; Gupta, D.K.; Singh, R. Pathogenicity and drug resistance in *Candida albicans* and other yeast species. A review. *Acta Microbiol. Immunol. Hung.* **2007**, *54*, 201-235.

5. Karababa, M.; Coste, A.T.; Rognon, B.; Bille, J.; Sanglard, D. Comparison of gene expression profiles of *Candida albicans* azole-resistant clinical isolates and laboratory strains exposed to drugs inducing multidrug transporters. *Antimicrob. Agents Chemother.* **2004**, *48*, 3064–3079.

6. Costa, C.; Dias, P.J.; Sá-Correia, I.; Teixeira, M.C. MFS multidrug transporters in pathogenic fungi: Do they have real clinical impact? *Front. Physiol.* **2014**, *5*, 197.

7. Prasad, R.; Kapoor, K. Multidrug Resistance in Yeast *Candida*. In *International review of cytology*; **2004**, *242*, pp. 215–248.

8. Caudle, K.E.; Barker, K.S.; Wiederhold, N.P.; Xu, L.; Homayouni, R.; Rogers, P.D. Genomewide Expression Profile Analysis of the *Candida glabrata Pdr1* Regulon. *Eukaryot. Cell* **2011**, *10*, 373–383.

9. Huang, G. Regulation of phenotypic transitions in the fungal pathogen *Candida albicans*. *Virulence* **2012**, *3*, 251–261.

10. Lin, C.H.; Kabrawala, S.; Fox, E.P.; Nobile, C.J.; Johnson, A.D.; Bennett, R.J. Genetic Control of Conventional and Pheromone-Stimulated Biofilm Formation in Candida albicans. *PLoS Pathog.* **2013**, *9*, e1003305.

11. Mota, S.; Alves, R.; Carneiro, C.; Silva, S.; Brown, A.J.; Istel, F.; Kuchler, K.; Sampaio, P.; Casal, M.; Henriques, M.; *et al. Candida glabrata* susceptibility to antifungals and phagocytosis is modulated by acetate. *Front. Microbiol.* **2015**, *6*, 919.

12. Walker, L.A.; Gow, N.A.R.; Munro, C.A. Fungal echinocandin resistance. *Fungal Genet. Biol.* **2010**, *47*, 117–126.

13. Papon, N.; Courdavault, V.; Clastre, M.; Bennett, R.J. Emerging and emerged pathogenic *Candida* species: beyond the *Candida albicans* paradigm. *PLoS Pathog.* **2013**, *9*, e1003550.

14. Abdulrehman, D.; Monteiro, P.T.; Teixeira, M.C.; Mira, N.P.; Lourenco, A.B.; dos Santos, S.C.; Cabrito, T.R.; Francisco, A.P.; Madeira, S.C.; Aires, R.S.; *et al.* YEASTRACT: providing a programmatic access to curated transcriptional regulatory associations in *Saccharomyces cerevisiae* through a web services interface. *Nucleic Acids Res.* **2011**, *39*, D136–D140.

15. Monteiro, P.T.; Mendes, N.D.; Teixeira, M.C.; d'Orey, S.; Tenreiro, S.; Mira, N.P.; Pais, H.; Francisco, A.P.; Carvalho, A.M.; Lourenço, A.B.; *et al.* YEASTRACT-DISCOVERER: new tools to improve the analysis of transcriptional regulatory associations in Saccharomyces cerevisiae. *Nucleic Acids Res.* **2008**, *36*, D132-D136.

16. Teixeira, M.C.; Monteiro, P.; Jain, P.; Tenreiro, S.; Fernandes, A.R.; Mira, N.P.; Alenquer, M.; Freitas, A.T.; Oliveira, A.L.; Sá-Correia, I. The YEASTRACT database: a tool for the analysis of transcription regulatory associations in Saccharomyces cerevisiae. *Nucleic Acids Res.* **2006**, *34*, D446–D451.

17. Teixeira, M.C.; Monteiro, P.T.; Guerreiro, J.F.; Gonçalves, J.P.; Mira, N.P.; dos Santos, S.C.; Cabrito, T.R.; Palma, M.; Costa, C.; Francisco, A.P.; *et al.* The YEASTRACT database: An upgraded information system for the analysis of gene and genomic transcription regulation in *Saccharomyces cerevisiae*. *Nucleic Acids Res.* **2014**, *42*, D161-D166.

18. Matys, V.; Kel-Margoulis, O. V; Fricke, E.; Liebich, I.; Land, S.; Barre-Dirrie, A.; Reuter, I.; Chekmenev, D.; Krull, M.; Hornischer, K.; *et al.* TRANSFAC(R) and its module TRANSCompel(R): transcriptional gene regulation in eukaryotes. *Nucleic Acids Res.* **2006**, *34*, D108–D110.

19. Medina-Rivera, A.; Defrance, M.; Sand, O.; Herrmann, C.; Castro-Mondragon, J.A.; Delerce, J.; Jaeger, S.; Blanchet, C.; Vincens, P.; Caron, C.; *et al.* RSAT 2015: Regulatory Sequence Analysis Tools. *Nucleic Acids Res.* **2015**, *43*, W50–W56.

20. Binkley, J.; Arnaud, M.B.; Inglis, D.O.; Skrzypek, M.S.; Shah, P.; Wymore, F.; Binkley, G.; Miyasato, S.R.; Simison, M.; Sherlock, G. The Candida Genome Database: the new homology information page highlights protein similarity and phylogeny. *Nucleic Acids Res.* **2014**, *42*, D711-D716.

21. Ashburner, M.; Ball, C.A.; Blake, J.A.; Botstein, D.; Butler, H.; Cherry, J.M.; Davis, A.P.; Dolinski, K.; Dwight, S.S.; Eppig, J.T.; *et al.* Gene ontology: tool for the unification of biology. The Gene Ontology Consortium. *Nat. Genet.* **2000**, *25*, 25–29.

22. Gene Ontology Consortium: going forward. *Nucleic Acids Res.* **2015**, *43*, D1049–D1056.

23. Zhou, P.; Szczypka, M.S.; Sosinowski, T.; Thiele, D.J. Expression of a yeast metallothionein gene family is activated by a single metalloregulatory transcription factor. *Mol. Cell. Biol.* **1992**, *12*, 3766–3775.

24. Paul, S.; Schmidt, J.A.; Moye-Rowley, W.S. Regulation of the CgPdr1 Transcription Factor from the Pathogen *Candida glabrata*. *Eukaryot. Cell* **2011**, *10*, 187–197.

25. Shah, A.H.; Singh, A.; Dhamgaye, S.; Chauhan, N.; Vandeputte, P.; Suneetha, K.J.; Kaur, R.; Mukherjee, P.K.; Chandra, J.; Ghannoum, M.A.; *et al.* Novel role of a family of major facilitator transporters in biofilm development and virulence of *Candida albicans*. *Biochem. J.* **2014**, *460*, 223–235.

26. Costa, C.; Pires, C.; Cabrito, T.R.; Renaudin, A.; Ohno, M.; Chibana, H.; Sá-Correia, I.; Teixeira, M.C. *Candida glabrata* drug: H+antiporter CgQdr2 confers imidazole drug resistance, being activated by transcription factor CgPdr1. *Antimicrob. Agents Chemother.* **2013**, *57*, 3159-3167.

27. Merhej, J.; Thiebaut, A.; Blugeon, C.; Pouch, J.; Ali Chaouche, M.E.A.; Camadro, J.M.; Le Crom, S.; Lelandais, G.; Devaux, F. A Network of Paralogous Stress Response Transcription Factors in the Human Pathogen *Candida glabrata*. *Front. Microbiol.* **2016**, *7*, 645.

28. Costa, C.; Ribeiro, J.; Miranda, I.M.; Silva-Dias, A.; Cavalheiro, M.; Costa-de-Oliveira, S.; Rodrigues, A.G.; Teixeira, M.C. Clotrimazole Drug Resistance in *Candida glabrata* Clinical Isolates Correlates with Increased Expression of the Drug:H(+) Antiporters CgAqr1, CgTpo1_1, CgTpo3, and CgQdr2. *Front. Microbiol.* **2016**, *7*, 526.

29. Vargas, R.C.; García-Salcedo, R.; Tenreiro, S.; Teixeira, M.C.; Fernandes, A.R.; Ramos, J.; Sá-Correia, I. *Saccharomyces cerevisiae* multidrug resistance transporter Qdr2 is implicated in potassium uptake, providing a physiological advantage to quinidine-stressed cells. *Eukaryot. Cell* **2007**, *6*, 134–142.

30. Vargas, R.C.; Tenreiro, S.; Teixeira, M.C.; Fernandes, A.R.; Sá-Correia, I. *Saccharomyces cerevisiae* multidrug transporter Qdr2p (Yil121wp): localization and function as a quinidine resistance determinant. *Antimicrob. Agents Chemother.* **2004**, *48*, 2531–2537.

3 Membrane proteome-wide response to the antifungal drug clotrimazole in *Candida glabrata*: role of the transcription factor CgPdr1 and the Drug:H+ Antiporters CgTpo1_1 and CgTpo1_2

This chapter contains results published in:

Pais, P., Costa, C., Pires C., Shimizu, K., Chibana, H., Teixeira, M.C. 2016. Membrane proteome-wide response to the antifungal drug clotrimazole in *Candida glabrata*: role of the transcription factor CgPdr1 and the Drug:H+ Antiporters CgTpo1_1 and CgTpo1_2. *Mol Cell Proteomics*, **15:**57-72.

The PhD candidate is the first author of the work detailed in this chapter. The candidate was responsible for most of the experimental work and writing of the correspondent publication.

3.1 Abstract

Azoles are widely used antifungal drugs. This family of compounds includes triazoles, mostly used in the treatment of systemic infections, and imidazoles, such as clotrimazole, often used in the case of superficial infections. *Candida glabrata* is the second most common cause of candidemia worldwide and presents higher levels of intrinsic azole resistance when compared to *Candida albicans*, thus being an interesting subject for the study of azole resistance mechanisms in fungal pathogens.

Since resistance often relies on the action of membrane transporters, including drug efflux pumps from the ATP-Binding Cassette (ABC) family or from the Drug:H^+ Antiporter (DHA) family, an iTRAQ-based membrane proteomics analysis was performed to identify all the membrane-associated proteins whose abundance changes in *C. glabrata* cells exposed to the azole drug clotrimazole. Proteins found to have significant expression changes in this context were clustered into functional groups, namely: glucose metabolism, oxidative phosphorylation, mitochondrial import, ribosome components and translation machinery, lipid metabolism, multidrug resistance transporters, cell wall assembly and stress response, comprising a total of 37 proteins. Among these, the DHA transporter CgTpo1_2 (ORF *CAGL0E03674g*) was identified as overexpressed in the *C. glabrata* membrane in response to clotrimazole. Functional characterization of this putative drug:H^+ antiporter, and of its homolog CgTpo1_1 (ORF *CAGL0G03927g*), allowed the identification of these proteins as localized to the plasma membrane and conferring azole drug resistance in this fungal pathogen by actively extruding the drug to the external medium. The cell wall protein CgGas1 was also shown to confer azole drug resistance through cell wall remodeling. Finally, the transcription factor CgPdr1 in the clotrimazole response was observed to control the expression of 20 of the identified proteins, thus highlighting the existence of additional unforeseen targets of this transcription factor, recognized as a major regulator of azole drug resistance in clinical isolates.

3.2 Introduction

Systemic fungal infections are a problem of increasing clinical significance, since the extensive use of antifungal drugs, both as treatment and prophylaxis, has led to a huge increase in the number of intrinsically resistant infections with fungal pathogens [1,2]. This is particularly true for the non-albicans *Candida* species *Candida glabrata*.

Candidemia represents the 4th most common nosocomial infection in humans [3]. Over the past two decades there has been an increase in the number of infections concerning non-*albicans* species, with *C. glabrata* arising as the second most frequent pathogenic yeast in mucosal and invasive fungal infections in humans, representing 15-20% of all infections caused by *Candida* species, depending on the geographical region [4–6]. Together, *C. albicans* and *C. glabrata* represent 65%-75% of all systemic candidiasis, followed by *C. parapsilosis* and *C. tropicalis* [5].

Azoles are one of the main families of drugs currently used to treat or prevent fungal infections. *C. glabrata* presents higher level of intrinsic resistance to azoles than *C. albicans* and develops further resistance during prolonged azole therapy. The acquisition of azole drug resistance is commonly associated with the expression of multidrug efflux pumps such as those from the ATP-Binding Cassette (ABC) family and from the Major Facilitator Superfamily (MFS) responsible for the efflux of structurally and functionally unrelated compounds [2,7]. Expression of several of these transporters was shown to be dependent on the transcription factor CgPdr1, recognized as a major pleiotropic drug resistance mediator in *C. glabrata* [8–10]. Most studies conducted so far to study azole drug resistance focus mainly on fluconazole.

Despite the notion that azole resistance mechanisms are well established, this is not absolutely true for non-albicans *Candida* species and certainly it is not true for azole drugs other than fluconazole. Since fluconazole is a triazole, it is possible to assume that information gathered for fluconazole may be extrapolated for other triazoles, like itraconazole and posaconazole. However, this would not be the case for imidazole drugs, which are widely used for topical applications in mucosal infections. Among these drugs, ketoconazole and miconazole are the most well-known, but for clotrimazole very little information is available, regarding its action and resistance mechanisms in *C. glabrata*. In a study by Calahorra *et al.* [11] the mode of action and resistance mechanisms of ketoconazole and miconazole (both imidazoles) were studied

in the model *S. cerevisiae*. Although the primary mode of action involves the inhibition of sterol synthesis common to all azoles, these two drugs seem to also have an effect on cation transport systems. Ketoconazole and miconazole produced an efflux of K^+ at low concentrations (~200 μM) leading to an almost complete depletion of that ion in the cells. The drugs appear to bind to the surface of the cell due to their amphipathic and cationic nature, decreasing the surface charge of the membrane. As a consequence, both antifungals can stimulate efflux of K^+ at low concentrations, once at higher concentrations the uptake of H^+ can be stimulated. The change of the surface charge was yet hypothesized to lead to a disruption of the membrane structure due to the interaction of the antifungals with lipid rafts. These results were not found with two triazole antifungals, fluconazole and itraconazole, indicating that the active group of the molecules is the imidazole moiety of the molecule, thus showing a clear difference between imidazole and triazole modes of action. Ketoconazole and miconazole were found yet to affect respiration, probably related to the cationic nature of the imidazolic portion of the molecule. More studies highlighted the importance of mitochondrial function for tolerance to antifungal drugs and virulence, with functions in lipid homeostasis likely to be the center of mitochondrial action in tolerance to antifungal drugs, with some crosstalk between mitochondria and cell wall integrity; but the exact molecular mechanisms are not fully understood [12,13].

In this study, the *C. glabrata* response to clotrimazole, at the membrane proteome level was examined. Based on the identified proteins exhibiting altered concentrations in the membrane-enriched fraction, the effect of cell wall remodeling, in the dependency of CgGas1, in clotrimazole resistance was inspected. CgGas1 (ORF *CAGL0G00286g*) is a predicted GlicosylPhosphatidylInositol (GPI)-anchored cell wall bound protein [14], homologue of the *S. cerevisiae* Gas1 β-1,3-glucanosyltransferase, required for cell wall assembly. The deletion of *CgGAS1* was shown to lead to an aggregation phenotype and to lead to decreased growth rates [15].

Furthermore, the suggested role of the two uncharacterized homologs of *S. cerevisiae* Tpo1 drug:H+ antiporter in *C. glabrata*, encoded by ORFs *CAGL0G03927g* (*CgTPO1_1*) and *CAGL0E03674g* (*CgTPO1_2*) in clotrimazole drug resistance was also evaluated, given the observed upregulation of CgTpo1_2 in *C. glabrata* membrane-enriched fractions exposed to clotrimazole. *S. cerevisiae* Tpo1 is one of the best characterized of the eukaryotic Drug:H+ Antiporters [16,17]. The primary physiological

role attributed to ScTpo1 has been the transport of polyamines [18], particularly spermidine [19]. However, ScTpo1 has been shown to confer resistance to numerous chemical stress agents, from herbicides [20] and agricultural fungicides [21] to the antifungal drug caspofungin [22], among many others [16,17]. Interestingly, the ScTpo1 homolog in *C. albicans*, CaFlu1, was found to complement fluconazole hypersusceptibility in a *S. cerevisiae Δpdr5* mutant, but not to have a significant role in fluconazole resistance in *C. albicans* [23]. More recently, CaFlu1 was shown to confer resistance to the salivary human antimicrobial peptide histatin 5, playing a direct role in its efflux from *C. albicans* cells, thus reducing histatin 5 toxicity [24]. Based on the proteomics data, *CgTPO1_1* and *CgTPO1_2* were further analyzed, in this study. The subcellular localization of these transporters and their effect in antifungal drug resistance was assessed. Their action as clotrimazole resistance determinants was correlated with their action in the accumulation of radiolabeled clotrimazole in *C. glabrata*.

3.3 Experimental Procedures

3.3.1 Strains and growth media

Saccharomyces cerevisiae parental strain BY4741 (*MATa, ura3□0, leu2Δ0, his3Δ1, met15Δ0*) and the derived single deletion mutant BY4741_*Δtpo1* were obtained from Euroscarf (http://web.uni-frankfurt.de/fb15/mikro/euroscarf/). Cells were batch-cultured at 30ºC, with orbital agitation (250 rpm) in basal medium (BM), with the following composition (per liter): 1.7 g yeast nitrogen base without amino acids or NH_4^+ (Difco), 20 g glucose (Merck) and 2.65 g $(NH_4)_2SO_4$ (Merck), supplemented with 20 mg/L methionine, 20 mg/L histidine, 60 mg/L leucine, 20 mg/L uracil (all from Sigma). *Candida glabrata* parental strain KUE100 [25] and derived single deletion mutants KUE100_*Δcggas1,* KUE100_*Δcgtpo1_1* or KUE100_*Δcgtpo1_2*, as well as the *C. glabrata* strains 66032u and 66032u_*Δcgpdr1* [10] , kindly provided by Thomas Edlind, from the Department of Microbiology and Immunology, Drexel University, College of Medicine, Philadelphia, PA, were batch-cultured at 30ºC, with orbital agitation (250 rpm) in BM medium, with the following composition (per liter): 1.7 g yeast nitrogen base without amino acids or NH_4^+ (Difco), 20 g glucose (Merck) and 2.65 g $(NH_4)_2SO_4$ (Merck). *C. glabrata* strain L5U1 (*cgura3Δ0, cgleu2Δ0*) [26], kindly provided by John Bennett from the National Institute of Allergy and Infectious Diseases, NIH, Bethesda, USA, was grown in BM medium supplemented with 20 mg/L uracil and 60mg/L leucine. Solid media contained, besides the above-indicated ingredients, 20 g/L agar (Iberagar). The plasmid pGREG576 was obtained from the Drag&Drop collection.

3.3.2 Membrane proteome-wide analysis of *C. glabrata* response to clotrimazole

Wild-type 66032u *C. glabrata* strain and the derived 66032u_*Δcgpdr1* deletion mutant were cultivated in liquid BM medium at 30ºC with orbital agitation (250 rpm) in the absence of stress until the standardized culture OD_{600nm} (Optical Density at 600nm) of 0.8 ± 0.08 was reached. Cells were then transferred to fresh medium in the absence of stress (control conditions) or in the presence of 100 mg/L clotrimazole, with an initial OD_{600nm} of 0.4 ± 0.05. Upon 1h of cultivation, cells were harvested by centrifugation and resuspended in A Buffer (50 mM Tris, pH 7.5, with 0.5 mM EDTA and 20%

glycerol), with protease inhibitors (10 mg/L leupeptine, 1mg/L pepstatine A, 20 mg/L aprotinine, 2 mg/L trypsin/quimotrypsin inhibitor, 1.5 mg/L benzamindine and 1 mM PhenylMethylSulfonyl Fluoride (PMSF) – all obtained from Sigma). Cell lysis was accomplished by consecutive steps of vortexing and cooling in the presence of glass beads. The mixture was centrifuged for clarification (8000 rpm, 5 min, 4ºC) and the top phase collected. A Buffer was added to a final volume of 8 mL, this mix ultra-centrifuged on a Beckman XL-90 ultracentrifuge (24000 rpm, 90 min, 4ºC) and the pellet washed with 8 mL of 0,1 M Na_2CO_3 and incubated on ice for 30 min with orbital agitation (60 rpm). The mixture was then ultracentrifuged (26000 rpm, 60 min, 4ºC) and the pellet was washed with 8mL of 50 mM TEAB (Tetraethylammonium bromide, Sigma) and ultracentrifuged again (26000 rpm, 60 min, 4ºC). This procedure was repeated 2 more times and, finally, the pellet was resuspended in 325 µL of 50 mM TEAB with 8 M urea (Sigma).

Expression proteomics analysis of the obtained membrane-enriched fraction was carried out using and iTRAQ-MS procedure, carried out as a paid service at the Keck Foundation Biotechnology Resource Laboratory, Yale University, USA (http://medicine.yale.edu/keck/proteomics/index.aspx). Briefly, samples were sonicated and proteins reduced by adding 50 mM TCEP (tris(2-carboxyethyl)phosphine), followed by 200 mM MMTS (methyl methane thiosulfonate). Protein digestion was achieved by adding 10 µL of a solution of 1 mg/ml Lys-C, followed by incubation at 37ºC for 3 h, and 10 µL of 1mg/ml trypsin, followed by overnight incubation at 37ºC. Macro-spin desalt of the digests with C18 spin columns for cleanup and quantitation was carried out, followed by dissolution in 65 µL of 500 mM TEAB. iTRAQ labelling was carried out based on the AAA quant protocol. iTRAQ experiments were carried out through the SCX cartridge and experiments run on 5600.

The search parameters and acceptance criteria used were the following: Peaklist generating software: ProteinPilot 4.5 and Mascot; Search engine: Paragon Search Engine (ProteinPilot 4.2); Sequence Database/spectral library: *Candida glabrata* [5478] from SwissProt (May 2013); The database used was downloaded from UniProt, with a total of 5197 protein entries. Mass spectrometric analysis is done on an AB SCIEX TripleTOF® 5600 mass spectrometer with AB SCIEX ProteinPilot™ software used for protein identification and quantitation. ProteinPilot utilizes a Paragon™ algorithm with hybrid sequence tag and feature probability database searches. Hence, specific details

such as mass tolerances, specific modifications etc. are not utilized. All iTRAQ results are uploaded into the Yale Protein Expression database (YPED) for investigator viewing. Protein identification was considered reliable for a Protein Score > 2, corresponding to a confidence level of 99%. A reserve decoy database search, followed by filtering of all peptidesabove 1% False Discovery Rate was carried out before protein grouping.

Proteomics data analysis started from 3 iTRAQ sets (Complete raw data corresponding to each iTRAQ set is available online https://www.mcponline.org/content/suppl/2015/10/28/M114.045344.DC1). The samples present in each of the sets were randomized to prevent bias, and in different sets distinct labels were used to tag the samples, ensuring that protein identification in the MS step is not biased by the tags. For each sample in a given set, protein quantification was only considered for p-value<0.05. Protein expression changes above 1.4-fold or below 0.71-fold were considered relevant. Protein classification into functional groups was achieved based on their predicted function, according to the Candida Genome Database (www.candidagenome.org), or based on the function of their closest *S. cerevisiae* homolog, according to the Saccharomyces Genome Database (www.yeastgenome.org).

3.3.3 β-1,3-glucanase susceptibility assay

To monitor structural changes at the cell wall level, a lyticase (β-1,3-glucanase, Sigma) susceptibility assay was conducted as described before [27]. *C. glabrata* KUE100 and KUE100_*Δcggas1* cells were grown in BM medium, in the presence of 60 mg/L of clotrimazole, and harvested following 0 or 30min of cell incubation, during the period of early adaptation to stress, and at the exponential growth phase, when the standardized OD_{600nm} of 1.0 ± 0.1 was attained. The harvested cells were washed with distilled water and resuspended in 0.1 mM sodium phosphate buffer (pH 7). After the addition of 10 μg/mL lyticase, cell lysis was monitored by measuring the percent decrease of the initial OD_{600nm} of the cell suspensions every 30 min for a total period of 180 min. Statistical analysis of the results were performed using analysis of variance, and differences were considered significant for p-values<0.05.

3.3.4 Disruption of the *CgGAS1*, *CgTPO1_1* and *CgTPO1_2* genes

The deletion of the *C. glabrata GAS1*, *TPO1_1* and *TPO1_2* genes (ORFs *CAGL0G00286g*, *CAGL0G03927g* and *CAGL0E03674g*, respectively) was carried out in the parental strain KUE100, using the method described by Ueno *et al.* [28]. The target genes *CgGAS1*, *CgTPO1_1* and *CgTPO1_2* were replaced by a DNA cassette including the *CgHIS3* gene, through homologous recombination. The replacement cassette was prepared by PCR using the primers 5´-AGCTGTATCAAACAACTCACTGTATCAATCACTATTTTACTATAACTAGATC AATAGGCCGCTGATCACG-3´and 5'-CCCGTTGATCATATGAACATTAGGATTCATCAAATATTTAAATCATTCTGAA ATTACATCGTGAGGCTGG-3, for the *CgGAS1* gene, the primers 5´-GTTTTATCATTCGGTAGTCAACTGAATAAAAAAAATATATACATACATACAA AACGGGCCGCTGATCACG-3´and 5'-TTGATTCTCTCTTTTAAAGGAAGAGTAGGAATCAGGATGTGGTCGCTTGAAG CTTACATCGTGAGGCTGG-3, for the *CgTPO1_1* gene, and the primers 5´-CCAGTGCAGGAGAAGTAACAGCATATAATTCATCTCACGATAAGGAAGTTG GAGTGGGCCGCTGATCACG-3´and 5'-AAAAGAGGGCACCAATTTCGTTAAGATATTATTAGTTTTTATTCTTTTTGGA TTTACATCGTGAGGCTGG-3, for the *CgTPO1_2* gene. The pHIS906 plasmid including *CgHIS3* was used as a template and transformation was performed as described previously [25]. Recombination locus and gene deletion were verified by PCR using the following pairs of primers: 5'-GTCTGGTTTCTTTCATAATAGC-3' and 5'-TTGGAGTAGTTAGCGAAC-3'; 5'-CGCCAAAGTATACCAATG-3' and 5'-CGGTGTTCCACAAATCTGT-3'; and 5'-GGCTCATCCATCTTCGCT-3' and 5'-AGCGAAGATGGATGAGCC-3', respectively.

For the disruption of *CgTPO1_2* (ORF *CAGL0E03674g*) in the *Δcggas1* derivative, the *SAT1* cassette, encoding a nourseothricin selection marker was used for homologous recombination. The *SAT1* cassette was obtained by PCR, using the pA83 plasmid as template and the following specific primers: 5'-GATCCCAGTGCAGGAGAAGTAACAGCATATAATTCATCTCACGATAAGGAA GTTGGAGTG*ATGGACGGTGGTATGTTTTA*-3' and 5'-ATATAACTCTAGTCCCATTTTTTAATTTGGAAGTTGGGATATCGAGATAAGG ATAGGTGC*TTAGGCGTCATCCTGTGCTC*-3'. The designed primers contain, besides

a region with homology to the first and last 20 nucleotides of the *SAT1* coding region (italic); 60 nucleotide sequences with homology to the upstream and downstream regions of *CgTPO1_2* (underlined). The successful recombination of the *SAT1* cassette was verified by PCR using the following specific primers: 5'-TTTGCTGCTTCGCCAGTTAT-3' and 5'-TGTAAATGCACCTGCAATGG-3'. The designed primers are homologous to a sequence in the upstream region of *CgTPO1_2* and to a sequence in the coding region of the *SAT1* cassette, respectively.

3.3.5 Cloning of the *C. glabrata CgTPO1_1* and *CgTPO1_2* genes (ORFs *CAGL0G03927g* and *CAGL0E03674g*, respectively)

The pGREG576 plasmid from the Drag&Drop collection was used to clone and express the *C. glabrata* ORFs *CAGL0G03927g* and *CAGL0E03674g* in *S. cerevisiae*, as described before for other heterologous genes [29–31]. pGREG576 was acquired from Euroscarf and contains a galactose inducible promoter (*GAL1*), the yeast selectable marker *URA3* and the *GFP* gene, encoding a Green Fluorescent Protein (GFPS65T), which allows monitoring of the expression and subcellular localization of the cloned fusion protein. *CAGL0G03927g* or *CAGL0E03674g* DNA was generated by PCR, using genomic DNA extracted from the sequenced CBS138 *C. glabrata* strain, and the following specific primers: 5'-GAATTCGATATCAAGCTTATCGATACCGTCGACA*ATGGTGGAAGAGATATCGC*
C-3' and 5'-GCGTGACATAACTAATTACATGACTCGAGGTCGAC*TTAAGCGTAGTAAGCATC*
C-3'; or 5'-GAATTCGATATCAAGCTTATCGATACCGTCGACA*ATGTCCTCCACTAGTAGCG*
-3' and 5'-GCGTGACATAACTAATTACATGACTCGAGGTCGAC*TTATAACGAATATGCGTA*
C-3', respectively. The designed primers contain; besides a region with homology to the first 20 and last 19 nucleotides of the *CAGL0G03927g* coding region (italic), and the first and last 19 nucleotides of the *CAGL0E03674g* coding region (italic); nucleotide sequences with homology to the cloning site flanking regions of the pGREG576 vector (underlined). The amplified fragments were co-transformed into the parental *S. cerevisiae* strain BY4741 with the pGREG576 vector, previously cut with the restriction

enzyme SalI, to obtain the pGREG576_*CgTPO1_1* or pGREG576_*CgTPO1_2* plasmids. Since the *GAL1* promoter only allows a slight expression of downstream genes in *C. glabrata*, to visualize by fluorescence microscopy the subcellular localization of the CgTpo1_1 or CgTpo1_2 proteins in *C. glabrata*, new constructs were obtained. The *GAL1* promoter present in the pGREG576_*CgTPO1_1* and pGREG576_*CgTPO1_2* plasmids was replaced by the copper-induced *MTI C. glabrata* promoter, giving rise to the pGREG576_*MTI_CgTPO1_1* and pGREG576_*MTI_CgTPO1_2* plasmids. The *MTI* promoter DNA was generated by PCR, using genomic DNA extracted from the sequenced CBS138 *C. glabrata* strain, and the following specific primers: 5'-TTAACCCTCACTAAAGGGAACAAAAGCTGGAGCTC*TGTACGACACGCATCAT GTGGCAATC*-3' and 5'-GAAAAGTTCTTCTCCTTTACTCATACTAGTGCGGC*TGTGTTTGTTTTTGTATGT GTTTGTTG*-3'. The designed primers contain, besides a region with homology to the first 26 and last 27 nucleotides of the first 1000 bp of the *MTI* promoter region (italic), nucleotide sequences with homology to the cloning site flanking regions of the pGREG576 vector (underlined). The amplified fragment was co-transformed into the parental strain BY4741 with the pGREG576_*CgTPO1_1 or* pGREG576_*CgTPO1_2* plasmids, previously cut with SacI and NotI restriction enzymes to remove the *GAL1* promoter, to generate the pGREG576_MTI_*CgTPO1_1* and pGREG576_MTI_*CgTPO1_2* plasmids. The recombinant plasmids pGREG576_*CgTPO1_1*, pGREG576_*CgTPO1_2*, pGREG576_MTI_*CgTPO1_1* and pGREG576_MTI_*CgTPO1_2* were obtained through homologous recombination in *S. cerevisiae* and verified by DNA sequencing.

3.3.6 CgTpo1_1 and CgTpo1_2 subcellular localization assessment

The subcellular localization of the CgTpo1_1 and CgTpo1_2 proteins was determined based on the observation of BY4741 *S. cerevisiae* or L5U1 *C. glabrata* cells transformed with the pGREG576_*CgTPO1_1* and pGREG576_*CgTPO1_2* or pGREG576_MTI_*CgTPO1_1* and pGREG576_MTI_*CgTPO1_2* plasmids, respectively. These cells express the CgTpo1_1_GFP or CgTpo1_2_GFP fusion proteins, whose localization may be determined using fluorescence microscopy. *S.*

cerevisiae cell suspensions were prepared by cultivation in BM-U medium, containing 0.5% glucose and 0.1% galactose, at 30ºC, with orbital shaking (250 rpm), until a standard culture OD_{600nm} = 0.4 ± 0.04 was reached. At this point cells were transferred to the same medium containing 0.1% glucose and 1% galactose, to induce protein expression. *C. glabrata* cell suspensions were prepared in BM-U medium, until a standard culture OD_{600nm} = 0.4 ± 0.04 was reached and transferred to the same medium supplemented with 50 µM $CuSO_4$ (Sigma), to induce protein over-expression. After 5h of incubation, the distribution of CgTpo1_1_GFP or CgTpo1_2_GFP fusion proteins in *S. cerevisiae* or in *C. glabrata* living cells was detected by fluorescence microscopy in a Zeiss Axioplan microscope (Carl Zeiss MicroImaging), using excitation and emission wavelength of 395 and 509 nm, respectively. Fluorescence images were captured using a cooled CCD camera (Cool SNAPFX, Roper Scientific Photometrics).

3.3.7 Antifungal susceptibility assays in *C. glabrata*

The susceptibility of the parental strain KUE100 towards toxic concentrations of the selected drugs was compared to that of the deletion mutants KUE100_*Δcggas1*, KUE100_*Δcgtpo1_1*, KUE100_*Δcgtpo1_2* and KUE100_*Δcgtpo1_2_Δcggas1* by spot assays or by comparing growth in liquid medium. The ability of *CgTPO1_1* and *CgTPO1_2* gene expression to increase wild-type resistance to the tested chemical stresses was also examined in the URA3- strain L5U1 *C. glabrata* strain, using the pGREG576_*MTI_CgTPO1_1* and pGREG576_*MTI_CgTPO1_2* centromeric plasmids.

KUE100 *C. glabrata* cell suspensions used to inoculate the agar plates, or liquid medium, were mid-exponential cells grown in basal BM medium, until culture OD_{600nm} = 0.4 ± 0.02 was reached and then diluted in sterile water to obtain suspensions with OD_{600nm} = 0.05 ± 0.005. These cell suspensions and subsequent dilutions (1:5; 1:25) were applied as 4 µL spots onto the surface of solid BM medium, supplemented with adequate chemical stress concentrations. L5U1 *C. glabrata* cell suspensions used to inoculate the agar plates were mid-exponential cells grown in BM medium, supplemented with 50 µM $CuSO_4$ (Sigma), to induce protein over-expression, without uracil when using the L5U1 strain harboring the pGREG576 derived plasmids, until culture OD_{600nm} = 0.4 ± 0.02 was reached and then diluted in sterile water to obtain suspensions with OD_{600nm} = 0.05 ± 0.005. These cell suspensions and subsequent

dilutions (1:5; 1:25) were applied as 4 µL spots onto the surface of solid BM medium, without uracil for strains transformed with the pGREG576 derived plasmids, supplemented with 50 µM $CuSO_4$ and with adequate chemical stress concentrations. The tested drugs included the following compounds, used in the specified concentration ranges: the azole antifungal drugs ketoconazole (10 to 60 mg/L), fluconazole (20 to 80 mg/L), miconazole (0.08 to 0.14 mg/L), tioconazole (0.2 to 0.9 mg/L), itraconazole (5 to 40 mg/L), and clotrimazole (2.5 to 10 mg/L), the polyene antifungal drug amphotericin B (0.12 to 0.19 mg/L), the fluoropyrimidine 5-flucytosine (0.010 to 0.017 mg/L), the pesticide mancozeb (0.5 to 2.5 mg/L), and the polyamines spermine (2 to 4.5 mM) and spermidine (3 mM to 5 mM) (all from Sigma).

3.3.8 Antifungal susceptibility assays in *S. cerevisiae*

The susceptibility of the parental strain BY4741 towards toxic concentrations of the selected drugs was compared to that of the deletion mutant BY4741_*Δtpo1* by spot assays. The ability of *CgTPO1_1* and *CgTPO1_2* genes to increase wild-type resistance to the tested chemical stresses and to complement the susceptibility phenotype exhibited by the BY4741_*Δtpo1* single deletion mutants was also examined, using the pGREG576_*CgTPO1_1* and pGREG576_*CgTPO1_2* centromeric plasmids through which the *C. glabrata* genes are expressed under the *GAL1* promoter.

S. cerevisiae cell suspensions used to inoculate the agar plates were mid-exponential cells grown in BM-U medium, containing 0.5% glucose and 0.1% galactose, until culture OD_{600nm} = 0.4±0.02 was reached and then diluted in sterile water to obtain suspensions with OD_{600nm} = 0.05 ± 0.005. These cell suspensions and subsequent dilutions (1:5; 1:25) were applied as 4 µL spots onto the surface of solid BM-U medium, containing 0.1% glucose and 1% galactose, supplemented with growth inhibitory chemical stress concentrations. The tested drugs and other xenobiotics included the following compounds, used in the specified concentration ranges: the polyamines spermidine (2 mM) and spermine (2.5 mM), and the fungicide mancozeb (1.25 mg/L).

3.3.9 ^{3}H-clotrimazole accumulation assays

^{3}H-clotrimazole transport assays were carried out as described before [31]. The internal accumulation of clotrimazole was determined by calculating the ratio between the radiolabeled clotrimazole measured within the yeast cells and in the external medium (Intracellular/Extracellular). The parental strain KUE100 and the mutant strains KUE100_*Δcgtpo1_1* and KUE100_*Δcgtpo1_2* were grown in BM medium until mid-exponential phase and harvested by filtration. Cells were washed and resuspended in BM medium, to obtain dense cell suspensions (OD_{600nm} = 0.5 ± 0.1, equivalent to approximately 1.57 mg (dry weight) mL^{-1}). Readily, 0.1 μM of ^{3}H-clotrimazole (American Radiolabeled Chemicals; 1 mCi/ml) and 30 mg/L of unlabeled clotrimazole were added to the cell suspensions. Incubation proceeded for an additional period of 30 min. The intracellular accumulation of labeled clotrimazole was followed by filtering 200 μl of cell suspension, at adequate time intervals, through pre-wetted glass microfibre filters (Whatman GF/C). The filters were washed with ice-cold TM buffer and the radioactivity measured in a Beckman LS 5000TD scintillation counter. Extracellular ^{3}H-clotrimazole was estimated, by radioactivity assessment of 50 μl of the supernatant. Non-specific ^{3}H-clotrimazole adsorption to the filters and to the cells (less than 5% of the total radioactivity) was assessed and taken into consideration. To calculate the intracellular concentration of labeled clotrimazole, the internal cell volume (Vi) of the exponential cells, grown in the absence of drug and used for accumulation assays, was considered constant and equal to 2.5 μl (mg dry weight)$^{-1}$ [32]. Statistical analysis of the results was performed using analysis of variance, and differences were considered significant for p-values<0.05.

3.3.10 *CgTPO1_1* and *CgTPO1_2* expression measurements

The levels of *CgTPO1_1* and *CgTPO1_2* transcripts were assessed by real-time PCR. Synthesis of cDNA for real time RT-PCR experiments, from total RNA samples, was performed using the MultiscribeTM reverse transcriptase kit (Applied Biosystems) and the 7500 RT-PCR Thermal Cycler Block (Applied Biosystems), following the manufacturer's instructions. The quantity of cDNA for the following reactions was kept around 10 ng. The subsequent RT-PCR step was carried out using SYBR® Green reagents. Primers for the amplification of the *CgTPO1_1*, *CgTPO1_2* and *CgACT1*

cDNA were designed using Primer Express Software (Applied Biosystems) and are 5'-CGCTGCTTCCCCAGTTATCT-3' and 5'-CTAGCACACCACGTCTACCGTAA-3'; 5'-AGGACCCGCTCTATCGAAAAA-3' and 5'-GCTGCGACTGCTGACTCAAC-3'; and 5'-AGAGCCGTCTTCCCTTCCAT-3' and 5'-TTGACCCATACCGACCATGA-3', respectively. The RT-PCR reaction was carried out using a thermal cycler block (7500 Real-Time PCR System - Applied Biosystems). Default parameters established by the manufacturer were used and fluorescence detected by the instrument and registered in an amplification plot (7500 System SDS Software – Applied Biosystems). The *CgACT1* mRNA level was used as an internal control. The relative values obtained for the wild-type strain in control conditions were set as 1 and the remaining values are presented relative to that control. To avoid false positive signals, the absence of non-specific amplification with the chosen primers was confirmed by the generation of a dissociation curve for each pair of primers. Statistical analysis of the results was performed using analysis of variance, and differences were considered significant for p-values<0.05.

3.4 Results

3.4.1 Proteome-wide protein identification in *C. glabrata* membrane-enriched fraction

624 proteins were identified in the membrane-enriched fraction in *C. glabrata*, 131 encoded by characterized genes, while 493 are encoded by non-characterized ORFs, comprising around 10% of the predicted *C. glabrata* proteome. To the best of our knowledge this is the first membrane proteome-wide analysis carried out in *C. glabrata*, making this list of proteins an invaluable repository of information on the functional analysis of all of these 624 proteins. To obtain a global perspective of the functional distribution of these membrane-associated proteins, the online Gene Ontology term-based grouping tool GoToolBox (http://genome.crg.es/GOToolBox/) was used, considering their *S. cerevisiae* homologs. Using this tool, only 1.44% of the total proteins were found to have cytoplasm-localization associated GO terms, attesting the high specificity of the applied approach for the yield of membrane proteins. Figure 3.1 highlights the most enriched GO terms associated to the *C. glabrata* membrane proteome. As expected, they are all related to transmembrane transport functions and membrane associated metabolic processes, and include proteins involved in the synthesis of ergosterol and phospholipids, but also transmembrane transporters and proteins involved in cell trafficking. The whole list of positively identified membrane-associated proteins is available online (https://www.mcponline.org/content/suppl/2015/10/28/M114.045344.DC1). Details on the protein quantification can be assessed at the Mass spectrometry Interactive Virtual Environment (MassIVE) repository (http://massive.ucsd.edu/ProteoSAFe/datasets.jsp; MassIVE ID: MSV000079209). Annotated spectra for single peptide identification for each protein is provided in MS-viewer (http://prospector2.ucsf.edu/prospector/cgi-bin/msform.cgi?form=msviewer; Search keys: qrvm65goix; xffxn22szm; tm0y9x0hqd).

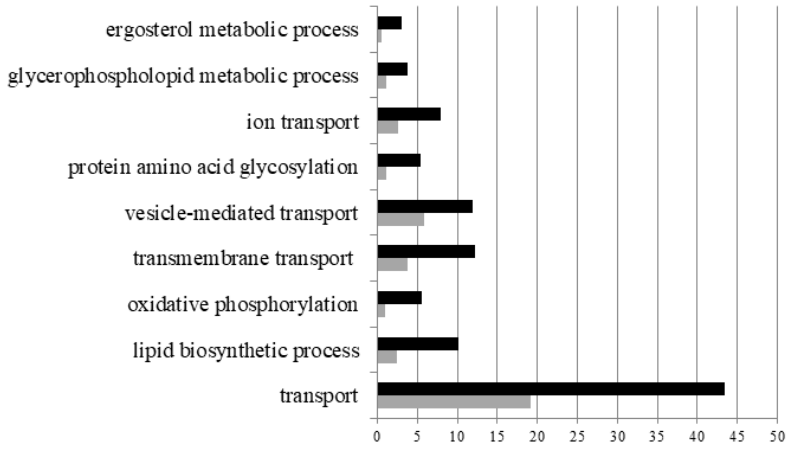

Figure 3.1 – Categorization, based on the biological process taxonomy of Gene Ontology, of the proteins identified in membrane-enriched fractions of *C. glabrata* cells. These genes were clustered using the GoToolBox software (http://genome.crg.es/GOToolBox/), and the most highly ranked statistically significant (p-value<10^{-10}) GO terms are displayed. The protein frequency within each class is indicated by the black bars, compared to the frequency registered for the *C. glabrata* whole genome, indicated by the grey bars, gene frequency being the percentage of the genes in a list associated to a specific GO term.

3.4.2 Membrane proteome-wide changes occurring in response to clotrimazole in *C. glabrata*

The analysis of the membrane-enriched fraction of the *C. glabrata* proteome obtained from cells exposed to clotrimazole when compared to control conditions allowed the identification of 12 proteins whose content increases and 25 proteins whose expression decreases upon exposure to the drug. Since only 4 of these 37 proteins had been previously characterized, their clustering was carried out based on the role of their predicted *S. cerevisiae* homologs (Table 3.1 and Figure 3.2). Among the obtained clusters, the most populated one is Ribosome components and translational machinery, with 2 ribosomal proteins being upregulated, while the remaining 20 are downregulated. This observation appears consistent with a decreased translation rate, which has been considered part of the so-called "Environmental Stress Response" [33]. This feature is consistent with growth arrest elicited by sudden exposure to clotrimazole induced stress.

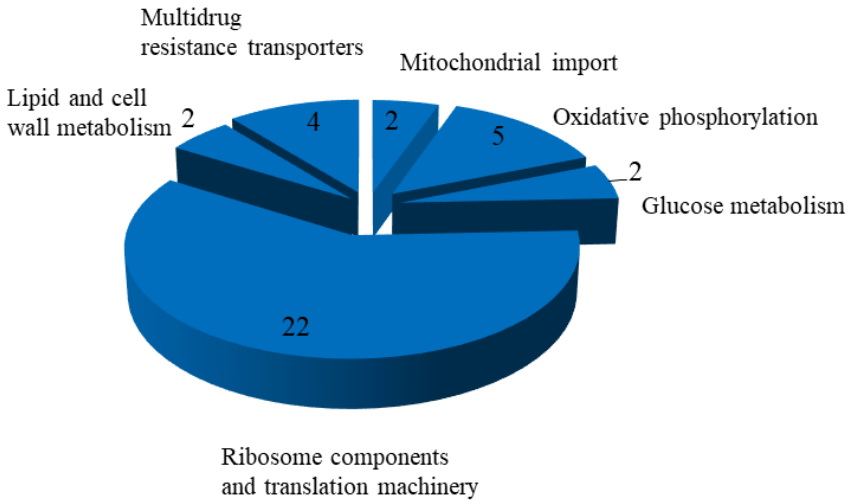

Figure 3.2 – Major functional groups found to have significant expression changes in the membrane-enriched proteome upon exposure to clotrimazole in *C. glabrata*. Proteins with significant expression changes include Ribosome components and translation machinery (22 proteins), Lipid and cell wall metabolism (2 proteins), Multidrug resistance transporters (4 proteins), Mitochondrial import (2 proteins), Oxidative phosphorylation (5 proteins) and Glucose metabolism (2 proteins).

Within the remaining classes, three are related to carbon and energy metabolism, comprising a total of 9 proteins: Glucose metabolism, Oxidative phosphorylation and Mitochondrial import. These 9 proteins include CgGsf2, an ER (Endoplasmic Reticulum) protein predicted to promote the traffic of hexose transporters.

All 4 proteins present in the Multidrug resistance transporters are upregulated upon exposure to clotrimazole. This is consistent with the characterization of several of these proteins as efflux pumps, despite a role in specific clotrimazole transport had only been described for CgQdr2 [31]. The most upregulated protein in this cluster is CgCdr1, widely characterized as an important ABC transporter. Accordingly, its *S. cerevisiae* homolog, ScPdr5, was previously found to be involved in clotrimazole extrusion [34]. Additionally, CgSnq2 has been characterized as a multidrug transporter [35], as well as its *S. cerevisiae* homolog [36]. The upregulation of CgSnq2 observed in this study predicts a possible role for this transporter in clotrimazole extrusion. CgTpo1_2 is the only protein from this cluster uncharacterized in *C. glabrata*, presenting here a slight upregulation upon clotrimazole exposure. Its *S. cerevisiae* homolog is known to confer resistance to spermine, putrescine and spermidine; catalyzing the extrusion of polyamines in *S. cerevisiae* [18,19]. The upregulation of CgTpo1_2 in clotrimazole exposed *C. glabrata* cells raises the possibility that this predicted MDR transporter

plays a role in imidazole transport in *C. glabrata*. This hypothesis will be addressed in this study.

The remaining cluster harbors two proteins related with Lipid and cell wall metabolism. The putative cell wall remodeling protein CgGas1, upregulated in this cluster, presumes some level of cell wall response against clotrimazole stress.

Table 3.1 – Set of 37 proteins found to have significant expression changes in *C. glabrata* wild-type cells in the presence of clotrimazole and correspondent fold changes in *Δcgpdr1* mutant cells upon exposure to the drug. Protein clustering was performed based on the role of their predicted *S. cerevisiae* homologs.

***C. glabrata* protein (ORF) name**	***S. cerevisiae* homolog**	**Description of the function of the *C. glabrata* protein or of its *S. cerevisiae* homolog[a]**	**Wild-type fold change (upon clotrimazole stress)**	***Δcgpdr1* fold change (upon clotrimazole stress)**
Glucose Metabolism				
CAGL0L01485g	*GSF2*	Uncharacterized. *S. cerevisiae* homolog encodes a ER localized integral membrane protein that may promote secretion of certain hexose transporters, including Gal2	2.26	2.30**
PGK1 (CAGL0L07722g)	*PGK1*	Uncharacterized. *S. cerevisiae* homolog encodes a 3-phosphoglycerate kinase; key enzyme in glycolysis and gluconeogenesis	6.31	4.93**
Oxidative phosphorylation				
CAGL0H05489g	*ATP4*	Uncharacterized. *S. cerevisiae* homolog encodes a subunit b of the stator stalk of mitochondrial F1F0 ATP synthase	1.68	1.49
CAGL0F04565g	*COR1*	Uncharacterized. *S. cerevisiae* homolog encodes a core subunit of the ubiquinol-cytochrome c reductase complex, a component of the mitochondrial inner membrane electron transport chain	0.32	4.79

Table 3.1 (continued)

C. glabrata **protein (ORF) name**	***S. cerevisiae*** **homolog**	**Description of the function of the *C. glabrata* protein or of its *S. cerevisiae* homolog[a]**	**Wild-type fold change (upon clotrimazole stress)**	***Δcgpdr1*** **fold change (upon clotrimazole stress)**
Oxidative phosphorylation				
RIP1 (CAGL0I03190g)	*RIP1*	Uncharacterized. *S. cerevisiae* homolog encodes a ubiquinol-cytochrome-c reductase; a Rieske iron-sulfur protein of the mitochondrial cytochrome bc1 complex	0.10	1.96**
CAGL0G10131g	*QCR2*	Uncharacterized. *S. cerevisiae* homolog encodes a subunit 2 of the ubiquinol cytochrome-c reductase complex, a component of the mitochondrial inner membrane electron transport chain	0.40	0.68
CAGL0G10153g	*QCR7*	Uncharacterized. *S. cerevisiae* homolog encodes a subunit 7 of the ubiquinol cytochrome-c reductase complex, a component of the mitochondrial inner membrane electron transport chain	0.21	1.24*
Mitochondrial import				
CAGL0I10472g	*PHB1*	Uncharacterized. *S. cerevisiae* homolog encodes a subunit of the prohibitin complex (Phb1p-Phb2p), a 1,2 MDa ring-shaped inner mitochondrial membrane chaperone that stabilizes newly synthesized proteins	3.09	2.18**
CAGL0L12936g	*TOM70*	Uncharacterized. *S. cerevisiae* homolog encodes a component of the TOM (translocase of outer membrane) complex; involved in the recognition and initial import steps for all mitochondrially directed proteins	0.57	0.37
Ribosome components and translation machinery				
CAGL0A03388g	*RPL15B*	Uncharacterized. *S. cerevisiae* homolog encodes a ribosomal 60S subunit protein L13B; not essential for viability	2.22	1.78**
CAGL0E02013g	*RPL18A*	Uncharacterized. *S. cerevisiae* homolog encodes a protein component of the small (40S) ribosomal subunit	2.21	2.17
CAGL0E03938g	*RPL8B*	Uncharacterized. *S. cerevisiae* homolog encodes a ribosomal 60S subunit protein L8B	0.16	0.13

Table 3.1 (continued)

C. glabrata protein (ORF) name	*S. cerevisiae* homolog	Description of the function of the *C. glabrata* protein or of its *S. cerevisiae* homolog[a]	Wild-type fold change (upon clotrimazole stress)	*Δcgpdr1* fold change (upon clotrimazole stress)
Ribosome components and translation machinery				
CAGL0F07073g	*RPS2*	Uncharacterized. *S. cerevisiae* homolog encodes a protein component of the small (40S) subunit	0.45	0.64
CAGL0F09031g	*RPS4A*	Uncharacterized. *S. cerevisiae* homolog encodes a protein component of the small (40S) ribosomal subunit	0.47	0.53
CAGL0G00990g	*RPP0*	Uncharacterized. *S. cerevisiae* homolog encodes a conserved ribosomal protein P0 of the ribosomal stalk	0.59	1.03**
CAGL0G01078g	*RPL26A*	Uncharacterized. *S. cerevisiae* homolog encodes a ribosomal 60S subunit protein L33B	0.22	0.11
CAGL0G06490g	*RPS7A*	Uncharacterized. *S. cerevisiae* homolog encodes a protein component of the small (40S) ribosomal subunit	0.22	0.36
CAGL0H00462g	*RPS5*	Uncharacterized. *S. cerevisiae* homolog encodes a protein component of the small (40S) ribosomal subunit	0.55	0.84*
CAGL0J03234g	*RPS24B*	Uncharacterized. *S. cerevisiae* homolog encodes a protein component of the small (40S) ribosomal subunit	0.33	0.31
CAGL0K06567g	*RPL27A*	Uncharacterized. *S. cerevisiae* homolog encodes a ribosomal 60S subunit protein L27A	0.13	0.24
CAGL0K07414g	*RPL20B*	Uncharacterized. *S. cerevisiae* homolog encodes a ribosomal 60S subunit protein L20A	0.36	0.33**
CAGL0K11748g	*RPS11A*	Uncharacterized. *S. cerevisiae* homolog encodes a protein component of the small (40S) ribosomal subunit	0.47	0.60
CAGL0L08114g	*RPS22A*	Uncharacterized. *S. cerevisiae* homolog encodes a protein component of the small (40S) ribosomal subunit	0.52	0.40**
CAGL0L12870g	*TMA19*	Uncharacterized. *S. cerevisiae* homolog encodes a protein that associates with ribosomes	0.26	3.24**
CAGL0M02695g	*RPL5*	Uncharacterized. *S. cerevisiae* homolog encodes a ribosomal 60S subunit protein L5	0.45	0.58

Table 3.1 (continued)

C. glabrata **protein (ORF) name**	***S. cerevisiae*** **homolog**	**Description of the function of the *C. glabrata* protein or of its *S. cerevisiae* homolog[a]**	**Wild-type fold change (upon clotrimazole stress)**	***Δcgpdr1*** **fold change (upon clotrimazole stress)**
Ribosome components and translation machinery				
EFT2 (CAGL0A03234g)	*EFT1*	Uncharacterized. *S. cerevisiae* homolog encodes an elongation factor 2	0.43	0.36
CAGL0H08976g	*RPL1A*	Uncharacterized. *S. cerevisiae* homolog encodes a ribosomal 60S subunit protein L15A	0.41	0.50**
CAGL0H03773g	*RPL7*	Uncharacterized. *S. cerevisiae* homolog encodes a nucleolar protein with similarity to large ribosomal subunit L7 proteins; constituent of 66S pre-ribosomal particles	0.36	0.47**
CAGL0I00792g	*RPS16A*	Uncharacterized. *S. cerevisiae* homolog encodes a protein component of the small (40S) ribosomal subunit	0.20	0.31
SSB1 (CAGL0C05379g)	*SSB2*	Uncharacterized. *S. cerevisiae* homolog encodes a cytoplasmic ATPase that is a ribosome-associated molecular chaperone	0.58	0.51**
TEF3 (CAGL0B03487g)	*TEF3*	Uncharacterized. *S. cerevisiae* homolog encodes a gamma subunit of translational elongation factor eEF1B	0.58	0.77
Lipid and cell wall metabolism				
HFD1 (CAGL0K03509g)	*HFD1*	Uncharacterized. Gene is upregulated in azole-resistant strain. *S. cerevisiae* homolog encodes a hexadecenal dehydrogenase	6.74	1.19*
GAS1 (CAGL0G00286g)	*GAS1*	Putative glycoside hydrolase of the Gas/Phr family; predicted GPI-anchor; *S. cerevisiae* homolog encodes a beta-1,3-glucanosyltransferase, required for cell wall assembly	3.92	1.61**
Multidrug resistance transporters				
CAGL0E03674g	*TPO1*	Uncharacterized. *S. cerevisiae* homolog encodes a polyamine transporter of drug:H(+) antiporter DHA1 family	1.44	1.57
CgQDR2 (CAGL0G08624g)	*QDR2*	Drug:H+ antiporter of the Major Facilitator Superfamily, confers imidazole drug resistance; activated by Pdr1p and in azole-resistant strain	4.29	3.11

Table 3.1 (continued)

C. glabrata protein (ORF) name	*S. cerevisiae* homolog	Description of the function of the *C. glabrata* protein or of its *S. cerevisiae* homolog[a]	Wild-type fold change (upon clotrimazole stress)	*Δcgpdr1* fold change (upon clotrimazole stress)
Multidrug resistance transporters				
CgSNQ2 (CAGL0I04862g)	*SNQ2*	Plasma membrane ATP-binding cassette (ABC) transporter; involved in Pdr1p-mediated azole resistance	2.78	0.72*
CgCDR1 (CAGL0M01760g)	*PDR5*	Multidrug transporter of ATP-binding cassette (ABC) superfamily; involved in Pdr1p-mediated azole resistance; increased abundance in azole resistant strains	6.40	0.20

* Fold change value outside of the chosen cut-off intervals (0.71 < fold change < 1.4)

**Fold change quantification considered as not reliable (p-value>0.05)

3.4.3 Effect of CgPdr1 deletion in the membrane proteome-wide changes occurring in response to clotrimazole in *C. glabrata*

The analysis of the membrane-enriched fraction of the *C. glabrata* proteome obtained from cells exposed to clotrimazole in the absence of the transcription factor CgPdr1 was assessed and compared to that of the *C. glabrata* wild-type cells exposed to clotrimazole. Among the 37 proteins whose expression was seen to change in the wild-type strain, 6 proteins were found to be repressed by CgPdr1, possibly in an indirect fashion, while 6 proteins were found to be activated by CgPdr1 (Table 3.1). For the remaining 25 proteins, no statistically significant change could be detected in the current experiment.

Particularly interesting in this context are the 6 proteins which were found to be induced by clotrimazole in the dependence of CgPdr1: the multidrug transporters CgSnq2 and CgCdr1; the hexadecenal dehydrogenase CgHfd1; the ribosomal protein CgRpl26A; the component of the TOM (translocase of outer membrane) complex CgTom70; and the β-1,3-glucanosyltransferase CgGas1. Interestingly, at least one CgPdr1-binding site is found in the promoter regions of the first 4 genes, suggesting that the action of CgPdr1 in their expression may be direct. These results are consistent with the characterization

of several of these proteins as efflux pumps and of their expression to be dependent on CgPdr1 in response to other chemical stress inducers [30,31,35,37]. The expression changes here observed reinforce CgPdr1 as a major pleiotropic drug resistance mediator and highlight its role in mediating the expression of multidrug transporters in response to clotrimazole. The observation regarding the lipid metabolism related protein CgHfd1 is consistent with previous microarray studies, reporting the activation of CgHfd1 upon exposure to fluconazole induced stress in the dependence of CgPdr1 [9]. It would be interesting to assess whether this result may relate to the imidazole mode of action on lipid raft binding, with CgHfd1 possibly intervening in plasma membrane lipid destabilization as a resistance mechanism dependent on CgPdr1.

3.4.4 CgTpo1_1 and CgTpo1_2 expression confer resistance to azoles and other chemical stress inducers

The deletion of *CgTPO1_1* and especially *CgTPO1_2* in *C. glabrata* was found to increase the susceptibility of this pathogen to clotrimazole, but also to other imidazoles such as miconazole, ketoconazole and tioconazole; as well as triazoles such as itraconazole and fluconazole (Figure 3.3A). Additionally, an effect in susceptibility to other antifungal drug families was observed, namely to the polyene amphotericin B, the pyrimide analog 5-flucytosine, the fungicide mancozeb and to the polyamine spermine (Figure 33.A). As determined by spot assays, the wild-type strain KUE100 is capable of growing in the tested concentrations, while the *Δcgtpo1_1* and especially *Δcgtpo1_2* mutants display reduced growth when compared to wild-type, suggesting a role of *CgTPO1_1* and *CgTPO1_2* as azole drug resistance determinants in *C. glabrata*. The over-expression of *CgTPO1_1* or *CgTPO1_2* in a wild-type strain was concordantly found to increase *C. glabrata* natural resistance towards the tested antifungal drugs (Figure 33.B). Consistent with the attributed role of *S. cerevisiae* Tpo1 in polyamine [18] and mancozeb [21] resistance, *CgTPO1_1* or *CgTPO1_2* expression was also found to increase *C. glabrata* resistance to the polyamine spermine and the fungicide mancozeb (Figure 3.3A and 3.3B).

Using *S. cerevisiae* has a heterologous expression system, the effect of *CgTPO1_1* and *CgTPO1_2* expression on yeast resistance to polyamines and mancozeb was further tested in order to assess if these genes are able to complement their *S. cerevisiae*

homolog. The deletion of the *S. cerevisiae TPO1* gene was found to increase the susceptibility to the polyamine spermine and the fungicide mancozeb. When expressed in the *Δtpo1 S. cerevisiae* background, the *CgTPO1_1* and *CgTPO1_2* genes were able to rescue the observed susceptibility phenotype to spermine and mancozeb (data not shown).

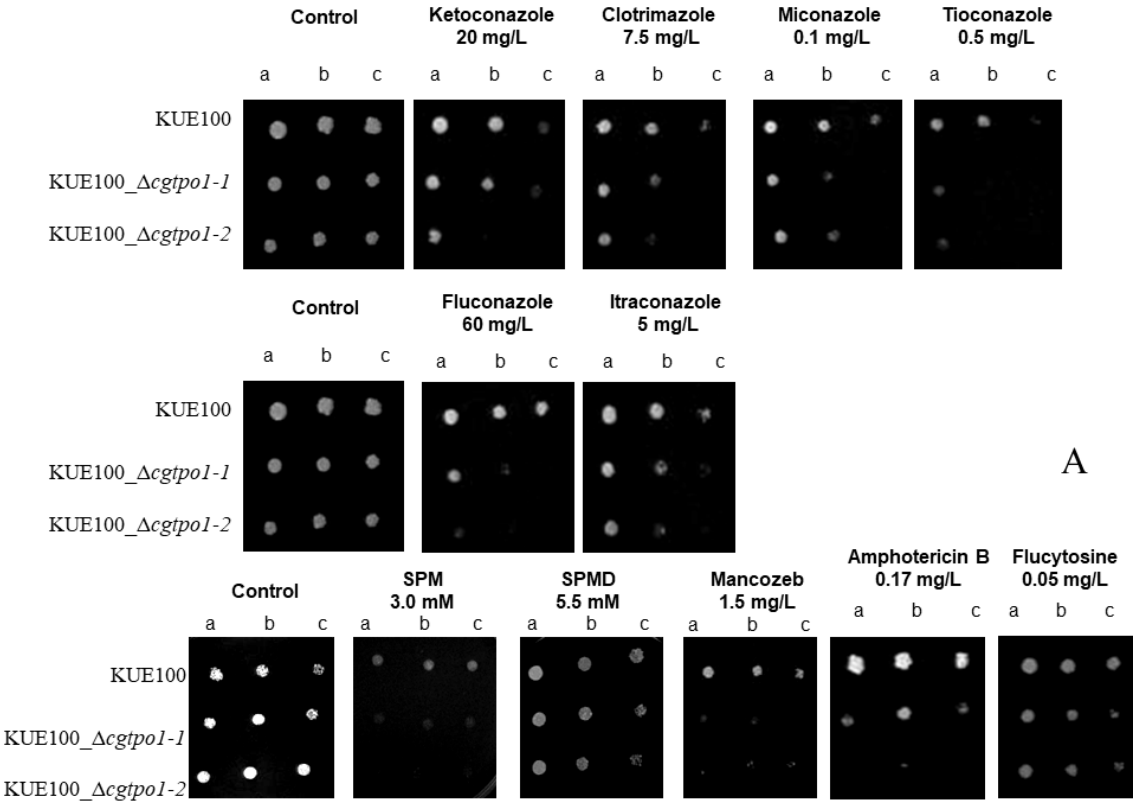

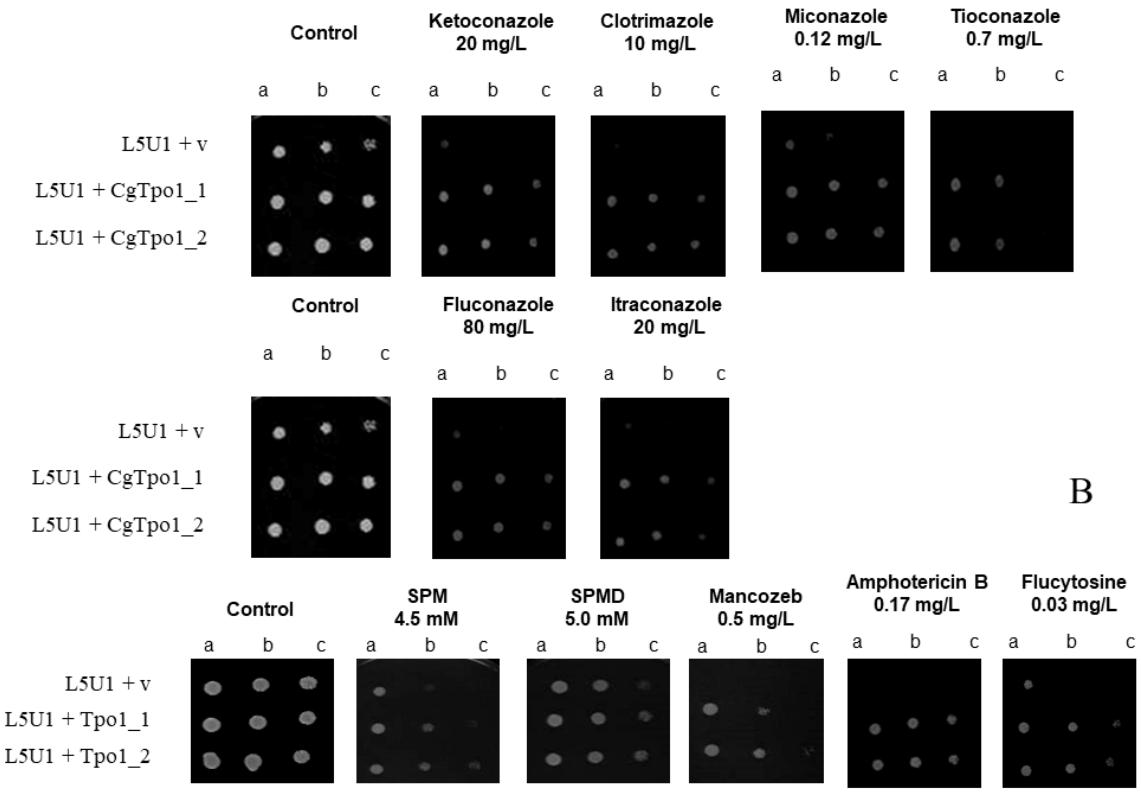

Figure 3.3 – CgTpo1_1 and CgTpo1_2 confer resistance to azole antifungal drugs in *C. glabrata* cells. (A) Comparison of the susceptibility to inhibitory concentrations of several chemical stress inducers, at the indicated concentrations, of the *C. glabrata* KUE100, KUE100_*Δcgtpo1_1* and KUE100_*Δcgtpo1_2* strains, in YPD agar plates (SPM - spermine and SPMD - spermidine) and BM plates (remaining drugs) by spot assays. (B) Comparison of the susceptibility to several drug stress inducers, at the indicated concentrations, of the *C. glabrata* L5U1 strain, harboring the pGREG576 cloning vector (v) or the pGREG576_MTI_*CgTPO1_1* or pGREG576_MTI_*CgTPO1_2* plasmids in YPD agar plates (SPM and SPMD) and BM agar plates (remaining drugs), without uracil, by spot assays. (c) Comparison of the vector pGREG576 (v) or the derived *CgTPO1_1* or *CgTPO1_2* expression plasmids pGREG576_*CgTPO1_1* or pGREG576_*CgTPO1_2*, on BM agar plates by spot assays. The inocula were prepared as described in Experimental Procedures. Cell suspensions used to prepare the spots were 1:5 (b) and 1:25 dilutions of the cell suspension used in (a). The displayed images are representative of at least three independent experiments.

3.4.5 CgTpo1_1 and CgTpo1_2 are localized to the plasma membrane in *C. glabrata* and when heterologously expressed in *S. cerevisiae*

C. glabrata cells harboring the pGREG576_MTI_*CgTPO1_1* and pGREG576_MTI_*CgTPO1_2* plasmids were grown to mid-exponential phase in minimal medium and then transferred to the same medium containing 50 µM $CuSO_4$ to induce fusion protein expression. At a standard OD_{600nm} of 0.5 ± 0.05, obtained after 5h of incubation, cells were inspected by fluorescence microscopy. In *C. glabrata* cells, the CgTpo1_1_GFP and CgTpo1_2_GFP fusion proteins were found to be localized to the

cell periphery (Figure 3.4). In a similar approach, *S. cerevisiae* cells harboring the pGREG576_*CgTPO1_1* and pGREG576_*CgTPO1_2* plasmids were grown to mid-exponential phase in minimal medium containing 0.5% glucose and 0.1% galactose, and then transferred to the same medium containing 0.1% glucose and 1% galactose, to promote protein over-expression. At a standard OD_{600nm} of 0.5 ± 0.05, cells were analyzed by fluorescence microscopy and the fusion proteins were found to be localized to the cell periphery (Figure 3.4). These results strongly suggest plasma membrane localization for both CgTpo1_1 and CgTpo1_2, similar to that observed for their *S. cerevisiae* homolog Tpo1.

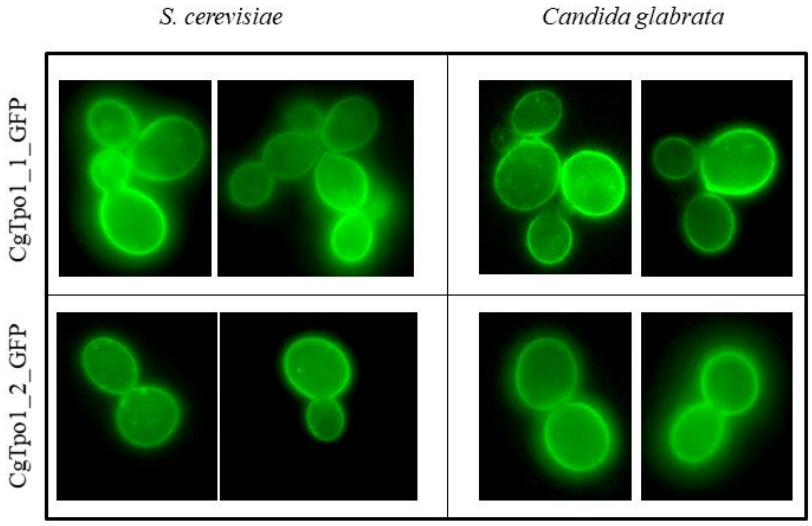

Figure 3.4 – Fluorescence of exponential phase BY4741 *S. cerevisiae* and L5U1 *C. glabrata* cells, harboring the expression plasmids pGREG576_*CgTPO1_1* and pGREG576_*CgTPO1_2*; or pGREG576_MTI_*CgTPO1_1* and pGREG576_MTI_*CgTPO1_2*, after galactose or copper-induced recombinant protein production, respectively.

3.4.6 CgTpo1_1 and CgTpo1_2 mediate ^{3}H-clotrimazole efflux in *C. glabrata*

Based on the identification of CgTpo1_1 and CgTpo1_2 as plasma membrane MDR transporters conferring resistance to azole drugs, their possible involvement in reducing clotrimazole accumulation in stressed yeast cells was examined. Under these conditions, the deletion of the *CgTPO1_1* gene, and especially the deletion of the *CgTPO1_2* leads to a very significant decrease in the exponential growth rate, when compared to the parental strain (Figure 3.5). ^{3}H-clotrimazole accumulation assays were carried out in the

absence or presence of the encoding genes. Consistent with the observed susceptibility phenotypes, *Δcgtpo1_1* and *Δcgtpo1_2* deletion mutants were found to accumulate four- and five-fold more radiolabeled clotrimazole than the corresponding parental KUE100 strain, respectively (Figures 3.6A and 3.6B). These results strongly suggest that CgTpo1_1 and CgTpo1_2 activities increase *C. glabrata* resistance towards clotrimazole by reducing its accumulation within yeast cells.

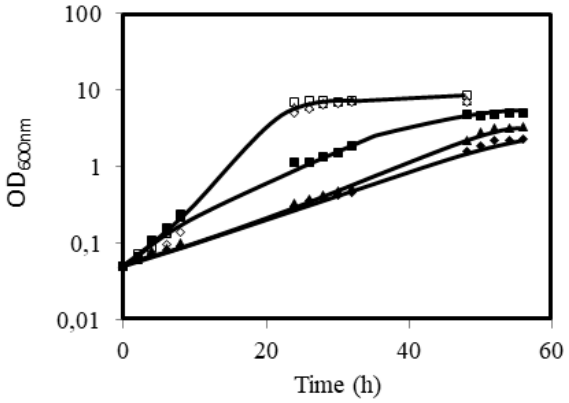

Figure 3.5 – Comparison of growth curves of *C. glabrata* KUE100 (■,□), KUE100_*Δcgtpo1_1* (▲,△) and KUE100_*Δcgtpo1_2* (◆,◇) cell populations, in liquid BM medium, in the absence (open symbols) or presence of 90 mg/L clotrimazole (filled symbols), measured in terms of variation in OD_{600nm}. The displayed growth curves are representative of at least three independent experiments.

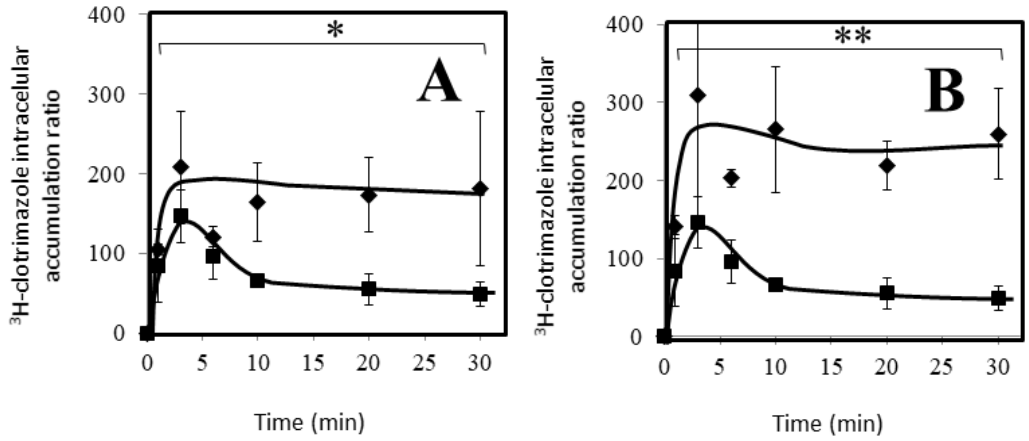

Figure 3.6 – Time-course accumulation of radiolabeled ^{3}H-clotrimazole in strains KUE100 (▪) wild-type and KUE100_*Δcgtpo1_1* (♦) (A) and KUE100 (▪) and KUE100_*Δcgtpo1_2* (♦) (B), during cultivation in BM liquid medium in the presence of 30 mg/L unlabeled clotrimazole. Accumulation values are the average of at least three independent experiments. Error bars represent the corresponding standard deviations. *p<0.05. **p<0.01.

3.4.7 *CgTPO1_1* and *CgTPO1_2* transcript levels are upregulated under clotrimazole stress

The effect of *C. glabrata* cell challenge with inhibitory concentrations of clotrimazole in *CgTPO1_1* and *CgTPO1_2* transcript levels were evaluated. The transcript levels of *CgTPO1_1* were seen to have no significant change upon 1h of exposure to inhibitory concentrations of clotrimazole (Figure 3.7A); whereas the transcript levels of *CgTPO1_2* were found to have a 7-fold increase upon clotrimazole exposure (Figure 3.7B). These results show *CgTPO1_2* transcript levels to be responsive to clotrimazole exposure, consistent with the observed increase of CgTpo1_2 concentration in the membrane of clotrimazole-exposed *C. glabrata* cells (Table 3.1). Expression values attained in *Δcgpdr1* mutant cells show a slight decrease in the case of *CgTPO1_1*, however, this decrease was not found to be statistically relevant (Figure 3.7A). On the other hand, the attained expression values confirm that CgPdr1 is not controlling the observed *CgTPO1_2* upregulation (Figure 3.7B).

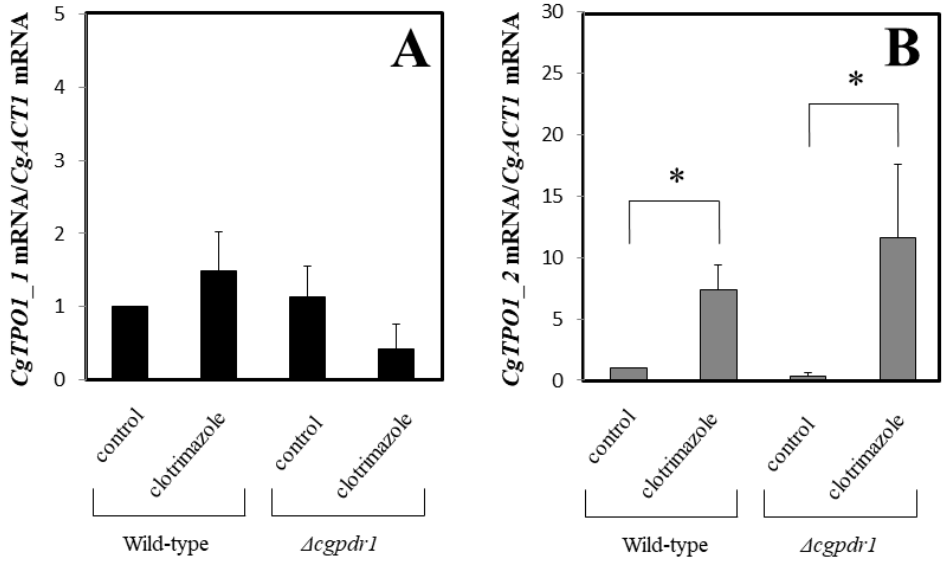

Figure 3.7 – Comparison of the variation of the *CgTPO1_1* (A) and *CgTPO1_2* (B) transcript levels in the 66032u *C. glabrata* wild-type strain and in the derived 66032u_*Δcgpdr1* deletion mutant, before (control) and after 1h of exposure 60 mg/L clotrimazole. The presented transcript levels were obtained by quantitative RT-PCR and are relative *CgTPO1_1*/*CgACT1* or *CgTPO1_2*/*CgACT1* mRNA, relative to the values registered in the 66032u parental strain in control conditions. The indicated values are averages of at least three independent experiments. Error bars represent the corresponding standard deviations. *p<0.05.

3.4.8 CgGas1 expression confers resistance to azoles

The deletion of *CgGAS1* in *C. glabrata* was found, based on spot assays, to increase the susceptibility of this pathogen to several azole antifungal drugs, such as clotrimazole, miconazole, ketoconazole, tioconazole (imidazoles); and fluconazole and itraconazole (triazoles). The wild-type strain (KUE100) is capable of growing in the tested concentrations, while the *Δcggas1* mutant displays very limited growth when compared to the wild-type, therefore showing a higher degree of susceptibility towards the tested azole drugs (Figure 3.8A).

3.4.9 Response to clotrimazole includes cell wall remodeling, mostly independently of CgGas1

A possible role of CgGas1 in cell wall resistance was assessed through the evaluation of lyticase susceptibility in yeast cells before and after adaptation to clotrimazole. The susceptibility to lyticase of exponential wild-type (KUE100) cells was seen to be lower than that exhibited by *Δcggas1* deletion mutant cells (Figure 3.8B), grown in the absence of clotrimazole. This result indicates that in the absence of stress, the cell wall of *Δcggas1* cells is more susceptible than that of wild-type cells. In wild-type or *Δcggas1* cells, sudden exposure to clotrimazole during 30 minutes leads to similarly increased susceptibility to lyticase, showing that clotrimazole appears to have a drastic effect at the level of the cell wall structure. However, once adapted to exponential growth in the presence of clotrimazole, either wild-type or *Δcggas1* cells exhibited levels of lyticase resistance which are even higher than those exhibited by non-stressed cells. This result suggests that adaptation to clotrimazole includes cell wall remodeling. Altogether, the lack of the CgGas1 putative cell wall assembly protein increases lyticase susceptibility at the level of cell wall in control conditions, eventually helping the *C. glabrata* cells to cope with sudden stress exposure. However, even in the absence of this protein cell wall remodeling taking place during adaptation to clotrimazole still takes place, but at a slower rate than observed in the wild-type cell population.

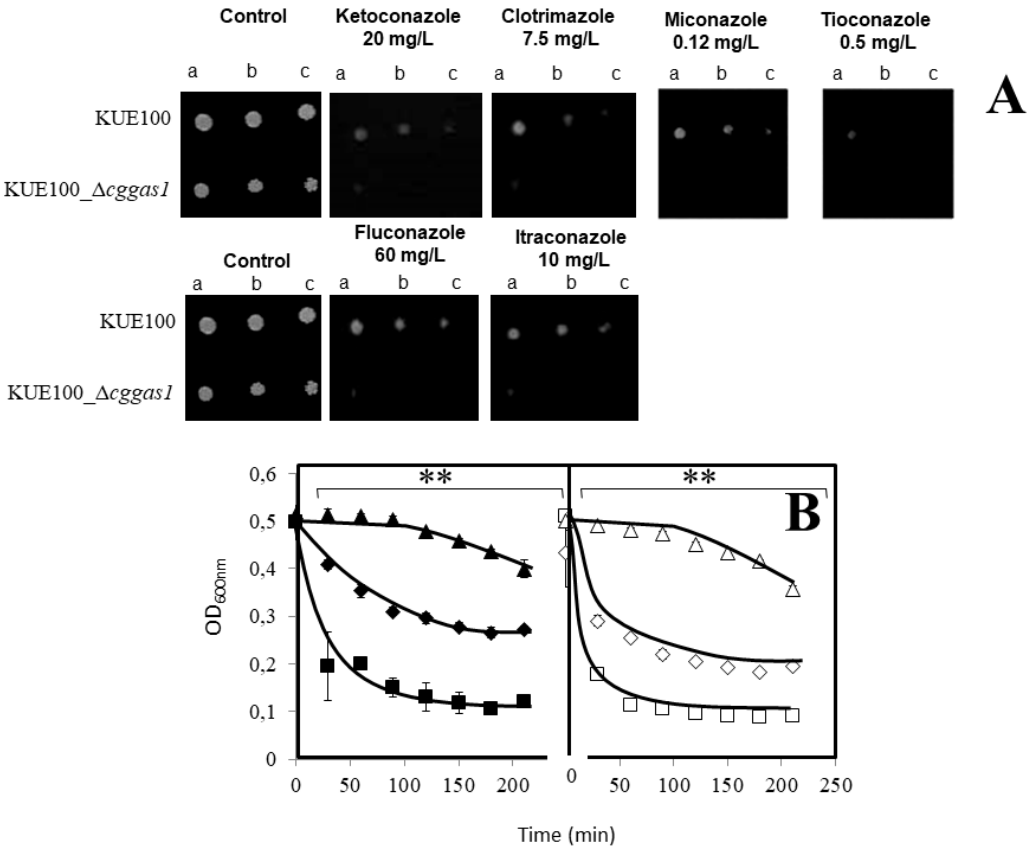

Figure 3.8 – CgGas1 confers resistance to azole antifungal drugs in *C. glabrata* cells. (A) Comparison of the susceptibility to azole antifungal drugs, at the indicated concentrations, of the *C. glabrata* KUE100 wild-type and KUE100_*Δcggas1* strains, in BM agar plates by spot assays. The inocula were prepared as described in Experimental Procedures. Cell suspensions used to prepare the spots were 1:5 (b) and 1:25 (c) dilutions of the cell suspension used in (a). The displayed images are representative of at least three independent experiments. (B) Lyticase susceptibility in *C. glabrata* KUE100 (♦,■,▲) and KUE100_*Δcggas1* (◊,□,Δ) cells harvested in the exponential phase of growth in the absence of stress (♦,◊) or upon 30 min of exposure to 30 mg/L clotrimazole (■,□), or in the exponential phase of growth reached upon adaptation to 30 mg/L clotrimazole (▲,Δ). After addition of 10 mg/L lyticase, the decrease in the OD_{600nm} of the cell suspension was measured periodically and indicated as a percentage of the initial OD_{600nm}. The indicated values are averages of at least three independent experiments. Error bars represent the corresponding standard deviations. **p<0.01.

3.4.10 CgGas1 reduces the intracellular accumulation of ^{3}H-clotrimazole in *C. glabrata*

Once the *C. glabrata* CgGas1 was identified as conferring resistance to azole drugs, its possible involvement in reducing clotrimazole accumulation in yeast cells was examined. The accumulation of radiolabeled clotrimazole in non-adapted *C. glabrata* cells suddenly exposed to 30 mg/L clotrimazole was seen to be approximately 2 times higher in cells devoid of CgGas1 when compared to the KUE100 wild-type cells (Figure 3.9C). These findings strongly suggest that CgGas1 contributes to *C. glabrata*

tolerance toward clotrimazole also by reducing its accumulation within yeast cells. These results show CgGas1 to be an important factor for cell wall composition, apparently necessary for clotrimazole resistance by catalyzing glucan linkage and chain elongation, thus reducing drug diffusion through the cell wall and into the cytosol.

Given that the deletion of the *CgTPO1_2* gene was previously found to significantly increase the susceptibility of this pathogen to azole drugs as well, a double deletion mutant was constructed in order to assess if both genes contribute in a cumulative manner to azole drug resistance. The deletion of both genes in *C. glabrata* was found, based on spot assays and growth curves, to further increase the susceptibility to the antifungal drugs clotrimazole, miconazole, tioconazole (imidazoles) and fluconazole (triazole), when compared to the susceptibility attained for the correspondent single mutants, leading to a drastic decrease in the growth rate of *C. glabrata* cells in the presence of clotrimazole (Figure 3.9A and 3.9B). The accumulation of radiolabeled clotrimazole was also tested in a KUE100*_Δcggas1_Δcgtpo1_2* double mutant. The accumulation of radiolabeled clotrimazole in non-adapted *C. glabrata* cells suddenly exposed to 30 mg/L clotrimazole was seen to be approximately 5 times higher in double mutant cells when compared to wild-type cells (Figure 3.9C). However, the deletion of *CgTPO1_2* in the *Δcggas1* background increases the amount of clotrimazole accumulation in *C. glabrata* cells, but only to levels close to the ones registered in the KUE100 *_Δcgtpo1_2* single mutant.

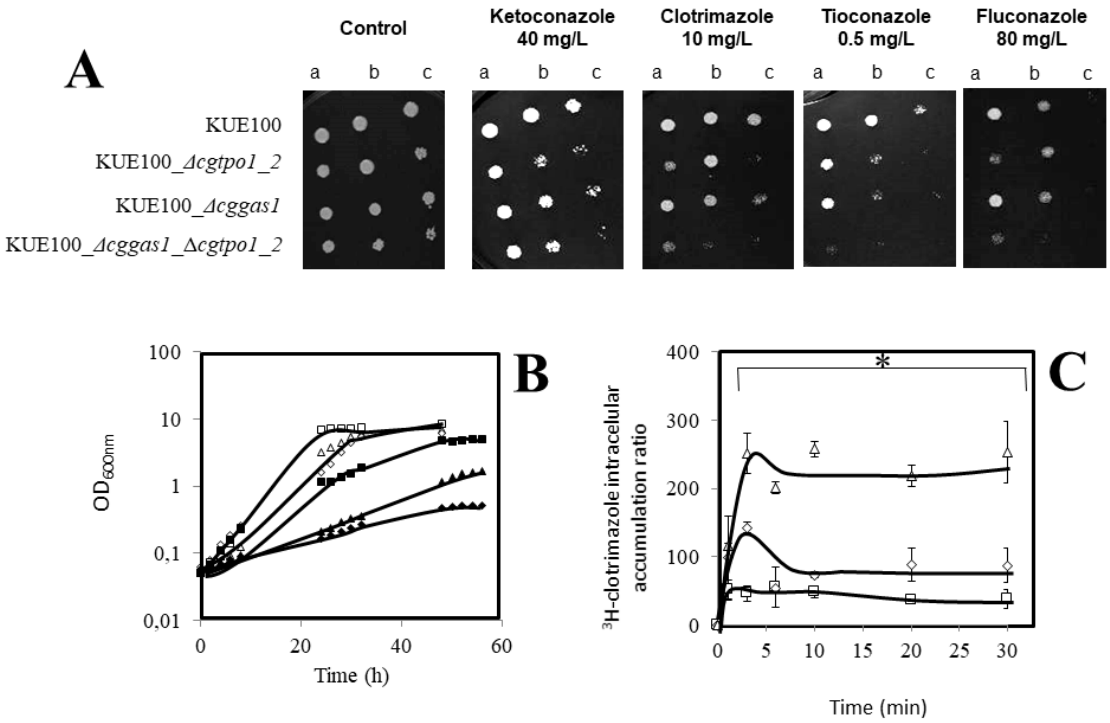

Figure 3.9 – The combined action of CgTpo1_2 and CgGas1 confers resistance to azole antifungal drugs in *C. glabrata* cells. (A) Comparison of the susceptibility to azole antifungal drugs, at the indicated concentrations, of the *C. glabrata* KUE100 wild-type and KUE100_*Δcggas1* strains, in BM agar plates by spot assays. The inocula were prepared as described in Experimental Procedures. Cell suspensions used to prepare the spots were 1:5 (b) and 1:25 (c) dilutions of the cell suspension used in (a). The displayed images are representative of at least three independent experiments. (B) Comparison of growth curves of *C. glabrata* KUE100 (■,□), KUE100_*Δcggas1* (▲,Δ) and KUE100_*Δcggas1_Δcgtpo1_2* (♦,◊), in liquid BM, in the absence (open symbols) or presence of 90 mg/L clotrimazole (filled symbols), measured in terms of variation in OD_{600nm}. The displayed growth curves are representative of at least three independent experiments. (C) Time-course accumulation of clotrimazole in KUE100 (□), KUE100_*Δcggas1* (◊) and KUE100_*Δcggas1_Δcgtpo1_2* (Δ) strains, during cultivation in BM liquid medium in the presence of radiolabeled ^{3}H-clotrimazole. Accumulation values are the average of at least three independent experiments. Error bars represent the corresponding standard deviations. *p<0.05.

3.5 Discussion

In this work, the first iTRAQ-based membrane proteomics study focused on the fungal pathogen *Candida glabrata* was undertaken, leading to functional characterization of the *C. glabrata* CgTpo1_1 and CgTpo1_2 drug:H^+ antiporters, and of the cell wall assembly protein CgGas1, in the context of clotrimazole drug resistance.

Using a membrane proteomics analysis, several proteins from distinct functional groups were found to be differentially expressed in *C. glabrata* clotrimazole response. Ribosomal proteins were amongst the downregulated ones, in accordance with the environmental stress response described by Gasch *et al.* [33], in which ribosomal proteins have a stress-dependent repression as a mechanism to conserve mass and energy while redirecting transcription to genes whose expression is induced by stress. The upregulated proteins encompass glucose metabolism, also in accordance with the predicted environmental stress response [33] and therefore were considered to be part of a general response. The more specific roles of CgCdr1 and CgSnq2 in clotrimazole response, registered in this study, could also eventually be predicted based on their known role in fluconazole adaptive response [38]. Interestingly, in a distinct proteomics study using fluconazole-resistant *C. glabrata* strains, and consistent with our work, several proteins involved in energy transfer and various metabolic pathways were identified [39]. In the referred study, resistant strains have been described to exhibit several upregulated membrane proteins, in contrast with the downregulation verified for several intracellular proteins in response to the drug. This data reinforces the relevance for directed membrane fraction proteomics studies, such as the work presented herein, as these proteins can reveal important factors and mechanisms of azole drug resistance in this pathogenic yeast.

More interesting was the observation that the multidrug transporter CgTpo1_2 and the cell wall related protein CgGas1 appear to be implicated in clotrimazole response. So far, CgTpo3 was the only transporter from the Tpo1-4 group to be associated with azole drug resistance in *C. glabrata* [30]. CgTpo1_1 and CgTpo1_2 (*ORFs CAGL0G03927g* and *CAGL0E03674g*, respectively) are described herein as the fourth and fifth members of the DHA1 family to be associated with azole drug resistance; after CgQdr2, CgAqr1 and CgTpo3 [29–31]. Azole antifungal drugs, to which CgTpo1_1 and CgTpo1_2 confer resistance to, were found to include the imidazoles clotrimazole, miconazole,

tioconazole and ketoconazole, used in the treatment of superficial skin and mucosal infections, but also the triazoles itraconazole and fluconazole, used against systemic infections. Given the observation that clotrimazole accumulation is three to five times higher in the absence of *CgTPO1_1* or *CgTPO1_2* than observed in wild-type *C. glabrata* cells, the mechanism underlying the role of CgTpo1_1 and CgTpo1_2 in clotrimazole resistance appears to be direct transport of the drug. Nonetheless, and similarly to what was observed for their *S. cerevisiae* homolog, Tpo1, *CgTPO1_1* and *CgTPO1_2* deletion was also found to increase susceptibility to spermine, suggesting a physiological role for these transporters in polyamine homeostasis. Interestingly, the homolog of these transporters in *C. albicans*, *FLU1*, was previously found to confer fluconazole resistance when expressed in *S. cerevisiae* [23]. These transporters were further found to confer resistance to the polyene antifungal drug amphotericin B and to the fungicide mancozeb. Interestingly, the related DHA transporter CgTpo3 does not appear to confer resistance to flucytosine or amphotericin B [30], while CgAqr1 is involved in flucytosine resistance [29]. These observations seem to imply that CgTpo1_1 and CgTpo1_2 are gifted with extraordinary substrate variety, even within their own DHA1 family [7]. Consistent with these results, their *S. cerevisiae* homolog was demonstrated to confer resistance to, at least, five different drugs besides polyamines, including the fungicide cycloheximide, the antiarrythmic drug quinidine, the polyene nystatin and the herbicides MCPA and 2,4-D [16,17].

The possibility that these transporters could be regulated by the major controller of the MDR phenomenon in *C. glabrata*, CgPdr1, was further investigated. As far as we could determine, the expression of these transporters appears to be independent on CgPdr1. Consistently, an analysis of the *CgTPO1_1* and *CgTPO1_2* promoter regions, performed in the Regulatory Sequence Analysis Tools web site (http://rsat.ulb.ac.be/), was unable to identify any of the CgPdr1-binding elements (BCCRYYRGD and TCCRYGGA) [9], supporting the possibility that these transporters may not be under direct control of CgPdr1.

This study further highlights the importance the cell wall protein CgGas1 in yeast resistance to clotrimazole. So far, *C. glabrata* Gas1 is described to be constitutively expressed, probably due to an important role in cell wall homeostasis, since its deletion was found to result in the formation of cell aggregates and growth defects, much in tune with the observed *S. cerevisiae* mutant phenotype [15]. The formation of aggregates has

been also reported for the *C. albicans* homolog gene deletion mutant [40]. Based on the obtained data, the changes undergone by the cell wall upon sudden clotrimazole challenge were studied using a lyticase susceptibility screening assay. It is remarkable to realize that just upon 30 min of clotrimazole exposure *C. glabrata* cell walls become more susceptible to lyticase, suggesting that this drug has a deleterious effect at the cell wall level. Also consistent with the harmful effect of clotrimazole in the cell wall is the observation that *C. glabrata* cells adapted to exponential growth in the presence of clotrimazole exhibit cell walls which are clearly more resistant to lyticase. The cell wall remodeling that underlies this observation is expected to depend on the cell wall related genes found to confer resistance to clotrimazole. Interestingly, the observed strengthening of the cell wall makes the clotrimazole adapted cells even more lyticase tolerant than non-stressed exponentially growing cells. The fact that clotrimazole has such an effect over the cell wall, a structure targeted directly by the new class of antifungal drugs, the echinocandins, suggests that a combined therapy using echinocandins and azoles may be a promising approach which, to the best of our knowledge, has not been attempted so far. The cell wall related protein CgGas1 was found to be required for clotrimazole resistance, with the correspondent deletion mutant displaying higher susceptibility to azole drugs and showing increased clotrimazole intracellular accumulation, suggesting a role in making the cell wall less permeable to this compound. The obtained results suggest that CgGas1 may have a protective effect in sudden exposure to clotrimazole, but it appears to have a limited role in the observed clotrimazole-induced cell wall remodeling.

Since two distinct mechanisms for antifungal resistance in *C. glabrata* were addressed in this study, namely drug efflux mediated by the transporter proteins CgTpo1_1 and CgTpo1_2, and cell wall integrity mediated by cell wall assembly protein CgGas1, the eventual crosstalk between these two mechanisms was assessed. In fact, *C. glabrata* cells devoid of both *CgTPO1_2* and *CgGAS1* were found to accumulate similar levels of clotrimazole to the ones attained for the single mutant *Δcgtpo1_2*. These results indicate that despite the fact that *C. glabrata* cells accumulate two times more drug in the absence of *CgGAS1*, the absence of *CgTPO1_2* appears to have a more deleterious effect in terms of drug accumulation. Despite this observation, the fact that the double deletion of *CgTPO1_2* and *CgGAS1* genes leads to an increased susceptibility to clotrimazole, when compared to each of the individual single mutants, highlights the

cooperative action of these proteins in providing protection against this drug. Indeed, the obtained results suggest that the effect of CgGas1 in clotrimazole resistance goes beyond cell wall remodeling and decreased drug accumulation. Interestingly, a very recent study by Eustice and Pillus [41] reported new functions for this protein in DNA damage response upon exposure to genotoxins, in the model *S. cerevisiae*, apparently through an unforeseen role in regulating transcriptional silencing. This line of evidence, still to be fully explored, expands immensely the possible effects of CgGas1 deletion that may contribute to the increased susceptibility exhibited by *Δcggas1* cells.

Altogether, the results described in this study highlight the importance of multidrug transporters from the MFS in antifungal resistance phenotypes. The characterization of *C. glabrata* CgTpo1_1 and CgTpo1_2 multidrug transporters involved in azole drug resistance reinforces the need for study remaining members of this family in this increasingly relevant pathogenic yeast, given that these transporters are likely to have clinical impact. This work also highlights the importance of genome/proteome-wide approaches in the identification of new antifungal resistance mechanisms.

3.6 Acknowledgements

We acknowledge Thomas Edlind, from the Department of Microbiology & Immunology, Drexel University, College of Medicine, Philadelphia, USA, and John Bennett, National Institute of Allergy and Infectious Diseases, NIH, Bethesda, USA, for kindly providing the 66032u and L5U1 derived strains, respectively. We further acknowledge the contribution of Mary LoPresti, Kathrin Wilczak, Thomas Abbott, Christopher Colangelo and TuKiet Lam, from the MS & Proteomics Resource at Yale, for their role in the iTRAQ-based proteomics analysis described in the paper.

This work was supported by FEDER and "Fundação para a Ciência e a Tecnologia" (FCT) (Contracts PTDC/EBB-BIO/119356/2010, UID/BIO/04565/2013 and PhD grants to PP and CC).

3.7 References

1. Fidel, P.L.; Vazquez, J.A.; Sobel, J.D. *Candida glabrata*: review of epidemiology, pathogenesis, and clinical disease with comparison to *C. albicans*. *Clin. Microbiol. Rev.* **1999**, *12*, 80-96.

2. Mishra, N.N.; Prasad, T.; Sharma, N.; Payasi, A.; Prasad, R.; Gupta, D.K.; Singh, R. Pathogenicity and drug resistance in *Candida albicans* and other yeast species. A review. *Acta Microbiol. Immunol. Hung.* **2007**, *54*, 201-235.

3. Pfaller, M.A.; Diekema, D.J. Epidemiology of invasive candidiasis: A persistent public health problem. *Clin. Microbiol. Rev.* **2007**, *20*, 133-163

4. Jandric, Z.; Schüller, C. Stress response in *Candida glabrata* : pieces of a fragmented picture. *Future Microbiol.* **2011**, *6*, 1475–1484.

5. Perlroth, J.; Choi, B.; Spellberg, B. Nosocomial fungal infections: Epidemiology, diagnosis, and treatment. *Med. Mycol.* **2007**, *45*, 321-346.

6. Roetzer, A.; Gabaldón, T.; Schüller, C. From *Saccharomyces cerevisiae* to *Candida glabrata* in a few easy steps: important adaptations for an opportunistic pathogen. *FEMS Microbiol. Lett.* **2011**, *314*, 1–9.

7. Costa, C.; Dias, P.J.; Sá-Correia, I.; Teixeira, M.C. MFS multidrug transporters in pathogenic fungi: Do they have real clinical impact? *Front. Physiol.* **2014**, *5*, 197.

8. Caudle, K.E.; Barker, K.S.; Wiederhold, N.P.; Xu, L.; Homayouni, R.; Rogers, P.D. Genomewide Expression Profile Analysis of the *Candida glabrata Pdr1* Regulon. *Eukaryot. Cell* **2011**, *10*, 373-383.

9. Tsai, H.F.; Krol, A.A.; Sarti, K.E.; Bennett, J.E. *Candida glabrata PDR1*, a transcriptional regulator of a pleiotropic drug resistance network, mediates azole resistance in clinical isolates and petite mutants. *Antimicrob. Agents Chemother.* **2006**, *50*, 1384–1392.

10. Vermitsky, J.P.; Edlind, T.D. Azole resistance in *Candida glabrata*: coordinate upregulation of multidrug transporters and evidence for a Pdr1-like transcription factor. *Antimicrob. Agents Chemother.* **2004**, *48*, 3773–81.

11. Calahorra, M.; Lozano, C.; Sánchez, N.S.; Peña, A. Ketoconazole and miconazole alter potassium homeostasis in *Saccharomyces cerevisiae*. *Biochim. Biophys. Acta - Biomembr.* **2011**, *1808*, 433–445.

12. Shingu-Vazquez, M.; Traven, A. Mitochondria and Fungal Pathogenesis: Drug Tolerance, Virulence, and Potential for Antifungal Therapy. *Eukaryot. Cell* **2011**, *10*, 1376–1383.

13. Singh, A.; Yadav, V.; Prasad, R. Comparative Lipidomics in Clinical Isolates of *Candida albicans* Reveal Crosstalk between Mitochondria, Cell Wall Integrity and Azole Resistance. *PLoS One* **2012**, *7*, e39812.

14. Weig, M.; Jänsch, L.; Gross, U.; De Koster, C.G.; Klis, F.M.; De Groot, P.W.J. Systematic identification in silico of covalently bound cell wall proteins and analysis of protein-polysaccharide linkages of the human pathogen *Candida glabrata*. *Microbiology* **2004**, *150*, 3129–3144.

15. Haynes, K.; Frosch, M.; Weig, M.; Kurzai, O.; Rogers, T.R.; Mühlschlegel, F.A. A GAS-like gene family in the pathogenic fungus *Candida glabrata*. *Microbiology* **2001**, *147*, 2007–2019.

16. dos Santos, S.C.; Teixeira, M.C.; Dias, P.J.; Sá-Correia, I. MFS transporters required for multidrug/multixenobiotic (MD/MX) resistance in the model yeast: understanding their physiological function through post-genomic approaches. *Front. Physiol.* **2014**, *5*, 180.

17. Sá-Correia, I.; dos Santos, S.C.; Teixeira, M.C.; Cabrito, T.R.; Mira, N.P. Drug:H+ antiporters in chemical stress response in yeast. *Trends Microbiol.* 2009, *17*, 22–31.

18. Tomitori, H.; Kashiwagi, K.; Sakata, K.; Kakinuma, Y.; Igarashi, K. Identification of a gene for a polyamine transport protein in yeast. *J. Biol. Chem.* **1999**, *274*, 3265–3267.

19. Albertsen, M.; Bellahn, I.; Krämer, R.; Waffenschmidt, S. Localization and Function of the Yeast Multidrug Transporter Tpo1p. *J. Biol. Chem.* **2003**, *278*, 12820–12825.

20. Teixeira, M.C.; Sá-Correia, I. *Saccharomyces cerevisiae* Resistance to Chlorinated Phenoxyacetic Acid Herbicides Involves Pdr1p-Mediated Transcriptional Activation of *TPO1* and *PDR5* Genes. *Biochem. Biophys. Res. Commun.* **2002**, *292*, 530–537.

21. Cabrito, T.R.; Teixeira, M.C.; Duarte, A.A.; Duque, P.; Sá-Correia, I. Heterologous expression of a Tpo1 homolog from *Arabidopsis thaliana* confers resistance to the herbicide 2,4-D and other chemical stresses in yeast. *Appl. Microbiol. Biotechnol.* **2009**, *84*, 927–936.

22. Markovich, S.; Yekutiel, A.; Shalit, I.; Shadkchan, Y.; Osherov, N. Genomic Approach to Identification of Mutations Affecting Caspofungin Susceptibility in *Saccharomyces cerevisiae*. *Antimicrob. Agents Chemother.* **2004**, *48*, 3871–3876.

23. Calabrese, D.; Sanglard, D.; Bille, J. A novel multidrug efflux transporter gene of the major facilitator superfamily from *Candida albicans* (*FLU1*) conferring resistance to fluconazole. *Microbiology* **2000**, *146*, 2743–2754.

24. Li, R.; Kumar, R.; Tati, S.; Puri, S.; Edgerton, M. *Candida albicans* Flu1-Mediated Efflux of Salivary Histatin 5 Reduces Its Cytosolic Concentration and Fungicidal Activity. *Antimicrob. Agents Chemother.* **2013**, *57*, 1832–1839.

25. Ueno, K.; Uno, J.; Nakayama, H.; Sasamoto, K.; Mikami, Y.; Chibana, H. Development of a Highly Efficient Gene Targeting System Induced by Transient Repression of *YKU80* Expression in *Candida glabrata*. *Eukaryot. Cell* **2007**, *6*, 1239–1247.

26. Chen, K.H.; Miyazaki, T.; Tsai, H.F.; Bennett, J.E. The bZip transcription factor Cgap1p is involved in multidrug resistance and required for activation of multidrug transporter gene *CgFLR1* in *Candida glabrata*. *Gene* **2007**, *386*, 63-72.

27. Simões, T.; Teixeira, M.C.; Fernandes, A.R.; Sá-Correia, I. Adaptation of *Saccharomyces cerevisiae* to the herbicide 2,4-dichlorophenoxyacetic acid, mediated by Msn2p- and Msn4p-regulated genes: important role of *SPI1*. *Appl. Environ. Microbiol.* **2003**, *69*, 4019–4028.

28. Ueno, K.; Matsumoto, Y.; Uno, J.; Sasamoto, K.; Sekimizu, K.; Kinjo, Y.; Chibana, H. Intestinal Resident Yeast *Candida glabrata* Requires Cyb2p-Mediated Lactate Assimilation to Adapt in Mouse Intestine. *PLoS One* **2011**, *6*, e24759.

29. Costa, C.; Henriques, A.; Pires, C.; Nunes, J.; Ohno, M.; Chibana, H.; Sá-Correia, I.; Teixeira, M.C. The dual role of *Candida glabrata* drug:H+ antiporter CgAqr1 (ORF *CAGL0J09944g*) in antifungal drug and acetic acid resistance. *Front. Microbiol.* **2013**.

30. Costa, C.; Nunes, J.; Henriques, A.; Mira, N.P.; Nakayama, H.; Chibana, H.; Teixeira, M.C. *Candida glabrata* drug:H+antiporter CgTpo3 (ORF *CAGL0I10384g*): Role in azole drug resistance and polyamine homeostasis. *J. Antimicrob. Chemother.* **2014**, *69*, 1767-1776.

31. Costa, C.; Pires, C.; Cabrito, T.R.; Renaudin, A.; Ohno, M.; Chibana, H.; Sá-Correia, I.; Teixeira, M.C. *Candida glabrata* drug: H+ antiporter CgQdr2 confers imidazole drug resistance, being activated by transcription factor CgPdr1. *Antimicrob. Agents Chemother.* **2013**, *57*, 3159–3167.

32. Rosa, M.F.; Sá-Correia, I. Intracellular acidification does not account for inhibition of *Saccharomyces cerevisiae* growth in the presence of ethanol. *FEMS Microbiol. Lett.* **1996**, *135*, 271–274.

33. Gasch, A.P.; Spellman, P.T.; Kao, C.M.; Carmel-Harel, O.; Eisen, M.B.; Storz, G.; Botstein, D.; Brown, P.O. Genomic Expression Programs in the Response of Yeast Cells to Environmental Changes. *Mol. Biol. Cell* **2000**, *11*, 4241–4257.

34. Golin, J.; Kon, Z.N.; Wu, C.P.; Martello, J.; Hanson, L.; Supernavage, S.; Ambudkar, S. V.; Sauna, Z.E. Complete Inhibition of the Pdr5p Multidrug Efflux Pump ATPase Activity by Its Transport Substrate Clotrimazole Suggests that GTP as Well as ATP May Be Used as an Energy Source †. *Biochemistry* **2007**, *46*, 13109–13119.

35. Torelli, R.; Posteraro, B.; Ferrari, S.; La Sorda, M.; Fadda, G.; Sanglard, D.; Sanguinetti, M. The ATP-binding cassette transporter–encoding gene *CgSNQ2* is contributing to the *CgPDR1*-dependent azole resistance of *Candida glabrata*. *Mol. Microbiol.* **2008**, *68*, 186–201.

36. Decottignies, A.; Lambert, L.; Catty, P.; Degand, H.; Epping, E.A.; Moye-Rowley, W.S.; Balzi, E.; Goffeau, A. Identification and characterization of *SNQ2*, a new multidrug ATP binding cassette transporter of the yeast plasma membrane. *J. Biol. Chem.* **1995**, *270*, 18150–18157.

37. Sanglard, D.; Ischer, F.; Calabrese, D.; Majcherczyk, P.A.; Bille, J. The ATP binding cassette transporter gene *CgCDR1* from *Candida glabrata* is involved in the resistance of clinical isolates to azole antifungal agents. *Antimicrob. Agents Chemother.* **1999**, *43*, 2753–2765.

38. Cannon, R.D.; Lamping, E.; Holmes, A.R.; Niimi, K.; Baret, P. V.; Keniya, M. V.; Tanabe, K.; Niimi, M.; Goffeau, A.; Monk, B.C. Efflux-mediated antifungal drug resistance. *Clin. Microbiol. Rev.* **2009**, *22*, 291-321.

39. Yoo, J. Il; Choi, C.W.; Kim, H.S.; Yoo, J.S.; Jeong, Y.H.; Lee, Y.S. Proteomic Analysis of Cellular and Membrane Proteins in Fluconazole-Resistant *Candida glabrata*. *Osong Public Heal. Res. Perspect.* **2012**, *3*, 74–78.

40. Mühlschlegel, F.A.; Fonzi, W.A. *PHR2* of *Candida albicans* encodes a functional homolog of the pH-regulated gene *PHR1* with an inverted pattern of pH-dependent expression. *Mol. Cell. Biol.* **1997**, *17*, 5960–5967.

41. Eustice, M.; Pillus, L. Unexpected Function of the Glucanosyltransferase Gas1 in the DNA Damage Response Linked to Histone H3 Acetyltransferases in *Saccharomyces cerevisiae*. *Genetics* **2014**, *196*, 1029–1039.

4 Membrane proteomics analysis of the *Candida glabrata* response to 5-flucytosine: unveiling the role and regulation of the drug efflux transporters CgFlr1 and CgFlr2

This chapter contains results published in:

Pais, P., Pires C., Costa, C., Okamoto, M., Chibana, H., Teixeira, M.C. 2016. Membrane proteomics analysis of the *Candida glabrata* response to 5-flucytosine: unveiling the role and regulation of the drug efflux transporters CgFlr1 and CgFlr2. *Front Microbiol*, **7:**2045.

The PhD candidate is the first author of the work detailed in this chapter. The candidate was responsible for most of the experimental work and writing of the correspondent publication.

4.1 Abstract

Resistance to 5-flucytosine (5-FC), used as an antifungal drug in combination therapy, compromises its therapeutic action.

In this work, the response of the human pathogen *Candida glabrata* to 5-flucytosine was evaluated at the membrane proteome level, using an iTRAQ-based approach. A total of 32 proteins were found to display significant expression changes in the membrane fraction of cells upon exposure to 5-flucytosine, 50% of which under the control of CgPdr1, the major regulator of azole drug resistance. These proteins cluster into functional groups associated to cell wall assembly, lipid metabolism, amino acid/nucleotide metabolism, ribosome components and translation machinery, mitochondrial function, glucose metabolism and multidrug resistance transport.

Given the obtained indications, the function of the drug:H+ antiporters CgFlr1 (ORF *CAGL0H06017g*) and CgFlr2 (ORF *CAGL0H06039g*) was evaluated. The expression of both proteins, localized to the plasma membrane, was found to confer 5-flucytosine resistance. CgFlr2 further confers azole drug resistance. The deletion of *CgFLR1* or *CgFLR2* was seen to increase the intracellular accumulation of 5-flucytosine, or 5-flucytosine and clotrimazole, suggesting that these transporters play direct roles in drug extrusion. The expression of *CgFLR1* and *CgFLR2* was found to be controlled by the transcription factors CgPdr1 and CgYap1, major regulator of oxidative stress resistance.

4.2 Introduction

Systemic fungal infections are a problem of increasing clinical significance, especially since the prophylactic and therapeutic use of antifungal drugs has led to an increased number of infections with drug resistant fungal pathogens [1,2].

The antifungal drug 5-flucytosine (5-FC) is a fluorinated pyrimidine which enters fungal cells through permeases [3–5] and is then converted, by cytosine deaminase, to its metabolically active form 5-fluorouracil (5-FU) [3,5,6]. This antifungal drug acts by inhibiting transcription, DNA replication and protein synthesis [3,6]. The specificity of this antimycotic relies on the absence of cytosine deaminase in mammalian cells [4,5]. However, 5-FU is considered toxic, mostly due to the conversion of 5-flucytosine to fluorouracil by gut bacteria [7]. Despite these side-effects, 5-flucytosine it is still used clinically, mostly in combination therapy [6].

Resistance to 5-flucytosine in clinically relevant *Candida* species develops rapidly under treatment [8]. Resistance is often related to decreased drug uptake by the Fcy2 cytosine permease or decreased conversion of 5-flucytosine to 5-FU or 5-FUMP by the Fcy1 and Fur1 enzymes [6,9,10]. Some epidemiological studies suggest, however, that resistance mechanisms, independent of the Fcy2-Fcy1-Fur1 pathway, may play an important role in this phenomenon [11]. For example, reduction of 5-flucytosine intracellular accumulation, mediated by the Drug:H+ Antiporter (DHA) CgAqr1 [12], or by the acquaglyceroporins CgFps1 and CgFps2 [13] were recently registered.

Given these observations, in this study the *Candida glabrata* response to 5-flucytosine was analysed at the membrane proteome level, using an iTRAQ-based approach. Among the obtained results, the concentration of the DHA transporter CgFlr1 was seen to increase in 5-flucytosine challenged cells. The role of CgFlr1 (ORF *CAGL0H06017g*), and of its very close homolog CgFlr2 (ORF *CAGL0H06039g*) [14,15], in the resistance to 5-flucytosine was then analysed.

The deletion of *CgFLR1* had been found to lead to increased susceptibility to benomyl, diamide, and menadione, but not to fluconazole [16]. As for CgFlr2, it remained uncharacterized until this study [15]. Both proteins, however, are close homologs of the *S. cerevisiae* Flr1 DHA transporter. ScFlr1 confers resistance to many unrelated chemical compounds (as reviewed in [17]), its expression being highly responsive to

chemical stress exposure [17–21]. The *ScFLR1* homolog in *Candida albicans*, *CaMDR1*, has been one of the few DHA transporters linked so far to azole drug resistance [12,15,22–25], being an important determinant of clinical acquisition of resistance against these antifungals [15,22,23]. These previous findings were used to guide the functional analysis of CgFlr1 and CgFlr2 in this study, in which the subcellular localization, role in antifungal drug resistance, and expression analysis was carried out.

4.3 Materials and Methods

4.3.1 Strains and growth media

Candida glabrata parental strain KUE100 [26] and derived single deletion mutants KUE100_*Δcgflr1* or KUE100_*Δcgflr2*, constructed in this study, as well as the *C. glabrata* strains 66032u and 66032u_*Δcgpdr1* [27], provided by Thomas Edlind, from Drexel University, College of Medicine, Philadelphia, PA, were batch-cultured at 30ºC, with orbital agitation (250 rpm) in BM (basal medium), with the following composition (per liter): 1.7 g yeast nitrogen base without amino acids or NH_4^+ (Difco), 20 g glucose (Merck) and 2.65 g $(NH_4)_2SO_4$ (Merck). *C. glabrata* strains L5U1 (*cgura3Δ0, cgleu2Δ0*), 84u (*cgura3Δ0*) and 84u_*Δyap1* [16], kindly provided by John Bennett from the National Institute of Allergy and Infectious Diseases, NIH, Bethesda, USA, was grown in BM supplemented with 20 mg/L uracil and 60 mg/L leucine. *Saccharomyces cerevisiae* parental strain BY4741 (*MATa, ura3□0, leu2Δ0, his3Δ1, met15Δ0*) and the derived single deletion mutant BY4741_*Δflr1* were obtained from Euroscarf (http://web.uni-frankfurt.de/fb15/mikro/euroscarf/). Cells were batch-cultured at 30ºC, with orbital agitation (250 rpm) in BM, with the following composition (per liter): 1.7 g yeast nitrogen base without amino acids or NH_4^+ (Difco), 20 g glucose (Merck) and 2.65 g $(NH_4)_2SO_4$ (Merck), supplemented with 20 mg/L methionine, 20 mg/L histidine, 60 mg/L leucine, 20 mg/L uracil (all from Sigma). Solid media contained, besides the above-indicated ingredients, 20 g/L agar (Iberagar). The plasmid pGREG576 was obtained from the Drag&Drop collection [28].

4.3.2 Membrane proteome-wide analysis of *C. glabrata* response to 5-flucytosine

Exponentially growing wild-type 66032u *C. glabrata* strain and the derived 66032u_*Δcgpdr1* deletion mutant were transferred to fresh BM in the absence of stress (control conditions) or in the presence of 4 μg/mL 5-flucytosine (Sigma). Upon 1h of cultivation, cells were harvested by centrifugation and the membrane protein fraction was obtained as described before [29]. Expression proteomics analysis of the obtained membrane-enriched fraction was carried out using and iTRAQ-MS procedure, carried out as a paid service at the Keck Foundation Biotechnology Resource Laboratory, Yale

University, USA (http://medicine.yale.edu/keck/proteomics/index.aspx), using the method followed in Pais *et al.* [29]. Briefly, samples were sonicated and proteins reduced by adding 50 mM TCEP (tris(2-carboxyethyl)phosphine), followed by 200 mM MMTS (methyl methane thiosulfonate). Protein digestion was achieved by adding 10 µL of a solution of 1 mg/ml Lys-C, followed by incubation at 37ºC for 3h, and 10 µL of 1mg/ml trypsin, followed by overnight incubation at 37ºC. Macro-spin desalt of the digests with C18 spin columns for cleanup and quantitation was carried out, followed by dissolution in 65 µL of 500 mM TEAB. iTRAQ labelling was carried out based on the AAA quant protocol. iTRAQ experiments were carried out through the SCX cartridge and experiments run on 5600.

The search parameters and acceptance criteria used were the following: Peaklist generating software: ProteinPilot 4.5 and Mascot; Search engine: Paragon Search Engine (ProteinPilot 4.2); Sequence Database/spectral library: *Candida glabrata* [5478] from SwissProt (May 2013); The database used was downloaded from UniProt, with a total of 5197 protein entries. Mass spectrometric analysis is done on an AB SCIEX TripleTOF® 5600 mass spectrometer with AB SCIEX ProteinPilot™ software used for protein identification and quantitation. ProteinPilot utilizes a Paragon™ algorithm with hybrid sequence tag and feature probability database searches. Hence, specific details such as mass tolerances, specific modifications etc. are not utilized. All iTRAQ results are uploaded into the Yale Protein Expression database (YPED) for investigator viewing. Protein identification was considered reliable for a Protein Score > 2, corresponding to a confidence level of 99%. A reserve decoy database search, followed by filtering of all peptides above 1% False Discovery Rate was carried out before protein grouping.

Proteomics data analysis started from 3 iTRAQ sets. The samples present in each of the sets were randomized to prevent bias, and in different sets distinct labels were used to tag the samples, ensuring that protein identification in the MS step is not biased by the tags. For each sample in a given set, protein quantification was only considered for p-value<0.05. Protein expression changes above 1.5-fold or below 0.66-fold were considered relevant. Protein classification into functional groups was achieved based on their predicted function, according to the Candida Genome Database (www.candidagenome.org), or based on the function of their closest *S. cerevisiae* homolog, according to the Saccharomyces Genome Database (www.yeastgenome.org).

4.3.3 Disruption of the *CgFLR1* and *CgFLR2* genes

The deletion of the *C. glabrata FLR1* and *FLR2* genes (ORFs *CAGL0H06017g* and *CAGL0H06039g*, respectively) was carried out in the parental strain KUE100, using the method described by Ueno *et al.* [30]. The target genes *CgFLR1* and *CgFLR2* were replaced by a DNA cassette including the *CgHIS3* gene, through homologous recombination. The replacement cassette was prepared by PCR using the primers 5' AGAGAAAAATAAAACCAATTCTAAAACCAAATCCATATTACAACCCAATTG CAAAGGGCCGCTGATCACG-3' and 5'-AATGTTAGTGTGAACTTGAATGTTAGATTTTCACGTGAATGAGAACTGAGA AATCACATCGTGAGGCTGG-3', for the *CgFLR1* gene, and the primers 5'-AGAATCATATTCATAAAGGTAACAAAACTACACAACAAATTATTAACTATT TTACAGGCCGCTGATCACG-3' and 5'-AAATAATTTGTTCGGGGTAAGCACAATTGGAGGCTCTATCTTTTTTCTCTTCT TCACATCGTGAGGCTGG-3', for the *CgFLR2* gene. The pHIS906 plasmid including *CgHIS3* was used as a template and transformation was performed as described previously [26]. Recombination locus and gene deletion were verified by PCR using the following pairs of primers: 5'-GAGGTGCTTAATATCGTCAC-3' and 5'-CAACAACGTGTCCTACATG-3'; and 5'-GTGCATTTCAGGACACACT-3' and 5'-GTATTTGTTCTTGTCCTGGTGTG-3', respectively.

4.3.4 Cloning of the *C. glabrata CgFLR1* and *CgFLR2* genes (ORFs *CAGL0H06017g* and *CAGL0H06039g*, respectively).

The pGREG576 plasmid from the Drag&Drop collection was used to clone and express the *C. glabrata* ORFs *CAGL0H06017g* and *CAGL0H06039g* in *S. cerevisiae*, as described before for other heterologous genes [12,24,25]. *CgFLR1* or *CgFLR2* DNA was generated by PCR, using genomic DNA extracted from the sequenced CBS138 *C. glabrata* strain, and the following specific primers: 5'-GAATTCGATATCAAGCTTATCGATACCGTCGACA*GCAAAGATGAATTATCTTC*-3' and 5'-GCGTGACATAACTAATTACATGACTCGAGGTCGAC*TCACCTGTTGTATTTAGA CATGG*-3'; or 5'-GAATTCGATATCAAGCTTATCGATACCGTCGACA*ATGTATATCGGTGCATTTC*

AGGAC-3' and 5'-GCGTGACATAACTAATTACATGACTCGAGGTCGAC*TCATGAATCTGGACTAAA TCTTG*-3', respectively. These plasmids include a *S. cerevisiae* CEN/ARS element which had been shown before to work in *C. glabrata* [31]. The *GAL1* promoter present in the pGREG576_*CgFLR1* and pGREG576_*CgFLR2* plasmids was then replaced by the copper-induced *MTI C. glabrata* promoter, giving rise to the pGREG576_MTI_*CgFLR1* and pGREG576_MTI_*CgFLR2* plasmids. The *MTI* promoter DNA was generated by PCR, using genomic DNA extracted from the sequenced CBS138 *C. glabrata* strain, and the following specific primers: 5'-TTAACCCTCACTAAAGGGAACAAAAGCTGGAGCTC*TGTACGACACGCATCAT GTGGCAATC*-3' and 5'-GAAAAGTTCTTCTCCTTTACTCATACTAGTGCGGC*TGTGTTTGTTTTTGTATGT GTTTGTTG*-3'. The recombinant plasmids pGREG576_*CgFLR1*, pGREG576_*CgFLR2*, pGREG576_MTI_*CgFLR1* and pGREG576_MTI_*CgFLR2* were obtained through homologous recombination in *S. cerevisiae* and verified by DNA sequencing. As before [12,24,25], the transformation of L5U1 *C. glabrata* cells with the pGREG576 plasmids, as well as plasmid propagation was ensured by growth in selective uracil depleted medium.

4.3.5 CgFlr1 and CgFlr2 subcellular localization assessment

The subcellular localization of the CgFlr1 and CgFlr2 proteins was determined based on the observation of BY4741 *S. cerevisiae* or L5U1 *C. glabrata* cells transformed with the pGREG576_*CgFLR1* and pGREG576_*CgFLR2* or pGREG576_MTI_*CgFLR1* and pGREG576_MTI_*CgFLR2* plasmids, respectively. These cells express the CgFlr1_GFP or CgFlr2_GFP fusion proteins, whose localization may be determined using fluorescence microscopy. *S. cerevisiae* cell suspensions were prepared by cultivation in BM-U medium, containing 0.5% glucose and 0.1% galactose, at 30ºC, with orbital shaking (250 rpm), until a standard culture OD_{600nm} = 0.4 ± 0.04 was reached. At this point cells were transferred to the same medium containing 0.1% glucose and 1% galactose, to induce protein expression. *C. glabrata* cell suspensions were prepared in BM-U medium, until a standard culture OD_{600nm} = 0.4 ± 0.04 was reached, and transferred to the same medium supplemented with 50 µM $CuSO_4$ (Sigma), to induce

the expression of the fusion protein. After 5h of incubation, the distribution of CgFlr1_GFP or CgFlr2_GFP fusion proteins in *S. cerevisiae* or in *C. glabrata* living cells was detected by fluorescence microscopy in a Zeiss Axioplan microscope (Carl Zeiss MicroImaging), using excitation and emission wavelength of 395 and 509nm, respectively. Fluorescence images were captured using a cooled CCD camera (Cool SNAPFX, Roper Scientific Photometrics).

4.3.6 Antifungal susceptibility assays

The susceptibility of the parental strain KUE100 towards toxic concentrations of the selected drugs was compared to that of the deletion mutants KUE100_*Δcgflr1* and KUE100_*Δcgflr2* by spot assays, using the steps described elsewhere [24]. The ability of *CgFLR1* and *CgFLR2* gene expression to increase wild-type resistance to the tested chemical stresses was also examined in the URA3- strain L5U1 *C. glabrata* strain, using the pGREG576_MTI_*CgFLR1* and pGREG576_MTI_*CgFLR2* centromeric plasmids. Additionally, the effect of *CgFLR1* and *CgFLR2* expression in *S. cerevisiae* BY4741 wild-type strain and BY4741_*Δflr1* single deletion mutant was also carried out as described elsewhere [24]. The tested drugs included the following compounds, used in the specified concentration ranges: the azole antifungal drugs ketoconazole (10 to 60 mg/L), fluconazole (150 to 250 mg/L), miconazole (0.10 to 0.50 mg/L), tioconazole (0.2 to 0.9 mg/L), itraconazole (0.1 to 0.5 mg/L), and clotrimazole (2.5 to 15 mg/L), the polyene antifungal drug amphotericin B (0.10 to 0.30 mg/L), the fluoropyrimidine 5-flucytosine (1 to 4 mg/L) and the pesticide mancozeb (0.5 to 2.5 mg/L) (all from Sigma).

4.3.7 Drug accumulation assays

The internal accumulation of 5-flucytosine or clotrimazole was determined by calculating the ratio between the radiolabeled compound measured within the yeast cells and in the external medium (Intracellular/Extracellular). The parental strain KUE100 and the mutant strains KUE100_*Δcgflr1* and KUE100_*Δcgflr2* were grown in BM medium until mid-exponential phase and harvested by filtration. Cells were washed and resuspended in BM medium, to obtain dense cell suspensions (OD_{600nm} = 0.5 ± 0.1,

equivalent to approximately 1.57 mg (dry weight) mL^{-1}). Readily, 0.1 µM of ^{3}H-5-flucytosine or ^{3}H- clotrimazole (American Radiolabelled Chemicals; 1 mCi/ml) and sub-inhibitory concentrations of the corresponding cold drug were added to the cell suspensions. Incubation proceeded for an additional period of 30 min. The intracellular accumulation of labeled antifungal was followed by filtering 200 µl of cell suspension, at adequate time intervals, through pre-wetted glass microfibre filters (Whatman GF/C). The filters were washed with ice-cold TM buffer and the radioactivity measured in a Beckman LS 5000TD scintillation counter. Extracellular ^{3}H-drug was estimated, by radioactivity assessment of 50 µl of the supernatant. Non-specific ^{3}H-drug adsorption to the filters and to the cells (less than 5% of the total radioactivity) was assessed and taken into consideration. To calculate the intracellular concentration of labeled antifungal drug, the internal cell volume (Vi) of the exponential cells, grown in the absence of drug and used for accumulation assays, was considered constant and equal to 2.5 µl (mg dry weight)$^{-1}$ [32]. Statistical analysis of the results was performed using analysis of variance, and differences were considered significant for p-values<0.05.

4.3.8 *CgFLR1* and *CgFLR2* expression measurements

The levels of *CgFLR1* and *CgFLR2* transcripts were assessed by real-time PCR, using the approach described before [24]. Synthesis of cDNA for real time RT-PCR experiments, from total RNA samples, was performed using the MultiscribeTM reverse transcriptase kit (Applied Biosystems) and the 7500 RT-PCR Thermal Cycler Block (Applied Biosystems), following the manufacturer's instructions. The quantity of cDNA for the following reactions was kept around 10 ng. The subsequent RT-PCR step was carried out using SYBR® Green reagents. Primers for the amplification of the *CgFLR1*, *CgFLR2* and *CgACT1* cDNA were designed using Primer Express Software (Applied Biosystems) and are 5'-TCTTATTCACGATGCTACAAATTGG-3' and 5'-GAATCACAAGGCCAGCAAAGTT-3'; 5'-GCAGCGGCATTCCCATTAT-3' and 5'-CGGGATACTTTTTTGTGCTCAAT-3'; and 5'-AGAGCCGTCTTCCCTTCCAT-3' and 5'-TTGACCCATACCGACCATGA-3', respectively. The RT-PCR reaction was carried out using a thermal cycler block (7500 Real-Time PCR System - Applied Biosystems). Default parameters established by the manufacturer were used and fluorescence detected by the instrument and registered in an amplification plot (7500

System SDS Software – Applied Biosystems). The *CgACT1* mRNA level was used as an internal control. The relative values obtained for the wild-type strain in control conditions were set as 1 and the remaining values are presented relative to that control. To avoid false positive signals, the absence of non-specific amplification with the chosen primers was confirmed by the generation of a dissociation curve for each pair of primers. Statistical analysis of the results was performed using analysis of variance, and differences were considered significant for p-values<0.05.

4.4 Results

4.4.1 Membrane proteome-wide changes occurring in response to 5-flucytosine in *C. glabrata*

Given the importance of membrane proteins as a first line of defense against external stress agents, the membrane proteome of *C. glabrata* cells exposed to 5-flucytosine-induced stress was compared to that of unstressed cells. Details on the protein quantification can be assessed at the Mass spectrometry Interactive Virtual Environment (MassIVE) repository (https://massive.ucsd.edu/ProteoSAFe/static/massive.jsp; MassIVE ID: MSV000079209). Annotated spectra for single peptide identification for each protein in the membrane-associated proteome is provided in MS-viewer (http://prospector2.ucsf.edu/prospector/cgi-bin/msform.cgi?form=msviewer; Search keys: qrvm65goix; xffxn22szm; tm0y9x0hqd) [29].

Among the identified membrane-associated proteins, 32 were found to exhibit more than 1.5-fold increased or decreased concentrations in *C. glabrata* cells exposed to inhibitory concentrations of 5-flucytosine, when compared to the same cells growing in the absence of stress. Within these proteins, 21 were found to be downregulated and 11 upregulated in 5-flucytosine challenged cells. Categorization of these proteins, based on their function predicted by homology to their *S. cerevisiae* homologs, enabled their clustering into 7 groups: Glucose metabolism; Mitochondrial function; Amino acid/Nucleotide metabolism; Ribosome components and translation machinery; Lipid metabolism; Cell wall assembly; Multidrug Resistance transporters (Figure 4.1; Table 4.1).

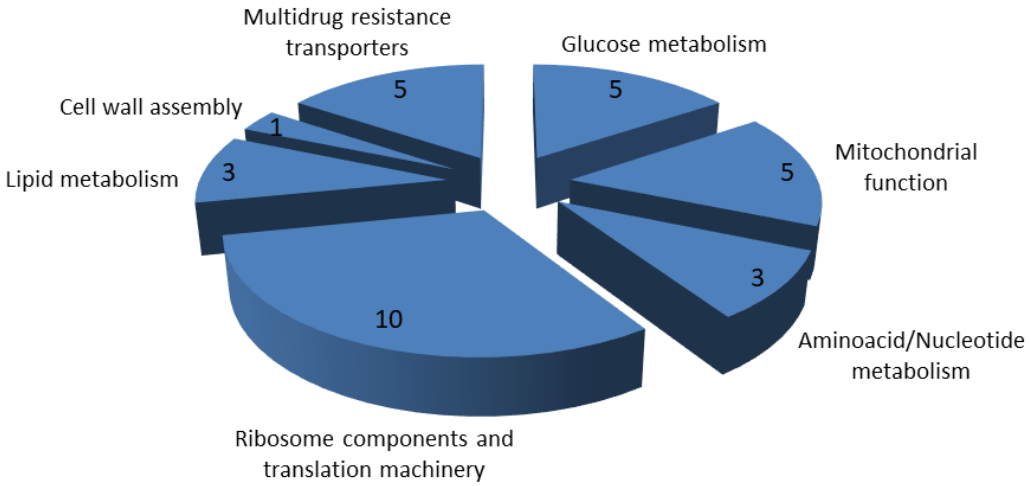

Figure 4.1 – Major functional groups found to have significant expression changes in the *C. glabrata* membrane-enriched proteome upon exposure to 5-flucytosine. Proteins with significant expression changes include Glucose metabolism (5 proteins), Mitochondrial function (5 proteins), Aminoacid/Nucleotide metabolism (3 proteins), Ribosome components and translation machinery (10 proteins), Lipid metabolism (3 proteins), Cell wall assembly (1 protein) and Multidrug resistance transporters (5 proteins).

The largest functional group identified in the 5-flucytosine membrane proteome response, including a third of the proteins with altered content, is related to RNA metabolism. The expression of 7 proteins involved in ribosome biogenesis and translation was found to increase in 5-flucytosine stressed cells, whereas 3 proteins of the same category were found to be downregulated in these conditions. It is difficult to say what the exact consequences of the altered expression of each of them individually may be. Additionally, the concentration of several proteins related to glucose metabolism and mitochondrial function related proteins was found to decrease in the presence of 5-flucytosine. The expression of 1 amino acid biosynthetic protein, Ilv5, and two pyrimidine biosynthetic proteins, Ura1 and Ura3, was also found to decrease in cells exposed to this antifungal agent. Interestingly, Ura3 is responsible for the conversion of 5-FOA into 5-fluorouracil, a key step in the conversion of 5-flucytosine into its toxic sub-products. The repressed expression of the Ura proteins may confer an advantage to 5-flucytosine stressed cells as it may delay the conversion of this pro-drug into its toxic subproducts. Finally, a group of 5 multidrug transporters was found to exhibit altered levels of expression in 5-flucytosine stressed cells. Four of them, previously implicated in azole drug resistance [24,33–35], were actually found to be down-regulated, while the fifth, CgFlr1, was found to be more than 2-fold upregulated upon *C. glabrata* exposure to 5-flucytosine.

Table 4.1 – Set of 32 proteins found to have significant expression changes in *C. glabrata* wild-type cells in the presence of 5-flucytosine and correspondent fold changes in *Δcgpdr1* mutant cells upon exposure to the drug. The name of the proteins whose expression change was found to vary more than 1.5-fold in the *Δcgpdr1* mutant when compared to the wild-type is underlined. Protein description and clustering was obtained from the Candida Genome Database (www.candidagenome.org) or, when completely uncharacterized, based on the role of their predicted *S. cerevisiae* homologs, obtained from the Yeast Genome Database (www.yeastgenome.org).

C. glabrata protein (ORF) name	*S. cerevisiae* homolog	Description of the function of the *C. glabrata* protein or of its *S. cerevisiae* homolog[a]	Wild-type fold change (upon 5-flucytosine stress)	*Δcgpdr1* fold change (upon 5-flucytosine stress)
Glucose Metabolism				
CgPDC1 (CAGL0M07920g)	*PDC1*	Pyruvate decarboxylase, involved in pyruvate metabolism	0.54	0.39
CAGL0L01485g	*GSF2*	Putative protein of the ER membrane involved in hexose transporter secretion	0.60	0.43
CgPGK1 (CAGL0L07722g)	*PGK1*	Putative 3-phosphoglycerate kinase	0.20	0.63
CgFBA1 (CAGL0L02497g)	*FBA1*	Fructose-bisphosphate aldolase	0.58	0.47
CAGL0G06138g	*YCK1*	*S. cerevisiae* ortholog encodes a palmitoylated plasma membrane-bound casein kinase I isoform; functions in morphogenesis, endocytic trafficking, and glucose sensing	0.44	0.90*
Mitochondrial function				
CgRIP1 (CAGL0I03190g)	*RIP1*	Putative ubiquinol-cytochrome C reductase iron-sulfur protein	1.68	0.28
CAGL0F04213g	*AAC2*	*S. cerevisiae* ortholog encodes a major ADP/ATP carrier of the mitochondrial inner membrane	0.64	1.00*
CAGL0C02695g	*MDM10*	Ortholog(s) have role in establishment of mitochondrion localization, mitochondrial outer membrane translocase complex assembly, phospholipid transport, protein import into mitochondrial outer membrane	0.51	0.91*

Table 4.1 (continued)

C. glabrata protein (ORF) name	*S. cerevisiae* homolog	Description of the function of the *C. glabrata* protein or of its *S. cerevisiae* homolog[a]	Wild-type fold change (upon 5-flucytosine stress)	*Δcgpdr1* fold change (upon 5-flucytosine stress)
Mitochondrial function				
CAGL0L06490g	*PHB2*	Ortholog(s) have role in mitochondrion inheritance, negative regulation of proteolysis, protein folding and replicative cell aging	0.63	0.85*
CAGL0M09713g	*YIM1*	Putative protein involved in DNA damage response	0.24	0.48
Amino acid / Nucleotide metabolism				
CgILV5 (CAGL0B03047g)	*ILV5*	Ketol-acid reducto-isomerase	0.50	0.70*
CgURA3 (CAGL0I03080g)	*URA3*	Orotidine 5'-phosphate decarboxylase, catalyzes a step in pyrimidine biosynthesis; converts 5-FOA into 5-fluorouracil, a toxic compound	0.44	2.92
CAGL0M12881g	*URA1*	Ortholog(s) have dihydroorotate oxidase (fumarate) activity, role in 'de novo' pyrimidine nucleobase biosynthetic process	0.26	2.62
Ribosome components and translation machinery				
CAGL0L03846g	*DBP2*	Ortholog(s) have RNA-dependent ATPase activity and role in mRNA catabolic process, nonsense-mediated decay, rRNA processing	3.94	2.15
CAGL0E03938g	*RPL4B*	*S. cerevisiae* ortholog encodes a ribosomal 60S subunit protein L13B	1.56	1.30*
CAGL0K07414g	*RPL20B*	*S. cerevisiae* ortholog encodes a ribosomal 60S subunit protein L20A	1.70	0.97*
CAGL0J03234g	*RPS24B*	Ortholog(s) have role in maturation of SSU-rRNA from tricistronic rRNA transcript	1.52	1.05*
CAGL0K01859g	*NOP1*	Ortholog(s) have mRNA binding, rRNA methyltransferase activity and role in box C/D snoRNA 3'-end processing, rRNA methylation	1.64	0.86*
CAGL0I00792g	*RPS16A*	Ortholog(s) have role in maturation of SSU-rRNA from tricistronic rRNA transcript (SSU-rRNA, 5.8S rRNA, LSU-rRNA) and 90S preribosome	1.97	1.27*

Table 4.1 (continued)

C. glabrata protein (ORF) name	*S. cerevisiae* homolog	Description of the function of the *C. glabrata* protein or of its *S. cerevisiae* homolog[a]	Wild-type fold change (upon 5-flucytosine stress)	*Δcgpdr1* fold change (upon 5-flucytosine stress)
Ribosome components and translation machinery				
CAGL0G01078g	*RPL26A*	Ortholog(s) have RNA binding, structural constituent of ribosome activity, role in cytoplasmic translation and cytosolic large ribosomal subunit	1.78	1.37*
CAGL0E02013g	*RPL18A*	*S. cerevisiae* ortholog encodes a ribosomal 60S subunit protein L18A	0.59	0.48
CAGL0L06886g	*RPL13B*	*S. cerevisiae* ortholog encodes a ribosomal 60S subunit protein L13B	0.62	0.96*
CAGL0A03278g	*RPL19A*	*S. cerevisiae* ortholog encodes a ribosomal 60S subunit protein L19A	0.33	0.55
Lipid and cell wall metabolism				
CAGL0L03828g	*CYB5*	Ortholog(s) have electron carrier activity, role in ergosterol biosynthetic process	2.14	0.98*
CAGL0E03201g	*CHO2*	Ortholog(s) have phosphatidylethanolamine N-methyltransferase activity, role in phosphatidylcholine biosynthetic process	1.56	1.56
CAGL0M08206g	*YJL171c*	*S. cerevisiae* ortholog encodes a GPI-anchored cell wall protein of unknown function; induced in response to cell wall damage	0.59	0.5
CgHFD1 (CAGL0K03509g)	*HFD1*	Putative mitochondrial fatty aldehyde dehydrogenase	0.29	0.24
Multidrug resistance transporters				
CgFLR1 (CAGL0H06017g)	*FLR1*	Multidrug transporter of the major facilitator superfamily;	2.08	1.89**
CgSNQ2 (CAGL0I04862g)	*SNQ2*	Predicted plasma membrane ATP-binding cassette (ABC) transporter, putative transporter involved in multidrug resistance	0.61	0.75*
CgCDR1 (CAGL0M01760g)	*PDR5*	Multidrug transporter of ATP-binding cassette (ABC) superfamily, involved in resistance to azoles	0.30	0.1
CgYOR1 (CAGL0G00242g)	*YOR1*	Putative ABC transporter involved in multidrug efflux	0.51	0.44

Table 4.1 (continued)

C. glabrata protein (ORF) name	*S. cerevisiae* homolog	Description of the function of the *C. glabrata* protein or of its *S. cerevisiae* homolog[a]	Wild-type fold change (upon 5-flucytosine stress)	*Δcgpdr1* fold change (upon 5-flucytosine stress)
Multidrug resistance transporters				
CgQDR2 (CAGL0G08624g)	*QDR2*	Drug:H+ antiporter of the Major Facilitator Superfamily, confers imidazole drug resistance	0.57	0.31

*Fold change value outside of the chosen cut-off intervals (0.67 < fold change < 1.5)

**Fold change quantification considered as not statistically significant (p-value>0.05)

4.4.2 Effect of CgPdr1 deletion in the membrane proteome-wide changes occurring in response to 5-flucytosine in *C. glabrata*

To assess the possible involvement of the transcription factor CgPdr1 in the resistance to the 5-flucytosine, the growth of the *C. glabrata* strains 66032u and 66032u_*Δcgpdr1* [27] was compared in solid medium containing inhibitory concentrations of 5-flucytosine, clotrimazole and fluconazole (Figure 4.2). *CgPDR1* deletion fully abrogates growth in the presence of the tested azole drug concentrations, as expected based on numerous reports on the pivotal role of this transcription factor in azole drug resistance. Interestingly, the *Δcgpdr1* deletion mutant was also found to display higher susceptibility to the antifungal drug 5-flucytosine than the wild-type parental strain, suggesting that it plays a role in the resistance to this drug as well. Based on this result, the analysis of the membrane-enriched fraction of the *C. glabrata* proteome obtained from cells exposed to 5-flucytosine in the absence of the transcription factor CgPdr1 was assessed and compared to that of the *C. glabrata* wild-type cells exposed to 5-flucytosine. Considering an at least 1.5-fold difference in protein expression activation in wild-type versus *Δcgpdr1* cells exposed to 5-flucytosine, 9 proteins were found to be repressed by CgPdr1; while 8 proteins were found to be activated by CgPdr1 (Table 4.1). The PDRE loci BCCRYYRGD, TCCRYGGA [36], TCCACGGA and HYCCGTGGR [37], were searched for the promoters of the referred genes using the PathoYeastract database [38]. Interestingly, considering these 17 proteins, at least one CgPdr1-binding site is found in the promoter regions of 9 genes, suggesting the action

of CgPdr1 in their expression may be direct. For the remaining 15 proteins, no statistically significant change could be detected in the current experiment. The proteins whose expression was found to be higher in the wild-type strain than in the *Δcgpdr1* deletion mutant include the multidrug transporters CgCdr1 and CgQdr2, but also two proteins related to mitochondrial function, CgCyb5 (ORF *CAGL0L03828g*) and CgRip1 (ORF *CAGL0I03190g*), and four proteins involved in RNA metabolism, CgDbp2 (ORF *CAGL0L03846g*), CgNop1 (ORF *CAGL0K01859g*), CgRpl20B (ORF *CAGL0K07414g*) and CgRps16A (ORF *CAGL0I00792g*).

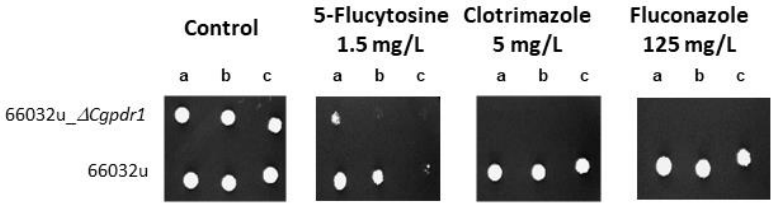

Figure 4.2 – CgPdr1 confers resistance to 5-flucytosine in *C. glabrata* cells. Comparison of the susceptibility to inhibitory concentrations of 5-flucytosine, clotrimazole and fluconazole, at the indicated concentrations, of the *C. glabrata* 66032u and 66032u_*Δcgpdr1* strains, in BM plates by spot assays. The inocula were prepared as described under "Materials and Methods". Cell suspensions used to prepare the spots were 1:5 (b) and 1:25 (c) dilutions of the cells suspension used in (a). The displayed images are representative of at least three independent experiments.

4.4.3 CgFlr1 and CgFlr2 expression confers resistance to other chemical stress inducers

The involvement of CgFlr1 and CgFlr2 in antifungal drug resistance was evaluated, through susceptibility assays, considering a total of nine antifungal drugs of four different families and one agricultural fungicide, mancozeb. The results obtained by screening the susceptibility phenotypes of *Δcgflr1* and *Δcgflr2* mutants, when compared to the wild-type strain, reveal that *CgFLR1* confers resistance to mancozeb, whereas *CgFLR2* confers resistance to azoles and amphotericin B (Figure 4.3).

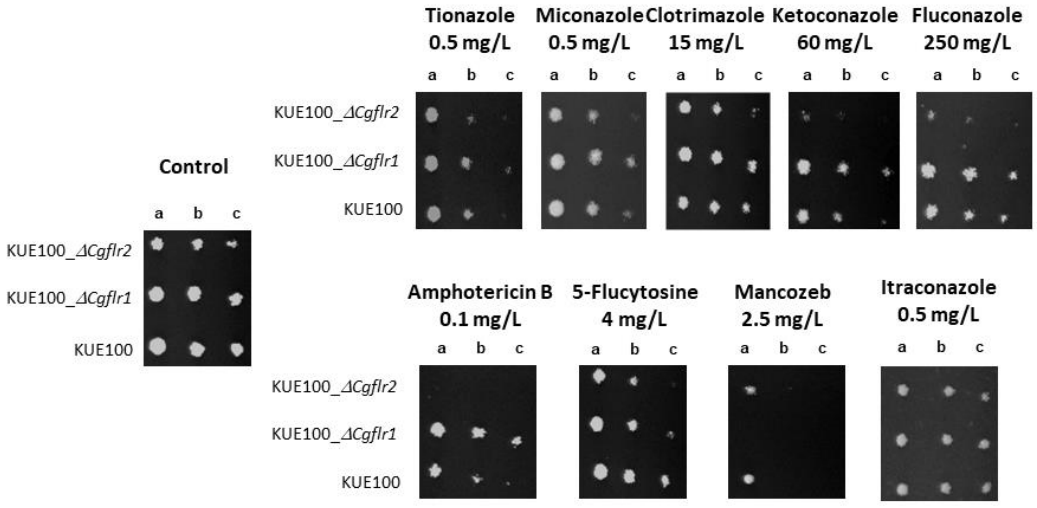

Figure 4.3 – CgFlr1 and CgFlr2 confer resistance to 5-flucytosine in *C. glabrata* cells. Comparison of the susceptibility to inhibitory concentrations of several chemical stress inducers, at the indicated concentrations, of the *C. glabrata* KUE100, KUE100_*Δcgflr1* and KUE100_*Δcgflr2* strains, in BM plates by spot assays. The inocula were prepared as described under "Materials and Methods". Cell suspensions used to prepare the spots were 1:5 (b) and 1:25 (c) dilutions of the cells suspension used in (a). The displayed images are representative of at least three independent experiments.

Both *CgFLR1* and *CgFLR2* were found to confer resistance to 5-flucytosine, although the effect of *CgFLR2* is stronger (Figure 4.3). The expression of *CgFLR1-GFP* or *CgFLR2-GFP* in the L5U1 *C. glabrata* wild-type strain, as verified by anti-GFP western analysis (Figure S4.1), was concordantly found to increase *C. glabrata* natural resistance towards the antifungal drugs to which the deletion of each gene was found to lead to a susceptibility phenotype (Figure 4.4).

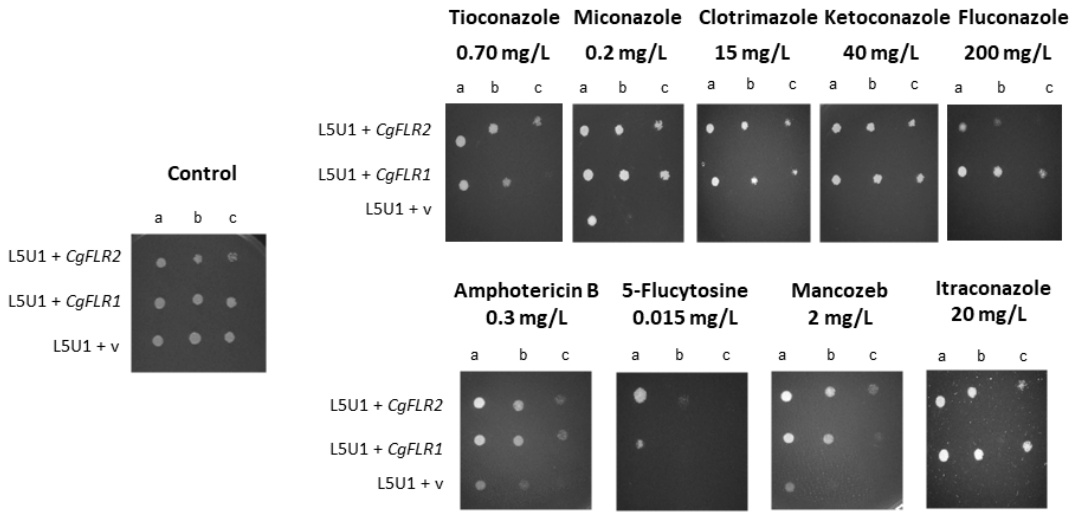

Figure 4.4 – CgFlr1 and CgFlr2 expression increases 5-flucytosine resistance in *C. glabrata* cells. Comparison of the susceptibility to inhibitory concentrations of several chemical stress inducers, at the indicated concentrations, of the *C. glabrata* L5U1 strain, harboring the pGREG576 cloning vector (v) or the pGREG576_MTI_*CgFLR1* or pGREG576_MTI_*CgFLR2* plasmids, in BM-U plates (50 µM $CuSO_4$ supplemented) by spot assays. The inocula were prepared as described under "Materials and Methods". Cell suspensions used to prepare the spots were 1:5 (b) and 1:25 (c) dilutions of the cells suspension used in (a). The displayed images are representative of at least three independent experiments.

Using *S. cerevisiae* as a heterologous expression system, the effect of *CgFLR1* and *CgFLR2* expression on yeast drug resistance was further investigated. When expressed in *S. cerevisiae*, the *CgFLR1* and *CgFLR2* genes were found to rescue the susceptibility phenotype exhibited by the *S. cerevisiae Δflr1* mutant against 5-flucytosine and mancozeb, and azole drugs, respectively (Figure 4.5).

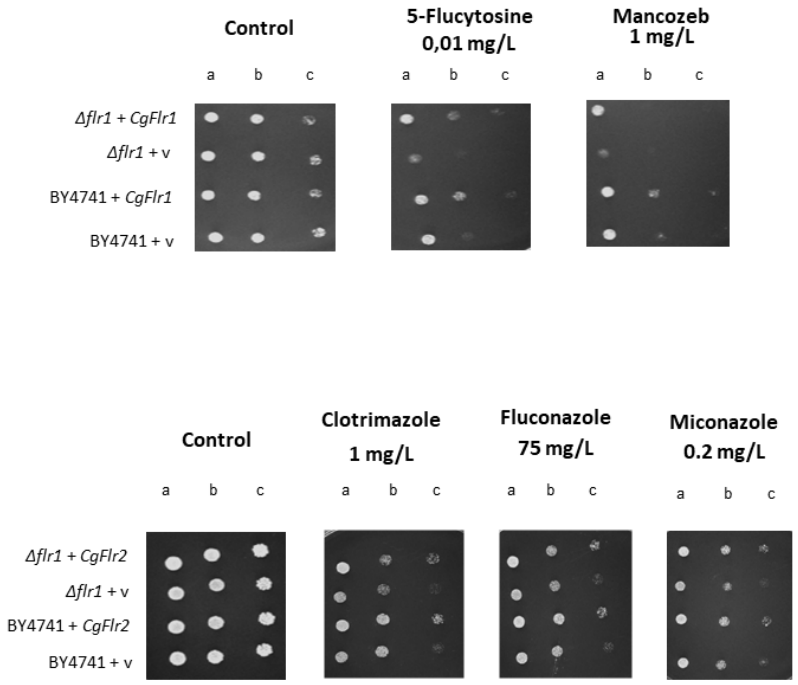

Figure 4.5 – CgFlr1 and CgFlr2 confer resistance to antifungal drugs when heterologously expressed in *S. cerevisiae* cells**.** Comparison of the susceptibility to inhibitory concentrations of several chemical stress inducers, at the indicated concentrations, of the *S. cerevisiae* BY4741 and BY4741_*Δflr1* strains, harboring the pGREG576 cloning vector (v) or the pGREG576_*CgFLR1* of pGREG576_*CgFLR2* plasmids, in BM-U plates by spot assays. The inocula were prepared as described under "Materials and Methods". Cell suspensions used to prepare the spots were 1:5 (b) and 1:25 (c) dilutions of the cells suspension used in (a). The displayed images are representative of at least three independent experiments.

4.4.4 CgFlr1 and CgFlr2 are localized to the plasma membrane

Upon expression induction, *C. glabrata* cells harboring the pGREG576_MTI_*CgFLR1* and pGREG576_MTI_*CgFLR2* plasmids were inspected by fluorescence microscopy. The CgFlr1_GFP and CgFlr2_GFP fusion proteins were found to be localized to the cell periphery (Figure 4.6). In a similar approach, CgFlr1_GFP and CgFlr2_GFP were found to be localized to the cell periphery when expressed heterologously in *S. cerevisiae* (Figure 4.6). These results strongly suggest plasma membrane localization for both CgFlr1 and CgFlr2.

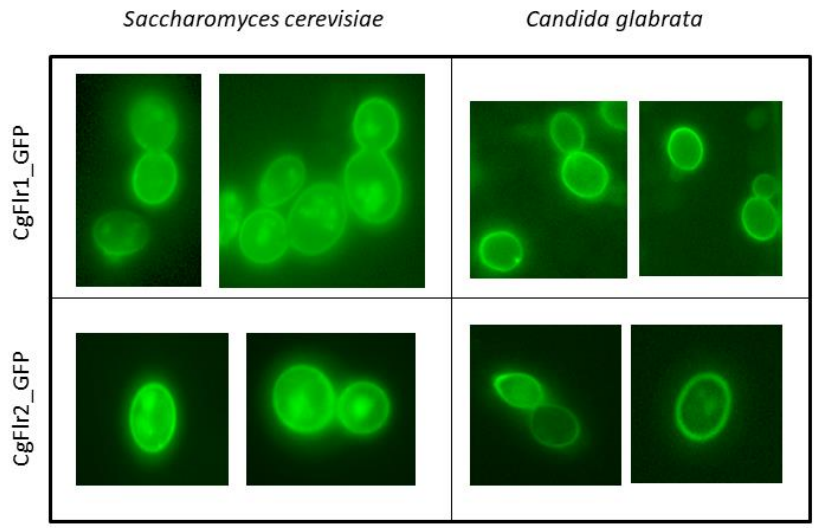

Figure 4.6 – CgFlr1 and GgFlr2 are plasma membrane proteins. Fluorescence of exponential phase BY4741 *S. cerevisiae* and L5U1 *C. glabrata* cells, harboring the expression plasmids pGREG576_*CgFLR1* and pGREG576_*CgFLR2* or pGREG576_MTI_*CgFLR1* and pGREG576_MTI_*CgFLR2*, after galactose or copper-induced recombinant protein production, respectively.

4.4.5 CgFlr1 and CgFlr2 reduce the intracellular accumulation of antifungal drugs in *C. glabrata*

Consistent with the observed susceptibility phenotypes, *Δcgflr1* and *Δcgflr2* deletion mutants were found to accumulate 2-fold more radiolabeled 5-flucytosine than the KUE100 parental strain (Figure 4.7A and 4.7B).

Additionally, *Δcgflr2* mutant cells were found to accumulate around 8-fold more radiolabeled clotrimazole than the parental strain (Figure 4.8). These results strongly suggest that CgFlr1 and CgFlr2 activities increase *C. glabrata* resistance towards 5-flucytosine, and in the case of CgFlr2 towards azoles, by reducing their accumulation in yeast cells.

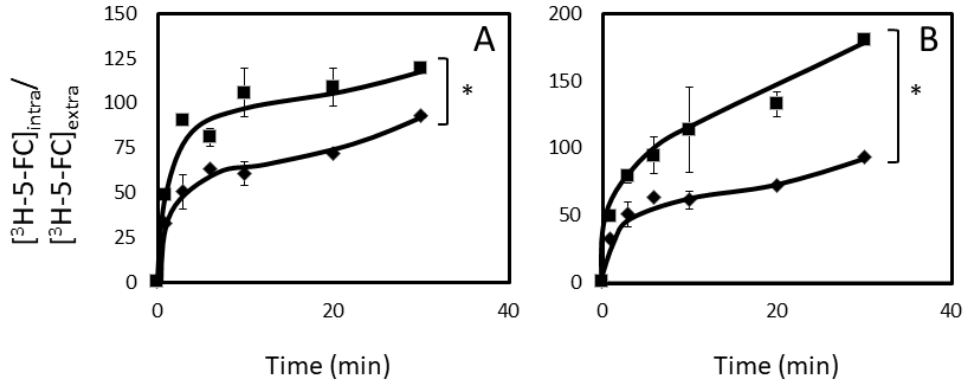

Figure 4.7 – CgFlr1 and CgFlr2 expression decreases the intracellular accumulation of ^{3}H-5-flucytosine. Time-course accumulation of radiolabeled ^{3}H-5-flucytosine in KUE100 wild-type (♦) and KUE100_*Δcgflr1* (■) (A) and KUE100 (♦) and KUE100_*Δcgflr2* (■) (B) strains, during cultivation in BM liquid medium in the presence of sub-lethal concentrations of unlabeled 5-flucytosine. Accumulation values are the average of at least three independent experiments. Errors bars represent the corresponding standard deviations. *p<0.05.

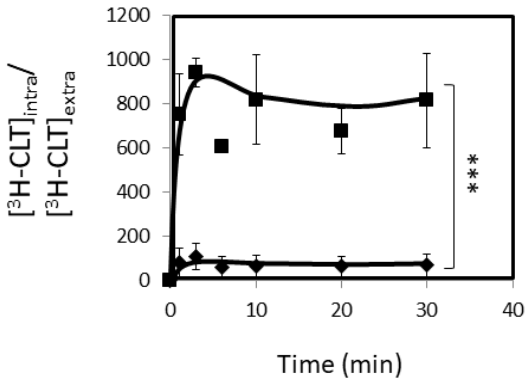

Figure 4.8 – CgFlr2 expression decreases the intracellular accumulation of ^{3}H-clotrimazole. Time-course accumulation of radiolabeled ^{3}H-clotrimazole in KUE100 wild-type (♦) and KUE100_*Δcgflr2* (■) strains, during cultivation in BM liquid medium in the presence of sub-lethal concentrations of unlabeled clotrimazole. Accumulation values are the average of at least three independent experiments. Errors bars represent the corresponding standard deviations. ***p<0.0001.

4.4.6 *CgFLR1* and *CgFLR2* transcript levels are upregulated under antifungal stress, their basal expression being controlled by CgPdr1 and CgYap1 transcription factors.

In order to evaluate whether or not the expression of *CgFLR1* and *CgFLR2* is affected upon drug exposure, quantitative RT-PCR was used to study the effect of 5-flucytosine, clotrimazole and mancozeb stress exposure in the transcript levels of these genes. No upregulation of *CgFLR1* or *CgFLR2* genes could be detected in wild-type cells upon 5-

flucytosine exposure. Interestingly, however, *CgFLR1* was found to be upregulated in mancozeb exposed cells, whereas both *CgFLR1* and *CgFLR2* were found to be upregulated upon exposure to clotrimazole or fluconazole stress, which is consistent with the role of *CgFLR1* and *CgFLR2* in mancozeb and azole drug resistance, respectively (Figure 4.9A and 4.9B).

Additionally, given the fact that the transcription factor CgPdr1 is the master regulator of azole drug resistance [39] and CgYap1 had been previously linked to the control of CgFlr1 expression [16], the effect of CgYap1 and CgPdr1 deletion in the control of the expression of *CgFLR1* and *CgFLR2* was further evaluated. *CgFLR1* and *CgFLR2* upregulation, registered under clotrimazole exposure – but not under fluconazole stress – was found to be abrogated in the absence of *CgPDR1* (Figure 4.9B), while CgPdr1 and CgYap1 were found to control the basal expression of both *CgFLR1* and *CgFLR2* (Figure 4.9A and 4.9B). As expected, based on the proteomics data, none of the genes was found to be controlled by CgPdr1 in 5-flucytosine exposed cells. Unexpectedly, the upregulation of *CgFLR1* and *CgFLR2* registered under mancozeb stress was found not to be controlled by CgYap1. Indeed, in *Δcgyap1* cells the mancozeb-induced upregulation of these genes was found to be even stronger than that registered in the wild-type strain (Figure 9A and 9B).

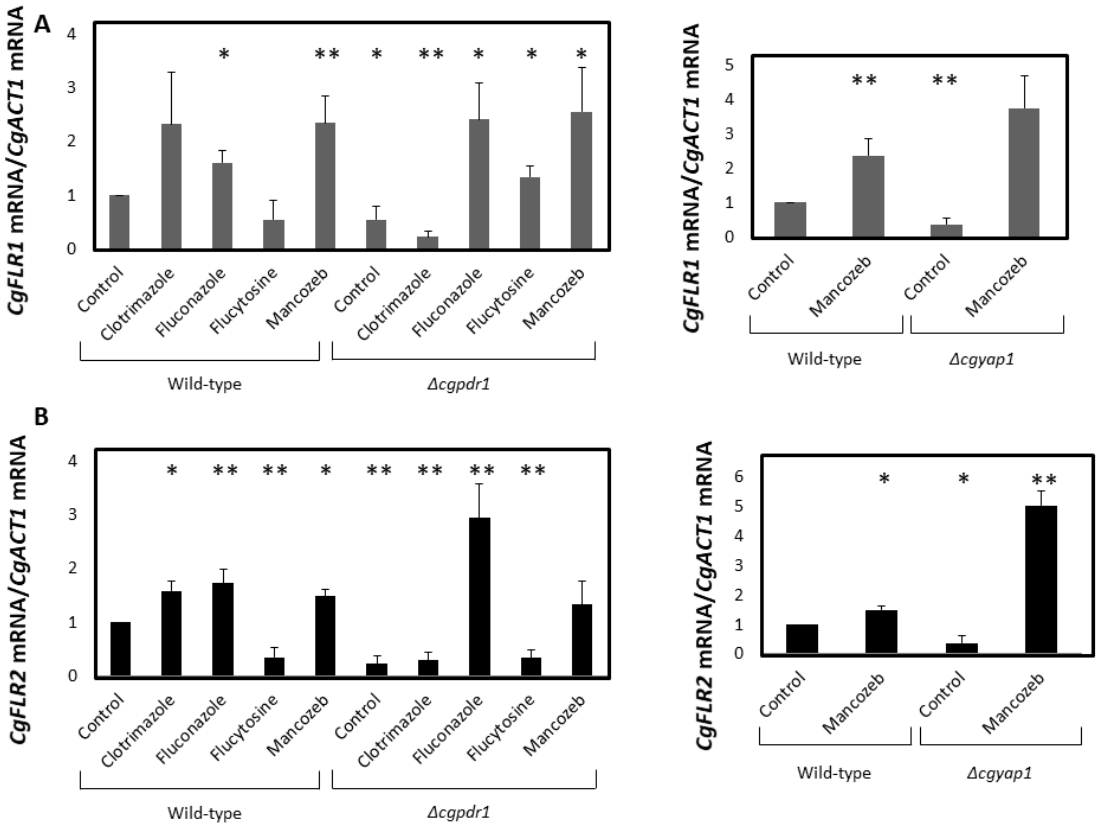

Figure 4.9 – *CgFLR1* and *CgFLR2* transcriptional control. Comparison of the variation of the *CgFLR1* (A) and *CgFLR2* (B) transcript levels in the 66032u *C. glabrata* wild-type strain and in the derived 66032u_*Δcgpdr1* deletion mutant; and in the 84u *C. glabrata* wild-type strain and in the derived 84u_*Δcgyap1* deletion mutant, before and after 1h of exposure to 60 mg/L clotrimazole, 80 mg/L fluconazole, 8 mg/L 5-flucytosine and 20 mg/L mancozeb. The presented transcript levels were obtained by quantitative RT-PCR and are relative *CgFLR1/CgACT1* or *CgFLR2/CgACT1* mRNA, relative to the values registered in the 66032u or 84u parental strains in control conditions. The indicated values are averages of at least three independent experiments. Error bars represent the corresponding standard deviations. *p<0.05; **p<0.01.

4.5 Discussion

5-flucytosine has fallen into disuse due to the rapid acquisition of resistance by fungal pathogens and to its moderate toxicity in humans, limiting the administration of higher dosages. The identification of the mechanisms underlying these phenomena is, thus, crucial to maintain the use of 5-flucytosine as a therapeutic option. In this work, the changes occurring at the membrane proteome level in *C. glabrata* cells exposed to 5-flucytosine were analysed, highlighting new mechanisms of resistance to this antifungal drug.

One of the most interesting aspects of this work concerns the identification of CgPdr1 transcription factor, a major factor of resistance to azoles [39], as a determinant of 5-flucytosine resistance. The deletion of CgPdr1 was consistently found to decrease the activation of about 50% of the membrane proteins found to be upregulated in response to 5-flucytosine. Among the proteins whose expression was seen to be affected by CgPdr1 deletion are the multidrug efflux transporter encoding genes *CgCDR1* and *CgQDR2*, but also *CgRIP1*, encoding a putative ubiquinol-cytochrome C reductase iron-sulfur protein, which were previously found to be controlled by this transcription factor [24,29,34,39,40]. New putative targets of CgPdr1 upregulated in the context of 5-flucytosine response include four proteins involved in RNA metabolism, CgDbp2, CgNop1, CgRpl20B and CgRps16A. Interestingly, the traditional targets of CgPdr1, including the ABC drug efflux pumps CgCdr1, CgYor1 and CgSnq2 are suppressed in response to 5-flucytosine, which suggests that, although being active in the response to azoles and to 5-flucytosine, the action of CgPdr1 at the level of transcriptional control appears to be different. It will be interesting to test whether this differential outcome of CgPdr1 activity is linked to differences in terms of the conformation of this transcription factor, whose activation is known to occur by the direct binding to the drug molecule [41]. To gain a full view on the extension of the participation of CgPdr1 in 5-flucytosine response, however, it would be necessary to conduct a transcriptomics study.

A large proportion of the 5-flucytosine response was found to be related to RNA and protein metabolism. Interestingly, an increased expression of some ribosome and translation associated proteins was observed, which may be related to the specific mechanism of action of 5-flucytosine. It is thus possible to assume that the RNA- and

protein-metabolism-related genes identified herein as responding to 5-flucytosine challenge may be involved in counteracting its primary toxic action. Previous analyses of the transcriptome-wide *S. cerevisiae* [11] or *C. albicans* [42] response to 5-flucytosine, also highlighted the relevance of RNA metabolism in the response to this antifungal drug. Indeed, Liu *et al.* found an upregulation of several genes involved in RNA metabolism and translation [42], while Zhang and co-workers showed a down regulation of a few ribosomal protein encoding genes in these conditions [11]. It is also in agreement with a previous chemogenomic analysis of the determinants of 5-flucytosine resistance in the model yeast *S. cerevisiae*, in which about one fourth of the determinants of resistance to this drug were found to be related to RNA and protein metabolism [13]. It appears that *C. glabrata* cells try to compensate, with the increased expression of translation associated proteins, the detrimental effect that 5-flucytosine exerts in this process.

Another interesting feature of the proteomics response includes the downregulation of two nucleotide biosynthesis related proteins, CgUra1 and CgUra3. CgUra1 catalyses the synthesis of ororate from dihydroorotate, which is, then converted to oritidine-5-phosphate. CgUra3 catalyses the next step of conversion of oritidine-5-phosphate to UMP, which is funneled into the production of UDP and UTP, used for RNA synthesis. This same pathway is used to process 5-flucytosine into its toxic products, including 5F-UDP, which upon incorporation in RNA molecules inhibit protein synthesis. It appears, thus, that the cell responds to 5-flucytosine induced stress by decreasing the expression of enzymes required for its conversion to toxic 5-flucytosine products. It is interesting to point out, in this context, that the expression level of CgUra1 and CgUra3 in the *Δcgpdr1* deletion mutant is much higher than in wild-type cells. The upregulation of these proteins in the *Δcgpdr1* background may underlie the increased susceptibility to 5-flucytosine exhibited by this deletion mutant, when compared to the wild-type strain.

Among the results obtained from the membrane proteomics analysis, the role of CgFlr1 and of its homolog CgFlr2, in 5-flucytosine response was further analysed. Although the concentration of CgFlr2 was not found to be increased in the membrane proteome of *C. glabrata* cells, both CgFlr1 and CgFlr2 were found to confer resistance to 5-flucytosine, apparently due to their role in controlling the levels of 5-flucytosine accumulation within *C. glabrata* cells. The fact that CgFlr2 is not upregulated in 5-flucytosine-exposed cells but is required for *C. glabrata* resistance to this stress,

although unexpected, is consistent with the frequent observation that the genes that are required for the resistance to a given stress are not necessarily up-regulated in response to that stress [43]. Interestingly, CgFlr1 was further found to confer resistance to mancozeb, while CgFlr2 was also found to confer resistance to azoles and amphotericin B, placing this transporter at the intersection of multiple antifungal resistance mechanisms. These two transporters constitute, thus, two additional players in the antifungal drug resistance phenomenon. Our group had previously shown that the acquaglyceroporins CgFps1 and CgFps2 [13], as well as the DHA transporters CgAqr1 [12] and CgTpo1_1 and CgTpo1_2 [29] are determinants of 5-flucytosine resistance as well, suggesting that 5-flucytosine extrusion is an important mechanism of resistance against this antifungal drug and showing this phenomenon to be the consequence of the additive contribution of several players.

The analysis of the expression of the *CgFLR1* and *CgFLR2* genes further highlighted their importance in the context of drug resistance in *C. glabrata*. Using the PathoYeastract database (http://pathoyeastract.org/cglabrata/index.php [38]), it is possible to verify that the *CgFLR1* was found to be upregulated upon the over-expression of CgPdr1, in control conditions [44], or upon benomyl or selenite exposure, in the dependency of CgYap1 [16,45,46]. Additionally, *CgFLR1* expression was shown to be repressed by the transcription factor CgStb5, a negative regulator of azole resistance in *C. glabrata* [44]. Chromatine ImmunoPrecipitation (ChIP) assays further showed that CgYap7 binds to the *CgFLR1* promoter in selenite exposed cells [46]. Information on the regulation of *CgFLR2* is much scarcer. RNA sequencing data have demonstrated that the predicted zinc cluster transcription factor encoded by ORF *CAGL0I07755g*, a homolog of the *S. cerevisiae* Hal9 and of the *C. albicans* Tac1 transcription factors, is a positive regulator of *CgFLR2* in control conditions [47]. The new data on the regulation of the *CgFLR1* and *CgFLR2* genes coming from this study shows that both genes are controlled at the transcription level by CgPdr1 in the presence of the azole drug clotrimazole, but not in the presence of fluconazole. The fact that in previous genome-wide expression analysis of fluconazole response in *Candida glabrata* the regulation of *CgFLR1* or *CgFLR2* by CgPdr1 had not been identified suggests that this effect may be specific to imidazole antifungals, such as clotrimazole, but not to triazole antifungals such as fluconazole. Despite the fact that a previous ChIP experiment probing CgPdr1 targets in ρ0 *C. glabrata* cells did not pinpoint *CgFLR1* or

CgFLR2 promoters as targets of CgPdr1 [37], a putative CgPdr1 binding site can be found in the promoter region of *CgFLR2*. The possibility, however, that CgPdr1 may regulate the expression of *CgFLR1* and *CgFLR2* in clotrimazole stressed cells through direct binding to their promoter regions remains to be established. Given the importance of CgPdr1 in the clinical acquisition of azole drug resistance, these results raise the hypothesis that CgFlr1 and CgFlr2 may be relevant in the clinical context. In a previous transcriptomics analysis of the impact of CgPdr1 GOF mutations in fluconazole resistant isolates, when compared to susceptible ones, no significant changes were detected in terms of the expression of *CgFLR1* or *CgFLR2* [36]. However, it would indeed be interesting to assess whether there is a possible correlation between the expression of these genes and the level of antifungal drug resistance in clinical isolates displaying differential clotrimazole or 5-flucytosine susceptibility phenotypes. Additionally, the fact that the transcript levels of both *CgFLR1* and *CgFLR2* genes is controlled, at least at the basal level, by CgPdr1 and CgYap1, appears to correlate with the complex regulation of their *S. cerevisiae* homolog Flr1. The observation that *S. cerevisiae FLR1* gene is also strongly upregulated by the transcription factor ScYap1 in mancozeb stressed cells [19] urged us to check for a similar effect in *CgFLR1* and *CgFLR2* genes. However, although an increased expression of *CgFLR1* and *CgFLR2* was indeed registered in *C. glabrata* cells exposed to mancozeb, this proved to be irrespective of CgYap1 activity, suggesting that the control of the expression of these genes is not fully conserved in *C. glabrata*. The transcriptional control of ScFlr1 was found to be highly complex, relying on the combined efforts of at least four transcription factors, ScYap1, ScPdr1, ScYrr1 and ScRpn4 [18,19,48]. The building of a mathematical model to describe the ScFlr1 regulatory network highlighted that this network is likely to require a fifth, still unidentified, transcription factor to explain the experimental observations, putting forward the hypothesis that its regulation may be even more complex than initially foreseen [20,49]. It would be interesting to check whether the homologs in *C. glabrata* of these additional *S. cerevisiae* transcription factors may also be important in the regulation of these genes, whose control appears to be phylogenetically conserved among these yeast species.

In conclusion, the results described in this study highlight the importance of the DHA transporters from the MFS in antifungal resistance. This work highlights the importance of proteome-wide approaches in the identification of new antifungal resistance

mechanisms. The newly identified processes stand out as promising targets for the development of new 5-flucytosine chemosensitizers, which would expectedly allow for the use of decreased therapeutic dosages of 5-flucytosine.

4.6 Acknowledgements

We acknowledge Thomas Edlind, from the Department of Microbiology & Immunology, Drexel University, College of Medicine, Philadelphia, USA, is acknowledged for kindly providing the 66032u derived strains. John Bennett, from the National Institute of Allergy and Infectious Diseases, NIH, Bethesda, USA, is acknowledged for kindly providing the L5U1 and 84u strains.

This work was supported by FEDER and "Fundação para a Ciência e a Tecnologia" (FCT) (Contract PTDC/BBB-BIO/4004/2014 and PhD and post-doctoral grants to PP (SFRH/BD/110956/2015) and CC (SFRH/BPD/100863/2014), respectively). Funding received by iBB-Institute for Bioengineering and Biosciences from FCT-Portuguese Foundation for Science and Technology (UID/BIO/04565/2013) and from Programa Operacional Regional de Lisboa 2020 (Project N. 007317) is acknowledged.

4.7 References

1. Fidel, P.L.; Vazquez, J.A.; Sobel, J.D. *Candida glabrata*: review of epidemiology, pathogenesis, and clinical disease with comparison to *C. albicans*. *Clin. Microbiol. Rev.* **1999**, *12*, 80-96.

2. Mishra, N.N.; Prasad, T.; Sharma, N.; Payasi, A.; Prasad, R.; Gupta, D.K.; Singh, R. Pathogenicity and drug resistance in *Candida albicans* and other yeast species. A review. *Acta Microbiol. Immunol. Hung.* **2007**, *54*, 201-235.

3. Ghannoum, M.A.; Rice, L.B. Antifungal agents: mode of action, mechanisms of resistance, and correlation of these mechanisms with bacterial resistance. *Clin. Microbiol. Rev.* **1999**, *12*, 501–517.

4. Hope, W.W.; Tabernero, L.; Denning, D.W.; Anderson, M.J. Molecular Mechanisms of Primary Resistance to Flucytosine in *Candida albicans*. *Antimicrob. Agents Chemother.* **2004**, *48*, 4377–4386.

5. Edlind, T.D.; Katiyar, S.K. Mutational Analysis of Flucytosine Resistance in *Candida glabrata*. *Antimicrob. Agents Chemother.* **2010**, *54*, 4733–4738.

6. Espinel-Ingroff, A. Mechanisms of resistance to antifungal agents: yeasts and filamentous fungi. *Rev. Iberoam. Micol.* **2008**, *25*, 101–106.

7. Vermes, A.; Guchelaar, H.J.; Dankert, J. Flucytosine: a review of its pharmacology, clinical indications, pharmacokinetics, toxicity and drug interactions. *J. Antimicrob. Chemother.* **2000**, *46*, 171–179.

8. Sanglard, D.; Odds, F.C. Resistance of *Candida* species to antifungal agents: molecular mechanisms and clinical consequences. *Lancet. Infect. Dis.* **2002**, *2*, 73–85.

9. Kontoyiannis, D.P.; Lewis, R.E. Antifungal drug resistance of pathogenic fungi. *Lancet* **2002**, *359*, 1135–1144.

10. Papon, N.; Noel, T.; Florent, M.; Gibot-Leclerc, S.; Jean, D.; Chastin, C.; Villard, J.; Chapeland-Leclerc, F. Molecular Mechanism of Flucytosine Resistance in *Candida lusitaniae*: Contribution of the *FCY2*, *FCY1*, and *FUR1* Genes to 5-Fluorouracil and Fluconazole Cross-Resistance. *Antimicrob. Agents Chemother.* **2007**, *51*, 369–371.

11. Zhang, L.; Zhang, Y.; Zhou, Y.; Zhao, Y.; Zhou, Y.; Cheng, J. Expression profiling of the response of *Saccharomyces cerevisiae* to 5-fluorocytosine using a DNA microarray. *Int. J. Antimicrob. Agents* **2002**, *20*, 444–450.

12. Costa, C.; Henriques, A.; Pires, C.; Nunes, J.; Ohno, M.; Chibana, H.; Sá-Correia, I.; Teixeira, M.C. The dual role of *Candida glabrata* drug:H+ antiporter CgAqr1 (ORF *CAGL0J09944g*) in antifungal drug and acetic acid resistance. *Front. Microbiol.* **2013**, *4*, 170.

13. Costa, C.; Ponte, A.; Pais, P.; Santos, R.; Cavalheiro, M.; Yaguchi, T.; Chibana, H.; Teixeira, M.C. New mechanisms of flucytosine resistance in *C. glabrata* unveiled by a chemogenomics analysis in *S. cerevisiae*. *PLoS One* **2015**, *10*, e0135110.

14. Gbelska, Y.; Krijger, J.J.; Breunig, K.D. Evolution of gene families: the multidrug resistance transporter genes in five related yeast species. *FEMS Yeast Res.* **2006**, *6*, 345–355.

15. Costa, C.; Dias, P.J.; Sá-Correia, I.; Teixeira, M.C. MFS multidrug transporters in pathogenic fungi: Do they have real clinical impact? *Front. Physiol.* **2014**, *5*, 197.

16. Chen, K.H.; Miyazaki, T.; Tsai, H.F.; Bennett, J.E. The bZip transcription factor Cgap1p is involved in multidrug resistance and required for activation of multidrug transporter gene *CgFLR1* in *Candida glabrata*. *Gene* **2007**, *386*, 63–72.

17. Sá-Correia, I.; dos Santos, S.C.; Teixeira, M.C.; Cabrito, T.R.; Mira, N.P. Drug:H+ antiporters in chemical stress response in yeast. *Trends Microbiol.* 2009, *17*, 22–31.

18. Brôco, N.; Tenreiro, S.; Viegas, C.A.; Sá-Correia, I. *FLR1* gene (ORF *YBR008c*) is required for benomyl and methotrexate resistance in *Saccharomyces cerevisiae* and its benomyl-induced expression is dependent on pdr3 transcriptional regulator. *Yeast* **1999**, *15*, 1595–1608.

19. Teixeira, M.C.; Dias, P.J.; Simões, T.; Sá-Correia, I. Yeast adaptation to mancozeb involves the up-regulation of *FLR1* under the coordinate control of Yap1, Rpn4, Pdr3, and Yrr1. *Biochem. Biophys. Res. Commun.* **2008**, *367*, 249–255.

20. Teixeira, M.C.; Dias, P.J.; Monteiro, P.T.; Sala, A.; Oliveira, A.L.; Freitas, A.T.; Sá-Correia, I. Refining current knowledge on the yeast *FLR1* regulatory network by combined experimental and computational approaches. *Mol. Biosyst.* **2010**, *6*, 2471-2481.

21. dos Santos, S.C.; Teixeira, M.C.; Dias, P.J.; Sá-Correia, I. MFS transporters required for multidrug/multixenobiotic (MD/MX) resistance in the model yeast: understanding their physiological function through post-genomic approaches. *Front. Physiol.* **2014**, *5*, 180.

22. White, T.C. Increased mRNA levels of *ERG16*, *CDR*, and *MDR1* correlate with increases in azole resistance in *Candida albicans* isolates from a patient infected with human immunodeficiency virus. *Antimicrob. Agents Chemother.* **1997**, *41*, 1482–1487.

23. Alarco, A.M.; Raymond, M. The bZip transcription factor Cap1p is involved in multidrug resistance and oxidative stress response in *Candida albicans*. *J. Bacteriol.* **1999**, *181*, 700–708.

24. Costa, C.; Pires, C.; Cabrito, T.R.; Renaudin, A.; Ohno, M.; Chibana, H.; Sá-Correia, I.; Teixeira, M.C. *Candida glabrata* drug: H+antiporter CgQdr2 confers imidazole drug resistance, being activated by transcription factor CgPdr1. *Antimicrob. Agents Chemother.* **2013**, *57*, 3159-3167.

25. Costa, C.; Nunes, J.; Henriques, A.; Mira, N.P.; Nakayama, H.; Chibana, H.; Teixeira, M.C. *Candida glabrata* drug:H+antiporter CgTpo3 (ORF *CAGL0I10384g*): Role in azole drug resistance and polyamine homeostasis. *J. Antimicrob. Chemother.* **2014**, *69*, 1767-1776.

26. Ueno, K.; Uno, J.; Nakayama, H.; Sasamoto, K.; Mikami, Y.; Chibana, H. Development of a Highly Efficient Gene Targeting System Induced by Transient Repression of *YKU80* Expression in *Candida glabrata*. *Eukaryot. Cell* **2007**, *6*, 1239–1247.

27. Vermitsky, J.P.; Edlind, T.D. Azole resistance in *Candida glabrata*: coordinate upregulation of multidrug transporters and evidence for a Pdr1-like transcription factor. *Antimicrob. Agents Chemother.* **2004**, *48*, 3773–81.

28. Jansen, G.; Wu, C.; Schade, B.; Thomas, D.Y.; Whiteway, M. Drag&Drop cloning in yeast. *Gene* **2005**, *344*, 43–51.

29. Pais, P.; Costa, C.; Pires, C.; Shimizu, K.; Chibana, H.; Teixeira, M.C. Membrane Proteome-Wide Response to the Antifungal Drug Clotrimazole in *Candida glabrata*: Role of the Transcription Factor CgPdr1 and the Drug:H+ Antiporters CgTpo1_1 and CgTpo1_2. *Mol. Cell. Proteomics* **2016**, *15*, 57–72.

30. Ueno, K.; Matsumoto, Y.; Uno, J.; Sasamoto, K.; Sekimizu, K.; Kinjo, Y.; Chibana, H. Intestinal resident yeast *Candida glabrata* requires Cyb2p-Mediated lactate assimilation to adapt in mouse intestine. *PLoS One* **2011**, *6*, e24759.

31. Willins, D.A.; Shimer, G.H.; Cottarel, G. A system for deletion and complementation of *Candida glabrata* genes amenable to high-throughput application. *Gene* **2002**, *292*, 141–149.

32. Rosa, M.F.; Sá-Correia, I. Intracellular acidification does not account for inhibition of *Saccharomyces cerevisiae* growth in the presence of ethanol. *FEMS Microbiol. Lett.* **1996**, *135*, 271–274.

33. Sanglard, D.; Ischer, F.; Calabrese, D.; Majcherczyk, P.A.; Bille, J. The ATP binding cassette transporter gene *CgCDR1* from *Candida glabrata* is involved in the resistance of clinical isolates to azole antifungal agents. *Antimicrob. Agents Chemother.* **1999**, *43*, 2753–2765.

34. Vermitsky, J.-P.; Earhart, K.D.; Smith, W.L.; Homayouni, R.; Edlind, T.D.; Rogers, P.D. Pdr1 regulates multidrug resistance in *Candida glabrata*: gene disruption and genome-wide expression studies. *Mol. Microbiol.* **2006**, *61*, 704–722.

35. Torelli, R.; Posteraro, B.; Ferrari, S.; La Sorda, M.; Fadda, G.; Sanglard, D.; Sanguinetti, M. The ATP-binding cassette transporter–encoding gene *CgSNQ2* is contributing to the *CgPDR1*-dependent azole resistance of *Candida glabrata*. *Mol. Microbiol.* **2008**, *68*, 186–201.

36. Tsai, H.F.; Sammons, L.R.; Zhang, X.; Suffis, S.D.; Su, Q.; Myers, T.G.; Marr, K.A.; Bennett, J.E. Microarray and molecular analyses of the azole resistance mechanism in *Candida glabrata* oropharyngeal isolates. *Antimicrob. Agents Chemother.* **2010**, *54*, 3308–3317.

37. Paul, S.; Bair, T.B.; Moye-Rowley, W.S. Identification of genomic binding sites for *Candida glabrata* Pdr1 transcription factor in wild-type and ρ0 cells. *Antimicrob. Agents Chemother.* **2014**, *58*, 6904–6912.

38. Monteiro, P.T.; Pais, P.; Costa, C.; Manna, S.; Sá-Correia, I.; Teixeira, M.C. The PathoYeastract database: An information system for the analysis of gene and genomic transcription regulation in pathogenic yeasts. *Nucleic Acids Res.* **2017**, *45*, D597-D603.

39. Tsai, H.F.; Krol, A.A.; Sarti, K.E.; Bennett, J.E. *Candida glabrata PDR1*, a transcriptional regulator of a pleiotropic drug resistance network, mediates azole resistance in clinical isolates and petite mutants. *Antimicrob. Agents Chemother.* **2006**, *50*, 1384–1392.

40. Ferrari, S.; Sanguinetti, M.; Torelli, R.; Posteraro, B.; Sanglard, D. Contribution of *CgPDR1*-Regulated Genes in Enhanced Virulence of Azole-Resistant *Candida glabrata*. *PLoS One* **2011**, *6*, e17589.

41. Thakur, J.K.; Arthanari, H.; Yang, F.; Pan, S.J.; Fan, X.; Breger, J.; Frueh, D.P.; Gulshan, K.; Li, D.K.; Mylonakis, E.; *et al.* A nuclear receptor-like pathway regulating multidrug resistance in fungi. *Nature* **2008**, *452*, 604–609.

42. Liu, T.T.; Lee, R.E.B.; Barker, K.S.; Lee, R.E.; Wei, L.; Homayouni, R.; Rogers, P.D. Genome-Wide Expression Profiling of the Response to Azole, Polyene, Echinocandin, and Pyrimidine Antifungal Agents in *Candida albicans*. *Antimicrob. Agents Chemother.* **2005**, *49*, 2226–2236.

43. Teixeira, M.C.; Mira, N.P.; Sá-Correia, I. A genome-wide perspective on the response and tolerance to food-relevant stresses in *Saccharomyces cerevisiae*. *Curr. Opin. Biotechnol.* **2011**, *22*, 150–156.

44. Noble, J.A.; Tsai, H.F.; Suffis, S.D.; Su, Q.; Myers, T.G.; Bennett, J.E. *STB5* is a negative regulator of azole resistance in *Candida glabrata*. *Antimicrob. Agents Chemother.* **2013**, *57*, 959–967.

45. Lelandais, G.; Tanty, V.; Geneix, C.; Etchebest, C.; Jacq, C.; Devaux, F. Genome adaptation to chemical stress: clues from comparative transcriptomics in *Saccharomyces cerevisiae* and *Candida glabrata*. *Genome Biol.* **2008**, *9*, R164.

46. Merhej, J.; Thiebaut, A.; Blugeon, C.; Pouch, J.; Ali Chaouche, M.E.A.; Camadro, J.-M.; Le Crom, S.; Lelandais, G.; Devaux, F. A Network of Paralogous Stress Response Transcription Factors in the Human Pathogen *Candida glabrata*. *Front. Microbiol.* **2016**, *7*, 645.

47. Wu, J.; Chen, X.; Cai, L.; Tang, L.; Liu, L. Transcription factors Asg1p and Hal9p regulate pH homeostasis in *Candida glabrata*. *Front. Microbiol.* **2015**, *6*, 843.

48. Alarco, A.M.; Balan, I.; Talibi, D.; Mainville, N.; Raymond, M. AP1-mediated multidrug resistance in *Saccharomyces cerevisiae* requires *FLR1* encoding a transporter of the major facilitator superfamily. *J. Biol. Chem.* **1997**, *272*, 19304–19313.

49. Monteiro, P.T.; Dias, P.J.; Ropers, D.; Oliveira, A.L.; Sá-Correia, I.; Teixeira, M.C.; Freitas, A.T. Qualitative modelling and formal verification of the *FLR1* gene mancozeb response in *Saccharomyces cerevisiae*. *IET Syst. Biol.* **2011**, *5*, 308–316.

5 *Candida glabrata* transcription factor Rpn4 mediates fluconazole resistance through regulation of ergosterol biosynthesis and plasma membrane permeability

This chapter contains results included in a submitted manuscript:

Pais, P., Califórnia, R., Galocha, M., Viana, R., Ola, M., Takahashi-Nakaguchi, A., Chibana, H., Butler, G., Teixeira, M.C. *Candida glabrata* transcription factor Rpn4 mediates fluconazole resistance through regulation of ergosterol biosynthesis and plasma membrane permeability.

The PhD candidate is the first author of the work detailed in this chapter. The candidate was responsible for most of the experimental work and writing of the correspondent manuscript.

5.1 Abstract

The ability to rapidly acquire azole resistance underlies the success of *Candida glabrata* as a fungal pathogen. As such, understanding the molecular basis of azole resistance in this pathogen is crucial to design more suitable therapeutic strategies.

In this study, we show that the *C. glabrata* transcription factor (TF) CgRpn4 is a determinant of azole drug resistance. The role of CgRpn4 in the transcriptome-wide response to fluconazole was evaluated through RNA-sequencing. CgRpn4 regulates expression of 212 genes, activating 80 genes and repressing, likely in an indirect fashion, 132 genes Targets include several proteasome and ergosterol biosynthesis genes, such as *CgERG1*, *CgERG2*, *CgERG3* and *CgERG11*. Localization of CgRpn4 to the nucleus increases upon fluconazole stress. Consistent with a role in ergosterol and plasma membrane homeostasis, CgRpn4 is required for the maintenance of ergosterol levels upon fluconazole stress, which is associated with a role in the upkeep of cell permeability and decreased intracellular fluconazole accumulation. Moreover, we provide evidence that CgRpn4 directly regulates expression of *CgERG11* through the TTGCAAA binding motif, reinforcing the relevance of this regulatory network in azole resistance.

In summary, CgRpn4 is a new regulator of the ergosterol biosynthesis pathway in *C. glabrata*, contributing to plasma membrane homeostasis and thus decreasing azole drug accumulation.

5.2 Introduction

Infections by fungal pathogens have become a worrying health concern worldwide. *Candida* species represent the most common cause of fungal infections and rank as the 4th leading cause of nosocomial bloodstream infections in the USA [1–3]. They are responsible for localized superficial infections in healthy individuals but can cause life-threatening scenarios in immunocompromised patients. After *Candida albicans*, *Candida glabra* is the second most commonly isolated species, mainly due to its ability to rapidly acquire azole resistance [1,4].

Due to their safety profile and availability in both oral and intravenous formulations, azoles have been the most widely used antifungals for decades both as a first line treatment and as prophylaxis, especially fluconazole [5]. Azoles disrupt ergosterol biosynthesis, the main sterol in fungal plasma membranes, which leads to loss of membrane structural properties. They act by binding and inhibiting the lanosterol 14-α-demethylase, a key enzyme of the ergosterol biosynthetic pathway encoded by *ERG11* [6,7]. The result is the accumulation of 14-α-methylated sterols, depletion of ergosterol and production of the toxic sterol dimethylcholesta-8,24(28)-dien-3β,6α-diol (DMCDD) in the membrane [8,9].

Investigation of the transcriptional regulation of antifungal resistance in *C. glabrata* is mostly focused on the role of the transcription factor CgPdr1, regarded as a master regulator of clinical acquisition of resistance to azole antifungals by activating the expression of multidrug resistance transporters [10–15]. In *C. albicans* Tac1 plays a similar role by regulating the expression of multidrug resistance transporters [16–18]. However, sequence similarity between CaTac1 and CgPdr1 is low. Apart from these pathways, knowledge about regulatory networks involved in response to antifungal stress is scarce, especially in *C. glabrata* [19].

In this study, we identified the transcription factor CgRpn4 as a regulator of fluconazole resistance in *C. glabrata*. In *Saccharomyces cerevisiae*, the Rpn4 homolog regulates expression of proteasome genes, affecting proteasome activity and ubiquitin-mediated proteolysis [20–23], and contributes to the unfolded protein response (UPR) [24]. Rpn4 has also been identified as a member of the multidrug resistance network in *S. cerevisiae* [25,26]. Consistently, deletion of *ScRPN4* results in increased sensitivity to fluconazole [27,28] and clotrimazole [29]. Moreover, expression of *ScRPN4* and

consequently the ubiquitin-proteasome system is regulated by the multidrug resistance regulators ScPdr1 and ScPdr3 [22]. In *C. albicans*, *RPN4* is also a regulator of proteasome genes and its absence results in enhanced sensitivity to fluconazole [30]. To the best of our knowledge, despite the apparent role of Rpn4 in azole resistance phenotypes, its actual role and mechanistic insights in antifungal resistance have not been addressed.

Given the identification of *CgRPN4* as a new determinant of azole drug resistance in *C. glabrata*, its role in the transcriptome-wide response to fluconazole was assessed. The determination of Rpn4 target genes enabled the identification of a new regulatory pathway towards azole resistance, which may provide the molecular basis of Rpn4-mediated azole resistance in pathogenic and non-pathogenic yeasts.

5.3 Materials and Methods

5.3.1 Strains, plasmids and growth media

Candida glabrata parental strain KUE100 [31] and derived single deletion mutants were batch-cultured at 30ºC, with orbital agitation (250 rpm) in basal medium (BM) medium or Yeast extract-Peptone-Dextrose (YPD) medium. BM has the following composition (per liter): 1.7 g yeast nitrogen base without amino acids or NH_4^+ (Difco), 20 g glucose (Merck) and 2.65 g $(NH_4)_2SO_4$ (Merck). YPD has the following composition (per liter): 20 g glucose (Merck), 20 g Peptone (Merck) and 10 g Yeast extract (Merck). *C. glabrata* strain L5U1 (*cgura3Δ0, cgleu2Δ0*) [32], kindly provided by John Bennett from the National Institute of Allergy and Infectious Diseases, NIH, Bethesda, USA, was grown in BM supplemented with 20 mg/L uracil and 60mg/L leucine. L5U1 strains harboring pGREG576 derived plasmids were grown in the same medium lacking uracil. Solid media contained, besides the above-indicated ingredients, 20 g/L agar (Iberagar). The plasmid pGREG576 was obtained from the Drag&Drop collection [33].

5.3.2 Disruption of *CgRPN4*

The deletion of the *C. glabrata RPN4* addressed in this study was carried out in the parental strain KUE100, using the method described by Ueno *et al.* [34]. *CgRPN4* was replaced by a DNA cassette including the *CgHIS3* gene, through homologous recombination. The PCR primers used to generate the replacement cassette were as follows: 5'-TATATAAAGGAGCACTGGTGGCGGTGGTGGCAATTCTATTAAAACTTTCCTCTCGAGGGCCGCTGATCACG-3' and 5'-AAAAAAAAATTATAATGATGTATCCGAAATTTTAAAAGAAATTTGAATGATGTTGGCATCGTGAGGCTGG-3'. The primers used for confirmation PCR were as follows: Fw – 5'-GATTTGGGACTGAAGAGG-3', Rv – 5'-ATAGTCCACATCGTCGTAG-3' and Check – 5'-TCCCTTTCTGATGTGGTGGC-3' The pHIS906 plasmid including *CgHIS3* was used as a template and transformation was performed as described previously [31].

5.3.3 Cloning of the *C. glabrata CgRPN4* (ORF *CAGL0K01727g*)

The pGREG576 plasmid from the Drag&Drop collection was used as described before to clone and express the *C. glabrata* ORF *CAGL0K01727g* [11,15,35–38]. pGREG576 was acquired from Euroscarf and contains a galactose inducible promoter (*GAL1*), the yeast selectable marker *URA3* and the *GFP* gene, encoding a Green Fluorescent Protein (GFPS65T), which allows monitoring of the expression and subcellular localization of the cloned fusion protein. *CgRPN4* DNA was generated by PCR, using genomic DNA extracted from the sequenced CBS138 *C. glabrata* strain, and the following specific primers: 5'-GAATTCGATATCAAGCTTATCGATACCGTCGACA*ATGACGTCTATAGATTTGG GAC*-3' and 5'-GCGTGACATAACTAATTACATGACTCGAGGTCGAC*TTATGCAGTGACAAATCC GATG*-3'. The designed primers contain, besides a region with homology to the first and last 22 nucleotides of the *CgRPN4* coding region (italic), nucleotide sequences with homology to the cloning site flanking regions of the pGREG576 vector (underlined). The amplified fragments were co-transformed into the parental *S. cerevisiae* strain BY4741 with the pGREG576 vector, previously cut with the restriction enzyme SalI, to obtain the pGREG576_*CgRPN4* plasmid. Since the *GAL1* promoter only allows a slight expression of downstream genes in *C. glabrata*, to visualize by fluorescence microscopy the subcellular localization of the CgRpn4 protein in *C. glabrata*, new constructs were obtained. The *GAL1* promoter present in the pGREG576_*CgRPN4* plasmid was replaced by the copper-inducible *MTI C. glabrata* promoter [39], giving rise to the pGREG576_MTI_*CgRPN4* plasmid. The *MTI* promoter DNA was generated by PCR, using genomic DNA extracted from the sequenced CBS138 *C. glabrata* strain, and the following specific primers: 5'-TTAACCCTCACTAAAGGGAACAAAAGCTGGAGCTC*CTGTACGACACGCATCA TGTGGCAATC*-3' and 5'-GAAAAGTTCTTCTCCTTTACTCATACTAGTGCGGC*TGTGTTTGTTTTTGTATGT GTTTGTTG*-3'. The designed primers contain, besides a region with homology to 27 nucleotides in the beginning and the last 27 nucleotides of the 1000 bp upstream region of the *MTI* coding sequence (italic), nucleotide sequences with homology to the cloning site flanking regions of the pGREG576 vector (underlined). The amplified fragment was co-transformed into the parental strain BY4741 with the pGREG576_*CgRPN4*

plasmid, previously cut with AscI and NotI restriction enzymes to remove the *GAL1* promoter, to generate the pGREG576_MTI_*CgRPN4* plasmid. The recombinant plasmids pGREG576_*CgRPN4* and pGREG576_MTI_*CgRPN4* were obtained through homologous recombination in *S. cerevisiae* and verified by DNA sequencing.

5.3.4 Antifungal susceptibility assays

The susceptibility of the parental strain KUE100 towards toxic concentrations of the selected drugs was compared to that of the deletion mutants KUE100_*Δcgrpn4* by spot assays. The ability of *CgRPN4* gene expression to increase wild-type resistance to the tested chemical stresses was also examined in the URA3- L5U1 *C. glabrata* strain, using the pGREG576_MTI_*CgRPN4* centromeric plasmids.

KUE100 *C. glabrata* cell suspensions used to inoculate agar plates were mid-exponential cells grown in BM until culture OD_{600nm} = 0.5 ± 0.05 was reached and then diluted in sterile water to obtain suspensions with OD_{600nm} = 0.05 ± 0.005. These cell suspensions and subsequent dilutions (1:5; 1:25) were applied as 4 µL spots onto the surface of solid BM, supplemented with adequate chemical stress concentrations. L5U1 *C. glabrata* cell suspensions used to inoculate the agar plates were mid-exponential cells grown in BM-U supplemented with leucine and 50 µM $CuSO_4$ when using the L5U1 strain harboring the pGREG576 derived plasmids, until culture OD_{600nm} = 0.5 ± 0.05 was reached and then diluted in sterile water to obtain suspensions with OD_{600nm} = 0.05 ± 0.005. These cell suspensions and subsequent dilutions (1:5; 1:25) were applied as 4 µL spots onto the surface of solid BM-U supplemented with leucine and 50 µM $CuSO_4$ for strains transformed with the pGREG576 derived plasmids and with adequate chemical stress concentrations. The tested drugs included the following compounds, used in the specified concentration ranges: the azole antifungal drugs ketoconazole (10 to 60 mg/L), fluconazole (100 to 250 mg/L), miconazole (0.10 to 0.50 mg/L), itraconazole (15 to 30 mg/L), and clotrimazole (2.5 to 15 mg/L), the polyene antifungal drug amphotericin B (0.10 to 0.35 mg/L) and the fluoropyrimidine 5-flucytosine (0.02 to 0.04 mg/L) (all from Sigma).

5.3.5 CgRpn4 subcellular localization assessment

The subcellular localization of the CgRpn4 protein was determined based on the observation of L5U1 *C. glabrata* cells transformed with the pGREG576_MTI_*CgRPN4* plasmid. These cells express the CgRpn4_GFP fusion protein, whose localization may be determined using fluorescence microscopy. *C. glabrata* cell suspensions were prepared in BM-U supplemented with leucine and 50 μM $CuSO_4$, until a standard culture OD_{600nm} = 0.5 ± 0.05 was reached and transferred to the same medium with or without fluconazole. After 1h of incubation, the distribution of CgRpn4_GFP fusion protein in *C. glabrata* living cells was detected by fluorescence microscopy in a Zeiss Axioplan microscope (Carl Zeiss MicroImaging), using excitation and emission wavelength of 395 and 509nm, respectively. Fluorescence images were captured using a cooled Zeiss Axiocam 503 color (Carl Zeiss Microscopy). For fluorescence signal localization a minimum of 50 cells/experiment were used. Statistical analysis of the results was performed using analysis of variance, and differences were considered significant for p-values<0.05.

5.3.6 Total RNA extraction

C. glabrata strains KUE100 and KUE100_Δ*cgrpn4* were grown in BM until mid-exponential phase. Subsequently, cells were transferred to fresh medium (control) or fresh medium containing 150 mg/L fluconazole were harvested after 1h of incubation. Total RNA was isolated using an Ambion Ribopure-Yeast RNA kit, according to manufacturer's instructions.

5.3.7 Library preparation

Prior to RNA-seq analysis quality control measures were implemented. Concentration of RNA was ascertained via fluorometric analysis on a Thermo Fisher Qubit fluorometer. Overall quality of RNA was verified using an Agilent Tapestation instrument. Following initial QC steps sequencing libraries were generated using the Illumina Truseq Stranded Total RNA library prep kit with ribosomal depletion via RiboZero Gold according to the manufacturer's protocol. Briefly, ribosomal RNA was

depleted via pull down with bead-bound ribosomal-RNA complementary oligomers. The RNA molecules were then chemically fragmented and the first strand of cDNA was generated using random primers. Following RNase digestion the second strand of cDNA was generated replacing dTTP in the reaction mix with dUTP. Double stranded cDNA then underwent adenylation of 3' ends following ligation of Illumina-specific adapter sequences. Subsequent PCR enrichment of ligated products further selected for those strands not incorporating dUTP, leading to strand-specific sequencing libraries. Final libraries for each sample were assayed on the Agilent Tapestation for appropriate size and quantity. These libraries were then pooled in equimolar amounts as ascertained via fluorometric analyses. Final pools were absolutely quantified using qPCR on a Roche LightCycler 480 instrument with Kapa Biosystems Illumina Library Quantification reagents.

5.3.8 Gene expression analysis

Strand specific RNA-seq library preparation and sequencing was carried out as a paid service by the NGS core from Oklahoma Medical Research Foundation, Oklahoma City, Oklahoma, USA. Paired-end reads (Illumina HiSeq 3000 PE150, 2x150 bp, 2 Gb clean data) were obtained from KUE100 and KUE100_Δ*cgrpn4*. Two replicates of each sample were obtained from three independent RNA isolations, subsequently pooled together. Raw data is available at Gene Expression Omnibus (GEO) under the accession number GSE129349. Samples reads were trimmed using Skewer (v0.2.2) [40] and aligned to the *C. glabrata* CBS138 reference genome, obtained from the Candida Genome Database (CGD) (http://www.candidagenome.org/), using TopHat (v2.1.1) [41] with parameters -p 12 (number of threads), -g 1 (maximum amount of times a read can be mapped to the genome), --b2-very-sensitive (preset option) and --library-type fr-firststrand (account for strand specificity). HTSeq (v0.7.1) [42] was used to count mapped reads per ORF Differentially expressed genes were identified using DESeq2 [43] with an adjusted p-value threshold of 0.05 and a log2 fold change threshold of -0.5 and 0.5. Default parameters in DESeq2 were used. *Candida albicans* and *Saccharomyces cerevisiae* homologs were obtained from the Candida Genome Database and Saccharomyces Genome Database (SGD) (https://www.yeastgenome.org/), respectively.

5.3.9 Ergosterol quantification

Ergosterol was extracted from cells using the methods adapted from Gong *et al.* 2001 [44]. Cells were cultivated in YPD medium with orbital agitation (250 rpm) until stationary phase, harvested by centrifugation and resuspended in 5 mL of methanol. 1 mL of a solution of 1 mg/mL of cholesterol (Sigma) was added as an internal standard to estimate ergosterol extraction yield. Homogenization was carried out with glass beads for 30s, followed by incubation at 320 rpm for 1h. Each sample was then centrifuged and 1,7 mL of the supernatant was collected, clarified and stored until HPLC analysis. The extracts were separated in a 250 mm × 4 mm C18 column (LiChroCART Purospher STAR RP-18 end- capped 5 µm) at 30ºC. Samples were eluted in 100% methanol at a flow rate of 1 mL/min. Detection of cholesterol and ergosterol was performed using an UV-Vis detector set at 282 and 210 nm, respectively. Under the conditions used the retention time of cholesterol was 15.4 ± 0.4 while ergosterol was eluted at 12.5 ± 0.2 minutes. Subsequent quantification of the two lipids was performed using appropriate calibration curves. The results are shown in µg of ergosterol per mg of wet cell weight. Statistical analysis of the results was performed using analysis of variance, and differences were considered significant for p-values<0.05.

5.3.10 Plasma membrane permeability

Plasma membrane permeability was assessed by the passive uptake of propidium iodide (PI; 20 mM in DMSO, Invitrogen). *C. glabrata* cell suspensions from strains KUE100 and KUE100_Δ*cgrpn4* were prepared in BM until a standard culture OD_{600nm} = 0.5 ± 0.05 was reached and transferred to the same medium with or without 150 mg/L fluconazole. After 1h of incubation, PI was added to 1 mL of 4×10^7 cells/mL to a final concentration of 20 µM and cell suspensions were incubated in the dark with orbital agitation (15 minutes, 250 rpm). Cells exposed to PI were centrifuged (17,500 × g for 5 minutes), washed twice and resuspended in PBS buffer to a final 10^7 cells/mL aliquots. PI-fluorescence was detected by fluorescence microscopy in a Zeiss Axioplan microscope (Carl Zeiss MicroImaging), using excitation and emission wavelength of 536 and 595nm, respectively. Fluorescence images were captured using a cooled Zeiss Axiocam 503 color (Carl Zeiss Microscopy) and the images were analyzed with the

ZEN lite software from ZEISS microscopy. Cell-to-cell fluorescence intensity was defined as the average of pixel by pixel intensity in the selected region of interest and a minimum of 50 cells/experiment were used. The fluorescence images were background corrected by using dark-current images. Statistical analysis of the results was performed using analysis of variance, and differences were considered significant for p-values<0.05.

5.3.11 ^{3}H-fluconazole accumulation assays

^{3}H-fluconazole transport assays were carried out as described before for other radiolabeled compounds [11,15,35–38]. The internal accumulation of fluconazole was determined by calculating the ratio between the radiolabeled fluconazole measured within the yeast cells and in the external medium (Intracellular/Extracellular). The parental strain KUE100 and the mutant strain KUE100_*Δcgrpn4* were grown in BM until mid-exponential phase and harvested by filtration. Cells were washed and resuspended in BM, to obtain dense cell suspensions (OD_{600nm} = 0.5 ± 0.1, equivalent to approximately 1.57 mg (dry weight) mL^{-1}). Readily, 0.1 µM of ^{3}H-fluconazole (Moravek Inc.; 1 mCi/ml) and 150 mg/L of unlabeled fluconazole were added to the cell suspensions. Incubation proceeded for an additional period of 20min. The intracellular accumulation of labeled fluconazole was followed by filtering 200 µl of cell suspension, at adequate time intervals, through pre-wetted glass microfibre filters (Whatman GF/C). The filters were washed with ice-cold TM buffer and the radioactivity measured in a Beckman LS 5000TD scintillation counter. Extracellular ^{3}H-fluconazole was estimated, by radioactivity assessment of 50 µl of the supernatant. Non-specific ^{3}H-fluconazole adsorption to the filters and to the cells (less than 5% of the total radioactivity) was assessed and taken into consideration. To calculate the intracellular concentration of labeled fluconazole, the internal cell volume (Vi) of the exponential cells, grown in the absence of drug and used for accumulation assays, was considered constant and equal to 2.5 µl (mg dry weight)$^{-1}$ [45]. Statistical analysis of the results was performed using analysis of variance, and differences were considered significant for p-values<0.05.

5.3.12 *In silico* prediction of overrepresented sequences in CgRpn4-activated promoters

The promoters (-1000 to -1 bp) upstream of the coding regions of genes whose expression was found to be activated by CgRpn4 were retrieved using the "Retrieve Upstream Sequence" tool from PathoYeastract (www.pathoyeastract.org) [46]. The obtained sequences were submitted to DREME (MEME suite) [47] for discovery of enriched sequences, using default parameters. The identified motifs were then cross checked with ScRpn4 motifs retrieved from the "TF-Consensus List" tool from YEASTRACT.

5.3.13 Cloning of the *CgERG11* promoter and site-directed mutagenesis

The pYPE354 plasmid was used as described before to clone and express the *lacZ* reporter gene [11]. pYEP354 contains the yeast selectable marker *URA3* and the bacterial selectable marker *AmpR* genes. *CgERG11* promoter DNA was generated by PCR, using genomic DNA extracted from the sequenced CBS138 *C. glabrata* strain, and the following specific primers: 5'-CCGGAATTC*GGTCGACTACTTCAAGGCTA*-3' and 5'-AACTGCAG*CTTCAGTGGACATGTTATTGT*-3'. The first primer contains a region with homology within the beginning of the *CgERG11* promoter (italic) and a recognition site for the EcoRI restriction enzyme, flanked by additional bases. The second primer contains a region with homology within the end of the *CgERG11* promoter and the beginning of the *CgERG11* coding sequence (italic) and a recognition site for the PstI restriction enzyme, flanked by additional bases. The amplified fragment was ligated into the pYEP354 vector (T4 Ligase, New England Biolabs), previously cut with the same restriction enzymes, to obtain the pYEP354_*CgERG11*prom_*lacZ* plasmid. The putative CgRpn4 consensus in the *CgERG11* promoter was mutated by site-directed mutagenesis using the following primers: 5'-GAGTGACATCTTTGTTAGCCCTTCCCATC-3' and 5'-GATGGGAAGGGCTAACAAAGATGTCACTC-3'. The designed primers contain two mutations within the potential consensus (underlined), resulting in the production of the mutated consensus by PCR amplification to obtain the

pYEP354_mut_*CgERG11*prom_*lacZ* plasmid. The original template was then degraded by DpnI digestion.

5.3.13 *LacZ* gene expression measurement

The transcript levels of the *lacZ* reporter gene encoding for β-galactosidase were determined by quantitative real-time PCR (RT-PCR). L5U1 cells transformed with the pYEP354_*CgERG11*prom_*lacZ* or pYEP354_mut_*CgERG11*prom_*lacZ* plasmids were grown in BM-U supplemented with leucine until mid-exponential phase. Subsequently, cells were transferred to fresh medium (control) or fresh medium containing 150 mg/L fluconazole and harvested after 1h of incubation. Samples were immediately frozen at -80ºC until RNA extraction. For total RNA extraction, the hot phenol method was applied [48]. Total RNA was converted to cDNA for the real-time Reverse-Transcription PCR (RT-PCR) using the MultiScribe Reverse Transcriptase kit (Applied Biosystems) and the 7500 RT-PCR thermal cycler block (Applied Biosystems). The real time PCR step was carried out using SYBR Green® reagents (Applied Biosystems) and the 7500 RT-PCR thermocycler block (Applied Biosystems), with the following primers for the *lacZ* gene: 5'-TGGCTGGAGTGCGATCTTC-3' and 5'-CGTGCATCTGCCAGTTTGAC-3'; and for the *CgRDN25* gene: 5'-AACAACTCACCGGCCGAAT-3' and 5'-CAAGCGTGTTACCTATACTCCGCCGTCA-3'. Default parameters set by the manufacturer were followed, and fluorescence was detected by the instrument and plotted in an amplification graph (7500 Systems SDS Software, Applied Biosystems). *CgRDN25* gene transcript levels were used as an internal reference.

5.4 Results and Discussion

5.4.1 The transcription factor *CgRPN4* is a determinant of fluconazole resistance in *Candida glabrata*

Based on the previous identification of Rpn4 as a member of the multidrug resistance network in several yeast species, the role of the uncharacterized *CgRPN4* gene was in azole resistance was determined. Figure 5.1A shows that deleting CgRpn4 increases sensitivity to 6 different azole drugs when compared to the KUE100 wild-type strain. Interestingly, over-expression of *CgRPN4* in the L5U1 wild-type *C. glabrata* strain increased its tolerance to the fluconazole and ketoconazole (Figure 5.1B).

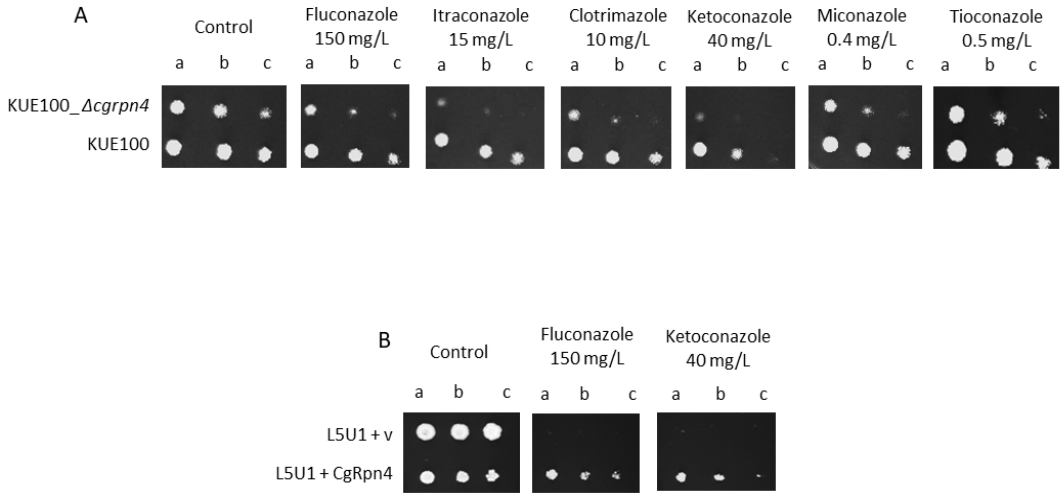

Figure 5.1 – *CgRPN4* confers resistance to fluconazole in *C. glabrata*. (A) Comparison of the susceptibility to azole antifungals, at the indicated concentrations, of the KUE100 and KUE100_*Δcgrpn4 C. glabrata* strains, in BM agar plates, by spot assays. (B) Comparison of the susceptibility to azole antifungals, at the indicated concentrations, of the L5U1 *C. glabrata* strain harboring the pGREG576 cloning vector (v) or the pGREG576_MTI_*CgRPN4* in BM-U agar plates supplemented with 50 μM $CuSO_4$, by spot assays. The inocula were prepared as described in the materials and methods section. Cell suspensions used to prepare the spots were 1:5 (b) and 1:25(c) dilutions of the cell suspensions used in (a). The displayed images are representative of at least three independent experiments.

The Minimum Inhibitory Concentration (MIC) levels for fluconazole and ketoconazole were further assessed, as well as for 5-flucytosine, amphotericin B and the echinocandin caspofungin. The MIC_{50} of the Δ*cgrpn4* mutant strain is 4 mg/L for fluconazole, which represents a 4-fold decrease in comparison to its parental wild-type strain (MIC_{50} 16 mg/L). The mutant strain also showed an 8-fold decrease in MIC relative to the wild-type for ketoconazole (MIC_{50} 0.0625 mg/L in the mutant vs MIC_{50} 0.500 mg/L in the wild-type). As expected, no MIC_{50} differences were observed for 5-flucytosine or amphotericin B However, a 2-fold decrease for caspofungin was observed (MIC_{50} 0.125 mg/L in the mutant vs MIC_{50} 0.25 in the wild-type). *CgRPN4* therefore plays a role in regulating azole drug resistance in *C. glabrata*.

5.4.2 Transcriptome-wide changes in response to mild fluconazole stress in *C. glabrata*

We used transcriptional profiling to determine the response of wild-type to treatment with fluconazole. Expression of 44 genes was altered in *C. glabrata* cells following exposure for 1 h to 150 mg/L fluconazole ($-0.5 < \log_2$ foldchange < 0.5; adjusted p-value<0.05) (Table 5.1; Supplementary Table S5.1). Expression of 29 (66%) genes is increased, whereas expression of 15 (34%) is decreased. The genes fall into 11 functional groups: Drug Resistance, Sterol Metabolism and Intracellular Traffic; which are exclusively associated to the upregulated genes; Lipid and Fatty Acid Metabolism, Nitrogen Metabolism, Carbon Metabolism, Heme Homeostasis, Mitochondrial Function, Stress Response, Cytoskeleton/Cell Cycle, and Unknown function.

Table 5.1 – List of genes differentially expressed in wild-type *C. glabrata* cells challenged with fluconazole. The effect of CgRpn4 deletion in their expression pattern is also shown. *Genes which expression levels are significantly altered in the absence of CgRpn4.

Functional Group	*C. glabrata* gene	Description	Log2 Fold Change WT FLC/WT control	Log2 Fold Change *Δcgrpn4* FLC/WT FLC
Drug Resistance	*CDR1*	Multidrug transporter of ATP-binding cassette (ABC) superfamily, involved in resistance to azoles; expression regulated by Pdr1p; increased abundance in azole resistant strains; expression increased by loss of the mitochondrial genome	0.806502278950904	0.417724117144525
Sterol Metabolism	*ERG1**	Squalene epoxidase with a role in ergosterol synthesis; involved in growth under conditions of low oxygen tension	0.826089155759605	-0.607762236567877
	*ERG2**	C-8 sterol isomerase	1.09725488322957	-0.707593953006031
	*ERG3**	Delta 5,6 sterol desaturase; C-5 sterol desaturase; predicted transmembrane domain and endoplasmic reticulum (ER) binding motif; gene used for molecular typing of *C. glabrata* strain isolates	1.07338746583993	-0.632736980812507
	ERG4	Putative C24 sterol reductase	0.829009537498708	-0.458637819498671
	ERG5	Putative C22 sterol desaturase	0.575941840120078	-0.23727206996668
	ERG6	C24 sterol methyltransferase; mutation confers resistance to amphotericin B and nystatin and increased sensitivity to azoles	0.51801680046259	-0.377305948226935
	*ERG11**	Putative cytochrome P-450 lanosterol 14-alpha-demethylase; target enzyme of azole antifungal drugs; increased protein abundance in azole resistant strain	0.962623735444949	-0.651350626785954
	ERG24	Ortholog(s) have delta14-sterol reductase activity and role in cellular response to drug, ergosterol biosynthetic process, filamentous growth of a population of unicellular organisms in response to biotic stimulus, pathogenesis	0.532441864386364	-0.315361825123651
	ERG25	Ortholog(s) have C-4 methylsterol oxidase activity, role in ergosterol biosynthetic process and endoplasmic reticulum membrane, plasma membrane localization	1.02400055032675	-0.407124188145839

Table 5.1 (continued)

Functional Group	*C. glabrata* gene	Description	Log2 Fold Change WT FLC/WT control	Log2 Fold Change *Δcgrpn4* FLC/WT FLC
Sterol Metabolism	*ERG29*	Ortholog(s) have role in cellular iron ion homeostasis, ergosterol biosynthetic process, mitochondrion organization and endoplasmic reticulum, nuclear envelope localization	0.836126107041274	-0.429774283229086
	*HES1**	Ortholog(s) have oxysterol binding, sterol transporter activity and role in endocytosis, exocytosis, maintenance of cell polarity, piecemeal microautophagy of nucleus, sterol transport	1.48301749340101	-0.964261714368453
	CYB5	Ortholog(s) have electron carrier activity, role in ergosterol biosynthetic process and endoplasmic reticulum membrane localization	0.729608818156223	-0.426890121278795
Lipid and Fatty Acid Metabolism	*CSR1**	Ortholog(s) have phosphatidylinositol transporter activity	0.590278326388826	-0.9007933257619
	HBN1	Ortholog(s) have oxidoreductase activity, acting on NAD(P)H, nitrogenous group as acceptor activity and role in cellular response to oxidative stress, negative regulation of fatty acid metabolic process	-0.512260055829125	-0.0962977434936838
	*CAGL0A03740g**	Ortholog(s) have role in fatty acid beta-oxidation, long-chain fatty acid catabolic process and peroxisome localization	-0.534771916510808	1.13052072581465
Stress Response	*RTA1**	Putative protein involved in 7-aminocholesterol resistance; gene is upregulated in azole-resistant strain	0.800609735652182	0.512744655158017
	*RAD14**	Ortholog(s) have damaged DNA binding, zinc ion binding activity and role in UV-damage excision repair, nucleotide-excision repair involved in interstrand cross-link repair, nucleotide-excision repair, DNA damage recognition	0.519884530303784	-0.534357546223619
	SSA3	Heat shock protein of the HSP70 family	-0.546692614140337	0.061620651017944
Nitrogen Metabolism	*PUT1**	Ortholog(s) have proline dehydrogenase activity, role in proline catabolic process to glutamate and mitochondrion localization	0.567275883582426	0.718766975891521
	MEP2	Ortholog(s) have high-affinity secondary active ammonium transmembrane transporter activity, methylammonium transmembrane transporter activity	-0.501876805164572	-0.0395670392027533

Table 5.1 (continued)

Functional Group	*C. glabrata* gene	Description	Log2 Fold Change WT FLC/WT control	Log2 Fold Change *Δcgrpn4* FLC/WT FLC
Carbon Metabolism	*PBI1**	Has domain(s) with predicted alcohol O-acetyltransferase activity and role in alcohol metabolic process	2.11441995123868	-1.92702652396821
	ATF2	Putative alcohol acetyltransferase involved in steroid detoxification; gene is upregulated in azole-resistant strain	0.70489628545683	-0.085334156678901
	*MLS1**	Ortholog(s) have malate synthase activity, role in acetate catabolic process, carbon utilization, fatty acid catabolic process, glyoxylate cycle and cytosol, glyoxysome, peroxisomal matrix localization	-0.530330935809311	0.739309139898255
Heme Biosynthesis	*HEM13**	Putative coproporphyrinogen III oxidase; protein differentially expressed in azole resistant strain	0.813076641463864	-0.670576605446651
	*HEM14**	Ortholog(s) have oxygen-dependent protoporphyrinogen oxidase activity, role in heme biosynthetic process and cytosol, mitochondrial inner membrane, nucleus localization	0.505151454333066	-0.695404641555594
	HMX1	Ortholog(s) have heme oxygenase (decyclizing) activity and role in cellular iron ion homeostasis, heme catabolic process, response to carbon monoxide, response to oxidative stress	-0.621061038857654	0.401565692370932
Cytoskeleton/Cell Cycle	*MSC7**	Ortholog(s) have role in reciprocal meiotic recombination and cytosol, endoplasmic reticulum, nucleus localization	0.88054792573548	-0.561596954228106
	NCE102	Ortholog(s) have role in actin cytoskeleton organization, eisosome assembly, establishment of protein localization to plasma membrane and negative regulation of protein phosphorylation, more	-0.547180919885947	0.426339595940746
	XBP1	Ortholog(s) have RNA polymerase II transcription factor activity, sequence-specific DNA binding, sequence-specific DNA binding activity	-0.694187016460997	0.473496054788794
	FMP45	Ortholog(s) have role in ascospore formation, cellular response to drug, fungal-type cell wall organization	-0.694187016460997	0.473496054788794
Mitochondrial Function	*COX26*	Ortholog(s) have mitochondrial respiratory chain complex IV, mitochondrial respiratory chain supercomplex localization	-0.63654948489126	0.124886776789974

Table 5.1 (continued)

Functional Group	*C. glabrata* gene	Description	Log2 Fold Change WT FLC/WT control	Log2 Fold Change *Δcgrpn4* FLC/WT FLC
Intracellular Traffic	*SRO7*	Ortholog(s) have Rab GTPase binding, SNARE binding activity and role in Golgi to plasma membrane transport, establishment of cell polarity, exocytosis, small GTPase mediated signal transduction	0.51380411792187	-0.0930282859186249
Unknown Function	*CAGL0M11660g**	Has domain(s) with predicted hydrolase activity	0.670671422559619	1.8125003048173
	*CAGL0G05632g**	Ortholog(s) have cytoplasm localization	-0.523893660022717	1.31525996174904
	*CAGL0K07337g**	Has domain(s) with predicted ion channel activity, role in ion transport and membrane localization	-0.633965284293892	0.660851633708788
	CAGL0A02277g	Protein of unknown function	-0.720087658281874	-0.106089387352821
	PET10	Ortholog(s) have lipid particle localization	-0.508798062098661	0.451013041160858
	MUP1	Protein of unknown function	-0.78025533259467	0.47428016797802
	SET4	Ortholog of *S. cerevisiae*: SET4 and *Saccharomyces cerevisiae* S288C: YJL105W	1.13502760003117	-0.296340043389294
	CAGL0L06776g	Has domain(s) with predicted sequence-specific DNA binding, transcription factor activity, sequence-specific DNA binding, zinc ion binding activity and role in regulation of transcription, DNA-templated	0.850825419903001	0.334126851565994
	CAGL0L08547g	Protein of unknown function	0.760275028834271	-0.0473638381153255
	CAGL0J00297g	Ortholog(s) have endoplasmic reticulum localization	0.630612006308276	-0.408271101001385
	CAGL0G00594g	Ortholog(s) have Golgi apparatus, endoplasmic reticulum localization	0.614359514487176	-0.30789676277002

As expected, expression of the multidrug resistance transporter encoding gene *CgCDR1*, a well-known biomarker of azole resistance [49–51], is upregulated 1.75-fold in fluconazole-challenged cells. Additionally, 41% of the upregulated genes are related to sterol metabolism, including components of the ergosterol biosynthetic pathway (*CgERG1*, *CgERG2*, *CgERG3*, *CgERG4*, *CgERG5*, *CgERG6*), and the azole target *CgERG11*. Upregulation of *ERG11* in response to azole stress in *C. glabrata* and other *Candida* species has been reported previously [52–55], as well as the upregulation of additional *ERG* genes in cases of azole resistance [56,57]. Two more genes with predicted roles in ergosterol biosynthesis, namely *CgHES1* and *CgCYB5*, are also present in this group. Upregulation of the ergosterol pathway is therefore a likely core response to mild fluconazole stress.

Genes in other functional classes are both up- and downregulated. For example, in the cluster of Lipid and Fatty Acid Metabolism, genes related to reduction/oxidation processes are downregulated (ORF *CAGL0A03740g* and *CgHBN1*), while a gene with a potential role in fatty acid metabolism during heme-depleted conditions is upregulated (*CgCSR1*). Additionally, the upregulated genes in Carbon Metabolism are related to alcohol metabolic processes: *CgPBI1* (*S. cerevisiae* homolog is induced during ketoconazole stress [58]); and *CgATF2*, previously reported to be upregulated in an azole-resistant strain [12]. Within the Stress Response cluster, the *CgRTA1* gene is upregulated, which is consistent with its expression being induced in azole resistant strains [12]. On the other hand, the heat shock protein encoding gene *CgSSA3* is downregulated. In turn, genes involved in the heme biosynthetic pathway are upregulated (*CgHEM13* and *CgHEM14*), while a gene involved in heme degradation is downregulated (*CgHMX1*). This profile suggests that the increased synthesis of heme, a vital prosthetic group of CgErg11, may be required to accompany the increased expression of CgErg11, aiming the increased levels of functional CgErg11 molecules.

5.4.3 Role of CgRpn4 in the transcriptome-wide changes occurring in response to fluconazole in *C. glabrata*

In order to study the role of CgRpn4 in the response of *C. glabrata* to fluconazole, gene expression changes occurring upon fluconazole exposure in the Δ*cgrpn4* mutant strain were compared to those observed in the wild-type strain. The expression of 80 genes

was found to be activated by CgRpn4, while 132 were found to be repressed, possibly in an indirect fashion, upon fluconazole exposure (Supplementary Table S5.2). The most prevalent functional groups activated by CgRpn4 include Proteasome and Ubiquitination, Lipid and Fatty Acid Metabolism, and Stress Response (Figure 5.2A); whereas repressed genes are enriched in Cell Wall Organization and Carbon Metabolism (Figure 5.2B).

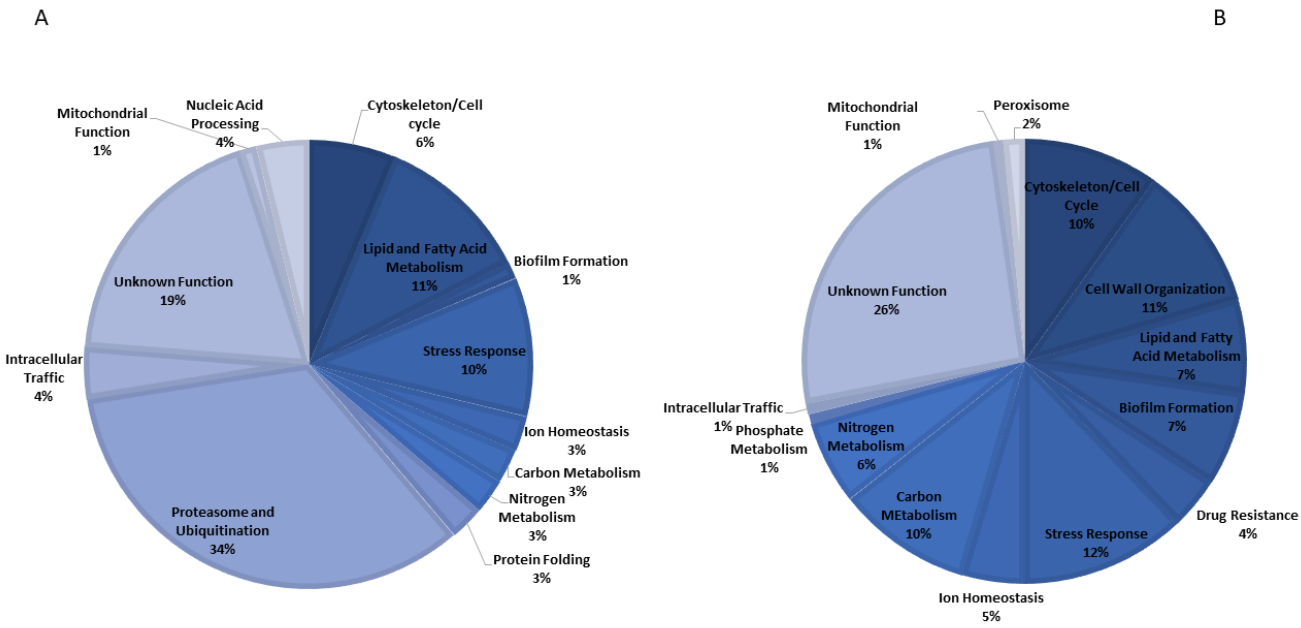

Figure 5.2 – *CgRPN4* regulated functional groups. Differentially expressed genes in exponential-phase KUE100_*Δcgrpn4 C. glabrata* cells, comparing to KUE100 cells, after 1h fluconazole exposure. (A) CgRpn4-activated genes (downregulated in the mutant strain). (B) CgRpn4-repressed genes (upregulated in the mutant strain).

The comparison of this regulon with differentially expressed genes in fluconazole-challenged wild-type cells enabled the identification of 18 genes that respond to fluconazole only when *CgRPN4* is present (Table 5.1). The most enriched functional group in this set comprises genes from the ergosterol biosynthetic pathway, namely *CgERG1*, *CgERG2*, *CgERG3* and *CgERG11*. A putative gene involved in regulation of ergosterol synthesis in *S. cerevisiae* (*HES1*) [59,60] is also found in this set. Interestingly, two genes involved in heme biosynthesis are also present: *CgHEM13* and *CgHEM14*. As described previously, heme is a key prosthetic group of several ergosterol biosynthesis enzymes, and increased CgHem13 protein levels were detected

in an azole resistant strain, concurrently with CgErg11 [51]. It is important to note that upregulation of ergosterol biosynthesis is the most dramatic response to fluconazole stress and that CgRpn4 functions as an activator of ergosterol and heme biosynthesis (Figure 5.3). Moreover, the activation of *ERG* and *HEM* genes constitutes a specific role of this TF during fluconazole stress, as CgRpn4 does not regulate their basal expression (Supplementary Table S5.3). Altogether, these data indicate that activation of the ergosterol biosynthetic pathway, mediated by CgRpn4, could be a major regulatory mechanism of azole antifungal resistance. Furthermore, Erg1 and Erg2 may influence resistance phenotypes, as they are targeted by other antifungals. Allylamines and thiocarbamates inhibit Erg1, whereas morpholines inhibit Erg2 [61]. The latter also inhibits the function of Erg24 [61] (*CAGL0I02970g*), which is upregulated in wild-type cells during fluconazole stress.

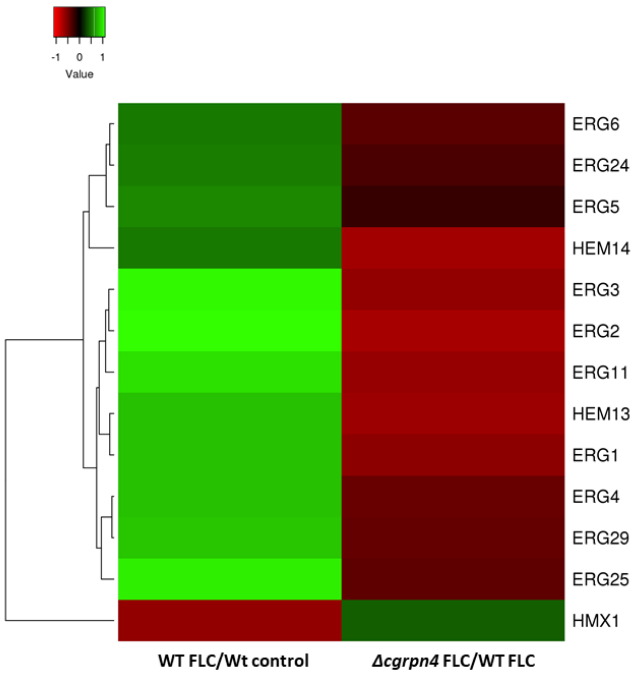

Figure 5.3 – Comparison of ergosterol and heme related genes expression patterns in wild-type and *Δcgrpn4* cells upon fluconazole stress. Expression profiles of differentially expressed *ERG* and *HEM* genes in at least one dataset. *C. glabrata* genes names are shown. In cases were no gene name has been assigned, the designation of their *S. cerevisiae* homolog is shown.

CgRpn4 was found to regulate expression of several additional genes irrespective of fluconazole treatment. The largest functional group includes Proteasome and Ubiquitination genes. This group comprises exclusively genes activated by CgRpn4, in

accordance with its role in both *C. albicans* and *S. cerevisiae* as an activator of proteasome genes [20,21,62]. *ScRPN4* is transcriptionally regulated under various stresses and ScRpn4 levels are also controlled by proteasome activity in a negative feedback loop [20]. The high enrichment of proteasome subunit-encoding genes in the CgRpn4 regulon strongly indicates that its physiological function is conserved with other species.

The functional group of cellular response to stress consists of genes involved in several stressful conditions, possibly representing responses activated by additional stress pathways other than fluconazole. Among the genes activated by CgRpn4 is *CAGL0L10186g*, a putative stress-induced gene upregulated in an azole-resistant strain [12], whose *S. cerevisiae* homolog (*ScTMC1*) is a stress-inducible transcriptional target of ScRpn4 [63]. Genes activated in the absence of CgRpn4 include typical stress response genes, such as the heat shock protein encoding *CgHSP12* and the calcineurin regulator *CgRCN2*. Transcription factors known to regulate the expression of stress response genes in either *S. cerevisiae* or *C. albicans*, such as the general stress regulator *MSN4* [64,65], the weak acid regulator *MNL1/COM2* [66,67] and alkaline pH-response regulator *RIM101* [68,69], are also expressed in the absence of CgRpn4. This suggests that CgRpn4 can affect several stress response networks. Interestingly, genes involved in oxidative stress resistance are also upregulated by CgRpn4 (*CgTSA1*, *CgSOD2*, *CgTRR1*).

Genes encoding five multidrug resistance transporters are repressed by CgRpn4: the MFS transporters encoded by *CAGL0L10912g*, *CAGL0B02343g*, *CgTPO1_1* and *CgQDR2*; as well as the ABC transporter *CgYOR1*. From these, *CgYOR1*, *CgTPO1_1* and *CgQDR2* have been implicated in azole resistance [11,12,15]. This indicates that CgRpn4 does not activate the expression of drug transporters, reinforcing its role as an activator of ergosterol biosynthesis as the main mechanism of fluconazole resistance.

5.4.4 CgRpn4 is activated upon fluconazole stress, leading to its nuclear accumulation

In order to examine possible CgRpn4 activation mechanisms, we investigated its subcellular localization. CgRpn4 was fused to GFP and expressed via the

pGREG576_MTI_*CgRPN4* plasmid in *C. glabrata* cells grown to mid-exponential phase in basal medium supplemented with 50 µM Cu_2SO_4 to induce fusion-protein expression, and then transferred to fresh medium (control) or to fresh medium containing 150 mg/L fluconazole. After 1h of incubation, cells were inspected through fluorescence microscopy.

In untreated *C. glabrata* cells, the CgRpn4_GFP fusion protein is distributed throughout the whole cell, with a stronger signal in the nucleus (Figure 5.4A). After fluconazole stress, an enrichment of nuclear localization was observed (Figure 5.4B). Fluconazole treatment therefore changes the relative distribution of CgRpn4 to the nucleus. Activation of its target genes could be partially dependent on translocation of the transcription factor.

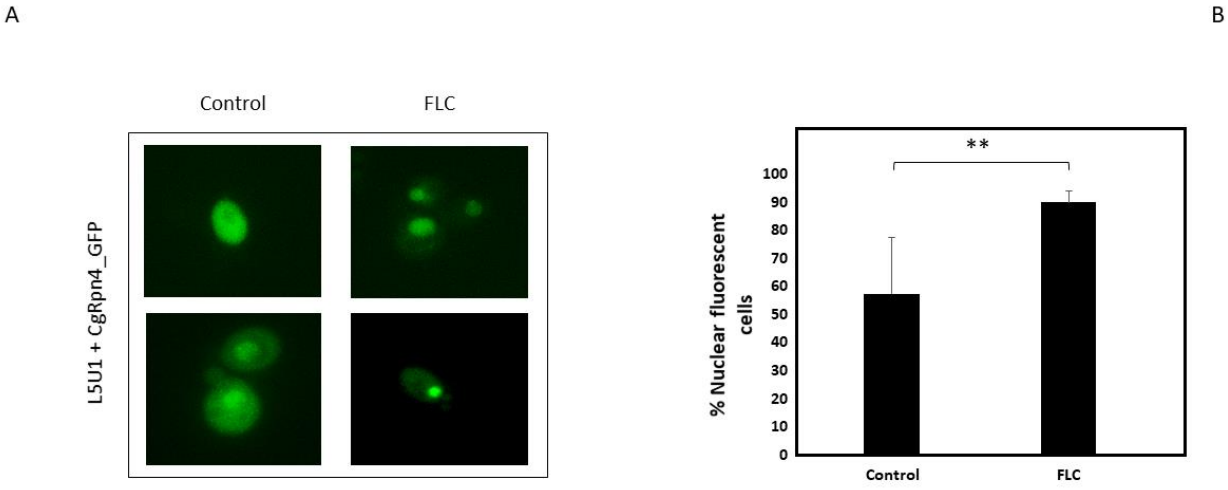

Figure 5.4 – CgRpn4 increases its relative distribution to the nucleus upon fluconazole stress. Assessment of the subcellular localization of fluorescence in exponential-phase L5U1 *C. glabrata* cells harboring the pGREG576_MTI_*CgRPN4* plasmid after 5h of recombinant protein production in control conditions or after 1h fluconazole exposure. (A) Representative images of CgRpn4_GFP localization in L5U1 *C. glabrata* cells. (B) Results are shown in the percentage of cells showing nuclear localization of the CgRpn4_GFP fusion protein. Error bars represent the corresponding standard deviation. **p<0.01.

5.4.5 *CgRPN4* plays a role in the maintenance of ergosterol levels, membrane permeability and fluconazole accumulation

Transcriptomics analysis of the KUE100 wild-type *C. glabrata* strain during fluconazole stress revealed a significant activation of the ergosterol biosynthesis pathway mediated by CgRpn4. This led us to hypothesize that CgRpn4 may contribute to preserve ergosterol levels in *C. glabrata* during upon fluconazole exposure.

C. glabrata cells were grown to mid-exponential phase and transferred to fresh medium (control) or to fresh medium containing 150 mg/L fluconazole. After 3h and 6h of incubation, cells were collected, total ergosterol was extracted and its levels quantified by High-Performance Liquid Chromatography (HPLC).

Deleting *CgRPN4* does not affect ergosterol levels in untreated cells (Figure 5.5A). Following exposure to fluconazole for 3h and 6h, the levels of ergosterol are reduced in both wild-type and deletion strains (Figure 5.5A). However, ergosterol levels in the Δ*cgrpn4* mutant are significantly lower than the wild-type strain during fluconazole treatment, indicating that CgRpn4 is necessary to maintain ergosterol levels upon fluconazole exposure (Figure 5.5A). Therefore, the activation of ergosterol biosynthesis genes during fluconazole stress may be part of a compensatory mechanism to counteract ergosterol synthesis targeted by the antifungal. Moreover, these results show that CgRpn4, through transcriptional regulation of the ergosterol biosynthesis pathway, has a measurable effect on ergosterol levels during fluconazole stress, which contributes to antifungal tolerance. Similar mechanisms have been reported in *C. albicans*, where fluconazole tolerant strains present higher levels of intermediate metabolites of sterol biosynthetic pathway and ergosterol ester, which was associated with the upregulation of ergosterol biosynthetic pathway genes [70]. Furthermore, reduction in the content of sphingolipids or ergosterol results in enhanced susceptibility to drugs [71–73].

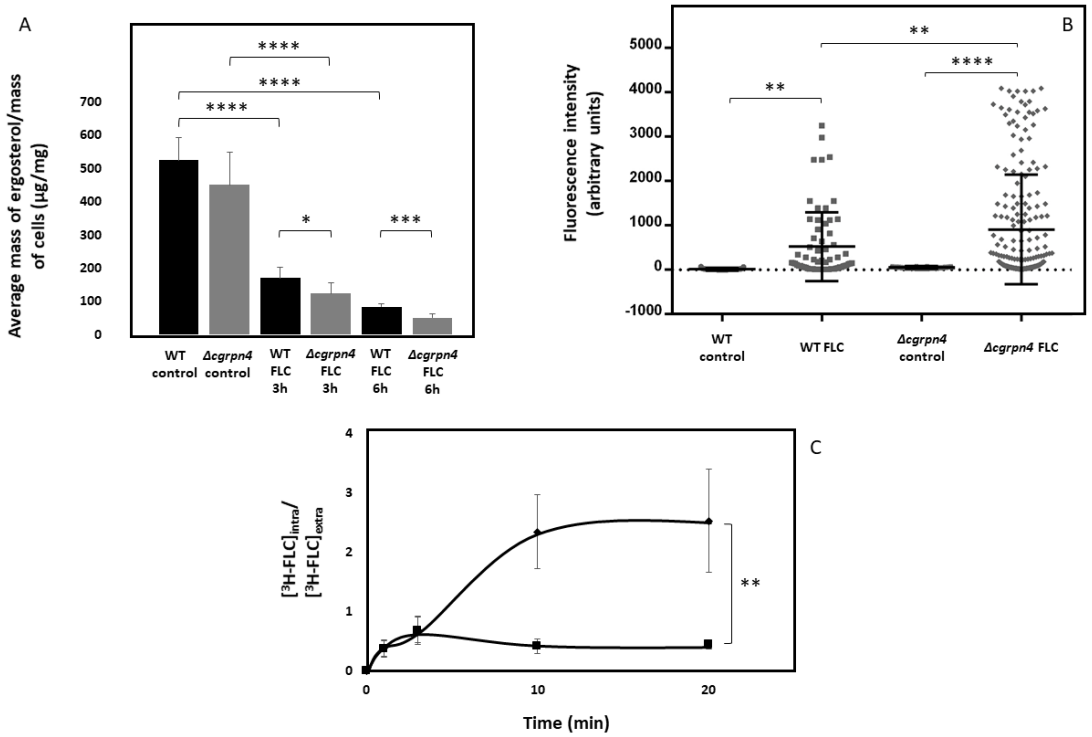

Figure 5.5 – CgRpn4 regulates ergosterol levels in *C. glabrata* cells during fluconazole stress, affecting permeability and drug accumulation. (A) KUE100 and KUE100_*Δcgrpn4 C. glabrata* cells were harvested after 15h of growth in YPD medium (control) or after 3h or 6h fluconazole stress. Ergosterol was extracted and quantified through HPLC. Cholesterol was used as an internal standard to evaluate yield of the ergosterol extraction. The displayed ergosterol content is representative of at least six independent experiments. Error bars represent the correspondent standard deviations. (B) Comparison of plasma membrane permeability of exponential-phase KUE100 (squares), KUE100_*Δcgrpn4* (diamonds) in control conditions or upon 1h fluconazole stress. The estimation of plasma membrane permeability is based on the fluorescence intensity values exhibited by yeast cells upon passive accumulation of propidium iodide. Error bars represent the corresponding standard deviation. (C) Time-course accumulation of radiolabeled ^{3}H-fluconazole in strains KUE100 (squares) and KUE100_*Δcgrpn4* (diamonds), during cultivation in liquid BM in the presence of 150 mg/L unlabeled fluconazole. Accumulation values are the average of at least three independent experiments. Error bars represent the corresponding standard deviations. *p<0.05, **p<0.01, ***p<0.001, ****p<0.0001.

Cell permeability in response to fluconazole was investigated using the fluorescent probe propidium iodide (PI), and the possible participation of CgRpn4 was evaluated. Upon 1h exposure to fluconazole, *C. glabrata* cell permeability increases significantly (Figure 5.5B). This observation is probably related to the inhibition of CgErg11 by fluconazole, resulting in the accumulation of the toxic sterol DMCDD that permeabilizes the plasma [74,75]. Permeability of untreated *Δcgrpn4* cells is not significantly different to wild-type. However, the permeability of *Δcgrpn4* cells significantly higher than the wild-type strain following fluconazole stress (Figure 5.5B). This data indicates that fluconazole increases *C. glabrata* cell permeability and that

CgRpn4 contributes to control its maintenance during fluconazole exposure, presumably by the upregulation of ergosterol biosynthesis.

The role of *CgRPN4* in ergosterol biosynthesis and plasma membrane permeability led us to investigate if this could be related with the increased azole susceptibility observed in the *Δcgrpn4* mutant. Consistent with the observed susceptibility and cell permeability phenotypes, the *Δcgrpn4* deletion mutant was found to accumulate 2.5-fold more radiolabeled fluconazole than the wild-type strain after 20 minutes of exposure to the antifungal (Figure 5.5C). These results suggest that CgRpn4 activity mediates *C. glabrata* resistance toward fluconazole by reducing its intracellular accumulation in yeast cells, possibly as a result of its regulation of ergosterol levels and membrane permeability.

5.4.6 Determination of promoter recognition motifs by CgRpn4 and direct regulation over *CgERG11* expression

In order to identify possible CgRpn4 DNA recognition sites and directly regulated target genes, the promoters of CgRpn4-activated genes during fluconazole stress were searched for enriched motifs using DREME [47]. Excluding TATA-box sequences, 4 overrepresented motifs were found (Figure 5.6A). Interestingly, one of the identified motifs (TGGCAAA) is identical to a core region of the ScRpn4 and CaRpn4 consensus (GGTGGCAAA and GAAGGCAAAA, respectively) found in promoters of proteasome genes [21,62]. This indicates that there is a high level of conservation in the promoter sequences recognized by Rpn4 across these species.

We found a near identical motif (TTGCAAA) located at positions -363 to -356 (Figure 5.6B) of *CgERG11*. To determine if this motif is required for CgRpn4-dependent activation of *CgERG11*, the *lacZ* reporter gene was placed downstream of the *CgERG11* promoter and site-directed mutagenesis was used to disrupt the putative binding site.

Upon 1h of fluconazole exposure, *lacZ* expression driven by *CgERG11* promoter increases 2-fold in comparison to control conditions (Figure 5.6C), which is in accordance with our transcriptomics data. When the motif TTGCAAA in the *CgERG11* promoter is disrupted, *lacZ* expression is significantly reduced in comparison to the wild-type promoter, even more so after fluconazole exposure (Figure 5.6C). These

results indicate that the identified motif is required for *CgERG11* basal expression and especially *CgERG11* activation during fluconazole stress, thus establishing a direct link between CgRpn4 regulatory control and ergosterol biosynthetic pathway gene expression.

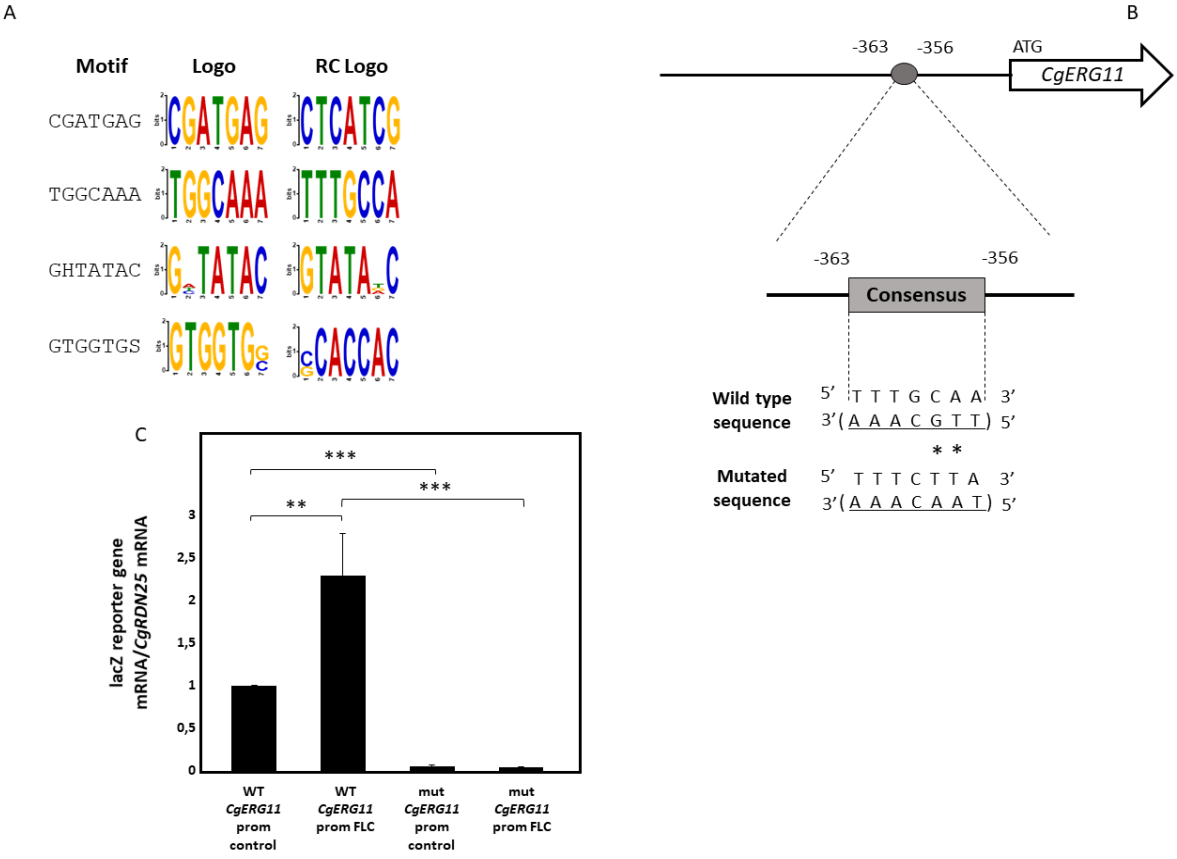

Figure 5.6 – Overrepresented sequences in the promoters of CgRpn4-activated genes and possible CgRpn4 recognition sequence. (A) Motifs found to be overrepresented in the promoters of CgRpn4-activated genes, as found by the DREME tool. Sequences located upstream (-1000 to -1 bp) of the genes found to be activated by CgRpn4 were retrieved from PathoYeastract and submitted to DREME. The prediction was made with default parameters. The sequences shown correspond to the motifs outputted by DREME, excluding TATA-box motifs. (B) The putative CgRpn4 recognition sequence in the promoter of *CgERG11* is in the complementary strand. The numbers refer to the position of the consensus site relative to the first ATG of the coding region. The wild-type sequence is shown underlined below the box, with asterisks denoting the base substitutions generated by site-directed mutagenesis. Below the resulting mutated sequence is shown. (C) Comparison of the variation of lacZ transcript levels determined by RT-PCR in L5U1 cells harboring the pYEP354_*CgERG11*prom_lacZ or pYEP354_mut_*CgERG11*prom_lacZ plasmids in control conditions or after 1h fluconazole exposure. Transcript levels of *CgRDN25* were used for normalization. Expression values are the average of at least three independent experiments. Error bars represent the corresponding standard deviations. **p<0.01, ***p<0.001.

Chapter 5

Here we show the role of the transcription factor CgRpn4 in mediating fluconazole resistance in *C. glabrata*. Through transcriptional control over the ergosterol biosynthesis pathway, CgRpn4 regulates ergosterol levels in the plasma membrane, thus affecting cell permeability and fluconazole accumulation. Additionally, CgRpn4 exerts direct control over *CgERG11* expression, reinforcing its role as a relevant player in *C. glabrata* fluconazole resistance, which is likely conserved among other yeast species. Based on these results, we propose CgRpn4 as a promising target to tackle acquisition of azole drug resistance.

5.5 Acknowledgements

We acknowledge John Bennett from the National Institute of Allergy and Infectious Diseases, NIH, Bethesda, USA, for kindly providing the L5U1 strain. This work was supported by “Fundação para a Ciência e a Tecnologia” (FCT) [Contracts PTDC/BBB-BIO/4004/2014 and PTDC/BII-BIO/28216/2017, PhD grants to PP and MG and post-doctoral grant to CC].

Funding received by iBB-Institute for Bioengineering and Biosciences from FCT-Portuguese Foundation for Science and Technology (UID/BIO/04565/2013) and from Programa Operacional Regional de Lisboa 2020 (Project N. 007317) is acknowledged. This study was partly supported by a Joint Usage/Research Program of the Medical Mycology Research Center, Chiba University.

5.6 References

1. Azie, N.; Neofytos, D.; Pfaller, M.; Meier-Kriesche, H.-U.; Quan, S.P.; Horn, D. The PATH (Prospective Antifungal Therapy) Alliance® registry and invasive fungal infections: update 2012. *Diagn. Microbiol. Infect. Dis.* **2012**, *73*, 293–300.

2. Wisplinghoff, H.; Bischoff, T.; Tallent, S.M.; Seifert, H.; Wenzel, R.P.; Edmond, M.B. Nosocomial Bloodstream Infections in US Hospitals: Analysis of 24,179 Cases from a Prospective Nationwide Surveillance Study. *Clin. Infect. Dis.* **2004**, *39*, 309–317.

3. Edmond, M.B.; Wallace, S.E.; McClish, D.K.; Pfaller, M.A.; Jones, R.N.; Wenzel, R.P. Nosocomial bloodstream infections in United States hospitals: a three-year analysis. *Clin. Infect. Dis.* **1999**, *29*, 239–244.

4. Khatib, R.; Johnson, L.B.; Fakih, M.G.; Riederer, K.; Briski, L. Current trends in candidemia and species distribution among adults: *Candida glabrata* surpasses *C. albicans* in diabetic patients and abdominal sources. *Mycoses* **2016**, *59*, 781–786.

5. Petrikkos, G.; Skiada, A. Recent advances in antifungal chemotherapy. *Int. J. Antimicrob. Agents* **2007**, *30*, 108–117.

6. Nakayama, H.; Nakayama, N.; Arisawa, M.; Aoki, Y. In Vitro and In Vivo Effects of 14alpha -Demethylase (*ERG11*) Depletion in *Candida glabrata*. *Antimicrob. Agents Chemother.* **2001**, *45*, 3037–3045.

7. Debnath, S.; Addya, S. Structural basis for heterogeneous phenotype of *ERG11* dependent Azole resistance in *C.albicans* clinical isolates. *Springerplus* **2014**, *3*, 660.

8. Revie, N.M.; Iyer, K.R.; Robbins, N.; Cowen, L.E. Antifungal drug resistance: evolution, mechanisms and impact. *Curr. Opin. Microbiol.* **2018**, *45*, 70–76.

9. Ghannoum, M.A.; Rice, L.B. Antifungal agents: mode of action, mechanisms of resistance, and correlation of these mechanisms with bacterial resistance. *Clin. Microbiol. Rev.* **1999**, *12*, 501–17.

10. Vermitsky, J.P.; Edlind, T.D. Azole resistance in *Candida glabrata*: coordinate upregulation of multidrug transporters and evidence for a Pdr1-like transcription factor. *Antimicrob. Agents Chemother.* **2004**, *48*, 3773–3781.

11. Costa, C.; Pires, C.; Cabrito, T.R.; Renaudin, A.; Ohno, M.; Chibana, H.; Sá-Correia, I.; Teixeira, M.C. *Candida glabrata* drug: H+antiporter CgQdr2 confers imidazole drug resistance, being activated by transcription factor CgPdr1. *Antimicrob. Agents Chemother.* **2013**, *57*, 3159-3167.

12. Vermitsky, J.P.; Earhart, K.D.; Smith, W.L.; Homayouni, R.; Edlind, T.D.; Rogers, P.D. Pdr1 regulates multidrug resistance in *Candida glabrata*: gene disruption and genome-wide expression studies. *Mol. Microbiol.* **2006**, *61*, 704–722.

13. Caudle, K.E.; Barker, K.S.; Wiederhold, N.P.; Xu, L.; Homayouni, R.; Rogers, P.D. Genomewide expression profile analysis of the *Candida glabrata* Pdr1 regulon. *Eukaryot. Cell* **2011**, *10*, 373–83.

14. Tsai, H.F.; Krol, A.A.; Sarti, K.E.; Bennett, J.E. *Candida glabrata PDR1*, a Transcriptional Regulator of a Pleiotropic Drug Resistance Network, Mediates Azole Resistance in Clinical Isolates and Petite Mutants. *Antimicrob. Agents Chemother.* **2006**, *50*, 1384–1392.

15. Pais, P.; Costa, C.; Pires, C.; Shimizu, K.; Chibana, H.; Teixeira, M.C. Membrane Proteome-Wide Response to the Antifungal Drug Clotrimazole in *Candida glabrata*: Role of the Transcription Factor CgPdr1 and the Drug:H+ Antiporters CgTpo1_1 and CgTpo1_2. *Mol. Cell. Proteomics* **2016**, *15*, 57–72.

16. Coste, A.; Turner, V.; Ischer, F.; Morschhäuser, J.; Forche, A.; Selmecki, A.; Berman, J.; Bille, J.; Sanglard, D. A mutation in Tac1p, a transcription factor regulating *CDR1* and *CDR2*, is coupled with loss of heterozygosity at chromosome 5 to mediate antifungal resistance in *Candida albicans*. *Genetics* **2006**, *172*, 2139–2156.

17. Coste, A.; Selmecki, A.; Forche, A.; Diogo, D.; Bougnoux, M.E.; D'Enfert, C.; Berman, J.; Sanglard, D. Genotypic evolution of azole resistance mechanisms in sequential *Candida albicans* isolates. *Eukaryot. Cell* **2007**, *6*, 1889–1904.

18. Coste, A.T.; Karababa, M.; Ischer, F.; Bille, J.; Sanglard, D. *TAC1*, Transcriptional Activator of *CDR* Genes, Is a New Transcription Factor Involved in the Regulation of *Candida albicans* ABC Transporters *CDR1* and *CDR2*. *Eukaryot. Cell* **2004**, *3*, 1639–1652.

19. Pais, P.; Costa, C.; Cavalheiro, M.; Romão, D.; Teixeira, M.C. Transcriptional Control of Drug Resistance, Virulence and Immune System Evasion in Pathogenic Fungi: A Cross-Species Comparison. *Front. Cell. Infect. Microbiol.* **2016**, *6*, 131.

20. Xie, Y.; Varshavsky, A. *RPN4* is a ligand, substrate, and transcriptional regulator of the 26S proteasome: A negative feedback circuit. *Proc. Natl. Acad. Sci.* **2001**, *98*, 3056–3061.

21. Mannhaupt, G.; Schnall, R.; Karpov, V.; Vetter, I.; Feldmann, H. Rpn4p acts as a transcription factor by binding to PACE, a nonamer box found upstream of 26S proteasomal and other genes in yeast. *FEBS Lett.* **1999**, *450*, 27–34.

22. Owsianik, G.; Balzi l, L.; Ghislain, M. Control of 26S proteasome expression by transcription factors regulating multidrug resistance in *Saccharomyces cerevisiae*. *Mol. Microbiol.* **2002**, *43*, 1295–308.

23. Johnson, E.S.; Ma, P.C.; Ota, I.M.; Varshavsky, A. A proteolytic pathway that recognizes ubiquitin as a degradation signal. *J. Biol. Chem.* **1995**, *270*, 17442–17456.

24. Schmidt, R.M.; Schessner, J.P.; Borner, G.H.; Schuck, S. The proteasome biogenesis regulator Rpn4 cooperates with the unfolded protein response to promote ER stress resistance. *Elife* **2019**, *8*, e43244.

25. Teixeira, M.C.; Dias, P.J.; Monteiro, P.T.; Sala, A.; Oliveira, A.L.; Freitas, A.T.; Sá-Correia, I. Refining current knowledge on the yeast *FLR1* regulatory network by combined experimental and computational approaches. *Mol. Biosyst.* **2010**, *6*, 2471-2481.

26. Teixeira, M.C.; Dias, P.J.; Simões, T.; Sá-Correia, I. Yeast adaptation to mancozeb involves the up-regulation of *FLR1* under the coordinate control of Yap1, Rpn4, Pdr3, and Yrr1. *Biochem. Biophys. Res. Commun.* **2008**, *367*, 249–255.

27. Parsons, A.B.; Brost, R.L.; Ding, H.; Li, Z.; Zhang, C.; Sheikh, B.; Brown, G.W.; Kane, P.M.; Hughes, T.R.; Boone, C. Integration of chemical-genetic and genetic interaction data links bioactive compounds to cellular target pathways. *Nat. Biotechnol.* **2004**, *22*, 62–69.

28. Kapitzky, L.; Beltrao, P.; Berens, T.J.; Gassner, N.; Zhou, C.; Wüster, A.; Wu, J.; Babu, M.M.; Elledge, S.J.; Toczyski, D.; *et al.* Cross-species chemogenomic profiling reveals evolutionarily conserved drug mode of action. *Mol. Syst. Biol.* **2010**, *6*, 451.

29. Hoepfner, D.; Helliwell, S.B.; Sadlish, H.; Schuierer, S.; Filipuzzi, I.; Brachat, S.; Bhullar, B.; Plikat, U.; Abraham, Y.; Altorfer, M.; *et al.* High-resolution chemical dissection of a model eukaryote reveals targets, pathways and gene functions. *Microbiol. Res.* **2014**, *169*, 107–120.

30. Homann, O.R.; Dea, J.; Noble, S.M.; Johnson, A.D. A phenotypic profile of the *Candida albicans* regulatory network. *PLoS Genet.* **2009**, *5*, e1000783.

31. Ueno, K.; Uno, J.; Nakayama, H.; Sasamoto, K.; Mikami, Y.; Chibana, H. Development of a highly efficient gene targeting system induced by transient repression of *YKU80* expression in *Candida glabrata*. *Eukaryot. Cell* **2007**, *6*, 1239–1247.

32. Chen, K.H.; Miyazaki, T.; Tsai, H.F.; Bennett, J.E. The bZip transcription factor Cgap1p is involved in multidrug resistance and required for activation of multidrug transporter gene *CgFLR1* in *Candida glabrata*. *Gene* **2007**, *386*, 63–72.

33. Jansen, G.; Wu, C.; Schade, B.; Thomas, D.Y.; Whiteway, M. Drag&Drop cloning in yeast. *Gene* **2005**, *344*, 43–51.

34. Ueno, K.; Matsumoto, Y.; Uno, J.; Sasamoto, K.; Sekimizu, K.; Kinjo, Y.; Chibana, H. Intestinal resident yeast *Candida glabrata* requires Cyb2p-Mediated lactate assimilation to adapt in mouse intestine. *PLoS One* **2011**, *6*, e24759.

35. Costa, C.; Henriques, A.; Pires, C.; Nunes, J.; Ohno, M.; Chibana, H.; Sá-Correia, I.; Teixeira, M.C. The dual role of *Candida glabrata* drug:H+ antiporter CgAqr1 (ORF *CAGL0J09944g*) in antifungal drug and acetic acid resistance. *Front. Microbiol.* **2013**, *4*, 170.

36. Costa, C.; Nunes, J.; Henriques, A.; Mira, N.P.; Nakayama, H.; Chibana, H.; Teixeira, M.C. *Candida glabrata* drug:H+antiporter CgTpo3 (ORF *CAGL0I10384g*): Role in azole drug resistance and polyamine homeostasis. *J. Antimicrob. Chemother.* **2014**, *69*, 1767–1776.

37. Romão, D.; Cavalheiro, M.; Mil-Homens, D.; Santos, R.; Pais, P.; Costa, C.; Takahashi-Nakaguchi, A.; Fialho, A.M.; Chibana, H.; Teixeira, M.C. A New Determinant of *Candida glabrata* Virulence: The Acetate Exporter CgDtr1. *Front. Cell. Infect. Microbiol.* **2017**, *7*, 473.

38. Pais, P.; Pires, C.; Costa, C.; Okamoto, M.; Chibana, H.; Teixeira, M.C. Membrane proteomics analysis of the *Candida glabrata* response to 5-flucytosine: Unveiling the role and regulation of the drug efflux transporters CgFlr1 and CgFlr2. *Front. Microbiol.* **2016**, *7*, 2045.

39. Zordan, R.E.; Ren, Y.; Pan, S.J.; Rotondo, G.; Peñas, A.D. Las; Iluore, J.; Cormack, B.P. Expression Plasmids for Use in *Candida glabrata*. *G3(Bethesda)* **2013**, *3*, 1675–1686.

40. Jiang, H.; Lei, R.; Ding, S.W.; Zhu, S. Skewer: a fast and accurate adapter trimmer for next-generation sequencing paired-end reads. *BMC Bioinformatics* **2014**, *15*, 182.

41. Trapnell, C.; Pachter, L.; Salzberg, S.L. TopHat: Discovering splice junctions with RNA-Seq. *Bioinformatics* **2009**, *25*, 1105–1111.

42. Anders, S.; Huber, W. Differential expression analysis for sequence count data. *Genome Biol.* **2010**, *11*, R106.

43. Love, M.I.; Huber, W.; Anders, S. Moderated estimation of fold change and dispersion for RNA-seq data with DESeq2. *Genome Biol.* **2014**, *15*, 550.

44. Gong, P.; Guan, X.; Witter, E. A rapid method to extract ergosterol from soil by physical disruption. *Appl. Soil Ecol.* **2001**, *17*, 285–289.

45. Rosa, M.F.; Sá-Correia, I. Intracellular acidification does not account for inhibition of *Saccharomyces cerevisiae* growth in the presence of ethanol. *FEMS Microbiol. Lett.* **1996**, *135*, 271–274.

46. Monteiro, P.T.; Pais, P.; Costa, C.; Manna, S.; Sá-Correia, I.; Teixeira, M.C. The PathoYeastract database: An information system for the analysis of gene and genomic transcription regulation in pathogenic yeasts. *Nucleic Acids Res.* **2017**, *45*, D597–D603.

47. Bailey, T.L. DREME: motif discovery in transcription factor ChIP-seq data. *Bioinformatics* **2011**, *27*, 1653–1659.

48. Köhrer, K.; Domdey, H. Preparation of high molecular weight RNA. *Methods Enzymol.* **1991**, *194*, 398–405.

49. Sanglard, D.; Ischer, F.; Calabrese, D.; Majcherczyk, P.A.; Bille, J. The ATP binding cassette transporter gene *CgCDR1* from *Candida glabrata* is involved in the resistance of clinical isolates to azole antifungal agents. *Antimicrob. Agents Chemother.* **1999**, *43*, 2753–65.

50. Bennett, J.E.; Izumikawa, K.; Marr, K.A. Mechanism of increased fluconazole resistance in *Candida glabrata* during prophylaxis. *Antimicrob. Agents Chemother.* **2004**, *48*, 1773–1777.

51. Rogers, P.D.; Vermitsky, J.P.; Edlind, T.D.; Hilliard, G.M. Proteomic analysis of experimentally induced azole resistance in *Candida glabrata*. *J. Antimicrob. Chemother.* **2006**, *58*, 434–438.

52. Henry, K.W.; Nickels, J.T.; Edlind, T.D. Upregulation of *ERG* genes in *Candida* species by azoles and other sterol biosynthesis inhibitors. *Antimicrob. Agents Chemother.* **2000**, *44*, 2693–700.

53. Marichal, P.; Vanden Bossche, H.; Odds, F.C.; Nobels, G.; Warnock, D.W.; Timmerman, V.; Van Broeckhoven, C.; Fay, S.; Mose-Larsen, P. Molecular biological characterization of an azole-resistant *Candida glabrata* isolate. *Antimicrob. Agents Chemother.* **1997**, *41*, 2229–2237.

54. Cavalheiro, M.; Costa, C.; Silva-Dias, A.; Miranda, I.M.; Wang, C.; Pais, P.; Pinto, S.N.; Mil-Homens, D.; Sato-Okamoto, M.; Takahashi-Nakaguchi, A.; *et al.* A Transcriptomics Approach To Unveiling the Mechanisms of In Vitro Evolution towards Fluconazole Resistance of a *Candida glabrata* Clinical Isolate. *Antimicrob. Agents Chemother.* **2019**, *63*, e00995-18.

55. Cernicka, J.; Subik, J. Resistance mechanisms in fluconazole-resistant *Candida albicans* isolates from vaginal candidiasis. *Int. J. Antimicrob. Agents* **2006**, *27*, 403–408.

56. Barker, K.S.; Crisp, S.; Wiederhold, N.; Lewis, R.E.; Bareither, B.; Eckstein, J.; Barbuch, R.; Bard, M.; Rogers, P.D. Genome-wide expression profiling reveals genes associated with amphotericin B and fluconazole resistance in experimentally induced antifungal resistant isolates of *Candida albicans*. *J. Antimicrob. Chemother.* **2004**, *54*, 376–385.

57. Liu, T.T.; Lee, R.E.B.; Barker, K.S.; Lee, R.E.; Wei, L.; Homayouni, R.; Rogers, P.D. Genome-Wide Expression Profiling of the Response to Azole, Polyene, Echinocandin, and Pyrimidine Antifungal Agents in *Candida albicans*. *Antimicrob. Agents Chemother.* **2005**, *49*, 2226–2236.

58. Agarwal, A.K.; Rogers, P.D.; Baerson, S.R.; Jacob, M.R.; Barker, K.S.; Cleary, J.D.; Walker, L.A.; Nagle, D.G.; Clark, A.M. Genome-wide Expression Profiling of the Response to Polyene, Pyrimidine, Azole, and Echinocandin Antifungal Agents in *Saccharomyces cerevisiae*. *J. Biol. Chem.* **2003**, *278*, 34998–35015.

59. Beh, C.T.; Cool, L.; Phillips, J.; Rine, J. Overlapping functions of the yeast oxysterol-binding protein homologues. *Genetics* **2001**, *157*, 1117–1140.

60. Jiang, B.; Brown, J.L.; Sheraton, J.; Fortin, N.; Bussey, H. A new family of yeast genes implicated in ergosterol synthesis is related to the human oxysterol binding protein. *Yeast* **1994**, *10*, 341–353.

61. Vandeputte, P.; Ferrari, S.; Coste, A.T. Antifungal Resistance and New Strategies to Control Fungal Infections. *Int. J. Microbiol.* **2012**, *2012*, 1–26.

62. Gasch, A.P.; Moses, A.M.; Chiang, D.Y.; Fraser, H.B.; Berardini, M.; Eisen, M.B. Conservation and Evolution of Cis-Regulatory Systems in Ascomycete Fungi. *PLoS Biol.* **2004**, *2*, e398.

63. Guerra-Moreno, A.; Hanna, J. Tmc1 Is a Dynamically Regulated Effector of the Rpn4 Proteotoxic Stress Response. *J. Biol. Chem.* **2016**, *291*, 14788–14795.

64. Estruch, F.; Carlson, M. Two homologous zinc finger genes identified by multicopy suppression in a *SNF1* protein kinase mutant of *Saccharomyces cerevisiae*. *Mol. Cell. Biol.* **1993**, *13*, 3872–3881.

65. Marchler, G.; Schüller, C.; Adam, G.; Ruis, H. A *Saccharomyces cerevisiae* UAS element controlled by protein kinase A activates transcription in response to a variety of stress conditions. *EMBO J.* **1993**, *12*, 1997–2003.

66. Mira, N.P.; Becker, J.D.; Sá-Correia, I. Genomic Expression Program Involving the Haa1p-Regulon in *Saccharomyces cerevisiae* Response to Acetic Acid. *Omi. A J. Integr. Biol.* **2010**, *14*, 587–601.

67. Ramsdale, M.; Selway, L.; Stead, D.; Walker, J.; Yin, Z.; Nicholls, S.M.; Crowe, J.; Sheils, E.M.; Brown, A.J.P. *MNL1* Regulates Weak Acid–induced Stress Responses of the Fungal Pathogen *Candida albicans*. *Mol. Biol. Cell* **2008**, *19*, 4393–4403.

68. Lamb, T.M.; Mitchell, A.P. The transcription factor Rim101p governs ion tolerance and cell differentiation by direct repression of the regulatory genes *NRG1* and *SMP1* in *Saccharomyces cerevisiae*. *Mol. Cell. Biol.* **2003**, *23*, 677–686.

69. Castrejon, F.; Gomez, A.; Sanz, M.; Duran, A.; Roncero, C. The *RIM101* Pathway Contributes to Yeast Cell Wall Assembly and Its Function Becomes Essential in the Absence of Mitogen-Activated Protein Kinase Slt2p. *Eukaryot. Cell* **2006**, *5*, 507–517.

70. Singh, A.; Yadav, V.; Prasad, R. Comparative Lipidomics in Clinical Isolates of *Candida albicans* Reveal Crosstalk between Mitochondria, Cell Wall Integrity and Azole Resistance. *PLoS One* **2012**, *7*, e39812.

71. Pasrija, R.; Prasad, T.; Prasad, R. Membrane raft lipid constituents affect drug susceptibilities of *Candida albicans*. *Biochem. Soc. Trans.* **2005**, *33*, 1219.

72. Pasrija, R.; Panwar, S.L.; Prasad, R. Multidrug Transporters CaCdr1p and CaMdr1p of *Candida albicans* Display Different Lipid Specificities: both Ergosterol and Sphingolipids Are Essential for Targeting of CaCdr1p to Membrane Rafts. *Antimicrob. Agents Chemother.* **2008**, *52*, 694–704.

73. Mukhopadhyay, K.; Prasad, T.; Saini, P.; Pucadyil, T.J.; Chattopadhyay, A.; Prasad, R. Membrane sphingolipid-ergosterol interactions are important determinants of multidrug resistance in *Candida albicans*. *Antimicrob. Agents Chemother.* **2004**, *48*, 1778–1787.

74. Vanden Bossche, H.; Koymans, L.; Moereels, H. P450 inhibitors of use in medical treatment: focus on mechanisms of action. *Pharmacol. Ther.* **1995**, *67*, 79–100.

75. Abe, F.; Usui, K.; Hiraki, T. Fluconazole modulates membrane rigidity, heterogeneity, and water penetration into the plasma membrane in *Saccharomyces cerevisiae*. *Biochemistry* **2009**, *48*, 8494–8504.

6 A novel pathway controlling fluconazole resistance in *Candida glabrata*: the CgMar1 transcription factor and sphingolipid metabolism

This chapter contains results included in a manuscript in preparation:

Pais, P., Galocha, M., Califórnia, R., Viana, R., Ola, M., Sato-Okamoto, M., Takahashi-Nakaguchi, A., Chibana, H., Butler, G., Teixeira, M.C. A novel pathway controlling fluconazole resistance in *Candida glabrata*: the CgMar1 transcription factor and sphingolipid metabolism.

The PhD candidate is the first author of the work detailed in this chapter. The candidate was responsible for most of the experimental work and writing of the correspondent manuscript.

6.1 Abstract

The ability to rapidly acquire azole resistance underlies the success of *Candida glabrata* as a fungal pathogen. As such, understanding the molecular basis of azole resistance in this pathogen is crucial to design more suitable therapeutic strategies.

In this study, the *C. glabrata* transcription factor (TF) encoded by ORF *CAGL0B03421g*, here denominated CgMar1 (Multiple Azole Resistance 1), is identified as a determinant of azole drug resistance. Additionally, CgMar1 was found to be activated upon fluconazole exposure, accumulating in the nucleus. Given these observations, the role of CgMar1 in the transcriptome-wide response to fluconazole was evaluated through RNA-sequencing. This TF was found to affect the expression of 337 genes, activating 134 genes and repressing, likely in an indirect fashion, 203 genes. The activated CgMar1 targets include a number of ergosterol, phospholipid and sphingolipid metabolism-related genes, among which, *CgLAM6*, *CgYPC1*, *CgRSB1* and *CgNTE1* were found to be determinants of azole resistance. Interestingly, fluconazole was found to act synergistically with the sphingolipid biosynthesis inhibitor, myriocin, suggesting that sphingolipid metabolism is crucial for *C. glabrata* cells to resist fluconazole stress. Consistent with a role in the control of sphingolipid metabolism, CgMar1 and its target gene *CgRBS1* were found to be required for sphingolipid incorporation in the plasma membrane, maintenance of cell permeability in fluconazole exposed cells, and decreased intracellular fluconazole accumulation.

Altogether, CgMar1 was found to control a new pathway towards azole drug resistance in *C. glabrata*, contributing to plasma membrane sphingolipid composition via, at least CgRbs1, and thus decreasing azole drug accumulation.

6.2 Introduction

Candida glabrata ranks second among the most commonly isolated *Candida* spp., only surpassed by *Candida albicans* [1,2]. *Candida* infections constitute the most common cause of fungal infections and are the 4th leading cause of nosocomial bloodstream infections in the USA [1,3,4].

Azole antifungals have been widely used in clinical practice as both treatment and prophylaxis of fungal infections, including candidiasis [5]. Azole treatment leads to loss of plasma membrane structural properties through inhibition of cytochrome P450-dependent enzyme lanosterol 14-α-demethylase (encoded by *ERG11* in *Candida* species), a key enzyme in the ergosterol biosynthetic pathway, resulting in ergosterol depletion and incorporation of the toxic sterol dimethylcholesta-8,24(28)-dien-3β,6α-diol (DMCDD) in the membrane [6,7]. Azole resistance mechanisms in *Candida* species are typically underscored by major transcription factors that regulate azole stress response, both in the intrinsically resistant *C. glabrata* and the commonly isolated *C. albicans*.

Current knowledge on the transcriptional regulation of antifungal resistance in *C. glabrata* is mostly focused on the transcription factor CgPdr1, regarded as a master regulator of clinical acquisition of resistance to azole antifungals by activating the expression of multidrug resistance transporters [8–12]. Similarly, *C. albicans* has in CaTac1 its own master regulator of azole resistance, which resembles CgPdr1 by having a central role in azole resistance by regulating the expression of multidrug resistance transporters [13–15], although sequence similarity between CaTac1 and CgPdr1 is low. Additionally, *C. albicans* carries another relevant regulator of azole resistance, the transcription factor CaMrr1, which activates the expression of the CaMdr1 drug:H+ antiporter from the Major Facilitator Superfamily (MFS) [16,17].

In order to identify additional regulators of antifungal resistance, twelve deletion mutants for predicted stress responsive TFs (*CgYAP1*, *CgCAD1*, *CgSKN7*, *CgHAP1*, *CgSTB5*, *CgNDT80*, *CgHAL9*, *CAGL0L04400g*, *CAGL0B03421g*, *CAGL0F07909g*, *CAGL0F09229g* and *CAGL0L04576g*) were screened for increased antifungal susceptibility phenotypes. The TF encoded by ORF *CAGL0B03421g* was identified as an azole resistance determinant, and designated *CgMAR1*. Given the identification of *CgMAR1* as a new determinant of azole drug resistance in *C. glabrata*, its role in the

transcriptome-wide response to fluconazole was assessed. The identification of CgMar1 target genes, enable the identification of a new pathway to azole resistance, whose characterization was conducted, from the process of CgMar1 activation to the role a few selected targets also identified as determinants of fluconazole resistance.

6.3 Materials and Methods

6.3.1 Strains, plasmids and growth media

Candida glabrata parental strain KUE100 [18] and derived single deletion mutants were batch-cultured at 30ºC, with orbital agitation (250 rpm) in basal medium (BM), with the following composition (per liter): 1.7 g yeast nitrogen base without amino acids or NH_4^+ (Difco), 20 g glucose (Merck) and 2.65 g $(NH_4)_2SO_4$ (Merck). *C. glabrata* strain L5U1 (*cgura3Δ0, cgleu2Δ0*) [19], kindly provided by John Bennett from the National Institute of Allergy and Infectious Diseases, NIH, Bethesda, USA, was grown in BM medium supplemented with 20 mg/L uracil and 60 mg/L leucine. L5U1 strains harboring pGREG576 derived plasmids were grown in the same medium lacking uracil. *S. cerevisiae* strain BY4741 (*MATa, ura3Δ0, leu2Δ0, his3Δ1, met15Δ0*) was obtained from Euroscarf (http://web.uni-frankfurt.de/fb15/mikro/euroscarf/) and grown in Yeast extract-Peptone-Dextrose (YPD) medium, with the following composition (per liter): 20 g glucose (Merck), 20 g Peptone (Merck) and 10 g Yeast extract (Merck). Solid media contained, besides the above-indicated ingredients, 20 g/L agar (Iberagar). The plasmid pGREG576 was obtained from the Drag&Drop collection [20].

6.3.2 Gene disruption

The deletion of the *C. glabrata* genes addressed in this study was carried out in the parental strain KUE100, using the method described by Ueno *et al.* [21]. Genes of interest were replaced by a DNA cassette including the *CgHIS3* gene, through homologous recombination. The PCR primers used to generate the replacement cassette for each gene and the primers used for PCR confirmation of gene deletion are present in Supplementary Table S6.1. The pHIS906 plasmid including *CgHIS3* was used as a template and transformation was performed as described previously [18].

6.3.3 Cloning of the *C. glabrata CgMAR1* (ORF *CAGL0B03421g*)

The pGREG576 plasmid from the Drag&Drop collection was used as described before to clone and express the *C. glabrata* ORF *CAGL0B03421g* [9,22–26]. pGREG576 was acquired from Euroscarf and contains a galactose inducible promoter (*GAL1*), the yeast

selectable marker *URA3* and the *GFP* gene, encoding a Green Fluorescent Protein (GFPS65T), which allows monitoring of the expression and subcellular localization of the cloned fusion protein. *CgMAR1* DNA was generated by PCR, using genomic DNA extracted from the sequenced CBS138 *C. glabrata* strain, and the following specific primers: 5'-GAATTCGATATCAAGCTTATCGATACCGTCGACA*ATGAGTACCACTACAACAA TACC*-3' and 5'-GCGTGACATAACTAATTACATGACTCGAGGTCGAC*CTACTCCCAGATTGAGC CAATG*-3'. The designed primers contain, besides a region with homology to the first 20 and last 22 nucleotides of the *CgMAR1* coding region (italic), nucleotide sequences with homology to the cloning site flanking regions of the pGREG576 vector (underlined). The amplified fragments were co-transformed into the parental *S. cerevisiae* strain BY4741 with the pGREG576 vector, previously cut with the restriction enzyme SalI, to obtain the pGREG576_*CgMAR1* plasmid. Since the *GAL1* promoter only allows a slight expression of downstream genes in *C. glabrata*, to visualize by fluorescence microscopy the subcellular localization of the CgMar1 protein in *C. glabrata*, new constructs were obtained. The *GAL1* promoter present in the pGREG576_*CgMAR1* plasmid was replaced by the constitutive *PDC1 C. glabrata* promoter [27], giving rise to the pGREG576_PDC1_*CgMAR1* plasmid. The *PDC1* promoter DNA was generated by PCR, using genomic DNA extracted from the sequenced CBS138 *C. glabrata* strain, and the following specific primers: 5'-TTAACCCTCACTAAAGGGAACAAAAGCTGGAGCTC*AGCATTTTTATACACGTT TTAC*-3' and 5'-GAAAAGTTCTTCTCCTTTACTCATACTAGTGCGGC*TGTTAATGTTTTTTGGCAA TTG*-3'. The designed primers contain, besides a region with homology to 22 nucleotides in the beginning and the last 22 nucleotides of the 1000 bp upstream region of the *PDC1* coding sequence (italic), nucleotide sequences with homology to the cloning site flanking regions of the pGREG576 vector (underlined). The amplified fragment was co-transformed into the parental strain BY4741 with the pGREG576_*CgMAR1* plasmid, previously cut with SacI and NotI restriction enzymes to remove the *GAL1* promoter, to generate the pGREG576_PDC1_*CgMAR1* plasmid. The recombinant plasmids pGREG576_*CgMAR1* and pGREG576_PDC1_*CgMAR1* were obtained through homologous recombination in *S. cerevisiae* and verified by DNA sequencing.

6.3.4 Antifungal susceptibility assays

The susceptibility of the parental strain KUE100 towards toxic concentrations of the selected drugs was compared to that of the deletion mutant KUE100_*Δcgmar1* by spot assays. The ability of *CgMAR1* gene expression to increase wild-type resistance to the tested chemical stresses was also examined in the URA3- L5U1 *C. glabrata* strain, using the pGREG576_PDC1_*CgMAR1* centromeric plasmids.

KUE100 *C. glabrata* cell suspensions used to inoculate agar plates or liquid medium, were mid-exponential cells grown in BM medium, until culture OD_{600nm} = 0.5 ± 0.05 was reached and then diluted in sterile water to obtain suspensions with OD_{600nm} = 0.05 ± 0.005. These cell suspensions and subsequent dilutions (1:5; 1:25) were applied as 4 µL spots onto the surface of solid BM medium, supplemented with adequate chemical stress concentrations. L5U1 *C. glabrata* cell suspensions used to inoculate the agar plates were mid-exponential cells grown in BM medium without uracil when using the L5U1 strain harboring the pGREG576 derived plasmids, until culture OD_{600nm} = 0.5 ± 0.05 was reached and then diluted in sterile water to obtain suspensions with OD_{600nm} = 0.05 ± 0.005. These cell suspensions and subsequent dilutions (1:5; 1:25) were applied as 4 µL spots onto the surface of solid BM medium without uracil for strains transformed with the pGREG576 derived plasmids and with adequate chemical stress concentrations. The tested drugs included the following compounds, used in the specified concentration ranges: the azole antifungal drugs ketoconazole (10 to 60 mg/L), fluconazole (100 to 250 mg/L), miconazole (0.10 to 0.50 mg/L), itraconazole (15 to 30 mg/L), and clotrimazole (2.5 to 15 mg/L), the polyene antifungal drug amphotericin B (0.10 to 0.35 mg/L) and the fluoropyrimidine 5-flucytosine (0.02 to 0.04 mg/L) (all from Sigma).

6.3.5 CgMar1 subcellular localization assessment

The subcellular localization of the CgMar1 protein was determined based on the observation of L5U1 *C. glabrata* cells transformed with the pGREG576_PDC1_*CgMAR1* plasmid. These cells express the CgMar1_GFP fusion protein, whose localization may be determined using fluorescence microscopy. *C. glabrata* cell suspensions were prepared in BM-U medium supplemented with leucine,

until a standard culture OD_{600nm} = 0.5 ± 0.05 was reached and transferred to the same medium with or without fluconazole. After 1h of incubation, the distribution of CgMar1_GFP fusion protein in *C. glabrata* living cells was detected by fluorescence microscopy in a Zeiss Axioplan microscope (Carl Zeiss MicroImaging), using excitation and emission wavelength of 395 and 509nm, respectively. Fluorescence images were captured using a cooled Zeiss Axiocam 503 color (Carl Zeiss Microscopy).

6.3.6 Total RNA extraction

C. glabrata strains KUE100 and KUE100_Δ*cgmar1* were grown in BM medium until mid-exponential phase. Subsequently, cells were transferred to fresh medium (control) or fresh medium containing 150 mg/L fluconazole were harvested after 1h of incubation. Total RNA was isolated using an Ambion Ribopure-Yeast RNA kit, according to manufacturer's instructions.

6.3.7 Library preparation

Prior to RNA-seq analysis quality control measures were implemented. Concentration of RNA was ascertained via fluorometric analysis on a Thermo Fisher Qubit fluorometer. Overall quality of RNA was verified using an Agilent Tapestation instrument. Following initial QC steps sequencing libraries were generated using the Illumina Truseq Stranded Total RNA library prep kit with ribosomal depletion via RiboZero Gold according to the manufacturer's protocol. Briefly, ribosomal RNA was depleted via pull down with bead-bound ribosomal-RNA complementary oligomers. The RNA molecules were then chemically fragmented and the first strand of cDNA was generated using random primers. Following RNase digestion the second strand of cDNA was generated replacing dTTP in the reaction mix with dUTP. Double stranded cDNA then underwent adenylation of 3' ends following ligation of Illumina-specific adapter sequences. Subsequent PCR enrichment of ligated products further selected for those strands not incorporating dUTP, leading to strand-specific sequencing libraries. Final libraries for each sample were assayed on the Agilent Tapestation for appropriate size and quantity. These libraries were then pooled in equimolar amounts as ascertained via fluorometric analyses. Final pools were absolutely quantified using qPCR on a

Roche LightCycler 480 instrument with Kapa Biosystems Illumina Library Quantification reagents.

6.3.8 Gene expression analysis

Strand specific RNA-seq library preparation and sequencing was carried out as a paid service by the NGS core from Oklahoma Medical Research Foundation, Oklahoma City, Oklahoma, USA. Paired-end reads (Illumina HiSeq 3000 PE150, 2x150 bp, 2 Gb clean data) were obtained from KUE100 and KUE100_Δ*cgmar1*. Two replicates of each sample were obtained from three independent RNA isolations, subsequently pooled together. Samples reads were trimmed using Skewer (v0.2.2) [28] and aligned to the *C. glabrata* CBS138 reference genome, obtained from the Candida Genome Database (CGD) (http://www.candidagenome.org/), using TopHat (v2.1.1) [29] with parameters -p 12 (number of threads), -g 1 (maximum amount of times a read can be mapped to the genome), --b2-very-sensitive (preset option) and --library-type fr-firststrand (account for strand specificity). HTSeq (v0.7.1) [30] was used to count mapped reads per gene. Differentially expressed genes were identified using DESeq2 [31] with an adjusted p-value threshold of 0.05 and a log2 fold change threshold of -0.5 and 0.5. Default parameters in DESeq2 were used. *Candida albicans* and *Saccharomyces cerevisiae* homologs were obtained from the Candida Genome Database and Saccharomyces Genome Database (SGD) (https://www.yeastgenome.org/), respectively.

6.3.9 NBD-DHS subcellular localization assessment

C. glabrata cell suspensions from strains KUE100, KUE100_Δ*cgmar1* and KUE100_Δ*cgrsb1* were prepared in BM medium until a standard culture OD_{600nm} = 0.5 ± 0.05 was reached. C_6 NBD-dihydrosphingosine (NBD-DHS; 1 mg/mL in methanol; Santa Cruz Biotechnology) was added to 1 mL of 4×10^7 cells/mL to a final concentration of 5 μM and cell suspensions were incubated in the dark with orbital agitation (30 minutes, 250 rpm). Cells exposed to C_6 NBD-DHS were centrifuged (17,500 × g for 5 minutes), washed twice and ressuspended in PBS buffer to final 10^7 cells/mL aliquots. NBD fluorescence was detected by fluorescence microscopy in a

Zeiss Axioplan microscope (Carl Zeiss MicroImaging), using excitation and emission wavelength of 395 and 509nm, respectively. Fluorescence images were captured using a cooled Zeiss Axiocam 503 color (Carl Zeiss Microscopy).

6.3.10 Plasma membrane permeability

Plasma membrane permeability was assessed by the passive uptake of propidium iodide (PI; 20 mM in DMSO, Invitrogen). *C. glabrata* cell suspensions from strains KUE100, KUE100_Δ*cgmar1* and KUE100_Δ*cgrsb1* were prepared in BM medium until a standard culture OD_{600nm} = 0.5 ± 0.05 was reached and transferred to the same medium with or without 150 mg/L fluconazole. After 1h of incubation, PI was added to 1 mL of 4×10^7 cells/mL to a final concentration of 20 µM and cell suspensions were incubated in the dark with orbital agitation (15 minutes, 250 rpm). Cells exposed to PI were centrifuged (17,500 × g for 5 minutes), washed twice and resuspended in PBS buffer to a final 10^7 cells/mL aliquots. PI-fluorescence was detected by fluorescence microscopy in a Zeiss Axioplan microscope (Carl Zeiss MicroImaging), using excitation and emission wavelength of 536 and 595nm, respectively. Fluorescence images were captured using a cooled Zeiss Axiocam 503 color (Carl Zeiss Microscopy) and the images were analyzed with the ZEN lite software from ZEISS microscopy. Cell-to-cell fluorescence intensity was defined as the average of pixel by pixel intensity in the selected region of interest and a minimum of 50 cells/experiment were used. The fluorescence images were background corrected by using dark-current images.

6.3.11 ^{3}H-fluconazole accumulation assays

^{3}H-fluconazole transport assays were carried out as described before for other radiolabeled compounds [9,22–26]. The internal accumulation of fluconazole was determined by calculating the ratio between the radiolabeled fluconazole measured within the yeast cells and in the external medium (Intracellular/Extracellular). The parental strain KUE100 and the mutant strains KUE100_*Δcgmar1* and KUE100_*Δcgrsb1* were grown in BM medium until mid-exponential phase and harvested by filtration. Cells were washed and resuspended in BM medium, to obtain dense cell suspensions (OD_{600nm} = 0.5 ± 0.1, equivalent to approximately 1.57 mg (dry

weight) mL^{-1}). Readily, 0.1 µM of ^{3}H-fluconazole (Moravek Inc.; 1 mCi/ml) and 150 mg/L of unlabeled fluconazole were added to the cell suspensions. Incubation proceeded for an additional period of 30 min. The intracellular accumulation of labeled fluconazole was followed by filtering 200 µl of cell suspension, at adequate time intervals, through pre-wetted glass microfibre filters (Whatman GF/C). The filters were washed with ice-cold TM buffer and the radioactivity measured in a Beckman LS 5000TD scintillation counter. Extracellular ^{3}H-fluconazole was estimated, by radioactivity assessment of 50 µl of the supernatant. Non-specific ^{3}H-fluconazole adsorption to the filters and to the cells (less than 5% of the total radioactivity) was assessed and taken into consideration. To calculate the intracellular concentration of labeled fluconazole, the internal cell volume (Vi) of the exponential cells, grown in the absence of drug and used for accumulation assays, was considered constant and equal to 2.5 µl (mg dry weight)$^{-1}$ [32]. Statistical analysis of the results was performed using analysis of variance, and differences were considered significant for p-values<0.05.

6.3.12 *In silico* prediction of overrepresented sequences in CgMar1-activated promoters

The promoters (-1000 to -1 bp) upstream of the coding regions of genes whose expression was found to be activated by CgMar1 were retrieved using the "Retrieve Upstream Sequence" tool from PathoYeastract (www.pathoyeastract.org) [33]. The obtained sequences were submitted to DREME (MEME suite) [34] for discovery of enriched sequences, using default parameters. The identified motifs were then cross checked with CaMar1 DNA-binding motifs retrieved from the "TF-Consensus List" tool from PathoYeastract.

6.4 Results and Discussion

6.4.1 The transcription factor CgMar1 (ORF *CAGL0B03421g*) is a determinant of azole resistance in *Candida glabrata*

In search of additional regulators of azole resistance among *C. glabrata* transcription factors (TFs), twelve TF deletion mutants were built and tested for differential fluconazole and ketoconazole Minimum Inhibitory Concentration (MIC) values, using standard CLSI microtiter plate assays. Among the tested TF mutants, only for the *ΔCAGL0B03421g* mutant strain a consistently lower MIC value for both azoles was found, when compared to the wild-type parental strain (Table 6.1). Indeed, the *ΔCAGL0B03421g* strain attained the fluconazole and ketoconazole MIC_{50} values 8 mg/L and 0.25 mg/L, respectively, corresponding to a 2-fold decrease when compared to the wild-type strain (16 mg/L and 0.5 mg/L, respectively). Consistently, the over-expression of *CAGL0B03421g* in the L5U1 wild-type *C. glabrata* strain resulted in a fluconazole and ketoconazole 16-fold MIC_{50} increase. Additionally, the deletion of ORF *CAGL0B03421g* was found to increase *C. glabrata* susceptibility to fluconazole, clotrimazole, ketoconazole and miconazole, as determined by spot assays (Figure 6.1A). Consistent with the previous results, the over-expression of *CAGL0B03421g* in the L5U1 wild-type *C. glabrata* strain was found to increase its tolerance to the same antifungal drugs (Figure 6.1B). Altogether, these results show that ORF *CAGL0B03421g* confers Multiple Azole Resistance, leading us to denominate this gene *CgMAR1*.

Table 6.1 – Fluconazole and ketoconazole MIC values for the tested TF deletion mutants.

Strain	Drug	
	Fluconazole (mg/mL)	**Ketoconazole (mg/mL)**
KUE100	16	0.5
KUE100_*Δcgyap1*	16	0.5
KUE100_*Δcgcad1*	16	0.5
KUE100_*Δcgskn7*	16	0.5
KUE100_*Δcghap1*	16	0.5
KUE100_*Δcgstb5*	16	0.5
KUE100_*Δcgndt80*	16	0.5
KUE100_*Δcghal9*	16	0.5
KUE100_*ΔCAGL0L04400g*	16	0.5
KUE100_*ΔCAGL0B03421g*	8	0.25
KUE100_*ΔCAGL0F07909g*	16	0.5
KUE100_*ΔCAGL0F09229g*	16	0.5
KUE100_*ΔCAGL0L04576g*	16	0.5

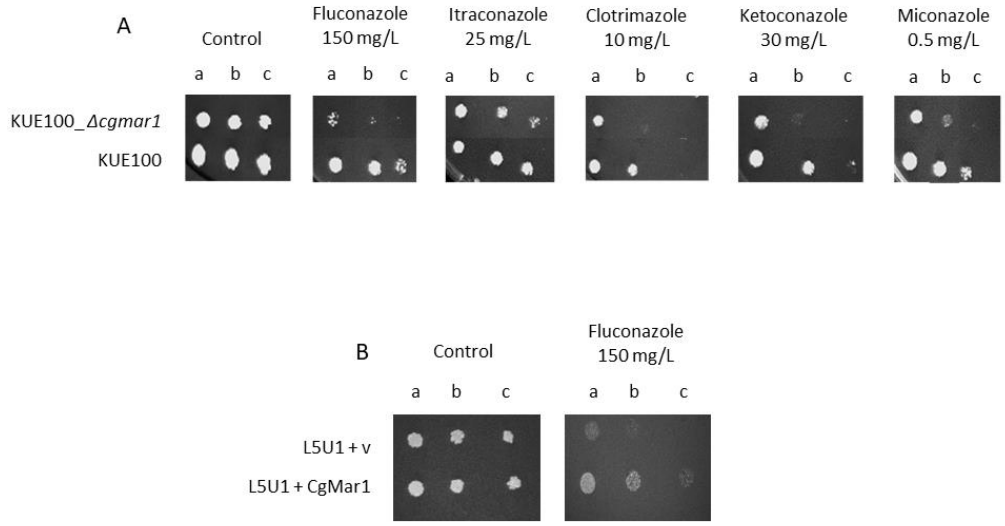

Figure 6.1 – *CgMAR1* confers resistance to fluconazole in *C. glabrata*. (A) Comparison of the susceptibility to azole antifungals, at the indicated concentrations, of the KUE100 and KUE100_*Δcgmar1 C. glabrata* strains, in BM agar plates, by spot assays. (B) Comparison of the susceptibility to azole antifungals, at the indicated concentrations, of the L5U1 *C. glabrata* strain harboring the pGREG576 cloning vector (v) or the pGREG576_PDC1_*CgMAR1* in BM-U agar plates, by spot assays.

6.4.2 CgMar1 is activated upon fluconazole stress, leading to its nuclear accumulation

In order to evaluate if fluconazole stress could lead to CgMar1 activation, we investigated its subcellular localization by fluorescence microscopy before and after fluconazole exposure. *C. glabrata* cells harboring the pGREG576_PDC1_*CgMAR1* plasmid were grown to mid-exponential phase in basal medium and then transferred to fresh medium (control) or fresh medium containing 150 mg/L fluconazole. After 1h of incubation, cells were inspected through fluorescence microscopy.

In *C. glabrata* cells, the CgMar1_GFP fusion protein was found to be predominantly localized indistinctly throughout the cell in control conditions (Figure 6.2A). After fluconazole stress, the CgMar1_GFP was found to accumulate in the nucleus (Figure 6.2B). These findings indicate that CgMar1 is indeed activated upon fluconazole stress, leading to its translocating from the cytosol to the nucleus.

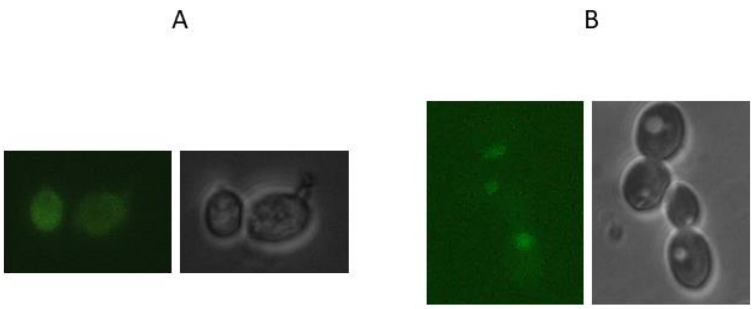

Figure 6.2 – CgMar1 is activated upon fluconazole stress. Fluorescence of exponential-phase L5U1 *C. glabrata* cells harboring the pGREG576_PDC1_*CgMAR1* plasmid after 5h of recombinant protein production in control conditions (A) or after 1h fluconazole exposure (B), respectively.

6.4.3 Role of CgMar1 in the transcriptome-wide changes occurring in response to fluconazole in *C. glabrata*

In order to determine the role of the transcription factor CgMar1 in fluconazole response, changes in gene expression occurring in Δ*cgmar1* cells were assessed and compared to that of wild-type cells (analyzed in the previous chapter). The expression of 134 genes was found to be activated by CgMar1, whereas 203 genes were found to be repressed by this transcription factor, possibly in an indirect fashion, in fluconazole exposed cells (Supplementary Table S5.2). From these, 30% are exclusively regulated during antifungal stress and CgMar1 deletions does not have an effect on their basal expression (Supplementary Table S5.3) The most prevalent functional groups of genes activated by CgMar1 comprise Carbon metabolism, Nitrogen metabolism and Lipid metabolism (Figure 6.3A), while genes indirectly repressed by CgMar1 are especially enriched in Nucleic acid processing and Ribosome biogenesis genes (Figure 6.3B).

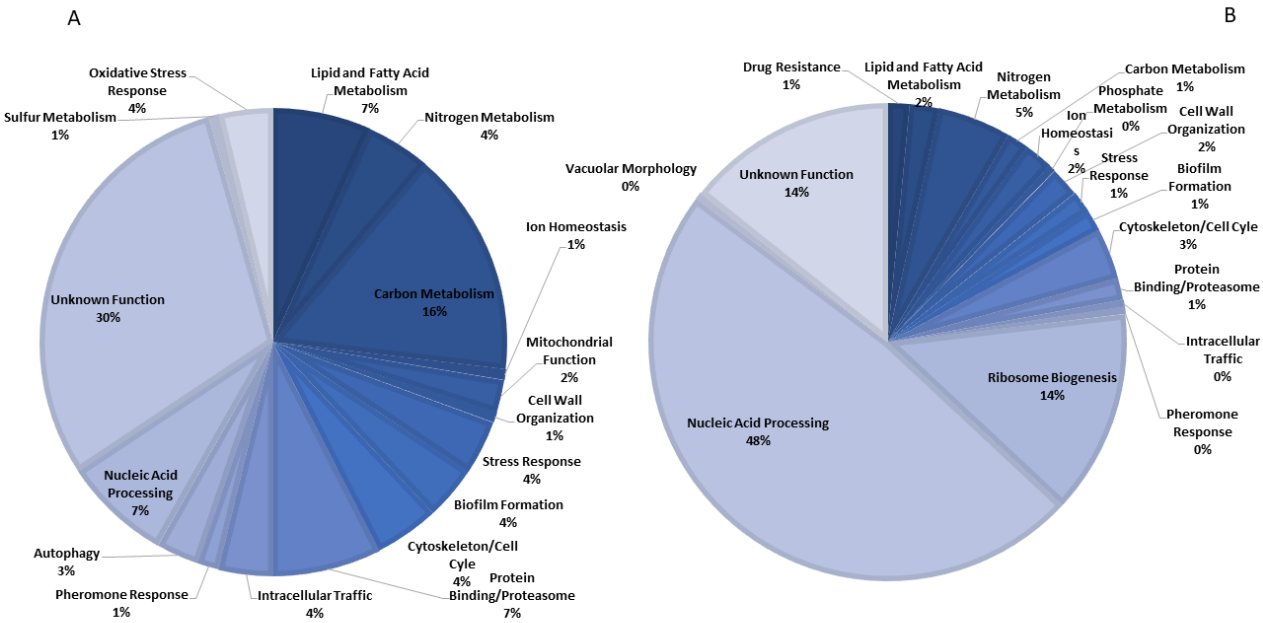

Figure 6.3 – *CgMAR1* regulated genes in response to fluconazole stress. Differentially expressed genes in exponential-phase KUE100_*Δcgmar1 C. glabrata* cells, comparing to KUE100 cells, after 1h fluconazole exposure. (A) CgMar1-activated genes (downregulated in the mutant strain). (B) CgMar1-repressed genes (upregulated in the mutant strain).

The comparison of this regulon with differentially expressed genes in fluconazole-challenged wild-type cells enabled the identification of 6 genes that respond to fluconazole only when *CgMAR1* is present. This include genes in Lipid and Fatty Acid Metabolism (*CgHNB1* and ORF *CAGL0A03740g*), Mitochondrial Function (*CgCOX26*), Stress Response (*CgSSA3*) and Unknown Function (ORFs *CAGL0M11660g* and *CAGL0K07337g*).

CgMar1 was found to regulate expression of several additional genes irrespective of fluconazole treatment. CgMar1-activated genes in the group of Carbon Metabolism are involved in carbon reserve metabolism, namely in the inter-conversion of glucose to glycogen or glucose to trehalose, part of the typical general stress response in yeast [35–37]; as well as alcohol catabolic processes. Other genes involved in alcohol metabolism were also observed to be activated in wild-type cells exposed to fluconazole. On the other hand, CgMar1-repressed genes comprise the putative transcriptional regulator encoding gene *CgMIG1*, involved in glucose catabolite repression [38], and the glucose transmembrane transporters *CgHXT3*, a predicted low affinity glucose transporter, and ORF *CAGL0D02640g*, encoding an homolog of the *S. cerevisiae* Hxt2 high-affinity glucose transporter, induced by low levels of glucose and repressed by high levels of

glucose [39,40]. Taken together, these results appear to indicate that CgMar1 is required to control central carbon metabolism during fluconazole stress.

The Nitrogen Metabolism group comprises genes involved in the metabolism of a number of amino acids, as well as genes involved in nucleotide catabolic processes. Genes activated by CgMar1 are involved in histidine (*CgHIS5*) and nucleotide (*CgGUD1*, *CgPRM15*, *CgNNR2* and *CgPHM8*) metabolism. Other CgMar1-activated genes involved in amino acid metabolism can be related with stress responses, such as cysteine (*CgSTR3*) and glutamate (*CgGDH2*, *CgGAD1* and *CgUGA1*) metabolism that are involved in oxidative stress resistance (OSR), together with glutathione metabolism (*CgOXP1*). Glutathione is a known antioxidant tripeptide in fungi that prevents damage to cellular components caused by reactive oxygen species (ROS) [41]. Cysteine and glutamate are two of the three constituents of glutathione [42]. Interestingly, *CgSTR3* was previously found to be upregulated in an azole resistant strain [10] and the protein encoded by *CgGAD1* is predicted to have a role in cellular response to oxidative stress. On the other hand, several genes repressed by CgMar1 comprise amino acid permeases, such as *CgLYP1*, *CgALP1* and *CgORT1*; the polyamine transporter *CgDUR3*; and the peptide transporter encoded by *CgPTR2*. Among these genes, the activator of nitrogen catabolite repression genes, *CgGAT1*, is also present.

Particularly interesting in this context, could be the genes activated in the functional category Lipid metabolism. CgMar1-activated genes comprise genes putatively involved in sterol transfer/transport: *CgLAM1*, *CgLAM5* and *CgLAM6*. Additionally, genes related to sphingolipid (*CgRSB1* and *CgYPC1*) and phospholipid (*CgOPI10* and *CgNTE1*) metabolism, as well as metabolism of carnitine (*CgYAT2*) and fatty acids (*CgHBN1*) are also present. Ceramides can be used as signaling molecules, while phospholipids and sphingolipids are structural components of the plasma membrane [43]. Lipid metabolism genes indirectly repressed by CgMar1 include *CgCDS1* (phospholipid biosynthesis), *CgBRL1* (lipid homeostasis), *CgCPT1* (choline pathway) and *CAGL0A03740g* (fatty acid oxidation). The differential expression of membrane lipid pathway genes other than sterol hints for additional mechanisms of cell membrane homeostasis in fluconazole resistance. In fact, plasma membrane alterations have been correlated with azole exposure and resistance, especially in *C. albicans*. In this species azole resistance can be associated with increased membrane fluidity due to decreased ergosterol content [44], defective phospholipid metabolism (lack of

phosphatidylethanolamine) leads to increased plasma membrane fluidity and increased accumulation of fluconazole [45] and altered sterol and phosphatidylcholine:phosphatidylethanolamine ratio was found in an azole-resistance isolate [46]. Further, response to fluconazole includes a significant increase of α-hydroxyphytoceramide (αHPC) and mannosylinositolphosphoceramide (MIPC), thus associating altered sphingolipid composition with azole resistance [47]. A lipidomics analysis of matched susceptible and resistant *C. albicans* clinical isolates revealed gradual changes in mannosylinositolphosphorylceramides and ergosterol [48]. Moreover, both ergosterol and the toxic sterol DMCDD integrate into the cell membrane through interaction with sphingolipids [49], thus suggesting a functional link between sphingolipids and azole resistance. Additionally, the lipid composition of the plasma membrane can influence the activity of MDR transporters. For example, ABC transporters are preferably localized in micro-domains, such as lipid rafts, which are rich in ergosterol and sphingolipids. The interactions between membrane sphingolipids and sterols are crucial for the sorting and functioning of ABC transporters, as shown by *C. albicans* transporter Cdr1 activity being affected by imbalances in raft lipid constituents (reviewed in Prasad *et al.*, 2016 [50]). Analysis of *C. albicans* plasma membrane physical properties upon fluconazole treatment revealed a decrease of ordered lipid domains containing integral proteins, accompanied by reduced protein content in the membrane [51].

Additional functional groups controlled by CgMar1 include Mitochondrial Function, Proteasome/Protein Processing, Autophagy and Intracellular Traffic. Genes activated by CgMar1 in Mitochondrial Function are relative to the respiratory chain (*CgCOX26*), cytochrome c degradation (*CgSUE1*) and regulation of ATP synthase activity (*CgSTF1*). As for the Proteasome/Protein Processing group, activated genes are composed mainly of ubiquitin-associated genes and proteases, including *CgHSP31* and *CgYPS8*. *CgHSP31* is upregulated in an azole-resistant strain [10], so is its protein levels [52]. *CgYSP8* is involved in virulence and was described to be induced under other stress conditions [53,54].

In the case of Stress Response genes, the heat-shock protein coding genes *CgHSP78* and *CgSSA3* are activated by CgMar1. Additionally, the putative heat shock binding protein encoded by *CgGAC1* is also positively regulated by CgMar1 and its *C. albicans* homolog was found to be fluconazole-induced [55]. Moreover, a putative stress

responsive gene (ORF *CAGL0M04763g*) and a gene with a predicted function in cellular response to drug (*CgRTC3*) were found to be activated by CgMar1.

Interestingly, CgMar1 was also found to activate the expression of genes involved in adhesion, namely the adhesin encoding genes *CgEPA11*, *CgEPA13* and *CgPWP6*, as well as the predicted adhesin encoding ORF *CAGL0I11011g*. On the other hand, CgMar1 was found to indirectly repress the adhesion encoding genes *CgEPA1* and *CgEPA3*, possibly indicating different roles for different adhesins according to environmental conditions.

Genes encoding three multidrug resistance transporters were here identified as repressed by CgMar1: the MFS transporters *CgTPO1_1* and *CAGL0L10912g*, and the ABC transporter *CgYOR1*. This indicates that CgMar1 is not an activator of multidrug resistance transporters, and thus the mechanisms of azole resistance controlled by CgMar1 are irrespective of drug transport.

6.4.4 CgMar1-activated sphingolipid and phospholipid genes mediate fluconazole resistance in *C. glabrata*

To investigate the possible involvement of CgMar1-activated genes in the observed fluconazole resistance phenotype, fluconazole MIC levels were assessed for 7 deletion mutants devoid of CgMar1-activated genes predicted to be related with sterol transfer (*CgLAM1*, *CgLAM5*, *CgLAM6*), sphingolipid (*CgYPC1*, *CgRSB1*) and phospholipid pathways (*CgNTE1*, *CgOPI10*). Their predicted functions were postulated given the function of their homologs in *S. cerevisiae*, ScLam1, ScLam5 and ScLam6 are sterol transporters that mediate sterol transfer between membranes [56], ScYpc1 displays ceramidase and ceramide synthase activities, involved in the breakdown/synthesis of phytoceramide [57], ScRsb1 is a putative sphingolipid flippase involved in the translocation of lipid chains to the outer side of the plasma membrane [58], ScNte1 is a serine esterase that mediates phosphatidylcholine turnover and influences the regulation of phospholipid biosynthesis [59,60] and ScOpi10 is involved in inositol excretion [61].

The strains *Δcglam6,* Δ*cgnte1*, *Δcgypc1* and *Δcgrsb1* exhibited a fluconazole MIC_{50} of 8 mg/L, corresponding to the same MIC_{50} of the *Δcgmar1* strain and a 2-fold decrease in comparison to the wild-type MIC_{50} (16 mg/L). This observation suggests that *CgMAR1*

is required for azole resistance through its action in multiple target genes. Two of the four genes are involved in sphingolipid pathways (*CgYPC1* and *CgRSB1*), indicating that sphingolipids metabolism may be required for fluconazole resistance. To test this hypothesis, the susceptibility of the wild-type and mutant strains to the sphingolipid biosynthesis inhibitor, myriocin, was performed. The susceptibility of *Δcgmar1* and *Δcgrsb1* mutants was comparable to the wild-type (MIC_{50} 16 mg/L), while the *Δcgypc1* mutant is more susceptible (MIC_{50} 8 mg/L). When cells are treated with both fluconazole and myriocin, all strains show higher susceptibility (MIC_{50} 4 mg/L) than to either fluconazole of myriocin individually. The synergistic effect between fluconazole and myriocin indicates that sphingolipid biosynthesis is required for full fluconazole tolerance. Moreover, the fact that both deletion mutants become equally more susceptible when treated with both fluconazole and myriocin indicates that they all are required for fluconazole resistance via sphingolipid homeostasis and that CgMar1 participates in this response. The relevance of sphingolipids in azole resistance has been recently shown in *C. albicans*, where fluconazole resistance was associated with the upregulation of sphingolipid biosynthesis genes [47].

In other transcriptomics studies, *CgRSB1* was found to be upregulated during fluconazole stress, including in a CgPdr1-depedent manner [10,62–64]. However, its actual role in fluconazole resistance remains to be addressed. To elucidate if *CgRSB1* could be an interesting target involved in *C. glabrata* fluconazole resistance, we investigated its homologs in other yeast species. In *S. cerevisiae*, *RSB1* has 4 homologs (*ScRTA1*, *ScRTM1*, *ScPUG1* and *YLR046C*) and is a member of the lipid-translocating exporter family that contributes to plasma membrane asymmetry and sphingoid long-chain base release [58,65]. Interestingly, *ScRSB1* is also upregulated by ScPdr1 [65]. In *C. albicans*, its homolog (*CaRTA2*) was found upregulated in clinical azole-resistant isolates and in an induced fluconazole-resistant strain [66,67]. Moreover, *CaRTA2* is required for fluconazole resistance by contributing to plasma membrane homeostasis and sphingoid long-chain base release [68]. It is localized to lipid rafts and is required for the association of additional proteins to such rafts, including CaErg11 [69]. Furthermore, the related lipid translocase gene *CaRTA3* is upregulated in response to ketoconazole exposure [70] and coordinately upregulated with *CaCDR1* and *CaCDR2* during fluconazole stress, being required for full fluconazole resistance [71]. The relevance of lipid flippases in azole resistance has also been demonstrated in other

pathogenic fungi. For example, in *C. neoformans*, the lipid flippase subunit CnCdc50 contributes to fluconazole tolerance [72].

Altogether, it seems that genes involved in the regulation of lipid distribution and homeostasis in the plasma membrane are relevant players in yeast azole response. Jointly with our transcriptomics and phenotypic data, *CgRSB1* stands out as promising target to study in the context of azole resistance and membrane stability in *C. glabrata*.

6.4.5 CgMar1 is required for sphingolipid incorporation in the plasma membrane, in a CgRsb1-dependent manner

To investigate a possible role of *CgMAR1* and of its target *CgRSB1* in the control of plasma membrane sphingolipid organization, we assessed the subcellular localization of fluorescently labeled dihydrosphingosine (NBD-DHS) in wild-type and Δ*cgrsb1* cells. After 30 minutes of incubation with 5 µM NBD-DHS, wild-type cells incorporated DHS in the cell periphery, consistent with a plasma membrane localization (Figure 6.4A), whereas the Δ*cgrsb1* mutant exhibited less incorporation of NBD-DHS in the plasma membrane and increased accumulation inside the cells (Figure 6.4B). This finding is consistent with the function described for *CaRTA2* in *C. albicans* in contributing to DHS export and reducing DHS accumulation [68]. To examine the role of *CgMAR1* in this instance, the subcellular localization of NBD-DHS was also assessed in Δ*cgmar1* cells. The Δ*cgmar1* mutant failed to incorporate NBD-DHS at the plasma membrane (Figure 6.4C). Overall, the evidence suggests *CgMAR1* controls the incorporation of DHS in the plasma membrane through, at least, *CgRSB1*, therefore being involved in plasma membrane organization.

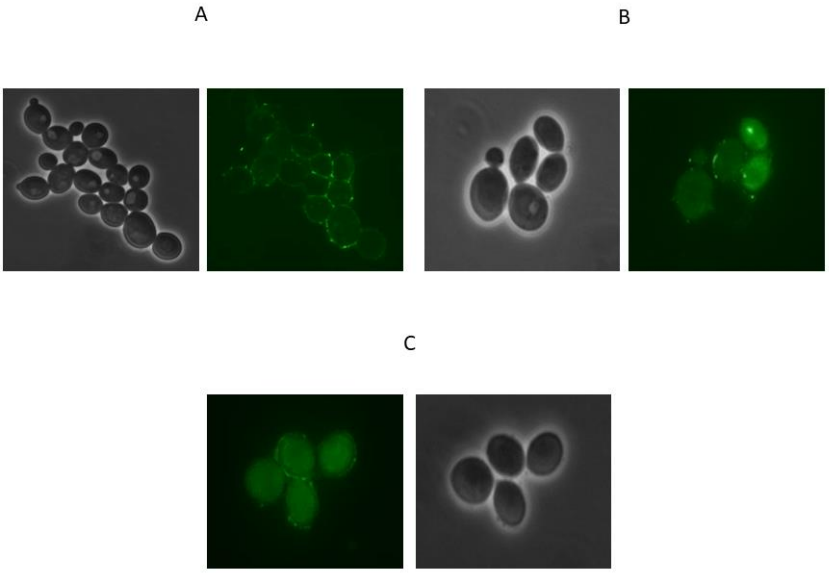

Figure 6.4 – CgMar1 and CgRbs1-dependent localization of NBD-DHS in *C. glabrata* cells. Comparison of 5 μM NBD-dihydrosphingosine (NBD-DHS) subcellular localization in *C. glabrata*, after 30 minutes incubation, in (A) KUE100 *C. glabrata* cells or (B) in KUE100_*Δcgrsb1* cells or (C) KUE100_*Δcgmar1* cells.

6.4.6 CgMar1 contributes to the maintenance of plasma membrane permeability and fluconazole accumulation of *C. glabrata* cells, mediated by CgRsb1

Although the identified *C. glabrata* Mar1 regulon did not include any MDR transporters, we found a positive association between this transcription factor and genes involved in sphingolipid pathways, such as *CgRSB1*. Based on these findings, and due to the targeting of plasma membrane by fluconazole, a possible role of CgMar1 and of its target CgRsb1 in the regulation of plasma membrane homeostasis was evaluated.

Cell permeability in response to fluconazole was investigated using the fluorescent probe propidium iodide (PI), and the possible participation of CgMar1 and its target CgRsb1 was evaluated. Upon 1h of exposure to fluconazole, *C. glabrata* cell permeability was found to increase significantly (Figure 6.5A). This observation is likely associated with the inhibition of CgErg11 by fluconazole and disruption of the ergosterol biosynthesis pathways, resulting in the accumulation of the toxic sterol DMCDD that permeabilizes the plasma membrane [73]. Accordingly, fluconazole treatment was associated with increased yeast cell permeability [74]. In comparison to wild-type cells, permeability of *Δcgmar1* cells was not significantly affected in control

conditions, however, upon fluconazole stress, it was seen to increase to levels higher than the wild-type strain (Figure 6.5A). Concurrently, the absence of *CgRSB1* results in increased permeability of *C. glabrata* upon fluconazole stress, comparable to levels registered in the Δ*cgmar1* and higher than those attained for the wild-type (Figure 6.5A). This data indicates that fluconazole increases *C. glabrata* cell permeability and that CgMar1, through at least CgRsb1, contributes to its maintenance during fluconazole exposure.

The influence of CgMar1 in plasma membrane organization and permeability via *CgRSB1* led us to investigate if this could be related with decreased accumulation of the drug, consequently leading to azole resistance.

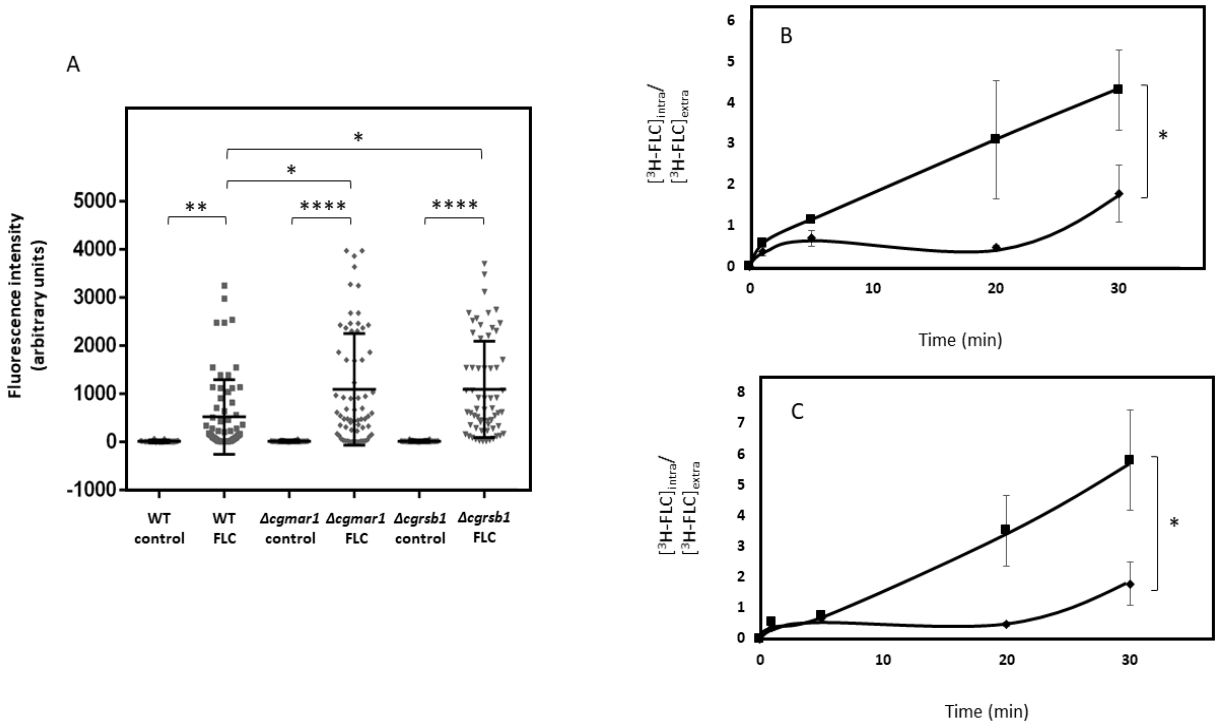

Figure 6.5 – CgMar1 and CgRsb1 regulate plasma membrane permeability and fluconazole accumulation in *C. glabrata* cells. (A) Comparison of plasma membrane permeability of exponential-phase KUE100 (squares), KUE100_*Δcgmar1* (diamonds) or KU100_*Δcgrsb1* (triangles) in control conditions or upon 1h fluconazole stress. The estimation of plasma membrane permeability is based on the fluorescence intensity values exhibited by yeast cells upon passive accumulation of propidium iodide. Error bars represent the corresponding standard deviation. (B) Time-course accumulation of radiolabeled ^{3}H-fluconazole in strains KUE100 (diamonds) and KUE100_*Δcgmar1* (squares) or (C) KUE100 (diamonds) and KUE100_*Δcgrsb1* (squares), during cultivation in BM liquid medium in the presence of 150 mg/L unlabeled fluconazole. Accumulation values are the average of at least three independent experiments. Error bars represent the corresponding standard deviations. *p<0.05, **p<0.01, ***p<0.001, ****p<0.0001.

Consistent with the observed susceptibility and cell permeability phenotypes, the *Δcgmar1* deletion mutant was found to accumulate 4.5-fold more radiolabeled fluconazole than the wild-type strain, after 30 minutes of exposure to the antifungal (Figure 6.5B). These results suggest that CgMar1 activity mediates *C. glabrata* resistance toward fluconazole by reducing its intracellular accumulation in yeast cells, possibly as a result of its role in controlling membrane permeability and organization. In order to understand if this phenotype could be, at least in part, due to regulation of CgMar1 over *CgRSB1*, the accumulation of radiolabeled fluconazole was also assessed in *Δcgrsb1* cells. In fact, the absence of *CgRSB1* was found to result in an increased of intracellular fluconazole accumulation in comparison to wild-type, to levels comparable to the *Δcgmar1* mutant (Figure 6.5C). These results indicate that *CgMAR1* mediates fluconazole resistance, at least, by reducing intracellular fluconazole levels, through regulation of *CgRSB1* and, eventually, other CgMar1-target genes.

6.4.7 Identification of the nucleotide binding site recognized by CgMar1

In order to identify possible CgMar1 DNA recognition sites and directly regulated target genes, the promoters of CgMar1-activated genes during fluconazole stress were searched for enriched motifs using DREME [34]. Excluding TATA-box sequences, 5 overrepresented motifs were found (Figure 6.6). From those, a CTCGA motif was located at positions -351 to -347 of *CgRSB1* promoter region. To determine if this motif is required for CgMar1-dependent activation of *CgRSB1*, *lacZ* reporter gene assay is being conducted to assess the effect of disrupting the putative binding site on *CgRSB1* promoter activation.

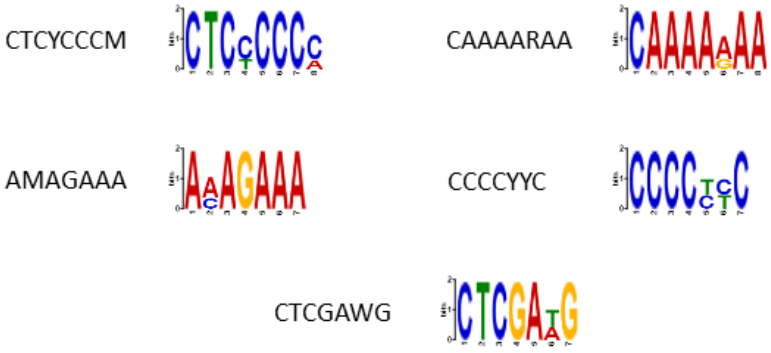

Figure 6.6 – Overrepresented sequences in the promoters of CgMar1-activated genes. Motifs found to be overrepresented in the promoters of CgMar1-activated genes, as found by the DREME tool. Sequences located upstream (-1000 to -1 bp) of the genes found to be activated by CgMar1 were retrieved from PathoYeastract and submitted to DREME. The prediction was made with default parameters. The sequences shown correspond to the motifs outputted by DREME, excluding TATA-box motifs.

6.5 Conclusions

The relevance of membrane lipid homeostasis during azole stress has been mostly associated with ergosterol synthesis and maintenance of the correspondent structural and functional properties. Here, we demonstrate a role for sphingolipid homeostasis in the plasma membrane in mediating fluconazole resistance in *C. glabrata*. Mechanistic insights are provided on how sphingolipid incorporation in the plasma membrane contributes to azole resistance, namely by decreasing plasma membrane permeability and, consequently, intracellular drug accumulation. This newly uncovered pathway towards azole resistance was found to be controlled, at least partially by the transcription factor CgMar1 and its target genes, particularly the sphingolipid flippase CgRsb1.

6.6 Acknowledgements

We acknowledge John Bennett from the National Institute of Allergy and Infectious Diseases, NIH, Bethesda, USA, for kindly providing the L5U1 strain.

This work was supported by “Fundação para a Ciência e a Tecnologia” (FCT) [Contracts PTDC/BBB-BIO/4004/2014 and PTDC/BII-BIO/28216/2017, PhD grants to PP and MG and post-doctoral grant to CC]. Funding received by iBB-Institute for Bioengineering and Biosciences from FCT-Portuguese Foundation for Science and Technology (UID/BIO/04565/2013) and from Programa Operacional Regional de Lisboa 2020 (Project N. 007317) is acknowledged. This study was partly supported by a Joint Usage/Research Program of the Medical Mycology Research Center, Chiba University.

6.7 References

1. Azie, N.; Neofytos, D.; Pfaller, M.; Meier-Kriesche, H.U.; Quan, S.P.; Horn, D. The PATH (Prospective Antifungal Therapy) Alliance® registry and invasive fungal infections: update 2012. *Diagn. Microbiol. Infect. Dis.* **2012**, *73*, 293–300.

2. Khatib, R.; Johnson, L.B.; Fakih, M.G.; Riederer, K.; Briski, L. Current trends in candidemia and species distribution among adults: *Candida glabrata* surpasses *C. albicans* in diabetic patients and abdominal sources. *Mycoses* **2016**, *59*, 781–786.

3. Wisplinghoff, H.; Bischoff, T.; Tallent, S.M.; Seifert, H.; Wenzel, R.P.; Edmond, M.B. Nosocomial Bloodstream Infections in US Hospitals: Analysis of 24,179 Cases from a Prospective Nationwide Surveillance Study. *Clin. Infect. Dis.* **2004**, *39*, 309–317.

4. Edmond, M.B.; Wallace, S.E.; McClish, D.K.; Pfaller, M.A.; Jones, R.N.; Wenzel, R.P. Nosocomial bloodstream infections in United States hospitals: a three-year analysis. *Clin. Infect. Dis.* **1999**, *29*, 239–244.

5. Petrikkos, G.; Skiada, A. Recent advances in antifungal chemotherapy. *Int. J. Antimicrob. Agents* **2007**, *30*, 108–117.

6. Revie, N.M.; Iyer, K.R.; Robbins, N.; Cowen, L.E. Antifungal drug resistance: evolution, mechanisms and impact. *Curr. Opin. Microbiol.* **2018**, *45*, 70–76.

7. Ghannoum, M.A.; Rice, L.B. Antifungal agents: mode of action, mechanisms of resistance, and correlation of these mechanisms with bacterial resistance. *Clin. Microbiol. Rev.* **1999**, *12*, 501–517.

8. Vermitsky, J.P.; Edlind, T.D. Azole resistance in *Candida glabrata*: coordinate upregulation of multidrug transporters and evidence for a Pdr1-like transcription factor. *Antimicrob. Agents Chemother.* **2004**, *48*, 3773–3781.

9. Costa, C.; Pires, C.; Cabrito, T.R.; Renaudin, A.; Ohno, M.; Chibana, H.; Sá-Correia, I.; Teixeira, M.C. *Candida glabrata* drug: H+antiporter CgQdr2 confers imidazole drug resistance, being activated by transcription factor CgPdr1. *Antimicrob. Agents Chemother.* **2013**, *57*, 3159-3167.

10. Vermitsky, J.P.; Earhart, K.D.; Smith, W.L.; Homayouni, R.; Edlind, T.D.; Rogers, P.D. Pdr1 regulates multidrug resistance in *Candida glabrata*: gene disruption and genome-wide expression studies. *Mol. Microbiol.* **2006**, *61*, 704–722.

11. Caudle, K.E.; Barker, K.S.; Wiederhold, N.P.; Xu, L.; Homayouni, R.; Rogers, P.D. Genomewide expression profile analysis of the *Candida glabrata* Pdr1 regulon. *Eukaryot. Cell* **2011**, *10*, 373–383.

12. Tsai, H.F.; Krol, A.A.; Sarti, K.E.; Bennett, J.E. *Candida glabrata PDR1*, a Transcriptional Regulator of a Pleiotropic Drug Resistance Network, Mediates Azole Resistance in Clinical Isolates and Petite Mutants. *Antimicrob. Agents Chemother.* **2006**, *50*, 1384–1392.

13. Coste, A.; Turner, V.; Ischer, F.; Morschhäuser, J.; Forche, A.; Selmecki, A.; Berman, J.; Bille, J.; Sanglard, D. A mutation in Tac1p, a transcription factor regulating *CDR1* and *CDR2*, is coupled with loss of heterozygosity at chromosome 5 to mediate antifungal resistance in *Candida albicans*. *Genetics* **2006**, *172*, 2139–2156.

14. Coste, A.; Selmecki, A.; Forche, A.; Diogo, D.; Bougnoux, M.E.; D'Enfert, C.; Berman, J.; Sanglard, D. Genotypic evolution of azole resistance mechanisms in sequential *Candida albicans* isolates. *Eukaryot. Cell* **2007**, *6*, 1889–1904.

15. Coste, A.T.; Karababa, M.; Ischer, F.; Bille, J.; Sanglard, D. *TAC1*, Transcriptional Activator of *CDR* Genes, Is a New Transcription Factor Involved in the Regulation of *Candida albicans* ABC Transporters *CDR1* and *CDR2*. *Eukaryot. Cell* **2004**, *3*, 1639–1652.

16. Morschhäuser, J.; Barker, K.S.; Liu, T.T.; Blaß-Warmuth, J.; Homayouni, R.; Rogers, P.D. The Transcription Factor Mrr1p Controls Expression of the *MDR1* Efflux Pump and Mediates Multidrug Resistance in *Candida albicans*. *PLoS Pathog.* **2007**, *3*, e164.

17. Dunkel, N.; Blaß, J.; Rogers, P.D.; Morschhäuser, J. Mutations in the multi-drug resistance regulator *MRR1*, followed by loss of heterozygosity, are the main cause of *MDR1* overexpression in fluconazole-resistant *Candida albicans* strains. *Mol. Microbiol.* **2008**, *69*, 827–840.

18. Ueno, K.; Uno, J.; Nakayama, H.; Sasamoto, K.; Mikami, Y.; Chibana, H. Development of a highly efficient gene targeting system induced by transient repression of *YKU80* expression in *Candida glabrata*. *Eukaryot. Cell* **2007**, *6*, 1239–1247.

19. Chen, K.H.; Miyazaki, T.; Tsai, H.F.; Bennett, J.E. The bZip transcription factor Cgap1p is involved in multidrug resistance and required for activation of multidrug transporter gene *CgFLR1* in *Candida glabrata*. *Gene* **2007**, *386*, 63–72.

20. Jansen, G.; Wu, C.; Schade, B.; Thomas, D.Y.; Whiteway, M. Drag&Drop cloning in yeast. *Gene* **2005**, *344*, 43–51.

21. Ueno, K.; Matsumoto, Y.; Uno, J.; Sasamoto, K.; Sekimizu, K.; Kinjo, Y.; Chibana, H. Intestinal resident yeast *Candida glabrata* requires Cyb2p-Mediated lactate assimilation to adapt in mouse intestine. *PLoS One* **2011**, *6*, e24759.

22. Costa, C.; Henriques, A.; Pires, C.; Nunes, J.; Ohno, M.; Chibana, H.; Sá-Correia, I.; Teixeira, M.C. The dual role of *Candida glabrata* drug:H+ antiporter CgAqr1 (ORF *CAGL0J09944g*) in antifungal drug and acetic acid resistance. *Front. Microbiol.* **2013**, *4*, 170.

23. Costa, C.; Nunes, J.; Henriques, A.; Mira, N.P.; Nakayama, H.; Chibana, H.; Teixeira, M.C. *Candida glabrata* drug:H+antiporter CgTpo3 (ORF *CAGL0I10384g*): Role in azole drug resistance and polyamine homeostasis. *J. Antimicrob. Chemother.* **2014**, *69*, 1767–1776.

24. Pais, P.; Pires, C.; Costa, C.; Okamoto, M.; Chibana, H.; Teixeira, M.C. Membrane proteomics analysis of the *Candida glabrata* response to 5-flucytosine: Unveiling the role and regulation of the drug efflux transporters CgFlr1 and CgFlr2. *Front. Microbiol.* **2016**, *7*, 2045.

25. Pais, P.; Costa, C.; Pires, C.; Shimizu, K.; Chibana, H.; Teixeira, M.C. Membrane Proteome-Wide Response to the Antifungal Drug Clotrimazole in *Candida glabrata* : Role of the Transcription Factor CgPdr1 and the Drug:H+ Antiporters CgTpo1_1 and CgTpo1_2. *Mol. Cell. Proteomics* **2016**, *15*, 57-72.

26. Romão, D.; Cavalheiro, M.; Mil-Homens, D.; Santos, R.; Pais, P.; Costa, C.; Takahashi-Nakaguchi, A.; Fialho, A.M.; Chibana, H.; Teixeira, M.C. A New Determinant of *Candida glabrata* Virulence: The Acetate Exporter CgDtr1. *Front. Cell. Infect. Microbiol.* **2017**, *7*, 473.

27. Zordan, R.E.; Ren, Y.; Pan, S.J.; Rotondo, G.; Peñas, A.D. Las; Iluore, J.; Cormack, B.P. Expression Plasmids for Use in *Candida glabrata*. *G3(Bethesda)* **2013**, *3*, 1675–1686.

28. Jiang, H.; Lei, R.; Ding, S.W.; Zhu, S. Skewer: a fast and accurate adapter trimmer for next-generation sequencing paired-end reads. *BMC Bioinformatics* **2014**, *15*, 182.

29. Trapnell, C.; Pachter, L.; Salzberg, S.L. TopHat: Discovering splice junctions with RNA-Seq. *Bioinformatics* **2009**, *25*, 1105–1111.

30. Anders, S.; Huber, W. Differential expression analysis for sequence count data. *Genome Biol.* **2010**, *11*, R106.

31. Love, M.I.; Huber, W.; Anders, S. Moderated estimation of fold change and dispersion for RNA-seq data with DESeq2. *Genome Biol.* **2014**, *15*, 550.

32. Rosa, M.F.; Sá-Correia, I. Intracellular acidification does not account for inhibition of *Saccharomyces cerevisiae* growth in the presence of ethanol. *FEMS Microbiol. Lett.* **1996**, *135*, 271–274.

33. Monteiro, P.T.; Pais, P.; Costa, C.; Manna, S.; Sá-Correia, I.; Teixeira, M.C. The PathoYeastract database: An information system for the analysis of gene and genomic transcription regulation in pathogenic yeasts. *Nucleic Acids Res.* **2017**, *45*, D597–D603.

34. Bailey, T.L. DREME: motif discovery in transcription factor ChIP-seq data. *Bioinformatics* **2011**, *27*, 1653–1659.

35. Gasch, A.P.; Spellman, P.T.; Kao, C.M.; Carmel-Harel, O.; Eisen, M.B.; Storz, G.; Botstein, D.; Brown, P.O. Genomic Expression Programs in the Response of Yeast Cells to Environmental Changes. *Mol. Biol. Cell* **2000**, *11*, 4241–4257.

36. Causton, H.C.; Ren, B.; Koh, S.S.; Harbison, C.T.; Kanin, E.; Jennings, E.G.; Lee, T.I.; True, H.L.; Lander, E.S.; Young, R.A. Remodeling of Yeast Genome Expression in Response to Environmental Changes. *Mol. Biol. Cell* **2001**, *12*, 323–337.

37. Brion, C.; Pflieger, D.; Souali-Crespo, S.; Friedrich, A.; Schacherer, J. Differences in environmental stress response among yeasts is consistent with species-specific lifestyles. *Mol. Biol. Cell* **2016**, *27*, 1694–705.

38. Carlson, M. Glucose repression in yeast. *Curr. Opin. Microbiol.* **1999**, *2*, 202–207.

39. Ozcan, S.; Johnston, M. Three different regulatory mechanisms enable yeast hexose transporter (HXT) genes to be induced by different levels of glucose. *Mol. Cell. Biol.* **1995**, *15*, 1564–1572.

40. Ozcan, S.; Johnston, M. Function and regulation of yeast hexose transporters. *Microbiol. Mol. Biol. Rev.* **1999**, *63*, 554–569.

41. Briones-Martin-Del-Campo, M.; Orta-Zavalza, E.; Juarez-Cepeda, J.; Gutierrez-Escobedo, G.; Cañas-Villamar, I.; Castaño, I.; De Las Peñas, A. The oxidative stress response of the opportunistic fungal pathogen *Candida glabrata*. *Rev. Iberoam. Micol.* **2014**, *31*, 67-71.

42. Lu, S.C. Glutathione synthesis. *Biochim. Biophys. Acta - Gen. Subj.* **2013**, *1830*, 3143–3153.

43. Cowart, L.A.; Obeid, L.M. Yeast sphingolipids: recent developments in understanding biosynthesis, regulation, and function. *Biochim. Biophys. Acta* **2007**, *1771*, 421–431.

44. Mishra, N.N.; Prasad, T.; Sharma, N.; Gupta, D.K. Membrane fluidity and lipid composition of fluconazole resistant and susceptible strains of *Candida albicans* isolated from diabetic patients. *Brazilian J. Microbiol.* **2008**, *39*, 219–225.

45. Khandelwal, N.K.; Sarkar, P.; Gaur, N.A.; Chattopadhyay, A.; Prasad, R. Phosphatidylserine decarboxylase governs plasma membrane fluidity and impacts drug susceptibilities of *Candida albicans* cells. *Biochim. Biophys. Acta - Biomembr.* **2018**, *1860*, 2308–2319.

46. Löffler, J.; Einsele, H.; Hebart, H.; Schumacher, U.; Hrastnik, C.; Daum, G. Phospholipid and sterol analysis of plasma membranes of azole-resistant *Candida albicans* strains. *FEMS Microbiol. Lett.* **2000**, *185*, 59–63.

47. Gao, J.; Wang, H.; Li, Z.; Wong, A.H.H.; Wang, Y-Z.; Guo, Y.; Lin, X.; Zeng, G.; Wang, Y.; Wang, J. *Candida albicans* gains azole resistance by altering sphingolipid composition. *Nat. Commun.* **2018**, *9*, 4495.

48. Singh, A.; Yadav, V.; Prasad, R. Comparative Lipidomics in Clinical Isolates of *Candida albicans* Reveal Crosstalk between Mitochondria, Cell Wall Integrity and Azole Resistance. *PLoS One* **2012**, *7*, e39812.

49. Bittman, R.; Kasireddy, C.R.; Mattjus, P.; Slotte, J.P. Interaction of cholesterol with sphingomyelin in monolayers and vesicles. *Biochemistry* **1994**, *33*, 11776–11781.

50. Prasad, R.; Khandelwal, N.K.; Banerjee, A. Yeast ABC transporters in lipid trafficking. *Fungal Genet. Biol.* **2016**, *93*, 25–34.

51. Sgherri, C.; Porta, A.; Castellano, S.; Pinzino, C.; Quartacci, M.F.; Calucci, L. Effects of azole treatments on the physical properties of *Candida albicans* plasma membrane: A spin probe EPR study. *Biochim. Biophys. Acta - Biomembr.* **2014**, *1838*, 465–473.

52. Rogers, P.D.; Vermitsky, J.P.; Edlind, T.D.; Hilliard, G.M. Proteomic analysis of experimentally induced azole resistance in *Candida glabrata*. *J. Antimicrob. Chemother.* **2006**, *58*, 434–438.

53. Kaur, R.; Ma, B.; Cormack, B.P. A family of glycosylphosphatidylinositol-linked aspartyl proteases is required for virulence of *Candida glabrata*. *Proc. Natl. Acad. Sci.* **2007**, *104*, 7628-7633.

54. Bairwa, G.; Kaur, R. A novel role for a glycosylphosphatidylinositol-anchored aspartyl protease, CgYps1, in the regulation of pH homeostasis in *Candida glabrata*. *Mol. Microbiol.* **2011**, *79*, 900-913.

55. Copping, V.M.S.; Barelle, C.J.; Hube, B.; Gow, N.A.R.; Brown, A.J.P.; Odds, F.C. Exposure of *Candida albicans* to antifungal agents affects expression of *SAP2* and *SAP9* secreted proteinase genes. *J. Antimicrob. Chemother.* **2005**, *55*, 645–654.

56. Gatta, A.T.; Wong, L.H.; Sere, Y.Y.; Calderón-Noreña, D.M.; Cockcroft, S.; Menon, A.K.; Levine, T.P. A new family of StART domain proteins at membrane contact sites has a role in ER-PM sterol transport. *Elife* **2015**, *4*, e07253.

57. Mao, C.; Xu, R.; Bielawska, A.; Obeid, L.M. Cloning of an alkaline ceramidase from *Saccharomyces cerevisiae*. An enzyme with reverse (CoA-independent) ceramide synthase activity. *J. Biol. Chem.* **2000**, *275*, 6876–6884.

58. Kihara, A.; Igarashi, Y. Identification and Characterization of a *Saccharomyces cerevisiae* Gene, *RSB1* , Involved in Sphingoid Long-chain Base Release. *J. Biol. Chem.* **2002**, *277*, 30048–30054.

59. Fernández-Murray, J.P.; Gaspard, G.J.; Jesch, S.A.; McMaster, C.R. *NTE1* -encoded Phosphatidylcholine Phospholipase B Regulates Transcription of Phospholipid Biosynthetic Genes. *J. Biol. Chem.* **2009**, *284*, 36034–36046.

60. Fernández Murray, J.P.; McMaster, C.R. Nte1p-mediated Deacylation of Phosphatidylcholine Functionally Interacts with Sec14p. *J. Biol. Chem.* **2005**, *280*, 8544–8552.

61. Hancock, L.C.; Behta, R.P.; Lopes, J.M. Genomic Analysis of the Opi$^-$ Phenotype. *Genetics* **2006**, *173*, 621–634.

62. Tsai, H.F.; Sammons, L.R.; Zhang, X.; Suffis, S.D.; Su, Q.; Myers, T.G.; Marr, K.A.; Bennett, J.E. Microarray and molecular analyses of the azole resistance mechanism in *Candida glabrata* oropharyngeal isolates. *Antimicrob. Agents Chemother.* **2010**, *54*, 3308–3317.

63. Ferrari, S.; Sanguinetti, M.; Torelli, R.; Posteraro, B.; Sanglard, D. Contribution of *CgPDR1*-Regulated Genes in Enhanced Virulence of Azole-Resistant *Candida glabrata*. *PLoS One* **2011**, *6*, e17589.

64. Paul, S.; Bair, T.B.; Moye-Rowley, W.S. Identification of genomic binding sites for *Candida glabrata* Pdr1 transcription factor in wild-type and ρ0 cells. *Antimicrob. Agents Chemother.* **2014**, *58*, 6904–6912.

65. Kihara, A.; Igarashi, Y. Cross Talk between Sphingolipids and Glycerophospholipids in the Establishment of Plasma Membrane Asymmetry. *Mol. Biol. Cell* **2004**, *15*, 4949–4959.

66. Barker, K.S.; Crisp, S.; Wiederhold, N.; Lewis, R.E.; Bareither, B.; Eckstein, J.; Barbuch, R.; Bard, M.; Rogers, P.D. Genome-wide expression profiling reveals genes associated with amphotericin B and fluconazole resistance in experimentally induced antifungal resistant isolates of *Candida albicans*. *J. Antimicrob. Chemother.* **2004**, *54*, 376–385.

67. Jia, X.M.; Ma, Z.P.; Jia, Y.; Gao, P.H.; Zhang, J.D.; Wang, Y.; Xu, Y.G.; Wang, L.; Cao, Y.Y.; Cao, Y.B.; *et al. RTA2*, a novel gene involved in azole resistance in *Candida albicans*. *Biochem. Biophys. Res. Commun.* **2008**, *373*, 631–636.

68. Jia, X.M.; Wang, Y.; Jia, Y.; Gao, P.H.; Xu, Y.G.; Wang, L.; Cao, Y.Y.; Cao, Y.B.; Zhang, L.X.; Jiang, Y.Y. *RTA2* is involved in calcineurin-mediated azole resistance and sphingoid long-chain base release in *Candida albicans*. *Cell. Mol. Life Sci.* **2009**, *66*, 122–34.

69. Wang, L.; Jia, Y.; Tang, R.J.; Xu, Z.; Cao, Y.B.; Jia, X.M.; Jiang, Y.Y. Proteomic Analysis of Rta2p-Dependent Raft-Association of Detergent-Resistant Membranes in *Candida albicans*. *PLoS One* **2012**, *7*, e37768.

70. Liu, T.T.; Lee, R.E.B.; Barker, K.S.; Lee, R.E.; Wei, L.; Homayouni, R.; Rogers, P.D. Genome-Wide Expression Profiling of the Response to Azole, Polyene, Echinocandin, and Pyrimidine Antifungal Agents in *Candida albicans*. *Antimicrob. Agents Chemother.* **2005**, *49*, 2226–2236.

71. Whaley, S.G.; Tsao, S.; Weber, S.; Zhang, Q.; Barker, K.S.; Raymond, M.; Rogers, P.D. The *RTA3* Gene, Encoding a Putative Lipid Translocase, Influences the Susceptibility of *Candida albicans* to Fluconazole. *Antimicrob. Agents Chemother.* **2016**, *60*, 6060–6066.

72. Huang, W.; Liao, G.; Baker, G.M.; Wang, Y.; Lau, R.; Paderu, P.; Perlin, D.S.; Xue, C. Lipid Flippase Subunit Cdc50 Mediates Drug Resistance and Virulence in *Cryptococcus neoformans*. *MBio* **2016**, *7*, e00478-16.

73. Vanden Bossche, H.; Koymans, L.; Moereels, H. P450 inhibitors of use in medical treatment: focus on mechanisms of action. *Pharmacol. Ther.* **1995**, *67*, 79–100.

74. Abe, F.; Usui, K.; Hiraki, T. Fluconazole modulates membrane rigidity, heterogeneity, and water penetration into the plasma membrane in *Saccharomyces cerevisiae*. *Biochemistry* **2009**, *48*, 8494–504.

7 General Discussion

Antifungal resistance, especially to the commonly used azole drugs, is particularly frequent in some of the pathogenic *Candida* species, such as *C. glabrata*. Due to the limitation of therapeutic options available to treat candidiasis patients, it is crucial to gain full understanding of the molecular basis of antifungal drug resistance to devise more effective antifungal therapies. Transcription networks represent promising therapeutic targets, as they enable the inhibition in a single step of entire pathways, potentially hindering multiple effectors of antifungal resistance.

With that aim in mind, this thesis focused on the disclosure of new pathways involved in antifungal resistance and on providing valuable knowledge on the understanding of resistance mechanisms, in their full complexity. Figure 7.1 provides a comprehensive representation of the data gathered in this thesis and its integration with previous knowledge on azole and 5-flucytosine resistance.

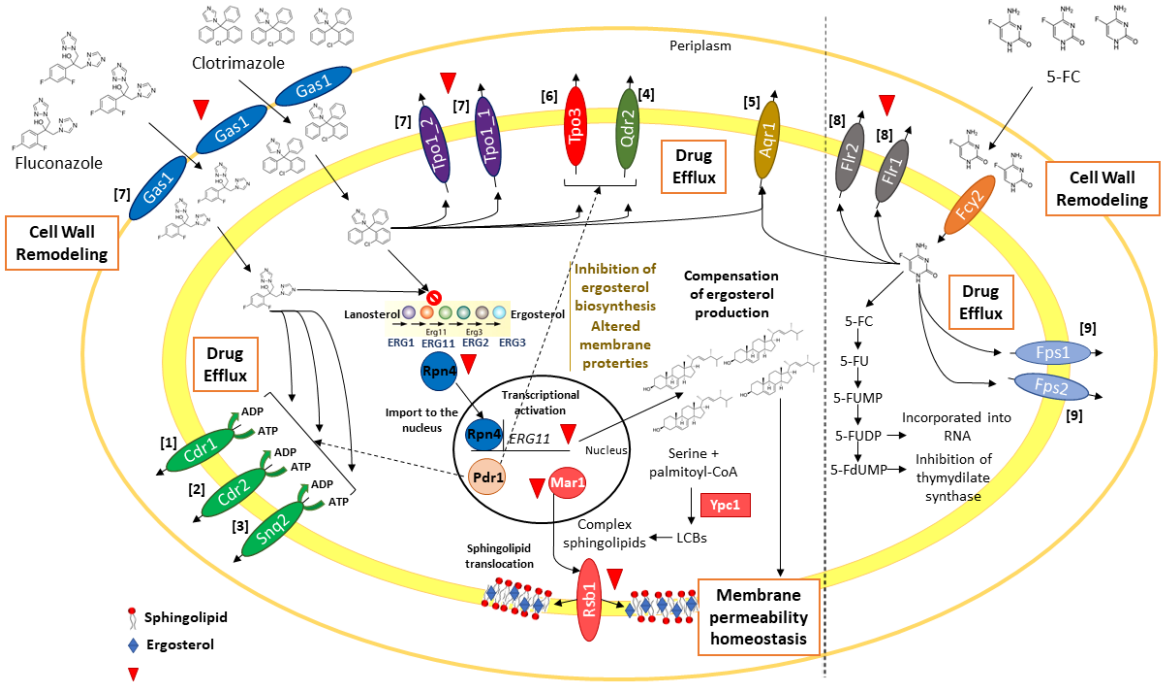

Figure 7.1 – Proposed model for the knowledge gathered in this thesis work on new regulators and effectors involved in azole and flucytosine resistance, integrated with known resistance mechanisms in *C. glabrata*. Red inverted triangles represent novel genes or mechanisms identified in this thesis. [1] Sanglard *et al.* AAC 43:2753-2765, 1999.; [2] Miyazaki *et al.* AAC 42(7):1695-701, 1998.; [3] Torelli *et al.* Mol Microbiol 68:186-201, 2008.; [4] Costa *et al.* AAC 57(7):3159-67, 2013.; [5] Costa *et al.* Front Microbiol 4:170, 2013.; [6] Costa *et al.* JAC 69:1767-76, 2014.; [7] Pais *et al.* MCP 15(1):57-72, 2016.; [8] Pais *et al.* Front Microbiol 7:2045, 2016.; [9] Costa *et al.* PLoS One 10(8):e0135110, 2015.

First, clotrimazole and 5-flucytosine exposure was found to result in the occurrence of cell wall remodeling. Through a membrane proteomics study, the cell wall assembly protein CgGas1 was found to be overexpressed upon clotrimazole stress and required for basal cell wall structure, contributing to reduced drug accumulation. Cell wall remodeling could therefore play a role in reducing the diffusion of antifungal molecules before reaching the plasma membrane, working as a passive first line barrier. Once antifungals reach the cell, distinct pathways focused on reducing intracellular drug accumulation take place, either by drug efflux or modulation of plasma membrane permeability. In response to 5-flucytosine, the MFS transporters CgFlr1 and CgFlr2 were found to mediate 5-flucytosine resistance by reducing its intracellular accumulation in *C. glabrata* cells [1]. Resistance to clotrimazole has been associated with drug efflux as well. Together with the well-known role of ABC drug efflux pumps in this context, the MFS transporters CgTpo1_1 and CgTpo1_2 were also found to mediate clotrimazole resistance, which complements the observed cell wall remodeling in the reduction of intracellular clotrimazole accumulation. Interestingly, reduced clotrimazole levels were also associated with CgFlr2 action, putting this transporter directly in the crossroads of the MDR phenomenon. Knowledge gathered in this work highlights that clotrimazole resistance is based on a multifactorial nature and crosstalk between resistance mechanisms.

In what concerns fluconazole, resistance is not only supported by the known role of ABC transporters [2–4] but was here found to be regulated by two new TFs in pathways unrelated with drug efflux. Once fluconazole reaches yeast cells, the TF CgRpn4 is activated via translocation to the nucleus and upregulates the expression of *ERG* genes, including direct activation of *CgERG11*. This was found to minimize the reduction of ergosterol levels due to fluconazole inhibition of CgErg11, resulting in maintenance of plasma membrane permeability and consequently reduced fluconazole accumulation in *C. glabrata* cells. On the other hand, sphingolipid metabolism was found to be required for full fluconazole resistance in *C. glabrata*. The TF CgMar1 regulates membrane sphingolipid composition by activation of *CgRSB1*, which catalyzes sphingosine integration into the lipid bilayer. This pathway was found to modulate membrane permeability and reduce intracellular drug accumulation. Given that both azoles and 5-flucytosine have intracellular targets, it is consistent that resistance to these antifungals is based on reducing their intracellular load. The data collected in this thesis elucidates

new networks and mechanisms on how such result is achieved. The cell wall acts as passive barrier against diffusion of drugs, reducing the number of antifungal molecules reaching the cells. The drug molecules that reach the plasma membrane see their diffusion limited by ergosterol and sphingolipids that confer plasma membrane impermeabilization, and finally those drug molecules that do enter the cell are pumped out. Altogether, these mechanisms, regulated by different transcription factors, act in a sequential and complementary way to prevent antifungal build-up in *C. glabrata*.

The regulon of the TF CgPdr1 and its contribution in *C. glabrata* azole resistance, especially fluconazole, has been addressed in several transcriptomics studies [5–10]. CgPdr1-mediated azole resistance has been associated with the upregulation of MDR transporter genes such as *CgCDR1*, *CgCDR2*, *CgSNQ2*, *CgQDR2* and *CgTPO3*; in the clinical context CgPdr1-mediated azole resistance develops through the acquisition of GOF mutations in the *CgPDR1* gene [5,11–13]. The proteomics approach detailed in this thesis provides a broader view on the role of this TF by assessing its role in the resistance to antifungals other than fluconazole at the membrane proteome levels. CgPdr1 regulation over 50% of the membrane proteome changes occurring in response to clotrimazole highlights the role of CgPdr1 as a determinant of resistance to imidazoles and the existence of additional targets of this TF. Moreover, this approach enabled the identification of two new MFS transporters, CgTpo1_1 and CgTpo1_2, as clotrimazole resistance determinants. This indicates that imidazole resistance, just as registered for triazoles, is mediated by antifungal transport, albeit mediated by additional transporters from the MFS family. Traditionally, ABC transporters have been associated with acquisition of azole resistance in *C. glabrata* clinical isolates. Additional work performed by our group has highlighted the relevance of MFS transporters in clinical azole resistance phenotypes, including both CgTpo1_1 and CgTpo1_2 [11,14,15], which further supports the relevance of their functional characterization conducted in the work presented in this thesis.

Although regarded as a master regulator of azole resistance, this work described the participation of CgPdr1 in 5-flucytosine resistance. CgPdr1 was found to regulate a significant portion of the membrane proteome response to 5-flucytosine in *C. glabrata*. The used membrane proteomics approach enabled the identification of the MFS transporters CgFlr1 and CgFlr2 as mediators of 5-flucytosine resistance. Regarded as a major azole resistance factor, drug efflux is here described as a mechanism of 5-

flucytosine resistance, highlighting the relevance of this mechanism in *C. glabrata* MDR. Knowledge gathered with this work reinforces the notion that inhibition of membrane transporters could be a viable strategy to counteract antifungal resistance phenotypes, as it could potentially disrupt the basis for resistance to multiple antifungals. The ability of *C. glabrata* to acquire MDR has been reinforced with an increasing number of studies that report strains resistant to two or more classes antifungal drugs, often by the development of specific resistance mechanisms [16–21]. Indeed, our results suggest that there is potential for cross-resistance development between 5-flucytosine and azoles, as reported in *Candida lusitaniae* [22]. Work in this thesis contributed to uncover CgPdr1 as a common resistance regulator against antifungals from distinct classes, but also two drugs that can be used in combination therapy [23,24]. Evolutionary studies could be useful to determine if this could be part of an adaptive response to concurrent or sequential treatment regiments in the clinical practice, consequently used to delineate better therapeutic strategies. Furthermore, the finding that response to both clotrimazole and 5-flucytosine can result from a common regulator underscores the relevance of targeting regulatory networks as promising therapeutic options.

Further, *CgTPO1_1* and *CgTPO1_2* expression during azole stress was found to be irrespective of CgPdr1 regulation [25], highlighting the existence of additional regulatory networks taking place in efflux pump control. Beyond a role in 5-flucytosine resistance, CgFlr2 was also found to contribute to clotrimazole resistance [1], and previous work in our group has identified the MFS transporter CgAqr1 as a mediator of both clotrimazole and 5-flucytosine resistance [26]. This emphasizes the pertinence of MDR transporters in resistance phenotypes to multiple drugs, but also the existence of additional networks of antifungal resistance.

Other than the role of MDR transporters in reducing antifungal accumulation inside *C. glabrata* cells, the work detailed in this thesis also describes the occurrence of cell wall remodeling upon clotrimazole or 5-flucytosine stress. This is especially surprising once these antifungals are not known to target the cell wall, unlike the echinocandins. The data collected indicates that clotrimazole or 5-flucytosine can have a deleterious effect in the cell wall, triggering a remodeling response. This mechanism acts in conjunction with drug efflux by CgTpo1_2 to mediate clotrimazole resistance [25]. Data gathered in this study hints for a passive role of the cell wall to reduce the diffusion of antifungal

molecules reaching *C. glabrata* cells and drug efflux as complementary mechanisms, providing valuable insight on the crosstalk between pathways of antifungal resistance.

The potential for CgPdr1 or MDR transporters targeting to provide better therapeutic options could also benefit from their overlapping role in host interaction. The contribution of CgPdr1 GOF mutations is not only associated with the acquisition of azole resistance in clinical isolates, but also with enhancing virulence [27–30]. Mitochondrial dysfunction has been associated with antifungal resistance phenotypes and the participation of CgPdr1 in this phenotype has been reported [7]. Interestingly, mitochondrial dysfunction has also been associated with increased virulence, as an azole-resistant *C. glabrata* clinical isolate not only exhibited mitochondrial dysfunction and upregulation of *CgCDR1* and *CgCDR2*, but also was more virulent than its susceptible counterpart in both systemic and vaginal murine infection models [31]. Current knowledge seems to indicate a connection between antifungal resistance and virulence in *C. glabrata*. MDR transporters, particularly from the MFS family, have also been associated with host interaction functions. After the work conducted in this thesis, relative to the functional characterization of CgTpo1_1 and CgTpo1_2, other studies from our group have implicated these membrane transporters in virulence pathways. CgTpo1_1 mediates resistance to the human antimicrobial peptide histatin-5 [32], CgTpo1_2 plays a role in biofilm formation [32] and CgDtr1 confers resistance to hemocyte-related stress [33]; each resulting in decreased virulence in the *Galleria mellonella* infection model. The uncover of new effectors of antifungal therapy, which also participate in other fungal pathways that underlie important virulence features, represent promising targets for more effective therapeutic strategies. In fact, a thorough review of the host-pathogen interactions mediated by MDR transporters clearly shows the promiscuity of these proteins and their intricated roles in multiple processes [34]. In light of this knowledge, the inhibition of efflux pumps appears more and more to be a promising therapeutic option. Optimally, disruption of these proteins can have impact not only in the abrogation of drug resistance, but also virulence features, which could prove to be highly effective in the treatment of fungal infections.

Despite the central role of CgPdr1 and GOF mutations as the basis for the acquisition of azole resistance in *C. glabrata* clinical isolates, some studies have reported the finding of azole resistant isolates that exhibit no GOF mutations in the *CgPDR1* gene [5,35–37]. Due to the prevalence of this pathway among resistant isolates, most studies probing

azole resistant isolates focus on the characterization of CgPdr1 mutations and their effect in the expression of ABC efflux pumps. As a result, multiple GOFs have been identified in *CgPDR1* in azole resistant clinical isolates (e.g., [8,27,38]). However, a fraction of azole resistant isolates that do not harbor *CgPDR1* mutations are often overlooked and the mechanisms responsible for azole resistance remain uncharacterized. An ongoing work in our group is indeed focused in screening a collection of more than one hundred *C. glabrata* clinical isolates for isolates exhibiting azole resistance but not *CgPDR1* GOF mutations; so far, such isolates appear to account for a minority, but still a significant part of the collection. Therefore, the study of azole resistance mechanisms beyond the CgPdr1 network is warranted and could provide new clues on how the acquisition of azole resistance evolves in *C. glabrata* in the clinical setting.

C. glabrata is more prone to acquire mutations with significant phenotypes due to its haploid nature [38]. This is reflected in the number of resistance mechanisms arising from this process, such as resistance to azoles mediated by *CgPDR1* GOFs or echinocandin resistance mediated by *FKS* mutations. On the contrary, unlike *C. albicans*, where azole resistance also includes CaErg11 mutations, such mechanism is not believed to have clinical impact in *C. glabrata* [39–42]. It appears that *ERG* mediated azole resistance in *C. glabrata* could be achieved by increased gene expression rather than mutations, resembling the *ERG11* upregulation observed in other *Candida* species [11,43–45]. This work details the role of the TF CgRpn4 in the upregulation of ergosterol biosynthesis genes, especially *CgERG11*, and how it contributes to minimize plasma membrane permeability and fluconazole accumulation in *C. glabrata* cells. It is plausible that *ERG* gene upregulation could be achieved by mutations in regulators of the ergosterol pathway, resembling the network of CgPdr1 and MDR transporters. Although not part of the studies detailed in this thesis, work carried out in our group identified CgRpn4 mutations in azole resistant *C. glabrata* clinical isolates. Notably, these strains harbor wild-type *CgPDR1* genes, indicating that the resistance phenotypes are irrespective of the master regulator. Future perspectives include functional characterization of the identified CgRpn4 mutations to assess their potential as GOF mutations and basis for azole resistance in these strains. Moreover, these preliminary results hint for a possible participation of CgRpn4 in the acquisition of clinical azole resistance.

Together with the role of CgRpn4 in regulation of plasma membrane properties during azole stress, this work also identified the TF CgMar1 in the regulation of the lipid composition of the *C. glabrata* membrane, namely through upregulation of *CgRSB1* and control of sphingolipid homeostasis. The plasma membrane is a complex structure of multiple components, each contributing to structural and functional properties [46,47]. Regulation of sphingolipid homeostasis by CgMar1 and its role in azole resistance indicates that despite ergosterol being the azole target, other lipid components of the plasma membrane contribute to alleviate azole stress. This rational could justify the role of CgMar1 in controlling membrane permeability and consequently drug accumulation, as sphingolipids can also play important structural and functional roles [47,48] and their regulation could be part of a compensatory mechanism to membrane stress, regardless of not being the primary antifungal target.

The role of plasma membrane homeostasis in azole resistance may go beyond permeability control. One could discuss that it can also be linked to its role in the localization of plasma membrane proteins. As discussed above, expression of MDR transporters is one of the most common resistance mechanisms to antifungal stress, especially azoles. It has been shown that defects in lipid raft constituents can affect the correct sorting of transporters to the membrane in *C. albicans* [49]. This could signal that expression of efflux pumps may not be enough to confer azole resistance if the underlying plasma membrane composition is not maintained. The role of sphingolipids gains special emphasis in this scenario, as they are main constituents in lipid raft domains [47] and imbalances in *C. albicans* raft lipids affects susceptibility to drugs [50]. As such, the incorporation of sphingolipids in the membrane influences several of its structural and functional properties. On the other hand, some MDR transporters are known to transport lipids across the bilayer or even incorporate lipid molecules in the membrane [46]. In *C. glabrata*, CgAus1 is a known ABC transporter involved in sterol uptake and consequently azole resistance [51,52]. In *S. cerevisiae*, the ABC pump ScPdr18 is involved in multi-stress resistance by mediating the incorporation of ergosterol in the membrane, influencing lipid order, permeability and membrane potential [53]. A similar role was found for *C. glabrata CgTPO1_2* expression, which modulates ergosterol and fatty acid content and plasma membrane potential [32]. Altogether, evidence shows the plasma membrane is a dynamic structure that alters its lipid composition according to multiple environmental stimuli. Consequently, lipid

homeostasis is a key feature that underlies the ability of yeasts to tolerate stress and is maintained through multiple mechanisms that act in a comprehensive system to protect a fine-tuned balance. The knowledge gathered with this work suggests that targeting lipid homeostasis could represent an alternative approach for innovative antifungal therapy, as it would have the advantage of disrupting multiple pathways as primary mode of action and/or facilitate the action of already established drugs. On one hand, disruption of multiple lipid components could effectively decrease *C. glabrata* cell viability through loss of structural properties, thus resulting in growth arrest. On the other hand, hindering membrane lipid homeostasis could be a relevant target for co-adjuvant therapy. The increased cell permeability would make current intracellular drug targets more available to current antifungals, which can be used to boost the effectiveness of current drugs. Additionally, the potential for disrupting MDR transporter sorting to the membrane can represent an alternative approach to the design of efflux pump inhibitors and effectively circumvent acquired resistance phenotypes by limiting drug efflux.

The biological knowledge obtained so far on transcriptional control in *C. glabrata* is complemented with the opportunities made available by the PathoYeastract database. Its bioinformatics tools that can be used, among other applications, to explore transcriptional networks involved in antifungal resistance to identify potentially new or overlooked targets to be studied as drug resistance determinants. On the other hand, regulatory networks governing known resistance determinants can also be predicted, providing clues to uncover potential unforeseen pathways in fungal pathogenesis. These tools can be used to make a comprehensive analysis of the experimental data gathered with this thesis. New MDR transporters and their regulation via CgPdr1 and CgYap1 were identified in this thesis. The newly gathered data can be crosschecked with the associations in PathoYeastract to draw a global regulatory network and further increase the knowledge on efflux pump regulation (Figure 7.2), thus providing further insight that could provide valuable information to target antifungal resistance networks. The possibility of cross species comparison and prediction means that there is room for gathering knowledge across the *Candida* genus. The participation of the new regulators of azole resistance described in this thesis has been associated to specific target genes. The use of PathoYeastract to compare their regulons with the correspondent networks in order species provides clues for additional regulators that could be involved in these

pathways, as well as the identification of complementary target genes directly involved in antifungal resistance networks. This can also help to assess network conservation among *Candida* species and assess the effectiveness of new therapeutic options in multiple species, according to the presence or absence of conserved therapeutic targets.

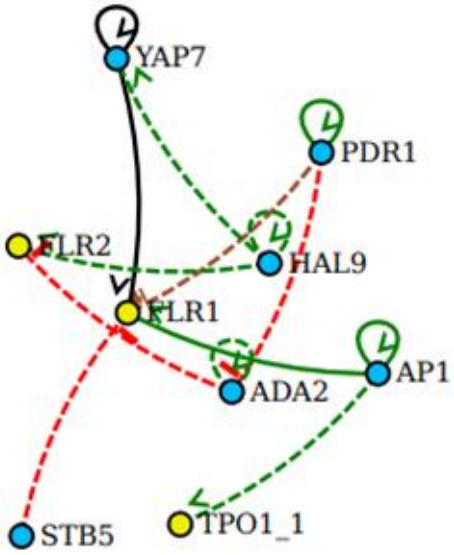

Figure 7.2 – Comprehensive regulatory network of the MDR transporters identified in this thesis as antifungal resistance determinants. The presented associations were drawn using the tools available at the PathoYeastract database.

Overall, his work contributes to enlighten how the membrane proteome changes upon antifungal stress and how membrane composition plays a role in antifungal susceptibility. The TF CgPdr1 is described as a relevant regulator of membrane proteome during antifungal stress response, while drug efflux mediated by MDR transporters is highlighted in imidazole resistance and discovered to be involved in 5-flucytosine resistance as well. The newly discovered TFs CgRpn4 and CgMar1 regulate distinct lipid components in the membrane, each of those in turn play different roles that contribute to overcome azole stress. This represents a complex structural and functional response at the plasma membrane level, lined by compensatory and possibly overlapping mechanisms to preserve a viable structure. The observation that three regulators of antifungal resistance act via membrane property regulation reveals

possible new targets to counteract the acquisition of resistance phenotypes and adds to the knowledge of additional resistance pathways taking place in *C. glabrata*.

With the inherent hardships for the development of antifungal drugs and the lack of known specific fungal targets available, therapeutic options focused on circumventing efflux-based resistance to conventional drugs look like a viable option. It would potentially save years of hard work and a lot of money in drug discovery pipelines, as the targets (efflux pumps or transcription factors) are already known proteins and their structural features well defined. This would mean successful reintegration of currently ineffective drugs in treatment regiments, potentially decreasing duration of treatment and healthcare associated costs, while improving patient clinical outcome. Ultimately, this would also contribute to decrease the rapid acquisition of clinical resistant phenotypes, with huge expected impact in improving the currently terrible prognosis associated to systemic *Candida* infections.

7.1 References

1. Pais, P.; Pires, C.; Costa, C.; Okamoto, M.; Chibana, H.; Teixeira, M.C. Membrane proteomics analysis of the *Candida glabrata* response to 5-flucytosine: Unveiling the role and regulation of the drug efflux transporters CgFlr1 and CgFlr2. *Front. Microbiol.* **2016**, *7*, 2045.

2. Sanglard, D.; Ischer, F.; Calabrese, D.; Majcherczyk, P.A.; Bille, J. The ATP binding cassette transporter gene *CgCDR1* from *Candida glabrata* is involved in the resistance of clinical isolates to azole antifungal agents. *Antimicrob. Agents Chemother.* **1999**, *43*, 2753–2765.

3. Miyazaki, H.; Miyazaki, Y.; Geber, A.; Parkinson, T.; Hitchcock, C.; Falconer, D.J.; Ward, D.J.; Marsden, K.; Bennett, J.E. Fluconazole resistance associated with drug efflux and increased transcription of a drug transporter gene, *PDH1*, in *Candida glabrata*. *Antimicrob. Agents Chemother.* **1998**, *42*, 1695–1701.

4. Torelli, R.; Posteraro, B.; Ferrari, S.; La Sorda, M.; Fadda, G.; Sanglard, D.; Sanguinetti, M. The ATP-binding cassette transporter–encoding gene *CgSNQ2* is contributing to the *CgPDR1*-dependent azole resistance of *Candida glabrata*. *Mol. Microbiol.* **2008**, *68*, 186–201.

5. Vermitsky, J.P.; Edlind, T.D. Azole resistance in *Candida glabrata*: coordinate upregulation of multidrug transporters and evidence for a Pdr1-like transcription factor. *Antimicrob. Agents Chemother.* **2004**, *48*, 3773–81.

6. Vermitsky, J.P.; Earhart, K.D.; Smith, W.L.; Homayouni, R.; Edlind, T.D.; Rogers, P.D. Pdr1 regulates multidrug resistance in *Candida glabrata*: gene disruption and genome-wide expression studies. *Mol. Microbiol.* **2006**, *61*, 704–722.

7. Tsai, H.F.; Krol, A.A.; Sarti, K.E.; Bennett, J.E. *Candida glabrata PDR1*, a transcriptional regulator of a pleiotropic drug resistance network, mediates azole resistance in clinical isolates and petite mutants. *Antimicrob. Agents Chemother.* **2006**, *50*, 1384–1392.

8. Tsai, H.F.; Sammons, L.R.; Zhang, X.; Suffis, S.D.; Su, Q.; Myers, T.G.; Marr, K.A.; Bennett, J.E. Microarray and molecular analyses of the azole resistance mechanism in *Candida glabrata* oropharyngeal isolates. *Antimicrob. Agents Chemother.* **2010**, *54*, 3308–3317.

9. Paul, S.; Schmidt, J.A.; Moye-Rowley, W.S. Regulation of the CgPdr1 Transcription Factor from the Pathogen *Candida glabrata*. *Eukaryot. Cell* **2011**, *10*, 187–197.

10. Caudle, K.E.; Barker, K.S.; Wiederhold, N.P.; Xu, L.; Homayouni, R.; Rogers, P.D. Genomewide expression profile analysis of the *Candida glabrata* Pdr1 regulon. *Eukaryot. Cell* **2011**, *10*, 373–383.

11. Cavalheiro, M.; Costa, C.; Silva-Dias, A.; Miranda, I.M.; Wang, C.; Pais, P.; Pinto, S.N.; Mil-Homens, D.; Sato-Okamoto, M.; Takahashi-Nakaguchi, A.; *et al.* A Transcriptomics Approach To Unveiling the Mechanisms of In Vitro Evolution towards Fluconazole Resistance of a *Candida glabrata* Clinical Isolate. *Antimicrob. Agents Chemother.* **2019**, *63*, e00995-18.

12. Costa, C.; Pires, C.; Cabrito, T.R.; Renaudin, A.; Ohno, M.; Chibana, H.; Sá-Correia, I.; Teixeira, M.C. *Candida glabrata* drug: H+antiporter CgQdr2 confers imidazole drug resistance, being activated by transcription factor CgPdr1. *Antimicrob. Agents Chemother.* **2013**, *57*, 3159-3167.

13. Costa, C.; Nunes, J.; Henriques, A.; Mira, N.P.; Nakayama, H.; Chibana, H.; Teixeira, M.C. *Candida glabrata* drug:H+antiporter CgTpo3 (ORF *CAGL0I10384g*): Role in azole drug resistance and polyamine homeostasis. *J. Antimicrob. Chemother.* **2014**, *69*, 1767-1776.

14. Costa, C.; Dias, P.J.; Sá-Correia, I.; Teixeira, M.C. MFS multidrug transporters in pathogenic fungi: Do they have real clinical impact? *Front. Physiol.* **2014**, *5*, 197.

15. Costa, C.; Ribeiro, J.; Miranda, I.M.; Silva-Dias, A.; Cavalheiro, M.; Costa-de-Oliveira, S.; Rodrigues, A.G.; Teixeira, M.C. Clotrimazole Drug Resistance in *Candida glabrata* Clinical Isolates Correlates with Increased Expression of the Drug:H+ Antiporters CgAqr1, CgTpo1_1, CgTpo3, and CgQdr2. *Front. Microbiol.* **2016**, *7*, 526.

16. Alexander, B.D.; Johnson, M.D.; Pfeiffer, C.D.; Jiménez-Ortigosa, C.; Catania, J.; Booker, R.; Castanheira, M.; Messer, S.A.; Perlin, D.S.; Pfaller, M.A. Increasing Echinocandin Resistance in *Candida glabrata*: Clinical Failure Correlates With Presence of *FKS* Mutations and Elevated Minimum Inhibitory Concentrations. *Clin. Infect. Dis.* **2013**, *56*, 1724–1732.

17. Pfaller, M.A.; Castanheira, M.; Lockhart, S.R.; Ahlquist, A.M.; Messer, S.A.; Jones, R.N. Frequency of Decreased Susceptibility and Resistance to Echinocandins among Fluconazole-Resistant Bloodstream Isolates of *Candida glabrata*. *J. Clin. Microbiol.* **2012**, *50*, 1199–1203.

18. Farmakiotis, D.; Tarrand, J.J.; Kontoyiannis, D.P. Drug-Resistant *Candida glabrata* Infection in Cancer Patients. *Emerg. Infect. Dis.* **2014**, *20*, 1833–1840.

19. Bizerra, F.C.; Jimenez-Ortigosa, C.; Souza, A.C.R.; Breda, G.L.; Queiroz-Telles, F.; Perlin, D.S.; Colombo, A.L. Breakthrough Candidemia Due to Multidrug-Resistant *Candida glabrata* during Prophylaxis with a Low Dose of Micafungin. *Antimicrob. Agents Chemother.* **2014**, *58*, 2438–2440.

20. Pham, C.D.; Iqbal, N.; Bolden, C.B.; Kuykendall, R.J.; Harrison, L.H.; Farley, M.M.; Schaffner, W.; Beldavs, Z.G.; Chiller, T.M.; Park, B.J.; *et al.* Role of *FKS* Mutations in *Candida glabrata*: MIC Values, Echinocandin Resistance, and Multidrug Resistance. *Antimicrob. Agents Chemother.* **2014**, *58*, 4690–4696.

21. Cho, E.J.; Shin, J.H.; Kim, S.H.; Kim, H.K.; Park, J.S.; Sung, H.; Kim, M.N.; Im, H.J. Emergence of multiple resistance profiles involving azoles, echinocandins and amphotericin B in *Candida glabrata* isolates from a neutropenia patient with prolonged fungaemia. *J. Antimicrob. Chemother.* **2014**, *70*, 1268–1270.

22. Noël, T.; François, F.; Paumard, P.; Chastin, C.; Brèthes, D.; Villard, J. Flucytosine-fluconazole cross-resistance in purine-cytosine permease-deficient *Candida lusitaniae* clinical isolates: indirect evidence of a fluconazole uptake transporter. *Antimicrob. Agents Chemother.* **2003**, *47*, 1275–1284.

23. Polak, A. Antifungal combination therapy in localized candidosis. *Mycoses 33*, 353–358.

24. Chandra, J.; Mohammad, S.; Ghannoum, M.A. Flucytosine: Site of Action, Mechanism of Resistance and Use in Combination Therapy. In *Antimicrobial Drug Resistance*; Humana Press: Totowa, NJ. **2009**; pp. 313–326.

25. Pais, P.; Costa, C.; Pires, C.; Shimizu, K.; Chibana, H.; Teixeira, M.C. Membrane Proteome-Wide Response to the Antifungal Drug Clotrimazole in *Candida glabrata*: Role of the Transcription Factor CgPdr1 and the Drug:H+ Antiporters CgTpo1_1 and CgTpo1_2. *Mol. Cell. Proteomics* **2016**, *15*, 57–72.

26. Costa, C.; Henriques, A.; Pires, C.; Nunes, J.; Ohno, M.; Chibana, H.; Sá-Correia, I.; Teixeira, M.C. The dual role of *Candida glabrata* drug:H+ antiporter CgAqr1 (ORF *CAGL0J09944g*) in antifungal drug and acetic acid resistance. *Front. Microbiol.* **2013**, *4*, 170.

27. Ferrari, S.; Ischer, F.; Calabrese, D.; Posteraro, B.; Sanguinetti, M.; Fadda, G.; Rohde, B.; Bauser, C.; Bader, O.; Sanglard, D. Gain of function mutations in *CgPDR1* of *Candida glabrata* not only mediate antifungal resistance but also enhance virulence. *PLoS Pathog.* **2009**, *5*, e1000268.

28. Vale-Silva, L.; Ischer, F.; Leibundgut-Landmann, S.; Sanglard, D. Gain-of-Function Mutations in *PDR1* , a Regulator of Antifungal Drug Resistance in *Candida glabrata*, Control Adherence to Host Cells. *Infect. Immun.* **2013**, *81*, 1709–1720.

29. Vale-Silva, L.A.; Moeckli, B.; Torelli, R.; Posteraro, B.; Sanguinetti, M.; Sanglard, D. Upregulation of the Adhesin Gene *EPA1* Mediated by *PDR1* in *Candida glabrata* Leads to Enhanced Host Colonization. *mSphere* **2016**, *1*, e00065-15.

30. Ni, Q.; Wang, C.; Tian, Y.; Dong, D.; Jiang, C.; Mao, E.; Peng, Y. *CgPDR*1 gain-of-function mutations lead to azole-resistance and increased adhesion in clinical *Candida glabrata* strains. *Mycoses* **2018**, *61*, 430–440.

31. Ferrari, S.; Sanguinetti, M.; Torelli, R.; Posteraro, B.; Sanglard, D. Contribution of *CgPDR1*-Regulated Genes in Enhanced Virulence of Azole-Resistant *Candida glabrata*. *PLoS One* **2011**, *6*, e17589.

32. Santos, R.; Costa, C.; Mil-Homens, D.; Romão, D.; de Carvalho, C.C.C.R.; Pais, P.; Mira, N.P.; Fialho, A.M.; Teixeira, M.C. The multidrug resistance transporters CgTpo1_1 and CgTpo1_2 play a role in virulence and biofilm formation in the human pathogen *Candida glabrata*. *Cell. Microbiol.* **2017**, *19*, e12686.

33. Romão, D.; Cavalheiro, M.; Mil-Homens, D.; Santos, R.; Pais, P.; Costa, C.; Takahashi-Nakaguchi, A.; Fialho, A.M.; Chibana, H.; Teixeira, M.C. A New Determinant of *Candida glabrata* Virulence: The Acetate Exporter CgDtr1. *Front. Cell. Infect. Microbiol.* **2017**, *7*, 473.

34. Cavalheiro, M.; Pais, P.; Galocha, M.; Teixeira, M. Host-Pathogen Interactions Mediated by MDR Transporters in Fungi: As Pleiotropic as it Gets! *Genes (Basel).* **2018**, *9*, 332.

35. Tian, Y.; Gao, N.; Ni, Q.; Mao, Y.; Dong, D.; Huang, X.; Jiang, C.; Li, Z.; Zhang, L.; Wang, X.; *et al.* Sequence modification of the master regulator Pdr1 interferes with its transcriptional autoregulation and confers altered azole resistance in *Candida glabrata*. *FEMS Yeast Res.* **2018**, *18*.

36. Hou, X.; Xiao, M.; Wang, H.; Yu, S.Y.; Zhang, G.; Zhao, Y.; Xu, Y.C. Profiling of *PDR1* and *MSH2* in *Candida glabrata* Bloodstream Isolates from a Multicenter Study in China. *Antimicrob. Agents Chemother.* **2018**, *62*, e00153-18.

37. Katiyar, S.; Shiffrin, E.; Shelton, C.; Healey, K.; Vermitsky, J.P.; Edlind, T. Evaluation of polymorphic locus sequence typing for *Candida glabrata* epidemiology. *J. Clin. Microbiol.* **2016**, *54*, 1042-1050.

38. Healey, K.R.; Zhao, Y.; Perez, W.B.; Lockhart, S.R.; Sobel, J.D.; Farmakiotis, D.; Kontoyiannis, D.P.; Sanglard, D.; Taj-Aldeen, S.J.; Alexander, B.D.; *et al.* Prevalent mutator genotype identified in fungal pathogen *Candida glabrata* promotes multi-drug resistance. *Nat. Commun.* **2016**, *7*, 11128.

39. Sanguinetti, M.; Posteraro, B.; Fiori, B.; Ranno, S.; Torelli, R.; Fadda, G. Mechanisms of azole resistance in clinical isolates of *Candida glabrata* collected during a hospital survey of antifungal resistance. *Antimicrob. Agents Chemother.* **2005**, *49*, 668–679.

40. Brun, S.; Bergès, T.; Poupard, P.; Vauzelle-Moreau, C.; Renier, G.; Chabasse, D.; Bouchara, J.-P. Mechanisms of azole resistance in petite mutants of *Candida glabrata*. *Antimicrob. Agents Chemother.* **2004**, *48*, 1788–1796.

41. Salazar, S.B.; Wang, C.; Münsterkötter, M.; Okamoto, M.; Takahashi-Nakaguchi, A.; Chibana, H.; Lopes, M.M.; Güldener, U.; Butler, G.; Mira, N.P. Comparative genomic and transcriptomic analyses unveil novel features of azole resistance and adaptation to the human host in *Candida glabrata*. *FEMS Yeast Res.* **2018**, *18*.

42. Hull, C.M.; Parker, J.E.; Bader, O.; Weig, M.; Gross, U.; Warrilow, A.G.S.; Kelly, D.E.; Kelly, S.L. Facultative Sterol Uptake in an Ergosterol-Deficient Clinical Isolate of *Candida glabrata* Harboring a Missense Mutation in *ERG11* and Exhibiting Cross-Resistance to Azoles and Amphotericin B. *Antimicrob. Agents Chemother.* **2012**, *56*, 4223–4232.

43. Henry, K.W.; Nickels, J.T.; Edlind, T.D. Upregulation of *ERG* genes in *Candida* species by azoles and other sterol biosynthesis inhibitors. *Antimicrob. Agents Chemother.* **2000**, *44*, 2693–2700.

44. Marichal, P.; Vanden Bossche, H.; Odds, F.C.; Nobels, G.; Warnock, D.W.; Timmerman, V.; Van Broeckhoven, C.; Fay, S.; Mose-Larsen, P. Molecular biological characterization of an azole-resistant *Candida glabrata* isolate. *Antimicrob. Agents Chemother.* **1997**, *41*, 2229–2237.

45. Cernicka, J.; Subik, J. Resistance mechanisms in fluconazole-resistant *Candida albicans* isolates from vaginal candidiasis. *Int. J. Antimicrob. Agents* **2006**, *27*, 403–408.

46. Prasad, R.; Khandelwal, N.K.; Banerjee, A. Yeast ABC transporters in lipid trafficking. *Fungal Genet. Biol.* **2016**, *93*, 25–34.

47. Simons, K.; Sampaio, J.L. Membrane Organization and Lipid Rafts. *Cold Spring Harb. Perspect. Biol.* **2011**, *3*, a004697–a004697.

48. van Meer, G.; Voelker, D.R.; Feigenson, G.W. Membrane lipids: where they are and how they behave. *Nat. Rev. Mol. Cell Biol.* **2008**, *9*, 112–124.

49. Pasrija, R.; Panwar, S.L.; Prasad, R. Multidrug Transporters CaCdr1p and CaMdr1p of *Candida albicans* Display Different Lipid Specificities: both Ergosterol and Sphingolipids Are Essential for Targeting of CaCdr1p to Membrane Rafts. *Antimicrob. Agents Chemother.* **2008**, *52*, 694–704.

50. Pasrija, R.; Prasad, T.; Prasad, R. Membrane raft lipid constituents affect drug susceptibilities of *Candida albicans*. *Biochem. Soc. Trans.* **2005**, *33*, 1219.

51. Nakayama, H.; Tanabe, K.; Bard, M.; Hodgson, W.; Wu, S.; Takemori, D.; Aoyama, T.; Kumaraswami, N.S.; Metzler, L.; Takano, Y.; *et al.* The *Candida glabrata* putative sterol transporter gene *CgAUS1* protects cells against azoles in the presence of serum. *J. Antimicrob. Chemother.* **2007**, *60*, 1264–1272.

52. Nagi, M.; Tanabe, K.; Ueno, K.; Nakayama, H.; Aoyama, T.; Chibana, H.; Yamagoe, S.; Umeyama, T.; Oura, T.; Ohno, H.; *et al.* The *Candida glabrata* sterol scavenging mechanism, mediated by the ATP-binding cassette transporter Aus1p, is regulated by iron limitation. *Mol. Microbiol.* **2013**, *88*, 371–381.

53. Godinho, C.P.; Prata, C.S.; Pinto, S.N.; Cardoso, C.; Bandarra, N.M.; Fernandes, F.; Sá-Correia, I. Pdr18 is involved in yeast response to acetic acid stress counteracting the decrease of plasma membrane ergosterol content and order. *Sci. Rep.* **2018**, *8*, 7860.

8 Thesis Publications

Peer-reviewed scientific publications directly related to this thesis

Pais, P., Galocha, M., Califórnia, R., Viana, R., Ola, M., Takahashi-Nakaguchi, A., Chibana, H., Butler, G., Teixeira, M.C. A novel pathway controlling fluconazole resistance in *Candida glabrata*: the CgMar1 transcription factor and sphingolipid metabolism. (in preparation)

Pais, P., Califórnia, R., Galocha, M., Viana, R., Ola, M., Takahashi-Nakaguchi, A., Chibana, H., Butler, G., Teixeira, M.C. *Candida glabrata* transcription factor Rpn4 mediates fluconazole resistance through regulation of ergosterol biosynthesis and plasma membrane permeability. (submitted)

Pais, P., Galocha, M., Teixeira, M.C. 2019. Genome-wide response to drugs and stress in the pathogenic yeast *Candida glabrata*. Chapter In: Yeasts in Biotechnology and Human Health (Isabel Sá-Correia, Ed.), Springer, *Prog Mol Subcell Biol*, **58:**155-193.

Pais, P., Galocha, M., Viana, R., Cavalheiro, M., Pereira, D., Teixeira, M.C. 2019. Microevolution of the pathogenic yeasts *Candida albicans* and *Candida glabrata* during antifungal therapy and host infection. *Microb Cell*, **6:**142-159.

Monteiro, P. T., Pais, P., Costa, C., Manna, S., Sá-Correia, I., Teixeira, M.C. 2017. The PathoYeastract database: an information system for the analysis of gene and genomic transcription regulation in pathogenic yeasts. *Nucleic Acids Res*, **45:**D597-D603.

Pais, P., Costa, C., Cavalheiro, M., Romão, D., Teixeira, M.C. 2016. Transcriptional control of drug resistance, virulence and immune system evasion in pathogenic fungi: a cross-species comparison. *Front Cell Infect Microbiol*, **6:**131.

Pais, P., Pires C., Costa, C., Okamoto, M., Chibana, H., Teixeira, M.C. 2016. Membrane proteomics analysis of the *Candida glabrata* response to 5-flucytosine: unveiling the role and regulation of the drug efflux transporters CgFlr1 and CgFlr2. *Front Microbiol*, **7:**2045.

Pais, P., Costa, C., Pires C., Shimizu, K., Chibana, H., Teixeira, M.C. 2016. Membrane proteome-wide response to the antifungal drug clotrimazole in *Candida glabrata*: role of the transcription factor CgPdr1 and the Drug:H+ Antiporters CgTpo1_1 and CgTpo1_2. *Mol Cell Proteomics*, **15:**57-72.

Thesis Publications

Oral presentations in international scientific meetings

Pais, P., Califórnia, R., Galocha, M., Viana, R., Ola, M., Takahashi-Nakaguchi, A., Chibana, H., Butler, G., Teixeira, M.C. Candida glabrata transcription factor Rpn4 regulates fluconazole resistance through transcriptional control of ergosterol biosynthesis and plasma membrane stability. 29th ECCMID, Amsterdam, Netherlands, 13-16 April 2019.

Pais, P., Galocha, M., Califórnia, R., Pimenta, A., Mil-Homens, D., Fialho, A., Butler, G., Teixeira, M.C. Functional characterization of the transcription factor CgMar1 suggests new players governing azole drug resistance in *Candida glabrata*. 14th ASM Conference on Candida and Candidiasis, Providence, RI, USA, 15-19 April 2018.

Poster presentations in international scientific meetings

Pais, P., Costa, C., Pires, C. Cavalheiro, C., Teixeira, M.C. Using pathoproteomics to unveil new players in antifungal resistance in the human pathogen *Candida glabrata*. Human Fungal Pathogens 2017 Advanced Lecture Course in Molecular Mechanisms of Host-Pathogens Interactions and Virulence, Nice, France, 13-19 May 2017.

Pais, P., Costa, C. Pires, C., Romão, D., Cavalheiro, M., Teixeira, M.C. Membrane proteomics approaches unveil new mechanisms of 5-flucytosine and clotrimazole antifungal resistance in the human pathogen *Candida glabrata*. 6th Physiology of Yeast and Filamentous Fungi (PYFF), Lisbon, Portugal, 11-14 July 2016.

Oral presentations in national scientific meetings

Pais, P., Galocha, M., Califórnia, R., Butler, G., Teixeira, M.C. Beyond MDR-transporter mediated azole resistance in *Candida glabrata*: functional characterization of the transcription factors CgRpn4 and CgMar1. XXI Jornadas de Biologia de Leveduras "Professor Nicolau van Uden", Braga, Portugal, 8-9 June 2018.

Poster presentations in national scientific meetings

Pais, P., Galocha, M., Cavalheiro, M., Costa, C., Califórnia, R., Leitão, C., Pereira, D., Butler, G., Teixeira, M.C. deciphering transcriptional regulation of antifungal drug resistance in the pathogenic yeast *Candida glabrata*. Microbiotec'17, Porto, 7-9 December 2017.

Pais, P., Costa, C., Pires, C., Santos, R, Cavalheiro, M., Teixeira, M.C. New mechanisms of 5-flucytosine resistance in the human pathogen *Candida glabrata*: unveiled through chemogenomics and proteomics approaches. Microbiotec'15, Évora, 10-12 December, 2015.

Peer-reviewed scientific publications not included in this thesis

Galocha, M., Pais, P., Cavalheiro, M., Pereira, D., Viana, R., Teixeira, M.C. 2019. Divergent approaches to virulence in *C. albicans* and *C. glabrata*: two sides of the same coin. *Int J Mol Sci*, **20:**E2345.

Cavalheiro, M., Costa, C. Silva-Dias, A., Miranda, I.M., Wang, C., Pais, P., Pinto, S.N., Mil-Homens, D., Sato-Okamoto, M., Takahashi-Nakaguchi, A., Silva, R.M., Mira, N.P., Fialho, A.M., Chibana, H., Rodrigues, A.G., Butler, G., Teixeira, M.C. 2018. A transcriptomics approach to unveiling the mechanisms of *in vitro* evolution towards fluconazole resistance of a *Candida glabrata* clinical isolate. *Antimicrob Agents Chemother*, **63:**e00995-18.

Cavalheiro, M., Pais, P., Galocha, M., Teixeira, M.C. 2018. Host-pathogen interactions mediated by MDR transporters in fungi: as pleiotropic as it gets!. *Genes*, **9:**E332.

Teixeira, M.C., Monteiro, P.T., Palma, M., Costa, C., Godinho, C.P., Pais, P., Cavalheiro, M., Antunes, M., Lemos, A., Pedreira, T., Sá-Correia, I. 2018. *Nucleic Acids Res*, **46:**D348-D353.

Romão, D., Cavalheiro, M., Mil-Homens, D., Santos, R., Pais, P., Costa, C., Takahashi-Nakaguchi, A., Fialho, A, Chibana, H., Teixeira, M.C. 2017. *Front Cell Infect Microbiol*, **7:**473.

Thesis Publications

Santos, R., Costa, C., Mil-Homens, D., Romão, D., de Carvalho, C.C., Pais, P., Mira, N.P., Fialho, A.M., Teixeira, M.C. 2017. The multidrug resistance transporters CgTpo1_1 and CgTpo1_2 play a role in virulence and biofilm formation in the human pathogen *Candida glabrata*. *Cell Microbiol*, **19:**e12686.

Costa, C., Ponte, A., Pais, P., Santos, R., Cavalheiro, M., Yaguchi, T., Chibana, H., Teixeira, M.C. 2015. New mechanisms of flucytosine resistance in *C. glabrata* unveiled by a chemogenomics analysis in *S. cerevisiae*. *PLoS One*, **10:**e0135110.

9 Supplementary Material

9.1 Supplementary Figures

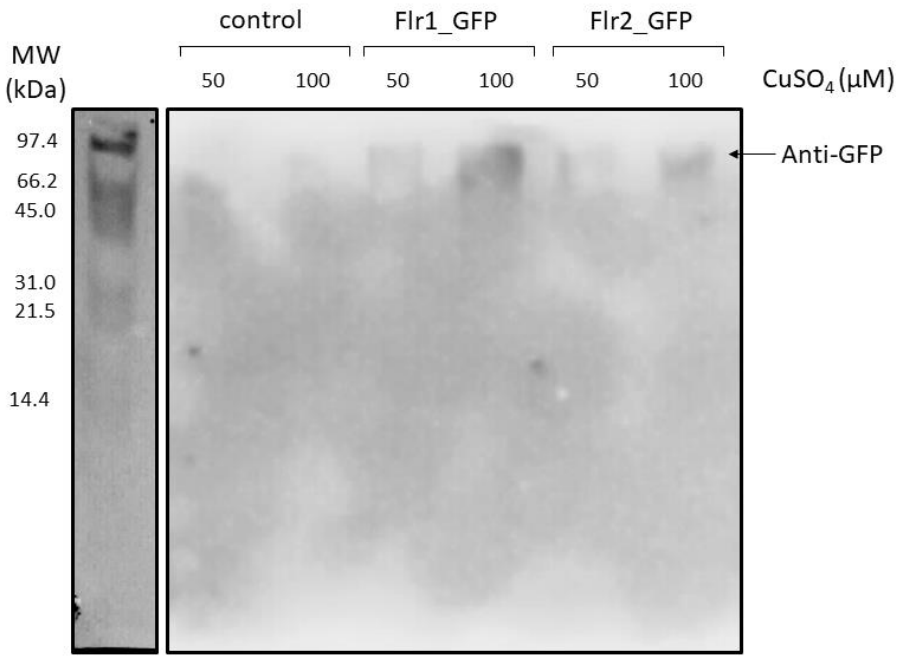

Supplementary Figure S4.1 – CgFlr1 and CgFlr2 are expressed in *C. glabrata* cells harboring the pGREG576_MT1_*CgFLR1* and the pGREG576_MT1_*CgFLR2* plasmids. Comparison of the level of expression of CgFlr1-GFP or CgFlr2-GFP fusion proteins in L5U1 *C. glabrata* cells upon exposure to the indicated CuSO4 concentrations, based on anti-GFP immuno-detection. Cells harboring the pGREG576 cloning vector (control), exposed to the same CuSO4 concentrations were used as a negative control.